THE KINETICS OF FORMATION OF COMPLEXES BETWEEN *ESCHERICHIA COLI* RNA POLYMERASE AND THE *rrnB* P1 AND P2 PROMOTERS OF *BACILLUS SUBTILIS*

By

Stephen Ross Wellington

B.Sc. , The University of British Columbia, 1985

A THESIS SUBMITTED IN PARTIAL FULFILLMENT OF
THE REQUIREMENTS FOR THE DEGREE OF
DOCTOR OF PHILOSOPHY

in

THE FACULTY OF GRADUATE STUDIES
(DEPARTMENT OF MICROBIOLOGY)

We accept this thesis as conforming to
the required standard

THE UNIVERSITY OF BRITISH COLUMBIA

August 1991

In presenting this thesis in partial fulfilment of the requirements for an advanced degree at the University of British Columbia, I agree that the Library shall make it freely available for reference and study. I further agree that permission for extensive copying of this thesis for scholarly purposes may be granted by the head of my department or by his or her representatives. It is understood that copying or publication of this thesis for financial gain shall not be allowed without my written permission.

Department of Microbiology

The University of British Columbia
Vancouver, Canada

Date Aug. 26, 1991

Abstract

In bacteria, a change in the growth rate (≥ 0.7 doublings per hour) is accompanied by a directly proportional change in the steady-state intracellular concentration of ribosomes. This growth rate dependent control of ribosome biosynthesis is apparently regulated at the level of ribosomal RNA (rRNA) transcription initiation by a feedback inhibition mechanism. One proposed effector of this feedback inhibition has been guanosine tetraphosphate (ppGpp). The effects of ppGpp on the kinetics of formation and dissociation of heparin resistant complexes between *Escherichia coli* RNA polymerase and the *rrnB* P1 (non growth rate regulated) and P2 (growth rate regulated) promoters from *Bacillus subtilis* were investigated as a function of temperature using a gel retardation assay. The results from this thesis suggest that the formation of polymerase/promoter complexes proceeded by way of three kinetically significant reaction steps. The initial bimolecular collision between free RNA polymerase and the promoter led to the formation of a heparin sensitive (HS) complex, which subsequently isomerized to an intermediate (HR1) and then final (HR2) heparin resistant complex. The temperature dependences of the forward isomerization rate constant (k_f), and the (overall) second-order association rate constant (k_a), were inconsistent with the proposal that free RNA polymerase and promoter fragments existed in rapid equilibrium with HS. If this rapid equilibrium existed, then the predicted equilibrium constant for binding ($K1 = k_a/k_f$) would be exothermic, contradicting the temperature dependence of K1 observed at other promoters. Consequently, it was proposed that a sequential mode of binding best described the bimolecular collision. The gel retardation assay described in this thesis examined the effects of ppGpp at a select number of steps in the overall path of transcription initiation. For the promoters in question, this analysis provided direct information regarding the formation of the HS and HR1 complexes, and indirect information regarding the

formation of HR2 and initiated ternary complexes. The cumulative results from studies of the *B. subtilis* and *E. coli rrnB* P1 and P2 promoters would suggest that ppGpp does not act to differentially inhibit transcription initiation at any of the steps investigated.

Table of contents

List of tables

List of figures

Abbreviations and Symbols.

Ap^r	Ampicillin resistant phenotype.
bp	Base pair.
BP1	*Bacillus subtilis rrnB* P1 promoter.
BP2	*Bacillus subtilis rrnB* P2 promoter.
BSA	Bovine serum albumin.
Cm^s/Cm^r	Chloramphenicol sensitive/resistant phenotype.
EP1	*Escherichia coli rrnB* P1 promoter.
EP2	*Escherichia coli rrnB* P2 promoter.
F	In a binding reaction, F represents the fraction of total promoter DNA which was found in complexes with RNA polymerase following gel retardation analysis.
HEPES	4-(2-Hydroxyethyl)-1-piperazineethanesulfonic acid.
HR	Heparin resistant polymerase/promoter complex.
HS	Heparin sensitive polymerase/promoter complex (or free RNA polymerase).
k_a	(Overall) second-order association rate constant.
k_d	Intrinsic overall dissociation rate constant.
k_f	Forward isomerization rate constant.
k_{obs}	Observed overall dissociation rate constant.
k_r	Reverse isomerization rate constant.
k_1, k_{-1}	The respective forward (second-order) and reverse rate constants which describe the formation and dissociation of the initial polymerase/promoter complex.
K1	Binding equilibrium constant (k_1/k_{-1}).

k_3, k_{-3}	The respective forward and reverse rate constants which describe the interconversion of the two heparin resistant complexes (HR1 and HR2).
KGlu	Potassium glutamate.
$1/\tau$	Overall (pseudo first-order) association rate constant.
nt	Nucleotide.
OMeGTP	3'-O-methylguanosine triphosphate.
ppGpp	Guanosine-3'-diphosphate-5'-diphosphate.
Puo	A purine nucleotide.
Pyd	A pyrimidine nucleotide.
S. D.	Standard deviation.
SDS	Sodium dodecyl sulfate.
Tc^r	Tetracycline resistant phenotype.

Acknowledgements

It is a pleasure to acknowledge my supervisor, George Spiegelman, for his valuable guidance and thoughtful criticism, without which my thesis could never have achieved this degree of preparedness. I would especially like to thank George for his patient answers to my many questions, and for selectively posing some key riddles of his own. I also wish to thank all the members of the Spiegelman lab, whose warm spirit and good humor have made my stay such an enjoyable one. These remarkable people are Vera Webb, Fereydoun Sajjadi, Terry Bird, Dick Pachal, and Loverne Duncan.

I would like to express my appreciation to the members of my thesis advisory committee, Tom Beatty, Gordon Tener, and Tony Warren, for their helpful suggestions.

Immeasurable thanks go to the members of my family for all their love and support, and I would like to acknowledge John McClean and Patrick Blaney for their constant friendship.

Most significantly, I wish to acknowledge my wife, Cheryl, whose love, strength, and patience were fundamental to the completion of this thesis.

Dedication

I wish to dedicate this thesis to my wife, Cheryl, for always being there to put the rest of the world into its proper perspective.

Introduction

I. General background.

It is well established that bacteria adjust their growth rate to match the nutritional capacity of their environment. This response primarily reflects the synthesis rate of protein, since protein may comprise up to 70% of the cell's total dry weight (for a review see Bremer and Dennis, 1987). Since it has been demonstrated that the synthetic activity of a translating ribosome is nearly constant under moderate to fast growth conditions (Pedersen, 1984; Bremer and Dennis, 1987), an altered capacity for protein synthesis must largely result from a change in the number of ribosomes relative to the total cellular mass. The linear increase in the steady-state concentration of ribosomes relative to increased cellular growth rate ($\geq$ 0.7 doublings per hour) has been well documented, and is referred to as the growth rate regulation of ribosome biosynthesis (for reviews see Nomura *et al.*, 1984; Lindahl and Zengel, 1986; Jinks-Robertson and Nomura, 1987).

The phenomenon of growth rate regulation raises some intriguing questions about the mechanisms by which the cell modulates ribosomal gene expression. Since the steady-state concentration of ribosomes is directly proportional to the cellular growth rate, the absolute synthesis rate of ribosomes must increase in proportion to the square of the growth rate. This relationship follows from the assumed condition of unrestricted balanced growth (Ingraham *et al.*, 1983), in which all cellular components of a bacterial culture increase at the same specific growth rate, such that $d[X]/dt = [X] (\mu \, Ln2)$ (where [X] is the concentration of a cellular component, and μ is the growth rate of the culture measured as doublings per hour). Under conditions where [X] is proportional to μ, then $d[X]/dt$ will be proportional to μ^2. The dramatic consequence of this relationship is apparent when one considers that over the range of 0.6 to 2.5 doublings per hour, the rate of

transcription initiation at an rRNA operon increases approximately 15 fold (Bremer and Dennis, 1987). The complexity of this regulation is compounded by the fact that over fifty r-proteins, and three species of rRNA, must be coordinately expressed and assembled into the two subunits which define the ribosome. Furthermore, in *E. coli*, these components are scattered over the genome between roughly thirty operons (Jinks-Robertson and Nomura, 1987). Thus, the phenomenon of growth rate regulation can be divided into two parts. First, the cell must be able to coordinate its expression of r-proteins and rRNA in order to satisfy the stoichiometry required by the intact ribosome. Secondly, the cell must be able to adjust the rate of ribosome biosynthesis to match the growth rate potential of the environment. Some insight as to how the cell coordinates the expression of its ribosomal components has come from studying the r-protein and rRNA genes in *E. coli*.

In general, the major form of control over r-protein synthesis seems to be autogenous feedback at the level of translation (Jinks-Robertson and Nomura, 1987). Both *in vivo* and *in vitro*, at least one of the r-proteins from each operon can interact with the leader region of its polycistronic message, thereby inhibiting the translation of some, or all, of the r-proteins encoded by that operon (Jinks-Robertson and Nomura, 1987). It should be noted that the presence of a translational feedback mechanism does not rule out the possibility for transcriptional regulation of r-protein gene expression (Lindahl and Zengel, 1986). However, the transcription of r-protein genes apparently takes place in excess of those levels actually required for r-protein synthesis (Nomura *et al.*, 1984), with the excess mRNA being selectively degraded as a consequence of the autogenous feedback described above (Cole and Nomura, 1986). Thus, it is primarily translational feedback inhibition which ensures the coordinate expression of all r-protein genes. A corollary to this observation is that the synthesis of r-proteins, and therefore ribosome assembly,

must be ultimately determined by the expression of another component that is rate limiting.

The rate of ribosome biosynthesis could be limited by the availability of rRNA binding sites for the regulatory r-proteins involved in the inhibition of r-protein expression (Noller and Nomura, 1987). To support this model, Lindahl and Zengel (1985) observed that during *in vivo* nutritional shift-up experiments, 23S rRNA synthesis rates increased immediately, whereas the release of the S10 operon from attenuation by L4 r-protein was delayed. It is interesting to note that this lag time was similar to the time required by the RNA polymerase to transcribe past the L4 binding region within the 23S RNA structural gene (Lindahl and Zengel, 1985). Furthermore, Yates and Nomura (1981) have demonstrated that *in vitro*, the translational inhibition of the L11 operon by L1 r-protein can be relieved by the addition of 23S rRNA.

II. Models for growth rate regulation.

Because it is generally accepted that the control of ribosome biosynthesis involves rRNA expression as a rate determining step, growth rate control of rRNA synthesis has received a great deal of attention. Since rRNA is not translated, and is known to be stable except at low growth rates (Gausing, 1977), any mechanism controlling its expression must act at the level of transcription. Three models for rRNA regulation have been developed.

1. Passive regulation.

Originally described by Maaløe (1969), the underlying principle of passive regulation is that the cell has only a limited capacity for transcription. Maaløe proposed that as the nutritional quality of the environment improves, the transcription 'equilibrium' within the cell is shifted from the expression of fueling

and biosynthetic operons (which become increasingly repressed), to the expression of genes involved with protein synthesis. A large number of the models for growth rate regulation have their foundations based on this principle of transcription equilibrium. For example, both Travers (1987) and Jensen and Pedersen (1990) have suggested that growth rate regulated promoters are more difficult to saturate with polymerase than their non-growth rate regulated counterparts. Consequently, a shift in either polymerase/promoter affinity (Travers, 1987), or polymerase concentration (Jensen and Pedersen, 1990), should lead to a large change in the steady state transcription initiation rate of a growth rate dependent promoter, compared to that of a non growth rate regulated one.

The Jensen and Pedersen model (1990) assumes that the majority of the total cellular polymerase is actively engaged in transcript elongation, and that the concentration of this 'active' fraction can be increased by slowing down polymerase elongation rates. The model suggests that modest decreases in the global elongation rates of polymerase could lead to larger decreases in the concentration of RNA polymerase available to initiate a new round of transcription at a promoter. Since the original assumption was that growth rate regulated promoters were more difficult to saturate with polymerase than their non growth rate regulated counterparts, the decrease in free RNA polymerase concentration would ultimately lead to the differential inhibition of transcription from growth rate regulated promoters.

The implication of the Jensen and Pedersen model is that the number of promoters in a cell are in molar excess over the amount of holoenzyme capable of initiating a new round of transcription (Jensen and Pedersen, 1990). If this were true, then changes in the copy number of an unregulated (constitutive) gene should lead to changes in the specific transcription initiation frequency from the promoter for that gene (i.e. as the copy number of a gene increased, the initiation frequency per individual promoter for that gene would decrease). However, it has been

observed that when the copy number of a constitutive gene is increased within *E. coli*, the specific transcription initiation frequency per promoter remains constant (Churchward *et al.*, 1982; Jinks-Robertson *et al.*, 1983; Gourse and Nomura, 1984). This would suggest that the polymerase concentration model (Jensen and Pedersen, 1990) might be incomplete as written (for additional arguments, see also Travers, 1987).

2. Feedback inhibition.

Studies by Nomura and co-workers have established that an excess of transcriptionally active ribosomes can serve to inhibit rRNA expression through a negative feedback mechanism. Initial evidence came from gene dosage experiments in *E. coli*, in which the total level of rRNA expression remained constant when the copy number of rRNA genes was increased two to three fold by plasmids bearing the intact *rrnD* or *rrnB* operons (Jinks-Robertson *et al.*, 1983). However, when structural portions of these plasmid-borne *rrn* operons were deleted, expression of total cellular rRNA became gene dosage dependent (Jinks-Robertson *et al.*, 1983; Gourse and Nomura, 1984). By measuring the transcription of tRNA genes uniquely encoded by the chromosomal and intact plasmid *rrn* operons, it was established that expression of the individual *rrn* operons was uniformly repressed by excess rRNA to compensate for the increased gene copy number, thereby maintaining a constant level of rRNA within the cell (Gourse and Nomura, 1984).

This feedback inhibition was determined to require intact ribosomes, since conditions which led to the blockage of ribosome assembly were found to increase the synthesis of rRNA (Takebe *et al.*, 1985). Furthermore, two studies suggested that the mechanism of rRNA regulation involved ribosomes active in the process of translation. First, by using an inducible promoter-fusion system, Cole *et al.* (1987) were able to limit the *in vivo* concentration of the translation initiation factor IF2, thereby decreasing the fraction of active ribosomes. If feedback inhibition of rRNA

synthesis involved free, non-translating ribosomes, as had been originally suggested (Jinks-Robertson *et al.*, 1983), the conditions induced by Cole *et al.* (1987) would have led to an inhibition of ribosome biosynthesis. Instead, a massive increase in the concentration of free ribosomal subunits was observed. A second experiment by Yamagishi *et al.* (1987), involved an *rrnB* operon which contained a mutation in the anti-Shine-Dalgarno region of the 16S rRNA gene. The over-expression of this mutant failed to exert feedback inhibition of rRNA synthesis (Yamagishi *et al.*, 1987), much like the original gene dosage experiments involving *rrn* operons deleted for rRNA structural genes (Jinks-Robertson *et al.*, 1983; Gourse and Nomura, 1984). Together, these results demonstrated that ribosomes inefficient in translation initiation were unable to cause feedback inhibition of rRNA synthesis, and suggested that the 'translational capacity' of the cell was an important sensing mechanism for the process of growth rate regulation.

3. ppGpp control.

A crucial link which is still missing from the negative feedback model, is the identification, and mode of action, of any effector(s) which might inhibit rRNA expression. The involvement of translating ribosomes is intriguing, for it resembles the requirements of the stringent response (for reviews on the stringent response, see Gallant, 1979; Cashel and Rudd, 1987). The stringent response is a global corrective mechanism which adjusts the metabolism of *E. coli* during conditions where the ratio of charged to uncharged tRNA falls below a minimum threshold (Rojiani *et al.*, 1989, 1990). The hallmark of the stringent response is a rapid decrease in the rate of RNA accumulation, which largely reflects a 10 - 20 fold reduction in the rate of stable RNA synthesis (Gallant, 1979; Cashel and Rudd, 1987). Concomitant with this decrease however, is a dramatic increase in the accumulation of guanosine tetraphosphate (ppGpp), whose concentration within the cell can rise from micromolar to millimolar levels during the onset of the stringent response

(Cashel and Gallant, 1969; Gallant, 1979; Cashel and Rudd, 1987). The synthesis of this unusual nucleotide during the stringent response requires the product of the *relA* gene (Cashel and Gallant, 1969), which catalyzes the formation of ppGpp from ATP and GTP under conditions where uncharged tRNA's block the A-site of a translating ribosome, thereby causing the ribosome to 'idle' (Haseltine and Block, 1973). *relA* mutants, while defective in the stringent response, are still able to accumulate ppGpp during steady-state growth, suggesting that an alternative synthetic pathway exists (Friesen, *et al.*, 1978; Atherly, 1979; Metzger *et al.*, 1989b). Due to the inverse correlation of rRNA synthesis with ppGpp concentration during the stringent response, many researchers have also investigated ppGpp as a possible effector of growth rate regulation.

By fractionating pulse-labelled cellular RNA, studies by Bremer and co-workers (Ryals *et al.*, 1982) demonstrated that the ratio of the rate of stable RNA synthesis (rs), to the total instantaneous rate of RNA synthesis (rt), was inversely related to the intracellular concentration of ppGpp. The relationship between the ratio rs/rt and ppGpp concentration was the same irrespective of the steady-state growth conditions of the bacteria, or whether the cells were starved for an amino acid (Ryals *et al.*, 1982). Furthermore, the function between rs/rt and ppGpp was independent of the *relA* gene product (Ryals *et al.*, 1982). Based on these observations, Ryals *et al.* (1982) concluded that ppGpp was the primary effector of growth rate regulation *in vivo*. These *in vivo* results conformed well to a model for ppGpp action originally suggested by Travers (1976), who proposed that RNA polymerase could adopt different conformations which displayed different promoter specificities, and that ppGpp could alter the relative equilibrium concentrations of these isomers. As the putative negative effector of both the stringent response (Travers, 1976) and growth rate regulation (Ryals *et al.*, 1982), ppGpp was suggested to cause polymerase to adopt that conformation which inefficiently initiated

transcription from stable RNA promoters. The next section will review some of the results which analyze whether ppGpp is an effector of growth rate regulation.

III. Evidence for ppGpp regulation.

1. Correlations.

The partitioning model of Travers (1976) and Ryals *et al.* (1982) would suggest that interaction of RNA polymerase with ppGpp is central to both the stringent response and growth rate regulation. Using photoaffinity labelling techniques, Owens *et al.* (1987) demonstrated that both GTP and ppGpp analogs could bind to the beta (β), beta' (β'), and sigma (σ) subunits of RNA polymerase (see Introduction section V.1 for a discussion of RNA polymerase). However, while the GTP analog preferentially labelled the β and β' subunits, the ppGpp analog primarily associated with the σ subunit, suggesting a unique ppGpp binding site(s) existed which was distinct from substrate binding (Owens *et al.*, 1987). This is consistent with the kinetic studies of Kingston *et al.* (1981), who concluded that ppGpp-induced pausing of transcription was not due to competitive inhibition of nucleoside triphosphate binding at the chain elongation site of RNA polymerase. Furthermore, the addition of ppGpp reduced the sedimentation coefficient of RNA polymerase, suggesting that a conformational change was induced (Debenham *et al.*, 1979; Travers *et al.*, 1980). Finally, Little *et al.* (1983a, 1983b) isolated an RNA polymerase mutant that displayed a hypersensitive response to ppGpp *in vivo*. The observed abnormal control of ribosome synthesis and ppGpp accumulation was consistent with the proposal that the regulation of protein synthesis is a mutual relationship between ppGpp-directed ribosome biosynthesis and ribosome-directed ppGpp metabolism (Little *et al.*, 1983a, 1983b).

Using purified RNA polymerase holoenzyme (holoenzyme is the core subunits of RNA polymerase β, β', and α_2, complexed with the σ subunit; see also

Introduction section V.1) and specific promoter bearing templates, several *in vitro* studies have reported a differential inhibition of transcription from rRNA promoters. Both Travers (1976) and van Ooyen *et al.* (1976) have investigated RNA synthesis from linear phage templates containing one or more *rrn* operons. Using continuous transcription assays, both Travers (1976) and van Ooyen *et al.* (1976) reported that ppGpp induced a 2 - 4 fold differential inhibition of rRNA transcription compared to the total synthesis of RNA. This differential inhibition was salt dependent, and displayed an optimum between 75 and 100 mM KCl (Travers, 1976; van Ooyen *et al.*, 1976). Alternatively, Glaser *et al.* (1983) employed a supercoiled plasmid containing the *rrnA* promoter region as a DNA template for their continuous transcription assay. It was observed that the absolute yield of RNA was far greater from supercoiled templates than from the same DNA linearized with the restriction endonuclease *Eco*R1. When ppGpp was included in the assay, a 2.5 - 5 fold differential inhibition of transcription was observed from the growth rate regulated *rrnA* P1 promoter, compared to that synthesis initiated from the non-growth rate regulated *rrnA* P2 promoter (Glaser *et al.*, 1983). It is interesting to note that while the supercoiled template was more efficient in promoting transcription, the differential inhibition obtained with ppGpp was comparable to that effect observed using the linear phage templates (Travers, 1976; van Ooyen *et al.*, 1976). Finally, by employing a mixed-template *in vitro* transcription assay (linear templates), Kajitani and Ishihama (1984) investigated the ability of ppGpp to determine promoter selectivity. Using the *trpP* promoter as an internal reference for transcription efficiency, Kajitani and Ishihama (1984) measured the effects of ppGpp on the relative partitioning of RNA polymerase between the *lac* UV5, *rrnE* P1, and *rrnE* P2 promoters. They observed a 2 - 4 fold inhibition of *rrnE* P1 activity compared to that repression induced at *rrnE* P2 (Kajitani and Ishihama, 1984), similar to the differential effect reported by Glaser *et al.* (1983) for the respective promoters of the *rrnA* operon. Even under altered reaction conditions (e.g.

increased glycerol, KCl replacing NaCl), Kajitani and Ishihama (1984) found that the upstream P1 promoter was always inhibited by ppGpp relative to the downstream P2 promoter.

2. Anomalies.

Not all *in vitro* transcription analyses have observed a differential effect of ppGpp on rRNA expression (see reviews in Gallant, 1979; Cashel and Rudd, 1987; Jinks-Robertson and Nomura, 1987). Early transcription assays were especially variable in their findings, and there have been several reports in which additional (Igarashi *et al.*, 1989) or alternative (Debenham *et al.*, 1980; Travers *et al.*, 1980) transcription factors were required to selectively inhibit expression from rRNA promoters. Furthermore, there have been reports of ppGpp effects *in vitro* which were demonstrated to be non-essential to growth rate regulation *in vivo*. For example, Kingston and Chamberlin (1981) observed that ppGpp enhanced the pausing of *in vitro* transcription at specific sites in the leader region of the *rrnB* operon, and suggested that an attenuation mechanism might contribute to the regulation of rRNA synthesis. However, deletion of these pause sites had no effect on the growth rate dependent expression of the *rrnB* P1 promoter *in vivo* (Gourse *et al.*, 1986), questioning the relevance of the pausing to growth rate regulation. Similarly, Glass *et al.* (1986) isolated RNA polymerase from *rpoB* (β subunit) mutants which were apparently relaxed in their stringent response *in vivo*. When used during *in vitro* transcription assays of the *rrnE* promoters, the mutant polymerases were resistant to ppGpp inhibition compared to the wild-type enzyme (Glass *et al.* , 1986). However, later investigations revealed that the apparent relaxed phenotype *in vivo* was due to an unusually low accumulation of ppGpp in the mutants, and that the function of rs/rt versus ppGpp concentration was identical for both mutant and wild-type strains (Baracchini *et al.*, 1988).

In addition to these inconsistencies *in vitro*, there was a recent *in vivo* study which suggested that feedback inhibition of rRNA expression by ppGpp is an incomplete description of growth rate regulation. The studies of Bremer and co-workers (Ryals *et al.*, 1982; Little *et al.*, 1983a, 1983b) demonstrated a strict relationship between the intracellular concentration of ppGpp and the specific stable RNA gene activity. However, as noted by the authors (Ryals *et al.*, 1982), an interdependent response between two parameters does not guarantee a specific causal relationship. In order to investigate the requirement of ppGpp for growth rate regulation *in vivo*, Gaal and Gourse (1990) measured the expression of the *rrnB* P1 promoter in a strain of *E. coli* deleted for genes responsible for ppGpp synthesis and degradation (*relA*$^-$, *spoT*$^-$). The *rrnB* P1 promoter was fused to the *lacZ* structural gene, and integrated as single copy into the *E. coli* genome. No ppGpp was detectable in the double mutant, and as expected, total RNA synthesis was not inhibited during the induction of a stringent response (Gaal and Gourse, 1990). However, under conditions of steady-state growth, expression of β-galactosidase increased in a growth rate dependent manner, both in the wild-type and mutant strains (Gaal and Gourse, 1990). Similarly, it was observed that an increase in rRNA gene dosage could decrease β-galactosidase activity about 40% in both the wild-type and double mutant strains, suggesting that ppGpp was not required for feedback inhibition of rRNA expression (Gaal and Gourse, 1990, see Introduction section II.2).

Therefore, the role of ppGpp as an effector of growth rate regulation is questionable. At one extreme, it could be argued that ppGpp is one of perhaps several redundant control mechanisms which regulate rRNA expression (Gallant, 1979). On the other hand, it could be that ppGpp has no role in rRNA transcription at all, and the observed correlation between rRNA expression and ppGpp concentration is only due to the involvement of ppGpp in another aspect of ribosome biosynthesis and/or function, such as translation fidelity (Dix and Thompson, 1986; see also Gaal and Gourse, 1990). It is clear however, that the

question still remains as to how the differential expression between growth rate dependent and non growth rate regulated rRNA promoters can be regulated. One of the goals for any model describing transcription is to understand the interactions between RNA polymerase and a promoter region, and how these interactions can be modulated to alter the frequency of productive transcript initiation. Thus, an understanding of the functional properties of rRNA promoters would greatly aid the description of growth rate regulation.

IV. Review of rRNA operon structure

1. General.

There are seven rRNA operons per haploid genome in *E. coli*, and their locations are centered around the initiation site for DNA replication (*oriC*) (for a review of *rrn* operon structure, see Lindahl and Zengel, 1986; Jinks-Robertson and Nomura, 1987). Each transcription unit contains one gene for each rRNA species (23S, 16S, and 5S), as well as several species of tRNA, and the gene order for each operon is 16S-spacer tRNA-23S-5S-(distal tRNA). It is generally assumed that the high copy number of *rrn* operons is necessary to maintain sufficient levels of rRNA within the cell during periods of rapid growth. However, at least one copy of the seven *rrn* operons can be deleted without any obvious impact on cell growth (Ellwood and Nomura, 1980). Note that the copy number of genes located near the origin of replication is amplified with increasing growth rates (Bremer and Dennis, 1987), and it has been proposed that such amplification is responsible for the growth rate dependent expression of rRNA. However, between a growth rate of 0.9 to 2.7 doublings per hour, the copy number of *rrn* operons per genome increases 20%, whereas the rate of transcription of these genes increases roughly 10 fold in this same growth rate range (Ellwood and Nomura, 1982). All seven operons direct transcription away from *oriC* (i.e. in the same direction as replication). The reason

for this is not clear, but is thought to be a consequence of the high level of expression which occurs from the rRNA promoters. Indeed, while the rRNA genes occupy approximately 0.5% of the *E. coli* genome, their expression can account for 73% of all transcription (Jinks-Robertson and Nomura, 1987; Bremer and Dennis, 1987). It has been proposed that the transcriptional orientation of the rRNA genes has evolved to minimize the frequency of collisions between the replicative apparatus and transcribing RNA polymerase (Brewer, 1988).

2. rRNA promoters.

A study of rRNA promoter regions reveals them to be highly complex (for a review see Lindahl and Zengel, 1986; Jinks-Robertson and Nomura, 1987). All seven *E. coli* rRNA operons have two tandem promoters (P1 and P2), each containing distinct - 35 and - 10 regions (the numbering of sequence positions within a promoter are relative to the transcription initiation site, which is designated as + 1; see also Introduction section V.2), and separated from one another by about 100 base pairs (bp). The P2 promoter is closest to the *rrn* structural genes, and is located approximately 200 bp upstream of the 5' end of the mature 16S rRNA. There is a high degree of DNA sequence homology between the promoter regions of the seven rRNA operons. Indeed, for *rrnA, B, C,* and *G,* the sequences are identical beginning upstream of the - 35 region of P1, and extending about 30 bp downstream of the P2 transcription initiation site (Lindahl and Zengel, 1986). While the sequences around P1 and P2 are highly conserved between the seven *rrn* operons, there is little homology between the actual P1 and P2 promoters themselves (Lindahl and Zengel, 1986; Jinks-Robertson and Nomura, 1987).

The sequence differences between *E. coli rrn* P1 and P2 apparently contribute towards the different levels of expression which are observed from these two promoters *in vivo.* Cashel and co-workers (Sarmientos *et al.,* 1983; Sarmientos and Cashel, 1983) studied the *in vivo* expression of the *rrnA* promoter region by creating

plasmids in which a strong transcriptional terminator was introduced approximately 400 bp downstream from the transcription initiation site of *rrnA* P2. Because of the separation between P1 and P2, transcripts originating from the two promoters could be independently monitored following gel electrophoresis of total cellular RNA. Three interesting observations were made. First, at growth rates above 1 doubling per hour, the P1 promoter was approximately 2 -3 times more active than the P2 promoter (Sarmientos and Cashel, 1983; see also de Boer and Nomura, 1979; Lund and Dahlberg, 1979). Second, as the steady-state growth rate of the bacteria increased, the expression from P1 increased in a growth rate dependent manner, whereas that from P2 did not (Sarmientos and Cashel, 1983). Third, while the P1 promoter was subject to stringent control during amino acid starvation, the P2 promoter was not (Sarmientos *et al.*, 1983). The same differential regulation between the P1 and P2 promoters was also observed at the *rrnB* and *rrnE* operons (Gourse *et al.*, 1986). By fusing the separate P1 and P2 promoter regions to a promoterless *lacZ* gene, and employing a bacteriophage lambda vector to integrate these constructs as single copy lysogens into the *E. coli* genome, Gourse *et al.* (1986) were able to measure the cellular concentration of β-galactosidase as an indication of expression from the promoters. They observed that the P1 promoters of *rrnB* and *rrnE* were growth rate regulated, whereas the P2 promoter from *rrnB* was not (Gourse *et al.*, 1986). Therefore in *E. coli*, the *rrn* P1 promoter is the target for both growth rate regulation (Sarmientos and Cashel, 1983; Gourse *et al.*, 1986) and stringent control (Sarmientos *et al.*, 1983). It is unclear what the physiological role of the downstream P2 promoter is, but Sarmientos and Cashel (1983) proposed that it might be important for maintaining low level expression of rRNA during adverse growth conditions (see also Gausing, 1977).

In order to determine the region(s) of the *E. coli rrnB* P1 promoter which were necessary to effect a growth rate dependent response *in vivo*, Gourse *et al.* (1986) tested the expression of a series of *rrnB* P1 mutants which carried deletions for

sequences flanking the promoter region. The *rrnB* P1 promoter and its deletion mutants were used to create single copy promoter fusion lysogens as described above, and the cellular concentration of the fusion product (β-galactosidase) was measured over a range of growth rates. Two important aspects of rRNA expression were discovered by this study. First, it was established that an upstream DNA sequence between - 154 and - 51 was necessary to optimize expression from the *rrnB* P1 promoter, and appeared to account for the high rates of transcription which are observed from rRNA operons *in vivo* (Gourse *et al.* , 1986; Jinks-Robertson and Nomura, 1987). The presence of this region could increase *rrnB* P1 expression at least 20-fold, and was associated with a highly A:T rich DNA sequence which displayed anomalous electrophoretic mobility (Gourse *et al.* , 1986). Recently, this upstream activating region has been shown to interact with Fis (Nilsson *et al.*, 1990; Ross *et al.*, 1990), a DNA binding protein known to bend the sequence with which it associates (Johnson *et al.*, 1987; Thompson and Landy, 1988), and whose presence seems responsible for stimulating the transcriptional activity of the *E. coli rrnB* P1 promoter both *in vivo* (5-fold) and *in vitro* (10 to 20-fold) (Ross *et al.*, 1990). However, it must be emphasized that the expression of β-galactosidase in *rrnB* P1 mutants which lacked this upstream activating sequence was still regulated in a growth rate dependent manner (Gourse *et al.* , 1986).

A second important aspect of rRNA expression that was observed during the study of Gourse *et al.* (1986), was that growth rate regulation and feedback inhibition of rRNA expression were both defined by sequences between the - 51 to - 4 positions of the *rrnB* P1 promoter (Gourse *et al.* , 1986). A much more detailed analysis was later performed by Gourse and co-workers (Gaal *et al.*, 1989; Dickson *et al.*, 1989), who measured the activities of 50 single copy promoter fusion lysogens from a collection of mutant and wild-type *rrnB* P1 promoters. As a set, the mutants spanned nearly the entire region of *rrnB* P1 between - 1 and - 48, and consisted primarily of single or multiple base pair substitutions, but also included single base

pair insertions and deletions (Gaal *et al.*, 1989; Dickson *et al.*, 1989). Mutants which deviated from the wild-type - 10 or - 35 hexamers, or which altered the 16 base pair spacing between the hexamers, were not regulated in a growth rate dependent manner (Dickson *et al.*, 1989). Since the growth rate dependent regulation of *rrnB* P1 was not linked in any way to its level of expression, it was suggested that rRNA promoters have evolved to maintain their regulatory abilities at the expense of optimizing their promoter strength (Gaal *et al.*, 1989; Dickson *et al.*, 1989).

By investigating the expression of rRNA in *Bacillus subtilis*, Spiegelman and co-workers established that the overall control of rRNA synthesis appears to be the same as that in *E. coli* (Leduc *et al.*, 1982; Webb and Spiegelman, 1984). Later, by fusing the *B. subtilis rrnB* promoter region to the structural gene for chloramphenicol acetyltransferase (CAT), Deneer and Spiegelman (1987) observed that the tandem rRNA promoters from the *B. subtilis rrnB* locus were functional in *E. coli*, and that the expression of CAT was regulated in a growth rate dependent manner (see also Deneer, 1986). However, when expression from the separate *B. subtilis rrnB* promoters was investigated, it was determined that only the downstream P2 promoter was subject to growth rate regulation, and was also the more transcriptionally active promoter of the P1-P2 pair (Deneer, 1986; Deneer and Spiegelman, 1987). These findings were in marked contrast to the situation described for the *E. coli* rRNA promoters (see above), and the significance of this functional reversal remains unclear. An important consideration for the present thesis is the lack of overall sequence homology between the *E. coli rrnB* P1 and the *B. subtilis rrnB* P2 promoters (Deneer and Spiegelman, 1987). Even in the core promoter region (- 35 hexamer, spacer region, - 10 hexamer), where sequence homologies are higher, there are significant differences between the two promoters. For example, the consensus sequence for the - 35 region of an *E. coli* (σ^{70}) promoter is 5' TTGACA (Hawley and McClure, 1983, Harley and Reynolds, 1987). Whereas the - 35 region of the *B. subtilis rrnB* P2 promoter displays a perfect match to the *E. coli*

consensus, the *rrnB* P1 promoter from *E. coli* deviates from this consensus at one position. It is noteworthy that a mutation which changed the *E. coli rrnB* P1 - 35 sequence towards consensus also destroyed growth rate regulation of this promoter (Dickson *et al.*, 1989). Similarly, for growth rate dependent expression of the *E. coli rrnB* P1 promoter to occur, the spacing between the - 35 and - 10 hexamers must be maintained at precisely 16 base pairs (Dickson *et al.*, 1989). However, the corresponding distance at the growth rate regulated *B. subtilis rrnB* P2 promoter is 17 base pairs (Deneer and Spiegelman, 1987). Because of the sequence differences between the growth rate regulated promoters isolated from *E. coli* compared to that of *B. subtilis*, the *Bacillus rrnB* P2 promoter represents a useful 'mutant' with which to study the growth rate dependent expression of rRNA in *E. coli*.

V. Review of transcription initiation.

The studies reviewed in the previous section would suggest that it is the core promoter region, and consequently the process of transcription initiation, that acts as a target for growth rate regulation. Presently, there have been very few detailed investigations of the specific mechanism for transcription initiation at a growth rate regulated rRNA promoter (Ishihama, 1986; Gourse, 1988). However a description of the general transcription initiation process is available from the large variety of studies performed at other promoter/polymerase systems. The following three sections outline the components, and the process, of transcription initiation at *E. coli* (σ^{70}) promoters.

1. RNA polymerase.

The DNA dependent RNA polymerase from *Escherichia coli* is most frequently used during studies of transcription. The enzyme is a large multimeric protein, whose core structure is formed by the three subunits, beta (β), beta' (β'), and

alpha (α), in a molar ratio of 1:1:2 respectively (Burgess, 1969). While catalytic activity is demonstrated by the core enzyme (Burgess *et al.*, 1969), a fourth subunit, sigma-70 (σ^{70}), is required for promoter specific transcription initiation (Burgess *et al.*, 1969), and together with core, defines the RNA polymerase holoenzyme (total molecular weight 449,058; Burgess *et al.*, 1987). In addition to the subunits which define RNA polymerase holoenzyme, the omega (ω) factor is an apparent accessory protein which binds to both core polymerase and holoenzyme at a molar ratio of 0.5 - 2 per enzyme (Burgess, 1969). The function of omega is unknown, but it is not required for growth rate regulation *in vivo*, since *E. coli* mutants which carry a deletion for the omega gene are still subject to growth rate dependent regulation of rRNA expression (Gaal and Gourse, 1990). Note that only 30 - 40% of the cellular RNA polymerase exists as holoenzyme (Iwakura *et al.*, 1974; Engbaek *et al.*, 1976), reflecting the transient, catalytic role of sigma in the overall transcription process (Travers and Burgess, 1969). However, since core polymerase can initiate transcription non-specifically at single strand breaks in a DNA template (Vogt, 1969; Ishihama *et al.*, 1971; Hinkle *et al.*, 1972), it is desirable to begin investigations of selective transcription *in vitro* with a preparation of sigma-saturated holoenzyme (for a review on purification schemes, see Burgess, 1976; and Results section I of this thesis).

2. Promoter structure.

One of the first events to occur during transcription initiation is the specific interaction between a promoter region and free RNA polymerase holoenzyme. The product of this bimolecular collision is referred to as the 'closed' complex (for reviews see von Hippel *et al.*, 1984; McClure, 1985; Travers, 1987; Gralla, 1990). While there are many aspects of closed complex formation which are still only partially understood, there are some general features of promoter structure which are believed to facilitate the initial polymerase/promoter collision, thereby

distinguishing the specific promoter sequence from surrounding non-specific regions of DNA. Some of these structural features are discussed below.

In addition to electrostatic interactions (Record *et al.*, 1978; Shaner *et al.*, 1983; Lohman, 1986; Record and Mossing, 1987), polymerase binding at a promoter is thought to be stabilized by hydrogen-bonds formed between the RNA polymerase and specific base-pairs in the major groove of the DNA helix (Seeman *et al.*, 1976; Woodbury *et al.*, 1980). The asymmetry of these interactions has been proposed to confer the directionality of transcription initiation (von Hippel *et al.*, 1984). In general, promoter architecture has two main features. First, there are two sets of highly conserved sequences located around the - 10 and - 35 positions of the promoter. Based on both statistical and mutant analyses (Siebenlist *et al.*, 1980; Hawley and McClure, 1983; Harley and Reynolds, 1987), it has been possible to designate an optimum 'consensus' sequence for both these regions for an *E. coli* σ^{70} promoter. The - 10 and - 35 elements are essential for interaction between the promoter and the RNA polymerase, and there is a strong correlation between the degree to which the promoter sequence matches the consensus, and the relative *in vitro* promoter strength (Stefano and Gralla, 1982a; Mulligan *et al.*, 1984). Second, there are spacing considerations between the - 10 and - 35 elements (Stefano and Gralla, 1982b; Auble *et al.*, 1986; Auble and deHaseth, 1988). In a recent compilation of 263 promoter sequences, Harley and Reynolds (1987) determined that 92% of all promoters had a separation distance between the - 10 and - 35 hexamers of 17 ± 1 base pairs. The importance of this spacing is realized when one considers that the recognition elements of a promoter are on the surface of a cylinder (i.e. the DNA helix), such that the addition or removal of a single base pair between two recognition sites will cause their relative alignment to be shifted by approximately 34° (this assumes that B-DNA in solution has an average of 10.5 bp per helical turn; Wang, 1979). While there is no real consensus sequence for the spacer region of a promoter in *E. coli*, it has been noted that in cases where the - 10 and - 35 spacing is

suboptimal, there are non-random tracts of either Puo-Puo and Pyd-Pyd dinucleotides, or Puo-Pyd and Pyd-Puo dinucleotides in the upstream sequence of the spacer region (Beutel and Record, 1990). It has been proposed that the aberrant helical twist associated with such dinucleotide sets might partially compensate the suboptimal spacing found at these promoters (Beutel and Record, 1990).

3. Transcription initiation.

After the formation of a closed complex between RNA polymerase and a promoter region, several conformational and catalytic transitions occur which ultimately commit the polymerase to transcription. These transitions begin with the sequential isomerizations of the closed complex into an open complex, in which the promoter DNA surrounding the transcription initiation site becomes denatured (Siebenlist, 1979; Siebenlist *et al.*, 1980). Originally, the conversion of the closed to open complex was proposed to occur by a single-step isomerization (Walter *et al.*, 1967; Chamberlin, 1974). However, for many promoters (see below), this simple model has proved to be inadequate, and it seems apparent that at least one intermediate complex is created prior to the formation of the open complex. An overall reaction mechanism for open complex formation is summarized below in equation (1). The interaction between free RNA polymerase (R) and a promoter (P) leads to the formation of a closed (C) complex, which subsequently isomerizes to form an intermediate (I) and then open (O) complex.

$$R + P \rightleftharpoons C \rightleftharpoons I \rightleftharpoons O \qquad (1)$$

The proposal for an intermediate complex has been largely based on the kinetic behavior of polymerase/promoter interactions. Comparative studies of mutant promoters (Hawley and McClure, 1982), and the thermodynamic response of an individual promoter to changes in salt concentration (Roe *et al.*, 1984) or temperature (Kadesch *et al.*, 1982; Rosenberg *et al.*, 1982; Buc and McClure, 1985; Roe

et al., 1984, 1985; Duval-Valentin and Ehrlich, 1987), showed that the rates of polymerase/promoter interactions were inconsistent with a direct closed-to-open conversion mechanism (Walter *et al.*, 1967; Chamberlin, 1974). Physical evidence for an intermediate complex also exists. DNA protection studies suggested that the temperature response of a polymerase/promoter 'footprint' underwent several shifts in both the extent of protection and the degree of single-stranded DNA formation (Spassky *et al.*, 1985; Duval-Valentin and Ehrlich, 1987; Cowing *et al.*, 1989; Schickor *et al.*, 1990). Similarly, gel retardation analyses of polymerase/promoter complexes at the *lac* UV5 promoter have demonstrated the formation of two different 'open' complexes (Straney and Crothers, 1985). The DNA melting profiles of these two complexes were consistent with a mechanism in which RNA polymerase induced a nucleation event at the promoter DNA (resulting in partial denaturation), followed by a temperature-dependent unwinding of the transcription initiation region (Straney and Crothers, 1987c).

The studies referred to above have indicated that the conversion of the closed to intermediate complex is an endothermic event, suggesting that this isomerization must be driven thermodynamically by entropy. A common source of mixing entropy during protein/DNA interactions is the release of cations from the specific DNA binding site (Record *et al.*, 1978; Shaner *et al.*, 1983; Lohman, 1986; Record and Mossing, 1987). In solution, DNA behaves as if 88% of its charge is shielded by counterions (Record *et al.*, 1978). Therefore, increased protection of the phosphate backbone by RNA polymerase would result in cation displacement and a favorable increase in entropy. The degree to which this entropy contributes towards polymerase/promoter complex stability should decrease as the salt concentration of the external solution increases. However, Roe *et al.* (1984) determined that the conversion of the closed to intermediate complex was largely salt insensitive at the λP_R promoter, implying that cation release did not contribute to the entropy of the process. Instead, they found that the difference in heat capacity (ΔC_p) between the

intermediate and closed complex was negative (Roe *et al.*, 1985). The negative ΔC_p associated with the closed to intermediate complex transition led these researchers to propose that RNA polymerase underwent a conformational change at this step which involved a burial of hydrophobic surfaces (Roe *et al.*, 1985). The release of 'caged' water molecules which accompanies such a conformational change was expected to provide the favorable increase in entropy required to drive the closed to intermediate complex formation process forward (Roe *et al.*, 1985; Record and Mossing, 1987; Ha *et al.*, 1989).

The predicted conformational change in the polymerase is consistent with evidence that demonstrates the requirement of 'stressed' DNA in order to form an open complex (Stefano and Gralla, 1982b; Auble *et al.*, 1986; Auble and deHaseth, 1988; Ayers *et al.*, 1989). One model (Stefano and Gralla, 1982b) involves polymerase/promoter contacts which are constrained at two offset points. In order to optimize polymerase interaction with these points, it would be necessary to bring these contacts into alignment by untwisting the intervening DNA helix. Mechanisms such as polymerase conformational changes or supercoiling effects (Borowiec and Gralla, 1987; Aoyama and Takanami, 1988) could facilitate the untwisting. Note that this untwisting mechanism is compatible with other conformational changes which have been suggested to involve RNA polymerase, such as DNA bending (Kuhnke, *et al.*, 1987; Heumann, *et al.*, 1988) and the formation of a polymerase 'channel' (Darst *et al.*, 1989; Schickor *et al.*, 1990). It was proposed that ultimately, the torsional stress of the DNA could be relieved by the formation of the open complex (Stefano and Gralla, 1982b). The formation of the open complex involves the localized 'melting' of DNA base-pairs (Saucier and Wang, 1972; Wang *et al.*, 1977; Melnikova *et al.*, 1978) surrounding the transcription initiation region of the promoter (Siebenlist, 1979; Siebenlist *et al.*, 1980). The extent of this denatured region depends on the promoter in question, and estimates between 10 bp (Hsieh and Wang, 1978) and 17 bp (Gamper and Hearst, 1982) have

been reported. In the absence of RNA polymerase, the enthalpy for DNA melting has been calculated between 6 to 10 (Roe *et al.*, 1984) kcal/mol base pair. Therefore, the formation of a 10 - 17 bp open complex at a specific promoter should be endothermic, with a theoretical enthalpy of 60 - 170 kcal/mol. Note that in the presence of RNA polymerase, this value may be lowered because of the nucleation of DNA associated with the intermediate complex. Indeed, when calculated in the presence of RNA polymerase, the enthalpy of open complex formation has been observed to range from 41 kcal/mol (Buc and McClure, 1985; Spassky *et al.*, 1985) to 73 kcal/mol (Cowing *et al.*, 1989), and is at the lower end of the theoretical spectrum.

In addition to being temperature dependent, the conversion from intermediate to open complex is affected by the salt concentration, such that the predicted levels of open complex decrease as the salt concentration increases (Strauss *et al.*, 1980; Roe *et al.*, 1984). It has been argued that this negative salt dependence reflects a decrease in the charge density of the DNA during the conversion from intermediate to open complex, such that there is a net release of cations from the phosphate backbone (for reviews see Shaner *et al.*, 1983; Lohman, 1986; Record and Mossing, 1987). Virtually all of this decreased charge density can be accounted for experimentally by the single-stranded DNA that is formed while denaturing the promoter transcription initiation region (Record *et al.*, 1978; Strauss *et al.*, 1980; Roe *et al.*, 1984). However, alternative sources of counterion release are possible, including the protection of additional phosphate groups by the RNA polymerase, or the release of anions from the DNA binding site of the RNA polymerase itself (Shaner *et al.*, 1983; Record and Mossing, 1987).

Following open complex formation, the polymerase/promoter complex can initiate the synthesis of the RNA transcript. However, the formation of a ternary complex does not guarantee a commitment to transcript elongation. It has been observed that *in vitro*, the commitment of a promoter-bound RNA polymerase to transcript elongation does not occur until after the synthesis of 8 - 14 nucleotides,

when the complex has released its upstream promoter contacts by ejection of the σ subunit (Hansen and McClure, 1980; Carpousis and Gralla, 1985; Straney and Crothers, 1985, 1987a; Stackhouse *et al.*, 1989; Krummel and Chamberlin, 1989). Until the expulsion of σ however, the initial short transcript can be released from the ternary complex without dissociation of the RNA polymerase from the promoter (Carpousis and Gralla, 1980). Many rounds of this 'abortive' transcription initiation can occur before the ternary complex successfully commits to elongation (McClure and Cech, 1978; Carpousis and Gralla, 1980; Munson and Reznikoff, 1981), however the yield of a particular abortive oligonucleotide transcript is decreased as the length of that transcript is increased (Carpousis and Gralla, 1980). As an extension of this last point, it has been proposed that the decision of whether to abort or commit to transcription is influenced by opposing upstream and downstream promoter contacts within the ternary complex (McClure *et al.*, 1978; Carpousis and Gralla, 1985; Straney and Crothers, 1987a, 1987c). While upstream promoter interactions are expected to be influenced by polymerase-σ-DNA contacts, the downstream interactions would be influenced by polymerase-RNA-DNA contacts. This view is supported by the results of both *in vivo* (Kammerer *et al.*, 1986) and *in vitro* (Straney and Crothers, 1987a) experiments, where changes to the transcribed region of a promoter influenced the overall promoter activity.

4. Transcription assays.

A variety of methods have been developed to investigate the kinetics of transcription initiation at a promoter. However, many of these assays rely upon the formation of an RNA transcript in order to measure the degree of promoter occupancy by the RNA polymerase (see for example Chamberlin, 1974; McClure, 1985). Due to the requirement of RNA synthesis, the investigation by these assays of early steps in the transcription initiation process is indirect, and often involves untested assumptions regarding the catalytic activity of the RNA polymerase

(McClure, 1985; Straney and Crothers, 1987b). In order to directly measure the rate of open complex formation at a specific promoter, it must be possible to directly measure the interaction of an RNA polymerase molecule with a specific promoter.

Two methods which permit a direct analysis of polymerase/promoter complexes are the filter-binding assays (Hinkle and Chamberlin, 1972; Roe *et al.*, 1984, 1985) and gel-retardation assays (Garner and Revzin, 1981; Fried and Crothers, 1981; Straney and Crothers, 1987b). The filter-binding assay relies on the observation that RNA polymerase (and hence a polymerase/DNA complex) is quantitatively retained on nitrocellulose filters, whereas free DNA is not (Hinkle and Chamberlin, 1972). The gel-retardation assay relies on the observation that polymerase/DNA complexes have a lower electrophoretic mobility on polyacrylamide gels than does free DNA (Straney and Crothers, 1987b). However, since polyacrylamide gel-electrophoresis can resolve small differences in mobility between different migrating species, the retardation assay has the potential to detect conformational isomers of a bound complex that would otherwise go unnoticed by the filter-binding assay (Straney and Crothers, 1985). Because of this potential advantage, I chose to use a gel-retardation assay to investigate the interactions between *E. coli* RNA polymerase and the various rRNA promoters which were studied during the course of this thesis.

VI. Summary and objectives.

The studies described above would suggest that it is the core promoter region, and consequently the process of transcription initiation, that acts as a target for regulating the growth rate dependent expression of an rRNA promoter. Analyses of rRNA expression *in vivo* demonstrated that a feedback inhibition mechanism was involved in the process of growth rate regulation. A longstanding candidate for the effector of this negative feedback system has been ppGpp, and there have been

strong correlations both *in vivo* and *in vitro* between ppGpp and the specific inhibition of expression from rRNA promoters. However, a recent report suggested that ppGpp was not required for growth rate regulation *in vivo*, and it remains to be seen whether ppGpp is perhaps one of several redundant control mechanisms which regulate rRNA expression, or if ppGpp is irrelevant to the process of transcription initiation at a growth rate dependent promoter.

To help understand the phenomenon of growth rate dependent expression, it would be beneficial to obtain a comparative account of the transcription initiation process which occurs at both growth rate regulated, and non-growth rate regulated, rRNA promoters. From such analyses, it could be possible to determine whether ppGpp can serve as a differential inhibitor of transcription initiation, and if so, establish the mechanism by which this putative effector might act. To this end, I wish to investigate the kinetics of complex formation between *E. coli* RNA polymerase and the *rrnB* P1 and P2 promoters from *B. subtilis*. While there are many differences between the growth rate regulated *rrnB* promoters of *E. coli* and *B. subtilis* in terms of overall sequence homology and spacing alterations, the *B. subtilis rrnB* P2 promoter is nonetheless able to utilize the *E. coli* transcriptional machinery *in vivo*, and its expression is regulated in a growth rate dependent manner. By regarding the *B. subtilis rrnB* P2 promoter as a mutant of *E. coli*, and using it as a model for transcription initiation, I wish to characterize the common features of rRNA promoters which make them subject to growth rate regulation.

Materials and Methods

I. Purification of RNA polymerase.

Initial steps in the purification of RNA polymerase, up to and including the Bio-Gel A-1.5m column, closely followed the methods of Spiegelman and Whiteley

(1974). A brief review of these steps is provided here. Approximately 20 g of frozen packed *E. coli* K12 (purchased from Iowa Grain Processing Corporation; 1/2 log, grown in rich media), were suspended in 28 ml of a Buffer A (10 mM Tris-HCl, pH 8.0, 1 mM EDTA, 10 mM $MgCl_2$, 50 μg/ml phenylmethylsulfonylfluoride), and supplemented with 4 ml of 2 M Tris-HCl (pH 8.0) and 200 mg of lysozyme Sigma Chemical Co.). Following digestion, the preparation was sonicated (20 ml batches for three 1 min periods, using the intermediate probe of the Branson Sonifier Model 350 at level 6) and cellular debris was eliminated by centrifugation. Note that these and all subsequent steps were performed at 0 - 7 °C, and that each step of the purification was started immediately upon completion of the preceding one. The RNA polymerase from the crude supernatant was extracted by the polyethylene glycol/dextran phase separation method of Babinet (1967). The final eluate from this separation protocol was precipitated with ammonium sulfate (Schwarz/Mann Biotech ultrapure), resuspended in 6 - 8 ml of Buffer B (Buffer A containing 10% glycerol (BDH Inc., AnalR®), 0.5 M NaCl, 20 mM β-mercaptoethanol), and applied to a Bio-Gel A-1.5m column (2.5 cm x 100 cm). The applied sample was eluted with ≥ 500 ml of Buffer B, at a flow rate of about 30 ml/h. Fractions of 5.5 ml were collected, and the absorbance at 280 nm was measured (all spectrophotometric analyses were performed in a 1 cm path-length cuvette using a Bausch and Lomb Spectronic® 601 spectrophotometer) along with RNA polymerase activity on ϕ29 DNA (Fig. 1A).

Those fractions containing the highest activity were combined, and the volume of this material was reduced to approximately 10 ml in an Amicon Diaflo 202 ultrafiltration cell (62 mm PM-10 membrane, ≤ 42 psi nitrogen). Buffer C (Buffer A containing 7.5% glycerol, 0.3 mM dithiothreitol) was added to this concentrated fraction until the conductivity of the flow-through from the Amicon apparatus was equal to that of Buffer C + 0.1 M KCl (approximately 5.5 milliohms as determined with a Radiometer type CDM2 conductivity meter at 0 °C). The volume of this

diluted sample was reduced in the Amicon cell as described above to a volume of approximately 10 ml, and was then loaded onto a 20 ml (2 x 7 cm) column of heparin-Sepharose. Heparin (Sigma Chemical Co., grade I at 181 USP unit/mg) was covalently bound to CNBr-activated Sepharose CL-4B (Pharmacia) according to the method of Davison *et al.* (1979), and the column had been equilibrated with 100 ml of Buffer C + 0.1 M KCl prior to sample application. Flow rates during sample addition and subsequent steps were maintained at 70 ml/h using a Pharmacia P1 peristaltic pump, and fractions of 5.5 ml were collected. When the sample had been loaded, the heparin-Sepharose column was washed with 100 ml of Buffer C + 0.1 M KCl, until the absorbance of the fractions at 280 nm had fallen below 0.01 units. A 300 ml linear gradient of 0.1 - 1.0 M KCl in Buffer C was then used to elute the column, and fractions were assayed for RNA polymerase activity on ϕ29 DNA, absorbance at 280 nm, and conductivity as described above (Fig. 1B). Eluted fractions containing the highest activity were combined and concentrated to a volume of approximately 6 ml in the Amicon cell as described above. This material was dialyzed (Spectra/Por 4 membrane, boiled for 10 min in 1 mM EDTA) overnight against 200 ml of Buffer D (10 mM HEPES (pH 8.0), 0.1 mM EDTA, 10 mM $MgCl_2$, 125 mM KCl, 1 mM dithiothreitol, 50% glycerol (BDH Inc., AnalR®)). Sample volumes were typically reduced 2 - 3 fold by this treatment, and the final concentrated material was stored at - 20 °C. Note that for RNA polymerase Batch #176 (Table II and III; Fig. 2A), dialysis was performed in the 50% glycerol buffer of Gonzalez *et al.* (1977), and the RNA polymerase was further purified over a phosphocellulose column (Gonzalez *et al.* , 1977).

II. RNA polymerase assays.

Reaction mixtures for monitoring RNA polymerase activity throughout the purification contained: 40 mM Tris-HCl (pH 8.0), 1 mM EDTA, 20 mM $MgCl_2$, 50

mM NaCl, 0.8 mM each of ATP, GTP, CTP, 80 μM UTP, 0.125 μCi [5,6 ^{3}H]-UTP (ICN Biomedicals Inc., 35 Ci/mmol (stock) or 6.9 x 10^3 dpm/nmol (assay)), 7 μg ϕ29 DNA (isolation described in Schachtele *et al.*, 1970), and RNA polymerase (5 - 20 μl samples) in a total volume of 0.5 ml. Assays were incubated at 37° C for 10 min and the samples precipitated with 1.0 ml of ice-cold 10% trichloroacetic acid. The precipitated material was collected on glass-fibre filters, dried, and the radioactivity was determined in a Beckman LS7500 liquid scintillation counter. For the determination of specific activities, fractions were assayed in triplicate over a fourfold range of sample volume input, and reported values represent an average of these results (Table II).

Protein concentrations were determined by a modification of the Lowry assay (Sandermann and Strominger, 1972), using bovine serum albumin (BSA from Sigma Chemical Co.) as a standard, and the appropriate buffer as a blank. The concentration of the BSA standard was initially calibrated at A_{278} using its extinction coefficient of $E_{278\ nm}$ (1%) = 6.6 (Burgess, 1976). Mangel and Chamberlin (1974) have noted that one mg of RNA polymerase measured relative to BSA protein is equivalent to an actual weight of 0.79 mg of RNA polymerase amino acids. Consequently, the reported molar concentrations of RNA polymerase protein were corrected by this factor (Table III).

III. Gel electrophoresis and the detection of proteins or DNA.

1. SDS-polyacrylamide gels.

Purity of the final RNA polymerase was determined on a 14 - 20% exponential gradient SDS-polyacrylamide (stock concentration 30% acrylamide, 0.174% N, N'-methylene-bis-acrylamide) gel as described by Dobinson and Spiegelman (1987). Gels were stained with 0.05% Coomassie Brilliant Blue R (Sigma Chemical Co.) in a solution of 10% acetic acid, 25% ethanol by heating to

approximately 50 °C, and allowing to cool to room temperature over approximately 15 min. This heating and cooling cycle was repeated once, and the gel was destained with 7.5% acetic acid, 25% ethanol. The gel was dehydrated for 2 h with 3% glycerol (w/v), 40% methanol, 10% acetic acid, and dried between sheets of cellophane membrane backing (Bio-Rad) in a Bio-Rad Model 483 slab dryer (80 °C, 2 - 3 h).

2. Agarose gel electrophoresis.

Intact plasmid and DNA fragments were analyzed on 0.7% agarose (Bio-Rad) 'mini-gels' (Sambrook *et al.*, 1989) which were made in TBE buffer (89 mM Trizma Base, 89 mM boric acid, 2 mM EDTA), and contained 1 μg/ml ethidium bromide. Gels were cast on 5 x 7 cm glass slides, loaded with DNA mixed in 0.1 x volume loading dye (2 x TBE, 50% glycerol, 0.25% bromophenol blue, 0.25% xylene cyanole FF), and electrophoresed at 60 mA in TBE. DNA was visualized by placing the gel on a UV transilluminator (Ultra-Violet Products Inc.). When required, gels were photographed with transmitted UV light using a Kodak MP-4 camera equipped with a Vivitar VMC orange filter and Polaroid Type 667 film.

3. Polyacrylamide gel electrophoresis.

A stock solution of 45% acrylamide (43.5% acrylamide, 1.5% N, N'-methylene bisacrylamide in H_2O) was used to prepare polyacrylamide gels in TBE buffer, 0.05% ammonium persulfate. The mixtures were polymerized by the addition of TEMED (N, N, N', N'-tetramethylenediamine) to a final concentration of 0.1% (v/v), and cast in 1.5 mm thick gels. DNA was loaded as described in section III.2, and the gels were electrophoresed at 17 volts/cm in TBE.

Denaturing gels were made as described above, using 0.5 x TBE buffer, and contained 7 M urea. DNA samples were mixed with 0.25 x volume of loading buffer (10 M urea, 2 x TBE, 0.05% bromophenol blue, 0.05% xylene cyanole FF), and denatured by heating at 80 °C for 2 min prior to gel application. Analytical gels were

0.75 mm thick, and electrophoresed at 30 - 40 volts/cm in 0.5 x TBE. Sequencing gels were 0.4 mm thick, and electrophoresed at 42 volts/cm in 0.5 x TBE.

Radioactive DNA fragments were detected by autoradiography (Sambrook *et al.*, 1989) using Kodak X-Omat™ RP X-ray film. Exposure times varied depending on the amount of label present in the DNA fragments, and when extra sensitivity was required, an intensifying screen (Dupont Cronex® Lightning-Plus) was placed on top of the X-ray film. Native acrylamide gels were exposed at 4 °C, whereas denaturing gels were exposed at - 70 °C. DNA sequencing gels were dried onto Whatman 3 MM filter paper using a Bio-Rad Model 483 slab dryer prior to autoradiography. Following exposure, X-ray film was developed in Kodak M35A X-Omat film processor. Non-radioactive DNA fragments were detected by fluorescence of ethidium bromide stained gels (Sambrook *et al.*, 1989), and visualized as described in section III.2.

IV. Quantitation of RNA polymerase subunits on gels.

The SDS-polyacrylamide gels stained with Coomassie Blue were scanned at 525 nm using a Helena Instruments Quick Scan R & D densitometer, and the areas under the peaks corresponding to the RNA polymerase subunits were calculated using a Quick Quant III integrator (Helena Instruments). It was noted that the peak areas of each subunit increased as a linear function of protein concentration (measured as BSA equivalents) as the amount of holoenzyme loaded onto the gel was increased from 3.2 to 12.8 μg (data not shown). This suggested that the absorbance of the dye was proportional to the mass of each protein band over the concentration range investigated (Burgess, 1976). The relative molar amount of each subunit was calculated using the molecular weights of Burgess *et al.* (1987): β (150,615), β' (155,159), α (36,511), σ^{70} (70,262).

V. Growth and maintenance of bacterial strains.

The *E. coli* bacterial strains used in this thesis have been previously described, and their relevant genotypes are listed in Table I. *E. coli* strains HB101 and DH5α were employed as hosts for the various plasmids used in these studies. All strains were grown in 2 x YT medium (Sambrook *et al.*, 1989), except for those cultures which were used for large-scale plasmid isolations, or analysis of growth rate dependent regulation (see sections VI and XV respectively). Plate cultures were grown on 1 x YT medium containing 15 g agar/l (Sambrook *et al.*, 1989). All strains were cultured at 37 °C. For the long-term maintenance of bacterial strains, 1.0 ml of culture (mid-log to stationary phase cells) was added to 1.0 ml 40% glycerol, and the resultant 20% glycerol stock was stored at - 70 °C. The antibiotics ampicillin and/or chloramphenicol (Sigma Chemical Co.) were used in both liquid and plate media at concentrations of 50 μg/ml to select resistant *E. coli* strains. Bacteriological supplies used for media preparation were obtained from Difco. Reagents used to prepare stock salt solutions for minimal media and other buffers were supplied by BDH Inc. and Sigma Chemical Co..

VI. Isolation of plasmid DNA.

For the rapid analysis of recombinant clones, the cells from 2.0 ml of an overnight culture were processed according to the small-scale alkaline-lysis method of Sambrook *et al.* (1989). Final DNA pellets were resuspended in 50 μl of TE buffer (pH 8.0; Sambrook *et al.*, 1989), and 10 - 20 μl of this solution (approximately 1 - 2 μg of plasmid DNA) was treated with the desired restriction enzyme(s) under the appropriate reaction conditions (section VIII.1).

For the purpose of DNA sequence analyses (section IX.5) or polymerase chain reactions (section XII), plasmid DNAs from 800 ml of culture were isolated by

Triton-X100 lysis followed by isopycnic centrifugation in a CsCl (Schwarz/Mann Biotech optical grade) gradient (Sambrook *et al.*, 1989). Briefly, a single isolated colony of the clone of interest was used to inoculate 2.0 ml of 2 x YT medium containing the appropriate antibiotic(s), and grown at 37 °C with vigorous shaking. When this culture had reached mid-log growth, 1.0 ml was transferred to 800 ml of pre-warmed M9 salts medium (Sambrook *et al.*, 1989), supplemented with 0.2% glucose, 0.1% casamino acids, 0.005% thiamine and the appropriate antibiotic(s). Growth was continued at 37 °C (200 rpm) for approximately 15 h, and cells were harvested and processed as described above. Ethidium bromide was extracted with water-saturated n-butanol, and plasmid DNA was precipitated from the CsCl solution with ethanol as described by Sambrook *et al.* (1989). The final DNA pellet was resuspended in approximately 200 µl of TE buffer (pH 8.0; Sambrook *et al.*, 1989), and stored at - 20 °C. The concentration and purity of the plasmid DNA was determined by measuring the absorbance of the DNA solution at both 260 nm and 280 nm (Sambrook *et al.*, 1989), and the integrity of the plasmid was confirmed by restriction enzyme analysis (section VIII.1).

VII. Purification and quantitation of DNA fragments following gel electrophoresis.

Following gel electrophoresis (section III), DNA fragments were recovered from agarose 'mini-gels' by trough-elution (Maniatis *et al.*, 1982), or from polyacrylamide gels by electroelution into a dialysis membrane bag (Spectra/Por 4 membrane, boiled for 10 min in 1 mM EDTA) (Sambrook *et al.*, 1989). In all cases, TBE was used as the elution buffer. The eluate containing the desired DNA fragment was extracted successively with phenol/chloroform, chloroform, and then precipitated with sodium acetate/ethanol as described in Sambrook *et al.* (1989). Final DNA pellets were resuspended in either 10 - 50 µl of TE (pH 8.0; Sambrook *et*

al. , 1989) for restriction fragments, or 200 µl 10 mM HEPES (pH 8.0) for polymerase chain reaction products, and stored at - 20 °C.

VIII. Cloning procedures.

The recombinant DNA techniques used in this thesis were essentially performed as described by Sambrook *et al.* (1989). Minor variations and/or additional comments will be noted here.

1. Digestion of DNA with restriction endonucleases.

Restriction endonuclease digestion of DNA was performed under the reaction conditions recommended by the suppliers (Bethesda Research Laboratories, New England Biolabs, and Pharmacia). Typically, 2 - 5 units of restriction enzyme per µg of DNA were added to a reaction, and incubated for 2 h at the appropriate temperature. When the source of DNA was from a small-scale alkaline-lysis preparation (section VI), DNase-free RNase (Sigma Chemical Co.) was included in the restriction enzyme digest at a final concentration of 25 µg/ml.

2. Ligation of DNA fragments and transformation of competent cells.

The ligation of DNA restriction fragments was performed in a total reaction volume of 20 µl under the conditions recommended by the suppliers of T4 DNA ligase (Bethesda Research Laboratories). The vector to insert molar ratio was 2 - 3, and the total amount of DNA per reaction was 0.1 µg. Ligations were incubated for 4 h at 25 °C for 'sticky' and 'blunt' ended DNA fragments, or 15 - 18 h at 15 °C for the addition of non-phosphorylated 'linkers' to the ends of DNA restriction fragments (Barnes, 1987).

Competent strains of *E. coli* were either created by the $CaCl_2$ method (Sambrook *et al.*, 1989), or purchased from Bethesda Research Laboratories. The

transformation of competent cells by recombinant plasmid DNA was performed as described by Sambrook *et al.*, 1989. In cases where non-phosphorylated linkers had been ligated to the ends of linearized plasmid DNA, the simplified 'linker-tailing' method of Barnes (1987) was used. Briefly, the ligation products were heated to 70 °C for 10 min and then rapidly cooled on ice. Dilutions of this reaction mixture were used directly to transform competent cells (Sambrook *et al.*, 1989).

IX. Construction and sequencing of recombinant plasmids containing promoter-bearing DNA inserts.

The plasmids used in this thesis are summarized in Table I. The *rrnB* P1 and P2 promoter fragments from *B. subtilis* and *E. coli* had been previously isolated (Deneer, 1986; Deneer and Spiegelman, 1987), however in some cases, the promoter bearing DNA fragments were considered to be too large for the purpose of gel retardation analysis. In other cases, the promoter fragment of interest was 'contaminated' by a residual - 35 or - 10 element from the complementary promoter of the original P1-P2 pair (Deneer, 1986; Deneer and Spiegelman, 1987). To avoid the possibility of RNA polymerase binding to a 'pseudo-promoter' region during gel retardation analysis, it was decided to further sub-clone the individual promoters as described below. In all cases, the promoter fragments were sub-cloned into the expression vector pKK232-8 (Brosius, 1984). This plasmid contains a promoterless gene for chloramphenicol acetyltransferase (CAT) which is located downstream of the M13mp8 polylinker (Brosius, 1984). Recombinant plasmids which have a promoter bearing fragment cloned in the correct orientation within this polylinker will confer a chloramphenicol resistant phenotype to a cell.

Table I. Bacterial strains, plasmids and phage.

E. coli bacterial strain	Relevant genotype	Source and/or reference
K12	wild type	Iowa Grain Processing Corporation
HB101	*hsdS20* (r_b- m_b-), *recA13*	Sambrook *et al.*, 1989
DH5α	*hsdR17* (r_k- m_k+), *recA1*	Bethesda Research Laboratories; Sambrook *et al.*, 1989

Plasmids and phage	Properties	Source and/or reference
pBR322	Ap^r, Tc^r	Maniatis *et al.*, 1982
pKK232-8	Ap^r, Cm^s	H. Deneer; Brosius, 1984
pKK282B	Ap^r, Cm^r; pKK232-8::*rrnB* P1 from *B. subtilis*	H. Deneer; Deneer and Spiegelman, 1987
pKK220B	Ap^r, Cm^r; pKK232-8::*rrnB* P2 from *B. subtilis*	as above
pKK351Ec	Ap^r, Cm^r; pKK232-8::*rrnB* P1 from *E. coli*	as above
pKK292Ec	Ap^r, Cm^r; pKK232-8::*rrnB* P1/P2 from *E. coli*	H. Deneer; Deneer, 1986
pKK220'	subclone of pKK220B	This thesis
pKK115B	subclone of pKK282B; *B. subtilis rrnB* P1 (- 87 to + 28)	as above
pKK183B	subclone of pKK220'; *B. subtilis rrnB* P2 (- 69 to + 114)	as above
pKK96E	subclone of pKK351Ec; *E. coli rrnB* P1 (- 64 to + 32)	as above
pKK131E	subclone of pKK292Ec; *E. coli rrnB* P2 (- 60 to + 71)	as above
ϕ29	*B. subtilis* phage	Schachtele *et al.*, 1970

1. Subcloning the *rrnB* P1 promoter from *B. subtilis* (BP1).

Plasmid pKK282B contained a 282 bp fragment from the *rrnB* P1 region of *B. subtilis* (Deneer, 1986; Deneer and Spiegelman, 1987) cloned into the *Sma* I site of the promoter-fusion expression vector pKK232-8 (Brosius, 1984). To facilitate detection and quantitation of the promoter bearing fragment during the sub-cloning procedure, pKK282B was first digested with *Hind* III, and the ends filled-in with the Klenow fragment of *E. coli* DNA polymerase I (Bethesda Research Laboratories) in a reaction mixture which contained 20 μCi [α-^{32}P] dATP (Sambrook, *et al.*, 1989). The plasmid pKK282B was then cut with *Eco* R1, and the promoter fragment was purified on a 5% polyacrylamide gel. The isolated promoter fragment was digested with *Mnl* I, gel-purified as described above, and following digestion with *Mae* I, the DNA restriction termini were filled-in with a Klenow reaction. These DNA restriction fragments were used directly in a ligation reaction with the *Sma* I-cut pKK232-8 vector. Portions of the ligation reaction were used to transform competent DH5α cells, and recombinant plasmids bearing promoter fragments were selected on 1 x YT plates containing chloramphenicol. The final construct was pKK115B, which contained sequences - 87 to + 28 relative to the transcription initiation site of the *B. subtilis rrnB* P1 promoter.

2. Subcloning the *rrnB* P2 promoter from *B. subtilis* (BP2).

Plasmid pKK220B contained a 220 bp fragment from the *rrnB* P2 region of *B. subtilis* (Deneer, 1986; Deneer and Spiegelman, 1987) cloned into the *Sma* I site of the promoter-fusion expression vector pKK232-8 (Brosius, 1984). However, I wished to eliminate the residual - 10 element which was still present from the upstream P1 promoter. The P2 promoter was released from pKK220B as an *Eco* RI/*Bam* HI fragment, gel purified, and treated with mung bean nuclease (Pharmacia) to create flush ends (Sambrook *et al.*, 1989). This fragment was ligated to pKK232-8, which had been cut with *Bam* HI and subsequently filled in by a Klenow reaction

(Sambrook *et al.*, 1989), to create pKK220'. Note that as a result of this ligation, the *Bam* HI site at the 3' end of the promoter fragment was restored. The plasmid pKK220' was linearized at a site upstream of the P2 promoter fragment by digestion with *Sma* I. From *Sma* I, a series of deletions were created in the 5' flanking region of the P2 promoter fragment by using *Bal* 31 exonuclease (Bethesda Research Laboratories) as described by Sambrook *et al.* (1989). Non-phosphorylated *Bam* HI linkers (New England Biolabs) were ligated to the ends of the deletion products by a linker-tailing reaction (Barnes, 1987), and competent HB101 were transformed as described in section VIII.2. Deletions which maintained promoter activity were selected by plating the transformants on 1 x YT media containing chloramphenicol. Deletion endpoints were roughly estimated by comparing the electrophoretic mobilities of the released *Bam* HI fragments from the deletion mutants and pKK220' to the mobilities of a series of DNA fragment molecular weight markers (pBR322 plasmid DNA cut with *Hinf* I). Based on these preliminary sizing experiments, the gel-purified *Bam* HI promoter fragments from several deletion mutants were independently ligated to *Bam* HI-cut pKK232-8. Portions of the ligation reaction were used to transform competent HB101 cells, and recombinant plasmids bearing deleted promoter fragments were selected on 1 x YT plates containing chloramphenicol. The promoter inserts of these deletion mutants were sequenced to determine which isolates had eliminated the residual - 10 element of the P1 promoter. The chosen construct was pKK183B, which contained sequences - 69 to + 114 relative to the transcription initiation site of the *B. subtilis rrnB* P2 promoter. Sequencing revealed the insertion of an extra A-residue between nucleotide position - 67 and - 68 compared to the published wild-type sequence (Stewart and Bott, 1983), but this insertion did not alter the growth rate dependent expression of this promoter *in vivo* (section XV).

3. Subcloning the *rrnB* P1 promoter from *E. coli* (EP1).

Plasmid pKK351Ec contained a 351 bp fragment from the *rrnB* P1 region of *E. coli* (Deneer, 1986; Deneer and Spiegelman, 1987) cloned into the *Sma* I site of the promoter-fusion expression vector pKK232-8 (Brosius, 1984). Initial sub-cloning steps were identical to those described above for the *rrnB* P1 promoter of *B. subtilis* (section IX.1). The isolated *Eco* RI/*Hind* III promoter fragment was cut with *Bst* U1, gel-purified, and following digestion with *Nci* I, the DNA restriction termini were filled-in with a Klenow reaction. Ligation reactions with *Sma* I-cut pKK232-8, transformation of competent DH5α cells, and selection of transformants on chloramphenicol plates were performed as described in section IX.1. The final construct was pKK96E, which contained sequences - 64 to + 32 relative to the transcription initiation site of the *E. coli rrnB* P1 promoter.

4. Subcloning the *rrnB* P2 promoter from *E. coli* (EP2).

Plasmid pKK292Ec contained a 292 bp fragment from the *rrnB* P1-P2 region of *E. coli* (Deneer, 1986) cloned into the *Sma* I site of the promoter-fusion expression vector pKK232-8 (Brosius, 1984). Initial sub-cloning steps were identical to those described above for the *rrnB* P1 promoter of *B. subtilis* (section IX.1). The isolated *Eco* RI/*Hind* III promoter fragment was cut with *Msp* I, gel-purified, and the DNA restriction termini were filled-in with a Klenow reaction. Ligation reactions with *Sma* I-cut pKK232-8, transformation of competent DH5α cells, and selection of transformants on chloramphenicol plates were performed as described in section IX.1. The final construct was pKK131E, which contained sequences - 60 to + 71 relative to the transcription initiation site of the *E. coli rrnB* P2 promoter.

5. Sequencing double-stranded plasmid DNA.

DNA fragments which had been cloned into the plasmid pKK232-8 were sequenced with the reagents from a Sequenase version 2.0 kit (United States

Biochemical Corporation) according to the Sequenase double-stranded plasmid sequencing protocol, with [α-^{32}P] dATP (Amersham Co., 3000 Ci/mmol). The CAT-primer described in section X was used as a sequencing primer.

X. Purification and quantitation of synthetic DNA oligonucleotides.

The non-phosphorylated DNA oligonucleotides used in this thesis were synthesized courtesy of Tom Atkinson (Department of Biochemistry, University of British Columbia) on an ABI Applied Biosystems Model 380B DNA synthesizer, and purified by reverse-phase chromatography on a C_{18} SEP-PAK column (Millipore®) as described by Atkinson and Smith (1984). The final DNA pellet was dissolved in a volume of TE buffer (pH 8.0; Sambrook *et al.*, 1989), and the absorbance of this solution at 260 nm was determined in a 1 cm path-length cuvette using a Bausch and Lomb Spectronic® 601 spectrophotometer. The molar extinction coefficient for an oligonucleotide was calculated from the number of times each base appeared in the oligonucleotide sequence, and the known molar extinction coefficients (ε_{260}) for the individual bases at pH 8.0 (Wallace and Miyada, 1987): dGTP (12,010); dATP (15,200); dTTP (8,400); dCTP (7,050). From the molar extinction coefficient of the oligonucleotide, and the measured A_{260} of the solution, the concentration (pmol/µl) of the DNA oligonucleotide was calculated.

To sequence the promoter fragments which were cloned into the expression vector pKK232-8 (Brosius, 1984), the DNA oligonucleotide 5'-dAATCTCGTCGAAGCTCGGC-3' was synthesized ($\varepsilon_{260} = 1.97 \times 10^5\ M^{-1}cm^{-1}$). The oligonucleotide is complementary to a region of pKK232-8 which is 15 nt downstream of the M13mp8 polylinker (Fig. 7 of Brosius, 1984), and spans the 5'-end of the structural gene for chloramphenicol acetyltransferase (CAT). The direction of DNA synthesis initiated from this CAT-primer was opposite to the direction of transcription initiated from the cloned promoter fragment.

To amplify the cloned promoter inserts in a polymerase chain reaction (section XII), a second non-phosphorylated DNA oligonucleotide was synthesized to be used in conjunction with the CAT-primer. The second oligonucleotide is identical to nucleotides 4331 to 4348 of pBR322 (5'-dGGCGTATCACGAGGCCCT-3' (ε_{260} = 1.85 x 10^5 $M^{-1}cm^{-1}$); see also Sutcliffe, 1979), and hybridizes to a region of pKK232-8 approximately 180 nt upstream of the M13mp8 polylinker (Fig. 7 of Brosius, 1984). This pBR322-primer served to initiate DNA synthesis in the same direction as transcription from the cloned promoter fragment.

XI. Kinase end-labelling of primers for the polymerase chain reaction.

Labelling of synthetic oligonucleotides by phosphorylation with bacteriophage T4 polynucleotide kinase was performed as described by Sambrook *et al.* (1989). Reactions contained 50 pmol of the CAT-primer (section X), 800 µCi [γ-^{32}P] ATP (ICN Biomedicals Inc., 7000 Ci/mmol), and 10 units of T4 polynucleotide kinase (Bethesda Research Laboratories), in a total reaction volume of 20 µl. Prior to heat inactivation of the enzyme, 1 µl of the reaction mixture was removed to 99 µl of H_2O, and samples of this dilution were electrophoresed on a 12% denaturing polyacrylamide gel. Unincorporated nucleotides and end-labelled CAT-primer were identified by autoradiography. The incorporation of radioactivity into the DNA oligonucleotide was quantitated by Cerenkov counting (Beckman LS6000IC liquid scintillation counter) of gel slices containing the CAT-primer. The specific activity of the CAT-primer was typically 2 x 10^6 cpm/pmol.

To remove excess unincorporated label from the kinase reaction, the remainder of the reaction mixture was diluted with 1 ml of H_2O and transferred to a Centricon™ 3 microconcentrator (Amicon). Samples were centrifuged at 6000 x *g* for 1.5 h, 10 °C. The dilution/centrifugation process was repeated twice. The final retentate was removed (approximately 100 µl), and the microconcentrator

membrane was rinsed with 50 µl H_2O. This rinse was combined with the final retentate, and samples were electrophoresed as described above to determine the recovery of the CAT-primer.

XII. Polymerase chain reactions.

Uniquely end-labelled DNA templates for the gel retardation assays (section XIII) and the DNase I protection analyses (section XIV) were obtained from amplification of the cloned promoter fragments (section IX) in a polymerase chain reaction (Sambrook *et al.*, 1989). Isolation of the pBR322/CAT-primer set and the end-labelling of the CAT-primer have already been described (sections X and XI respectively). Note that the specific activity of the amplified promoter fragment will be identical to that of the CAT-primer. Because of the location of the two primers relative to the cloned promoter inserts (section X), the amplified DNA products will be 266 bp longer than the original cloned promoter fragments discussed in section IX.

All polymerase chain reactions were performed in a final volume of 50 µl. The reaction buffer consisted of 20 mM Tris-HCl (pH 8.9 at 25 °C), 50 mM KCl, 1 mM $MgCl_2$, 10 mM 2-mercaptoethanol, and 0.1 mM each of dATP, dTTP, dCTP, and dGTP (Pharmacia Ultrapure deoxynucleoside 5'-triphosphates were stored as 5 mM stocks in equimolar $MgCl_2$). Reactions contained 10 pmol of each primer, and 50 ng of pKK232-8 recombinant plasmid (section IX) which had been previously linearized with *Pvu* I. The reactions were overlayed with mineral oil, heated at 100 °C for 3 min, and quickly transferred to an Ericomp Singleblock temperature cycler (block temperature 95 °C), where 2.5 units of *Taq* DNA polymerase (Bethesda Research Laboratories) were added. Each reaction was denatured at 95 °C for 15 s, annealed at 58 °C for 1 s, and extended at 72 °C for 30 s. These steps were repeated 30 times and completed with a 5 min extension at 72 °C. Excess mineral oil was removed, and the

samples were extracted with an equal volume of phenol/chloroform (Sambrook *et al.*, 1989). The amplified promoter fragments were gel-purified on a 4% polyacrylamide gel, and the final DNA pellets were resuspended in 200 µl of 10 mM HEPES (pH 8.0). To determine the yield of the polymerase chain reaction, samples from the 200 µl stock were electrophoresed on a 4% polyacrylamide gel, and the end-labelled promoter fragments were identified and quantitated by Cerenkov counting as described in section XI. Typically, 3 pmol of an end-labelled promoter fragment was obtained, an amount sufficient to perform ≥ 300 gel retardation reactions (≤ 10 fmol template in a 20 µl reaction).

XIII. Gel-retardation analyses.

The final volume of a standard binding reaction between RNA polymerase and a promoter template was 20 µl. The volumes given below are for a single reaction. For cases where a large reaction stock was required, all components were scaled up accordingly. Standard binding conditions included end-labelled promoter fragment (final concentration 0.025 to 0.5 nM), 40 mM HEPES (pH 8.0), 80 mM KCl, 10 mM $MgCl_2$, 1 mM dithiothreitol, and 0.1 mg/ml acetylated BSA (Bethesda Research Laboratories). When present, ribonucleotides (Pharmacia FPLC™ Ultrapure), OMeGTP (Pharmacia FPLC™ Ultrapure), and ApA (Sigma Chemical Co.) were each at final concentrations of 0.2 mM, and ppGpp (ICN Biomedicals Inc.) was at a final concentration of 0.1 mM. Prior to the addition of RNA polymerase, the above mixture was incubated for at least 2 min in a circulating water bath set at the desired reaction temperature (10 - 35 °C). RNA polymerase dilutions were made in Buffer D + 0.1 mg/ml acetylated BSA (see section I above), and 2 µl of this dilution was added per binding reaction to give a final concentration of 0.05 to 9.4 nM polymerase and 5% glycerol. Unless otherwise specified, the concentration of RNA polymerase was based on active binding, as determined in Results section I.1a.

Except for the association rate experiments (Results section II.4), RNA polymerase and the *B. subtilis* promoters were allowed to equilibrate for 10 min at the reaction temperature prior to the addition of 1 µl of heparin (Sigma grade I, final reaction concentration either 50 or 100 µg/ml).

The 21 µl binding reaction was loaded immediately onto a 4 - 5% polyacrylamide gel running at 17 volts/cm. To follow the progress of the gel electrophoresis, a dye solution (section III.2) was added to either an empty adjacent gel well, or added into the same well as the sample, but after a minimum of 5 min of sample electrophoresis (see Results section I.2c). Electrophoresis continued until the xylene cyanol was approximately 2 cm from the bottom of the gel. Unbound promoter fragments and polymerase/promoter complexes were identified by autoradiography (exposure with an intensifying screen at 4 °C for 18 h), cut out of the gel with a scalpel, and quantitated by Cerenkov counting (Beckman LS6000IC liquid scintillation counter). A gel slice containing neither free DNA nor polymerase/promoter complexes was always counted as a background control, and this value was subtracted from the Cerenkov counts associated with the promoter fragments. Unless otherwise specified, the results of a binding experiment were always expressed as a ratio (F) between the amount of polymerase/promoter complexes (RP) and the total promoter DNA (P_{total} = RP + free DNA). Note that the fraction ($F = RP/P_{total}$) is independent of the sample volume which was applied onto the gel, and therefore corrects for any loading errors which might occur.

XIV. DNase I protection studies.

Binding reaction conditions were identical to those described in section XIII, and contained 2 nM DNA template and 20 nM RNA polymerase holoenzyme. Following heparin addition, 3 µl of either 25 ng/µl (for 35 °C reactions) or 50 ng/µl (for 10 - 15 °C reactions) DNase I (Sigma Chemical Co.) was added to the 21 µl

binding reaction, gently mixed, and returned to the reaction temperature. Timing of the digestion began when the DNase I was first added to the reaction, and continued for 10 s before 10 µl of stop-mix (1% SDS, 50 mM EDTA, 0.2 mg/ml sonicated calf thymus DNA) was added. Under these digestion conditions, approximately 70% of the promoter fragments remained uncut. Samples were extracted with phenol/chloroform, precipitated with 95% ethanol, resuspended in 4 µl of loading buffer (95% formamide, 20 mM EDTA, 0.05% Bromophenol Blue, 0.05% Xylene Cyanol FF), and transferred to a fresh 0.65 ml Eppendorf tube. The recovery of the promoter fragments in these tubes was quantitated by Cerenkov counting, and the digestion products were analyzed on a 5% sequencing gel. To facilitate comparison of the different binding reaction footprints, each lane of the sequencing gel was loaded with the same number of total Cerenkov counts.

To map the DNase I-protected regions of the polymerase/promoter complexes to the DNA sequence of the promoter, a sequencing reaction (section IX.5) of the double-stranded recombinant plasmid containing the promoter of interest was run alongside the DNase I reactions on the sequencing gel. Note that the electrophoretic mobilities of the dideoxy sequencing reaction products are directly comparable to the mobilities of the DNase I digestion products, because the end-labelled DNA fragment lengths of both reactions are measured relative to the CAT-primer (sections IX.5 and XII respectively).

XV. Determining growth rate dependent expression *in vivo*.

To determine whether expression from the subcloned *B. subtilis rrnB* P2 promoter was still subject to growth rate dependent control *in vivo*, *E. coli* HB101 carrying pKK183B was cultured at a variety of growth rates as described by Deneer and Spiegelman (1987). The different growth rates were achieved by supplementing the basal media with either (a) 0.5% sodium acetate, 0.1% yeast extract; (b) 0.5%

sodium succinate, 0.4% tryptone; (c) 0.4% glucose, 0.2% casamino acids; or (d) 0.4% glucose, 0.2% yeast extract, 1% tryptone. The cells were harvested, sonicated, and the cell extracts were assayed for protein concentration and chloramphenicol acetyltransferase (CAT) activity as described in Deneer and Spiegelman (1987). As the growth rate of the cultures increased from 0.4 to 1.1 doublings per hour, the CAT specific activity (CAT activity/mg protein) increased approximately 2.6 fold (data not shown). This response in CAT specific activity was virtually identical to that observed for the original pKK220B construct over the same growth rate range (Deneer, 1986; Deneer and Spiegelman, 1987). Therefore, the subclone of the *B. subtilis rnnB* P2 promoter which was used in this thesis (pKK183B) is regulated *in vivo* in a growth rate dependent manner.

Results

I. Gel retardation analysis: Components and considerations.

1. Purification of RNA polymerase holoenzyme.

Approximately 20 g of frozen packed cells from *E. coli* K12 were broken, and RNA polymerase was purified through phase partitioning as described in the Materials and Methods. Following precipitation with ammonium sulfate, the crude RNA polymerase fraction was applied to a Bio-Gel A-1.5m column, and Figure 1A shows a typical RNA polymerase elution profile. Those fractions containing peak activity (fractions 48 - 58) were pooled, concentrated, and applied to the heparin-Sepharose column. The corresponding elution profile is shown in Fig. 1B, with the second (eluting at KCl = 0.25 M) and third (eluting at KCl = 0.35 M) A_{280} peaks displaying polymerase activity. To determine the subunit composition of these two activity peaks, samples from the heparin-Sepharose column fractions were analyzed on SDS-polyacrylamide gels. As Fig. 2A shows, RNA polymerase in the first activity

Figure 1A. Chromatography of *E. coli* K12 cell extracts on a Bio-Gel A-1.5m column.

Approximately 20 g of frozen packed cells from *E. coli* K12 were broken and polymerase was extracted using the polyethylene glycol/dextran separation described in the Materials and Methods. Following precipitation with ammonium sulfate, the crude RNA polymerase fraction was resuspended in 6.2 ml of Buffer B, and applied to a Bio-Gel A-1.5m column (2.5 cm x 100 cm). The applied sample was eluted with the same buffer, at a flow rate of about 30 ml/h. Fractions of 5.5 ml were collected, and 20 µl samples were assayed for RNA polymerase activity on ϕ29 DNA (closed circles), as described in the Materials and Methods. The absorbance of the fractions at 280 nm was also measured (open circles). Fractions 48 - 58 were pooled and concentrated as described in the Materials and Methods, and applied to the heparin-Sepharose column (Fig. 1B).

Figure 1B. Chromatography of *E. coli* K12 cell extracts on a heparin-Sepharose column.

The pooled, concentrated fraction from the Bio-Gel A-1.5m column of Figure 1A was diluted and re-concentrated successively in Buffer C, as described in the Materials and Methods. The final concentrated sample was applied to a 20 ml (2 cm x 7 cm) column of heparin-Sepharose, which had been previously equilibrated with 100 ml of Buffer C + 0.1 M KCl. The column was washed with 5 volumes of equilibration buffer, and the enzyme was eluted with a 300 ml linear gradient of 0.1 to 1.0 M KCl, as described in the Materials and Methods. Fractions of 5.5 ml were collected, and 20 µl samples were assayed for RNA polymerase activity on ϕ29 DNA (closed circles), as described in the Materials and Methods. The absorbance at 280 nm (open circles), and conductivity of the fractions were also measured. Conductivity is expressed as salt concentration (cross). Fractions 29 - 31 were pooled and concentrated to less than 3 ml.

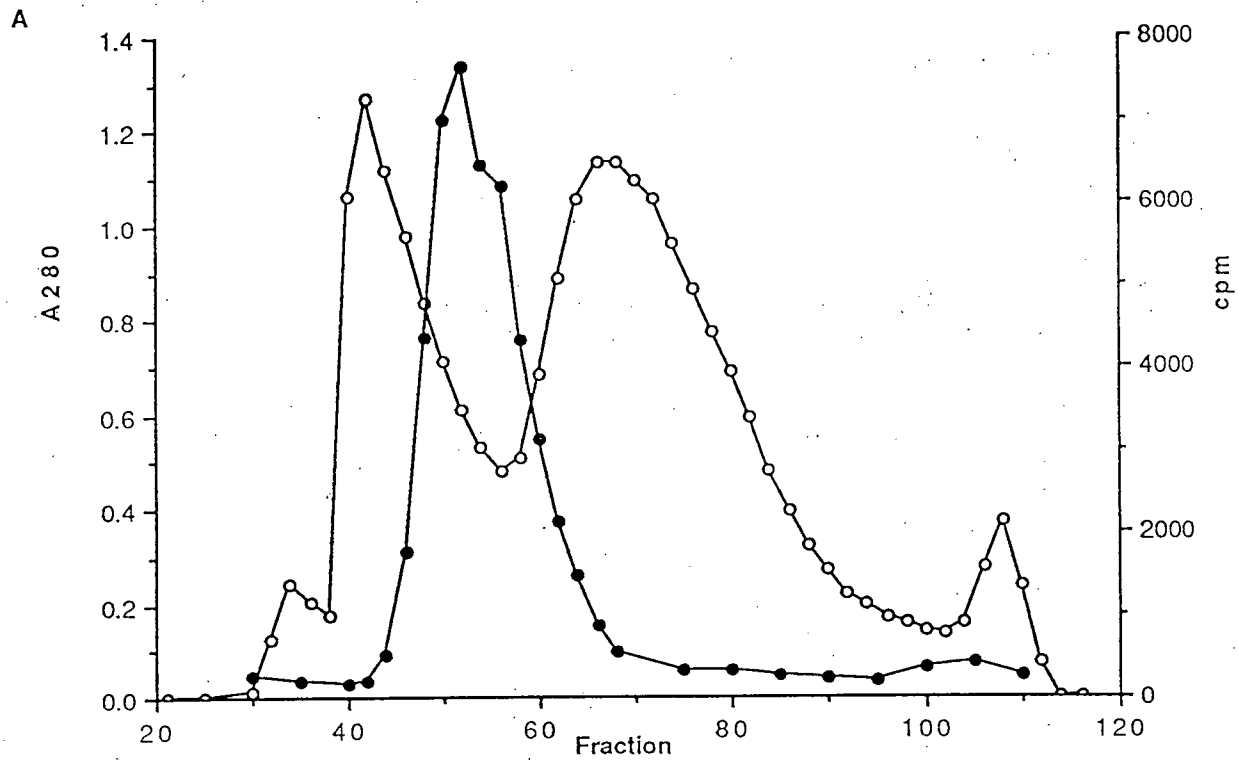
A
A280
cpm
Fraction
1.4
1.2
1.0
0.8
0.6
0.4
0.2
0.0
8000
6000
4000
2000
0
20
40
60
80
100
120

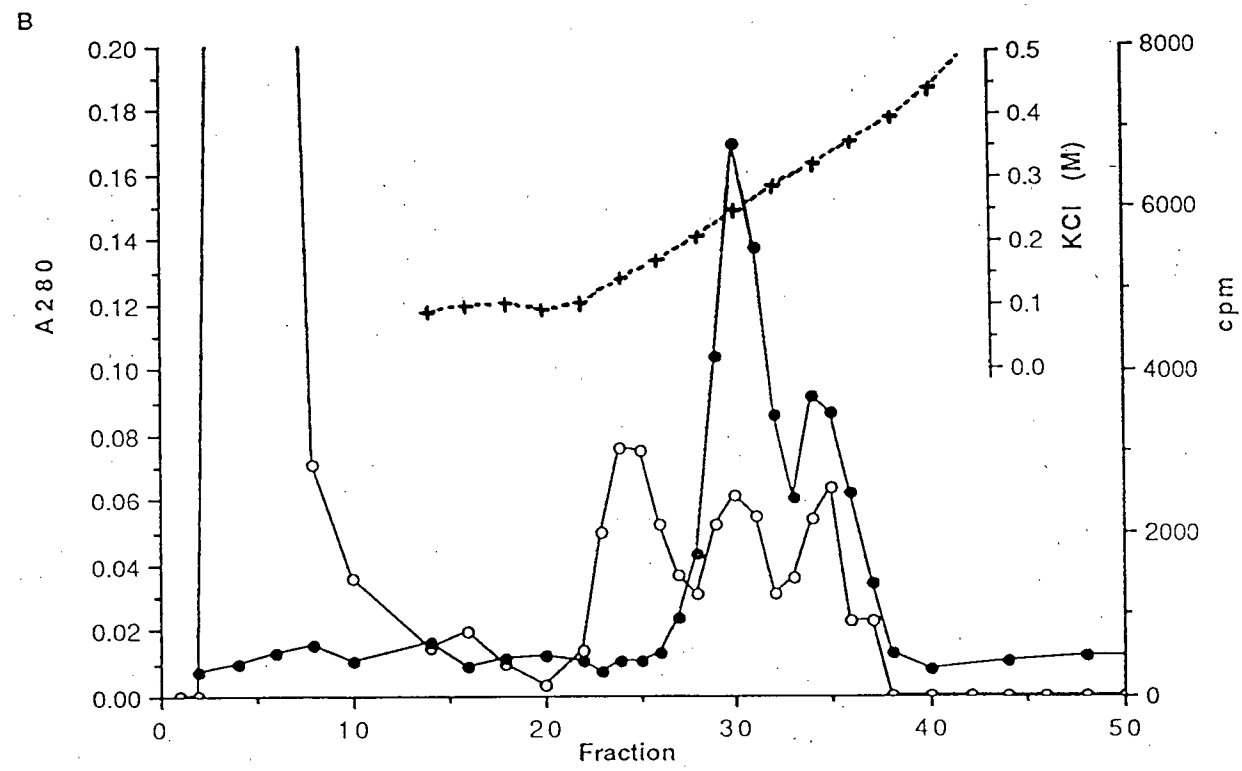
B
A280
KCl (M)
cpm
Fraction
0.20
0.18
0.16
0.14
0.12
0.10
0.08
0.06
0.04
0.02
0.00
0.5
0.4
0.3
0.2
0.1
0.0
8000
6000
4000
2000
0
0
10
20
30
40
50

Figure 2A. SDS-polyacrylamide gel electrophoresis of RNA polymerase at different stages of the purification method.

RNA polymerase holoenzyme Batch #233 was purified as described in the Materials and Methods. At various stages throughout this purification scheme, samples were removed and electrophoresed through a 14 - 20% exponential gradient SDS-polyacrylamide gel to evaluate protein composition (Materials and Methods). Positions of the RNA polymerase subunits β'/β, σ, and α are indicated to the right of the figure. A description of the fractions which were sampled is given in Table II. When indicated, protein content reflects BSA equivalents. Lane a: Clearing-spin supernatant (approximately 52 µg of loaded protein). Lane b: Bio-Gel load (approximately 32 µg of loaded protein). Lane c: Bio-Gel eluate (approximately 7.7 µg of loaded protein). Lanes 5, 22, 24, 26, 28, and 29 - 36: Designate the fraction numbers from the wash/elution steps of the heparin-Sepharose column (Fig. 1B). A 20 µl sample volume was loaded from each 5.5 ml fraction. Lanes d - f: Holoenzyme Batch #233 (3.2, 6.4, and 12.8 µg of loaded protein respectively). Lane g: Holoenzyme Batch #176 (6.0 µg of loaded protein). Lane h: Holoenzyme Batch #203 (12.6 µg of loaded protein).

Figure 2B. Densitometer tracing of the stained SDS-polyacrylamide gel.

The SDS-polyacrylamide gels stained with Coomassie Blue were scanned at 525 nm using a Helena Instruments Quick Scan R & D densitometer. The tracing shows the densitometry scan of Lane f from Figure 2A, which contained 12.8 µg (BSA equivalents) of RNA polymerase holoenzyme Batch #233. The polymerase subunits are indicated above their corresponding densitometry peaks.

A

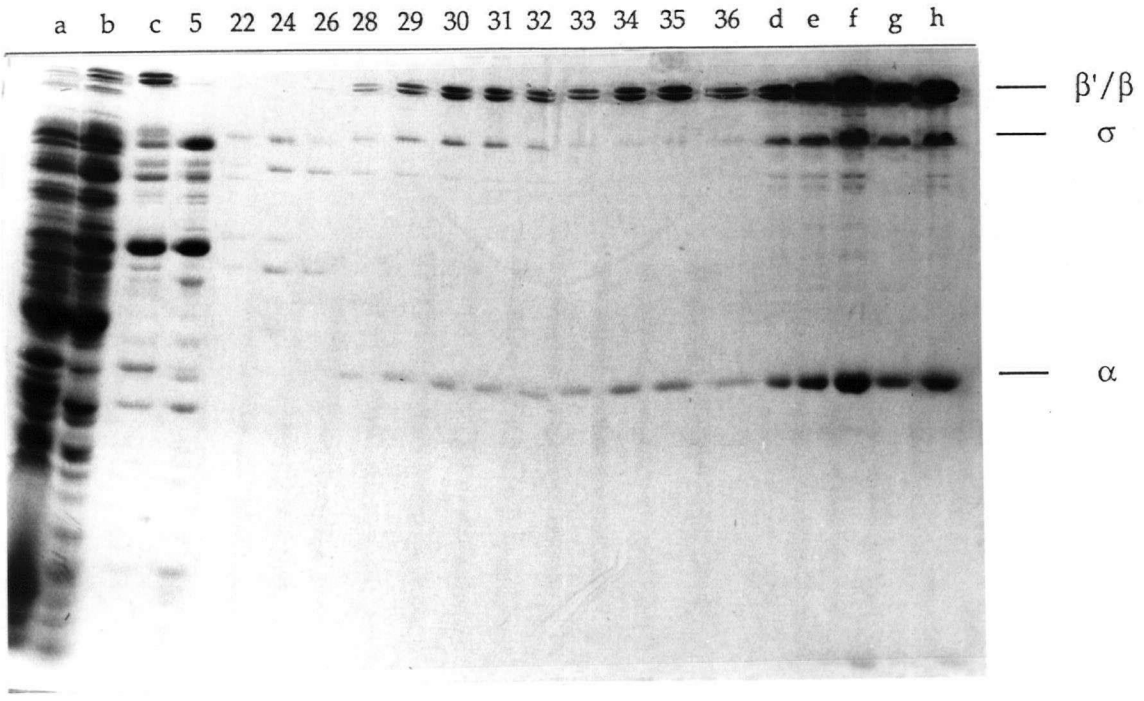

B

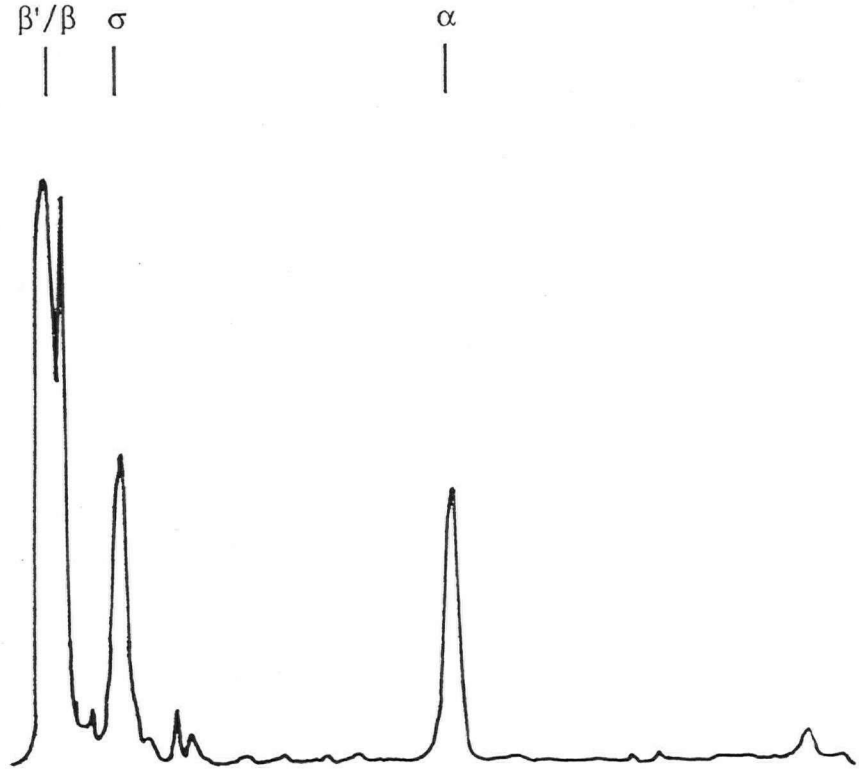

peak (Lanes 29 - 31) contained the σ-subunit whereas the enzyme in the second activity peak (Lanes 34 and 35) was associated with only trace amounts of σ. Thus, under the elution conditions employed, RNA polymerase holoenzyme from *E. coli* eluted at 0.25 M KCl, and was followed by core enzyme at 0.35 M KCl. The minor activity associated with the core enzyme can be ascribed to either the residual sigma contamination from the preceding holoenzyme peak, or non-specific transcription initiation at single stranded DNA breaks in the bacteriophage ϕ29 template (Vogt, 1969; Ishihama *et al.*, 1971; Hinkle *et al.*, 1972).

For holoenzyme Batch #233, fractions 29 - 31 from the heparin-Sepharose column (Fig. 1B) were pooled and concentrated. A summary of the overall purification of Batch #233 is shown in Table II. From 20 g of starting material, 1 mg of RNA polymerase holoenzyme was obtained. Based on the specific and total activities respectively, this procedure resulted in a 500-fold purification of the RNA polymerase, with a final yield of 16% of the original starting activity. The largest single purification step was due to the Bio-Gel chromatography, which resulted in a 13-fold increase in polymerase specific activity. Extractions following the clearing spin and chromatography over the heparin-Sepharose column each contributed about 5 - 7 fold purification. By comparing the total activity values of the heparin-Sepharose eluate and heparin-Sepharose load fractions, it would seem that about 28% of the total cellular RNA polymerase was holoenzyme. This is in good agreement with other studies (Iwakura *et al.*, 1974; Engbaek *et al.*, 1976), which have estimated that holoenzyme accounts for 30 - 40% of the total cellular population. Finally, Table II shows that this procedure was reproducible, with holoenzyme preparations #233 and #203 displaying similar final specific activities and purity (see also Fig. 2A Lane f versus h). Note that additional purification over a phosphocellulose column did not significantly increase the specific activity of the holoenzyme (Table II, Batch #176 versus Batch #233 and #203).

Table II. Summary of RNA polymerase purification.

Fraction	Activity x 10^{-3} (cpm/ml)	Protein (mg/ml BSA)	Total fraction volume (ml)	Total activity x 10^{-5} (cpm)	Specific activity x 10^{-4} (cpm/mg)
Clearing-spin supernatant	285	51.6	54	153	0.55
Bio-Gel (load)	952	31.8	6.2	59	2.99
Bio-Gel (eluate) [a]	150	0.385	55	82	38.9
Heparin-Sepharose (load)	995	1.83	8.3	82	54.4
Heparin-Sepharose (eluate) [b]	144	0.067	16	23	215
Holoenzyme (Batch #233)	1806	0.641	1.4	25	282
Holoenzyme (Batch #203)	2219	0.842	1.6	36	263
Holoenzyme (Batch #176)	1169	0.397	2.5	29	294

RNA polymerase holoenzyme Batch #233 was purified as described in the Materials and Methods. At various stages throughout this purification scheme, samples were removed and assayed for protein content (mg BSA per ml) and polymerase activity on ϕ29 DNA (cpm per ml) (see Materials and Methods). Samples were assayed in triplicate over a fourfold range of sample volume input, and reported values represent an average of these results. Fractions were tested either immediately before their application to a chromatography column, or represented the pooled eluate of those column fractions which displayed peak **(a)** RNA polymerase (Fig. 1A), or **(b)** holoenzyme (Fig. 1B), activity. In addition, the crude supernatant which was obtained following cell breakage/centrifugation, and the final dialyzed preparations of holoenzyme (Batch #233, 203, and 176), were also tested. Note that purification of holoenzyme Batch #176 included chromatography on a phosphocellulose column, as described in the Materials and Methods.

To determine the purity of Batch #233, increasing amounts of holoenzyme protein (BSA equivalents) were separated on an SDS-polyacrylamide gel, and the results are shown in Fig. 2A (Lanes d - f). Generally, an accurate determination of purity can be made if ≥ 10 μg of RNA polymerase has been applied to the gel (Burgess, 1976). Consequently, the apparent mass of each protein band in Figure 2A Lane f (12.8 μg of applied holoenzyme) was determined by a densitometry scan of the stained gel (see Fig. 2B and Materials and Methods). Although minor contaminating protein bands could be seen both above and below the σ-subunit, these comprised less than 5% of the total sample. Based on the integrated peak areas from this gel scan, the apparent mass ratio of σ/α_2 was calculated as 1.13. Since the theoretical σ/α_2 mass ratio is 0.962 (from the molecular mass of the polymerase subunits in Burgess *et al.*, 1987), this suggested that the RNA polymerase was saturated for the σ-subunit.

1a. Determining the active concentration of RNA polymerase holoenzyme.

Although the physical purity of the holoenzyme preparation was high, it is quite possible that some of these molecules are unable to initiate transcription. Since the kinetic analyses are only based on functional polymerase interactions, it is important to express a preparation of holoenzyme in terms of its active concentration, and not merely its protein concentration. Since the gel retardation assay is concerned only with active binding, this property will be considered below.

To determine the active binding concentration, a constant amount of RNA polymerase protein (final concentration 0.125 nM or 0.25 nM) was titrated with increasing levels of promoter template (final concentration 0.5 - 1.5 nM) under standard binding conditions in a gel retardation assay (see Materials and Methods). Note that the term 'protein' reflects actual polymerase concentrations, and not merely an equivalent concentration relative to BSA (see Materials and Methods, and Mangel and Chamberlin, 1974). Following electrophoresis, heparin resistant

complexes and unbound promoter fragments were identified and measured as described in the Materials and Methods. Results were expressed as the fraction (F) of total DNA (P_{total}) which formed a heparin resistant complex (RP) with RNA polymerase at a given template concentration. Based on the fraction ($F = RP/P_{total}$) of heparin-resistant complexes which were formed at saturating levels of promoter template, and the amount of template (P_{total}) present in a given reaction, the apparent concentration of active polymerase (RP) was averaged over three input concentrations of DNA. This is illustrated in Figure 3, which shows that at saturating levels of DNA, a constant plateau of (RP) was achieved, suggesting that all active enzyme had been bound by the molar excess of promoter fragments. Note that the plateau value of (RP) only represents an apparent active concentration of RNA polymerase, since the promoter being used to titrate the enzyme might have a low overall isomerization constant, such that saturating levels of one reactant does not cause all of the second reactant to form heparin resistant complexes. This discrepancy can be corrected by dividing the apparent active polymerase concentration, obtained at promoter excess, by the fraction of heparin resistant complexes observed at saturating RNA polymerase. However, for the promoters in question, this maximal binding approached 100%, and made such correction unnecessary (see Lanes 1 and 8 from Fig. 3). The results for holoenzyme Batches #176 and #233 are shown in Table III. Both BP1 and BP2 templates were used to titrate each stock. Note that for both preparations, the average active fraction of RNA polymerase was $\geq$ 100%, indicating that all of the polymerase protein was capable of binding to these promoters. Of equal importance, these results confirmed that the binding stoichiometry of polymerase/promoter complexes was 1:1. For example, an active fraction determination that was 50% could mean either that half of the polymerase molecules were unable to bind to the promoter, or that the binding stoichiometry of polymerase to the promoter was 2:1. Based on these results, the active stock concentrations of the holoenzyme were determined, and are

Figure 3. Titration of RNA polymerase with promoter-bearing DNA fragments.

A constant amount of RNA polymerase protein was titrated with increasing levels of promoter template under standard binding conditions (10 min at 35 °C, see Materials and Methods). Note that the term 'protein' reflects actual polymerase concentrations, and not merely an equivalent concentration relative to BSA (see Materials and Methods, and Mangel and Chamberlin, 1974). Following a heparin challenge (final concentration 100 μg/ml), binding reactions were immediately loaded onto a 4% polyacrylamide gel (1x TBE) running at 17 volts/cm (see Materials and Methods). Figure 3 shows a picture of the autoradiograph of a gel retardation analysis in which the *B. subtilis rrnB* P1 promoter (BP1) was used as a DNA template. Heparin resistant complexes (RP) and unbound promoter fragments (P) are indicated to the left of the figure. Lanes 1 - 7: Titration of RNA polymerase Batch #176. Lanes 8 - 14: Titration of RNA polymerase Batch #233. Control lanes 1 and 8: 0.5 nM of BP1 was bound with ≥ 2.0 nM of polymerase. Lanes 2 - 4 and 9 - 11: Titration of 0.25 nM polymerase with 0.5, 1.0, and 1.5 nM BP1 respectively. Lanes 5 - 7 and 12 - 14: Titration of 0.125 nM polymerase with 0.5, 1.0, and 1.5 nM BP1 respectively.

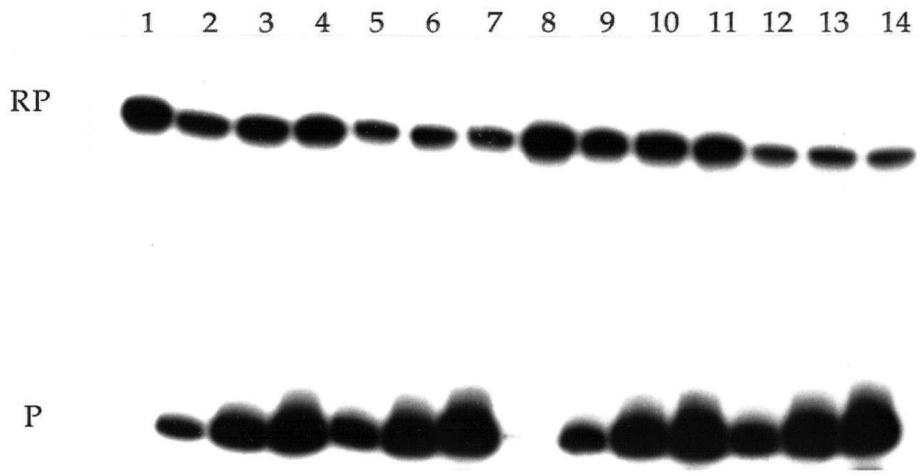
1 2 3 4 5 6 7 8 9 10 11 12 13 14
RP
P

Table III. Active binding concentrations of RNA polymerase Batch #176 and #233.

Holoenzyme stock	Stock dilution	(nM protein) [a]	(nM active binding) [b]	Average active binding fraction [c]	Active binding stock (nM ± 1 S. D)
Batch #176 DNA = BP1	3.58×10^{-4}	0.25	0.349		
	1.79×10^{-4}	0.125	0.158		
				1.08 ± 0.25	758 ± 187
Batch #176 DNA = BP2	3.58×10^{-4}	0.25	0.211		
	1.79×10^{-4}	0.125	0.105		
Batch #233 DNA = BP1	2.22×10^{-4}	0.25	0.328		
	1.11×10^{-4}	0.125	0.147		
				1.18 ± 0.10	1325 ± 137
Batch #233 DNA = BP2	2.23×10^{-4}	0.25	0.300		
	1.11×10^{-4}	0.125	0.128		

RNA polymerase holoenzyme Batch #176 and #233 (Table II) were diluted to either 0.25 or 0.125 nM of protein, and titrated with promoter-bearing DNA fragments, using either the *B. subtilis rrnB* P1 (BP1) or P2 (BP2) promoters as a DNA template (see Results section I.1a and Fig. 3 for details).

a) RNA polymerase protein concentrations = BSA equivalents x 0.79 (Mangel and Chamberlin, 1974). The molecular weight of holoenzyme ($\beta\beta'\alpha_2\sigma^{70}$) is 449,058 (Burgess *et al.*, 1987).

b) Active binding = average polymerase binding concentration obtained at saturating DNA, divided by the fraction of total DNA which forms heparin resistant complexes at saturating enzyme (see text for details).

c) Average (± 1 S. D.) of the ratio (nM active binding)/(nM protein) for a given batch of RNA polymerase.

reported (± 1 S.D.) in the final column of Table III. Unless otherwise specified, all subsequent references to polymerase concentration shall be based upon the active binding concentration of the RNA polymerase holoenzyme.

1b. Comments on the purification of RNA polymerase.

Several methods for the isolation of RNA polymerase holoenzyme have been published (Nüsslein and Heyden, 1972; Mukai and Iida, 1973; Sternbach *et al.*, 1975; Gonzalez *et al.*, 1977). However, these suffer from a variety of drawbacks including time-consuming protocols (Mukai and Iida, 1973), technically awkward chromatography systems (Gonzalez *et al.*, 1977), or the requirement of further purification steps to remove unwanted protein (Nüsslein and Heyden, 1972) or nucleic acid (Sternbach *et al.*, 1975) contaminants. The present report describes a rapid procedure for the isolation of RNA polymerase holoenzyme.

Similar separations of holoenzyme from core have been obtained using both DNA-cellulose (Mukai and Iida, 1973) and single stranded DNA-agarose (Nüsslein and Heyden, 1972) columns. However, both these reports include extra purification steps to obtain a pure holoenzyme preparation. Compared to the report of Mukai and Iida (1973), the concentrations of KCl required in the present system were higher (0.25 vs 0.15 M for the elution of holoenzyme, and 0.35 vs 0.25 M for core.) This difference is most probably due to a higher affinity of the RNA polymerase for heparin than for DNA cellulose. The higher stringency likely contributes to the observed purity of the preparations, and obviates any further purification steps, allowing the entire procedure to be completed in two days. From 20 g of starting material, 1 mg of RNA polymerase holoenzyme was obtained. This preparation was 95% pure with respect to protein, saturated for sigma, and had an active binding fraction of 100%.

2. General considerations for the gel retardation assay.

For the kinetic analyses of promoter/polymerase interactions to be meaningful, it is necessary that the binding reactions and subsequent gel retardation analyses fulfill three conditions:

1. RNA polymerase holoenzyme interactions with a DNA template must be directed towards a given promoter sequence, and not just reflect non-specific interactions (Shaner *et al.*, 1983).

2. Along with its function as a non-specific competitor, the addition of heparin must prevent any further polymerase/promoter interactions from occurring. Functionally, this requires that heparin can irreversibly bind free RNA polymerase at a rate that is much faster than the rate of closed complex formation.

3. Heparin resistant polymerase/promoter complexes must be stable during the gel retardation analysis.

The following set of experiments was designed to investigate whether the amount of bound complexes and free promoter fragments measured after gel electrophoresis reflected those same levels formed in solution following heparin addition.

2a. Promoter Specificity.

To demonstrate that the binding of RNA polymerase holoenzyme to a promoter template was specific, promoter-bearing and promoterless DNA templates (final concentrations 0.5 nM) were tested for their ability to form heparin resistant complexes with RNA polymerase holoenzyme. Figure 4 shows that under standard binding conditions (10 min at 35° C, see also Materials and Methods), polymerase would only form heparin resistant complexes on DNA templates bearing a promoter recognition sequence (compare Lane 2 with Lane 5). That this binding was specific to sigma saturated polymerase is shown in Lane 4, which demonstrates that at 34 nM of core enzyme (concentration based on BSA protein equivalents), less

Figure 4. Specificity of binding of RNA polymerase to various DNA templates.

Standard reaction conditions (10 min at 35 °C, see Materials and Methods) were used to test the specificity of binding of excess RNA polymerase (Batch #233) to DNA templates (0.5 nM). DNA templates were derived from either the recombinant plasmid pKK183B (*B. subtilis rrnB* P2), or from the promoterless vector pKK232-8 (see Table I and Materials and Methods). The binding reactions were challenged with heparin (final concentration 50 μg/ml), and immediately loaded onto a 4% polyacrylamide gel (1x TBE) running at 17 volts/cm (see Materials and Methods). Figure 4 shows a picture of the autoradiograph of this gel retardation analysis. The positions of heparin resistant complexes (RP) and unbound promoter fragments (P) are indicated to the left of the figure. Lanes 1, 2: DNA templates derived from the promoterless vector pKK232-8. Lanes 3 - 6: DNA templates derived from the recombinant plasmid pKK183B (BP2 promoter). Lanes 1 and 3: No RNA polymerase. Lane 4: 34 nM (BSA equivalents) of core RNA polymerase. Lanes 2, 5, and 6: ≥ 2 nM of RNA polymerase holoenzyme. Lane 6: Heparin was present in the binding reaction before the addition of RNA polymerase holoenzyme.

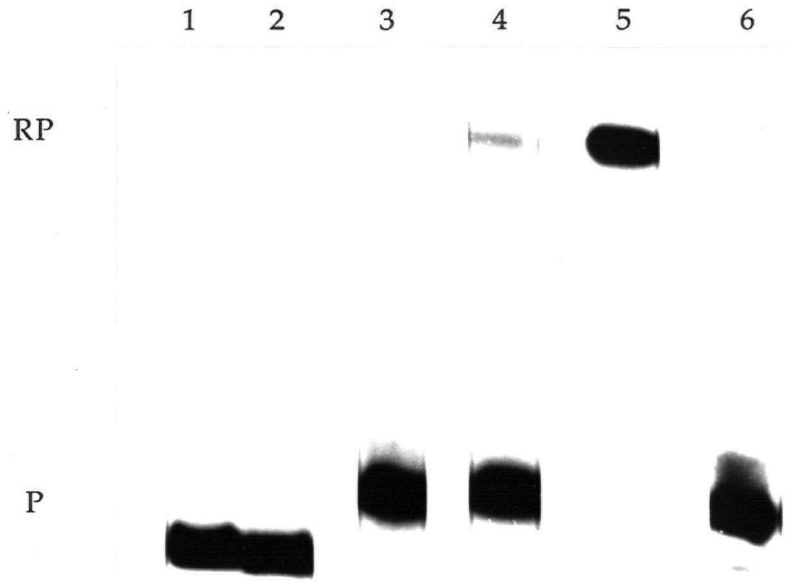
1
2
3
4
5
6
RP
P

than 7% of the BP2 template was bound following a heparin challenge. This residual binding may be due to carry over of the sigma subunit into the core enzyme fraction during the elution of the heparin-Sepharose column (see Fig. 1B). Only 0.1% contamination would be required to generate the observed levels of binding in Figure 4, Lane 4, and inspection of Figure 2A Lanes 34 - 35 would suggest that some sigma was indeed present in this core enzyme fraction. Lane 6 of Figure 4 confirms that under standard binding conditions, 50 μg/ml heparin was able to irreversibly bind all free holoenzyme and prevent any further promoter/polymerase complex formation (see also Results section I.2b). Finally, the observed complex formation was not an artifact of the binding buffer, since reactions which contained no polymerase failed to produce complexes (Lanes 1 and 3).

2b. Heparin as a non specific competitor.

The original binding conditions for the gel retardation assay included 125 mM KCl, since it was felt that the higher salt concentration would help prevent non-specific DNA/promoter interactions from occurring (Shaner *et al.*, 1983). However, as Figure 5 dramatically illustrates, heparin did not irreversibly bind free RNA polymerase at 125 mM KCl. Instead, an apparent equilibrium was established which involved the binding of polymerase to both heparin and the specific promoter. As expected for a binding competitor, increased levels of heparin reduced the amount of promoter/polymerase complexes formed.

The reversible association of holoenzyme with heparin in the binding assay can be compared to the elution of polymerase from a heparin-Sepharose column (see Fig. 1B). Accordingly, lowering the salt concentration in the binding reaction should lead to a condition at which heparin/polymerase interactions are essentially irreversible. This is shown in Figure 6, where the ability of the BP2 promoter to compete with heparin for polymerase binding was tested at various concentrations of KCl. There was a sharp inflection point at 120 mM KCl, but below this limit,

Figure 5. Polymerase/promoter interactions in the presence of heparin and 125 mM KCl.

Binding reactions containing RNA polymerase (3 nM) and promoter bearing DNA templates (0.5 nM) were performed at 35 °C, 125 mM KCl as described in the Materials and Methods. Lanes 1 - 7: DNA templates derived from pKK115B (*B. subtilis rrnB* P1). Lanes 8 - 14: DNA templates derived from pKK183B (*B. subtilis rrnB* P2). Binding reactions were incubated for either 10 min (Lanes 1 - 3; 8 - 10) or 3 h (Lanes 4 - 6; 11 - 13) prior to loading a 4% polyacrylamide gel (1x TBE) running at 17 volts/cm (see Materials and Methods). Figure 5 shows a picture of the autoradiograph of this gel retardation analysis. The positions of heparin resistant complexes (RP) and unbound promoter fragments (P) are indicated to the left of the figure. Lanes 1 - 3; 4 - 6; 8 - 10; 11 - 13: Heparin was added to the binding reactions at respective final concentrations of 5, 50 and 200 μg/ml before the addition of RNA polymerase holoenzyme. For control experiments (Lanes 7 and 14), heparin (final concentration 50 μg/ml) was added to the binding reaction following a 10 min incubation of RNA polymerase with the promoter fragment.

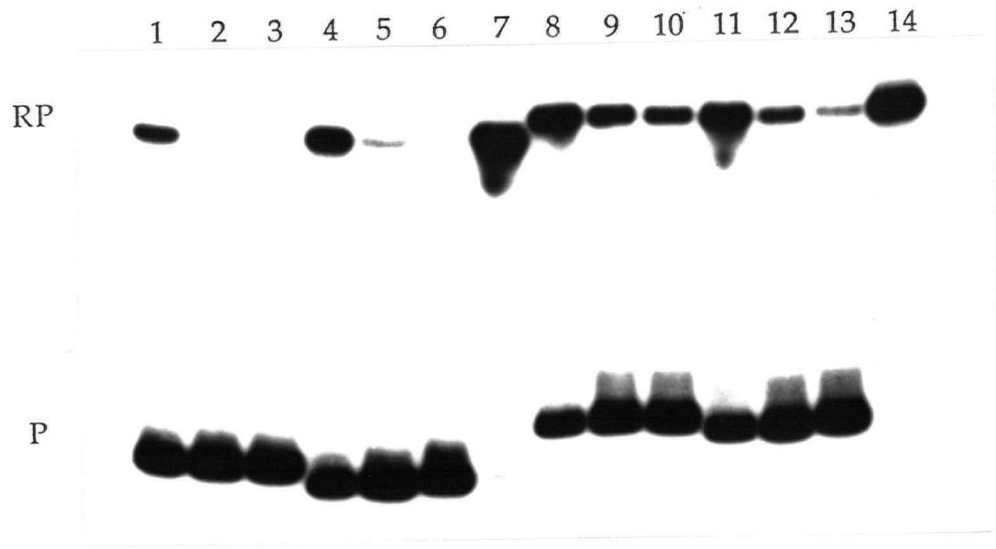
1 2 3 4 5 6 7 8 9 10 11 12 13 14
RP
P

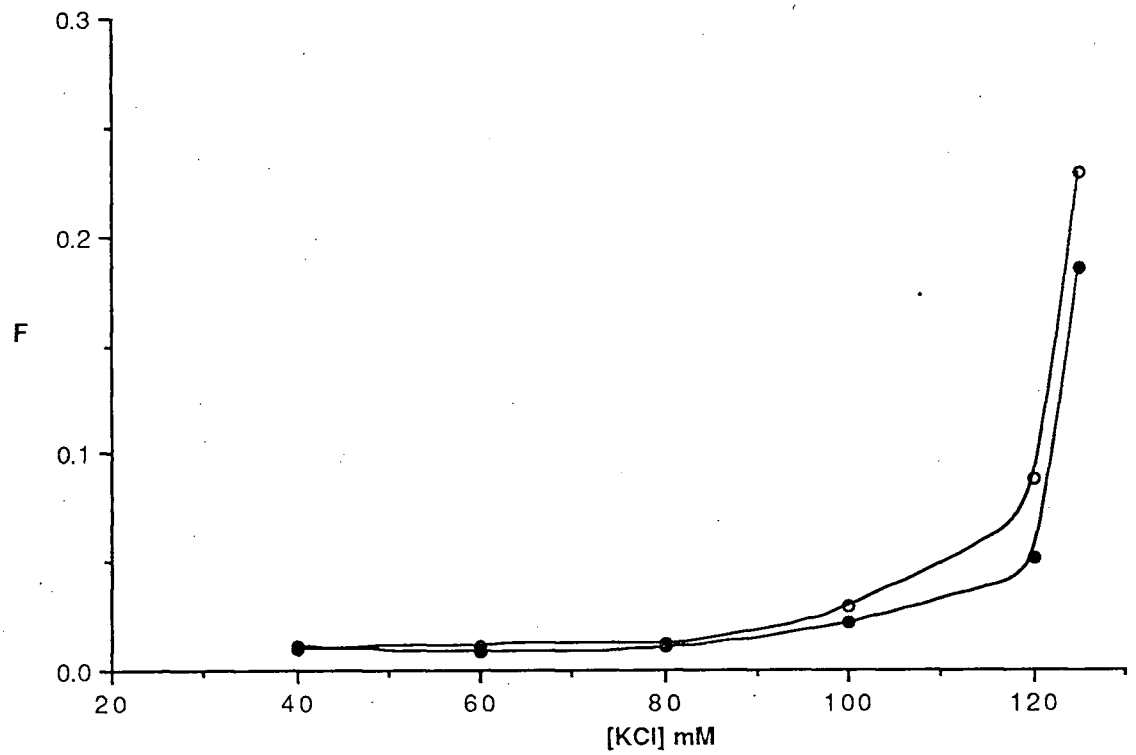

Figure 6. Polymerase/promoter interactions in the presence of heparin and 40 - 125 mM KCl.

Binding reactions were performed as described in Figure 5 (10 min at 35 °C) using DNA templates derived from pKK183B (*B. subtilis rrnB* P2). Heparin was added to the binding reaction at final concentrations of either 50 (open circles) or 200 (closed circles) μg/ml before the addition of RNA polymerase holoenzyme. The concentration of KCl in the binding reactions ranged from 40 - 125 mM. Following gel electrophoresis, heparin resistant complexes and unbound promoter fragments were identified and measured as described in the Materials and Methods. Results were expressed as the fraction (F) of total DNA which formed a heparin resistant complex with RNA polymerase at a given salt concentration.

heparin/polymerase interactions were essentially irreversible. Unless otherwise specified, subsequent experiments used 80 mM KCl as the standard binding condition.

2c. Stability of complexes during gel loading conditions.

In addition to a non-specific competitor, researchers often add a dye mixture containing either glycerol or sucrose to their binding reactions prior to gel electrophoresis (Garner and Revzin, 1981; Fried and Crothers, 1981; Straney and Crothers, 1987b). However, such a mixture might destabilize promoter/polymerase complexes, and lead to an underestimation of their apparent levels following gel electrophoresis. To test for this possibility, the apparent dissociation rates of polymerase/promoter complexes in the presence of various dye mixtures was investigated. As discussed in Appendix B.II.2, the irreversible conversion of heparin-resistant (HR) complexes into a heparin-sensitive (HS) state can be described by equation (2)

$$\mathrm{Ln}[HR] = -(k_{obs})\, t + \mathrm{Ln}[HR]_0 \qquad (2)$$

Where the time-dependent concentration of HR is related to the initial (time zero) concentration according to the observed dissociation rate constant (k_{obs}).

The observed dissociation rates of polymerase/promoter complexes were measured in an assay as follows. A reaction stock of RNA polymerase and promoter fragment was mixed and allowed to equilibrate for 10 min at 18° C (reaction buffer included 125 mM KCl and 0.1 mM ppGpp). Complexes formed under these conditions were relatively unstable to begin with (see Results section II.3a), and served as a sensitive probe for any perturbation the loading dye might have caused. At time zero, heparin and various loading dye mixtures were added, and after a brief vortex, the stock was returned to the reaction temperature. Samples were removed at intervals over a 5 min period, and analyzed by gel retardation as described in the Materials and Methods. Results were expressed as the fraction (F) of total DNA

which remained in heparin resistant complexes with RNA polymerase at a given time following the addition of loading dye.

As illustrated in Figure 7, the combination of dye/heparin and any one of sucrose, Ficoll, or glycerol, significantly destabilized the preformed complexes (average half-life = 37 s). This meant that in the 10 seconds it usually takes to load a gel, these complexes would decay by as much as 17%. The addition of dye/heparin alone increased complex stability by four-fold, but this condition was still about twelve-times less stable than if sucrose alone was added with the heparin challenge. In the end I decided to add nothing to the binding reactions following heparin addition, since the 5% glycerol present in all binding reactions (from the addition of polymerase) was sufficient to load the sample onto the gel. To follow the progress of the gel electrophoresis, a dye solution was added to either an empty adjacent gel well, or added into the same well as the sample, but after a minimum of 5 minutes of sample electrophoresis (see also below). It is not known what property of the dye mixtures caused complex instability, and this matter was not pursued.

Other factors which might also destabilize complexes include sample vortexing, and sudden shifts in the temperature and buffer composition that the sample might experience when loaded into the gel-well buffer. Figure 8A shows the effects of vortexing on complex stability. Initial complexes were formed under the same conditions as described for Figure 7. Following complex formation, samples were removed to a heparin challenge (final concentration 50 μg/ml), vortexed from 0 - 5 seconds, and analyzed by gel retardation as described above. While the complexes were sensitive to vortexing, the estimated half-life was 22 seconds. Since it generally took less than 1 second to vortex a sample, the maximum that a complex could decay is estimated to be about 3%. In many cases, this error was less than the absolute error of cpm measurement obtained for the individual gel slices (data not shown).

Figure 7. Stability of polymerase/promoter complexes to various loading dye mixtures.

A binding reaction containing RNA polymerase (0.9 nM) and promoter fragment (0.5 nM of *B. subtilis rrnB* P2 derived from pKK183B) was allowed to equilibrate for 10 min at 18° C (reaction buffer included 125 mM KCl and 0.1 mM ppGpp; see also Materials and Methods). At time zero, a loading dye (3 µl per 20 µl binding reaction) and heparin (final concentration 50 µg/ml) were added, and after a brief vortex, the mixture was returned to the reaction temperature. Samples were removed at intervals over a 5 min period, and analyzed by gel retardation as described in the Materials and Methods. Results were expressed as the fraction (F) of total DNA which remained in heparin resistant complexes with RNA polymerase at a given time following the addition of the loading dye, and a plot of Ln(100*F) versus time is shown. The lines through each data set were calculated by linear least-squares analysis, and the slopes from these lines yielded the observed dissociation rate constants (k_{obs}). The loading dye compositions are summarized in the figure insets, and the corresponding observed dissociation rate constants are indicated below. The final respective concentrations of sucrose, Ficoll, glycerol and dye (bromophenol blue and xylene cyanol) were 7.5%, 1.25%, 10.4% and 0.03%.

Loading dye	k_{obs} (s^{-1})
sucrose/dye/heparin	1.9×10^{-2}
Ficoll/dye/heparin	1.9×10^{-2}
glycerol/dye/heparin	1.8×10^{-2}
dye/heparin	4.8×10^{-3}
sucrose/heparin	4.1×10^{-4}
heparin	3.6×10^{-4}

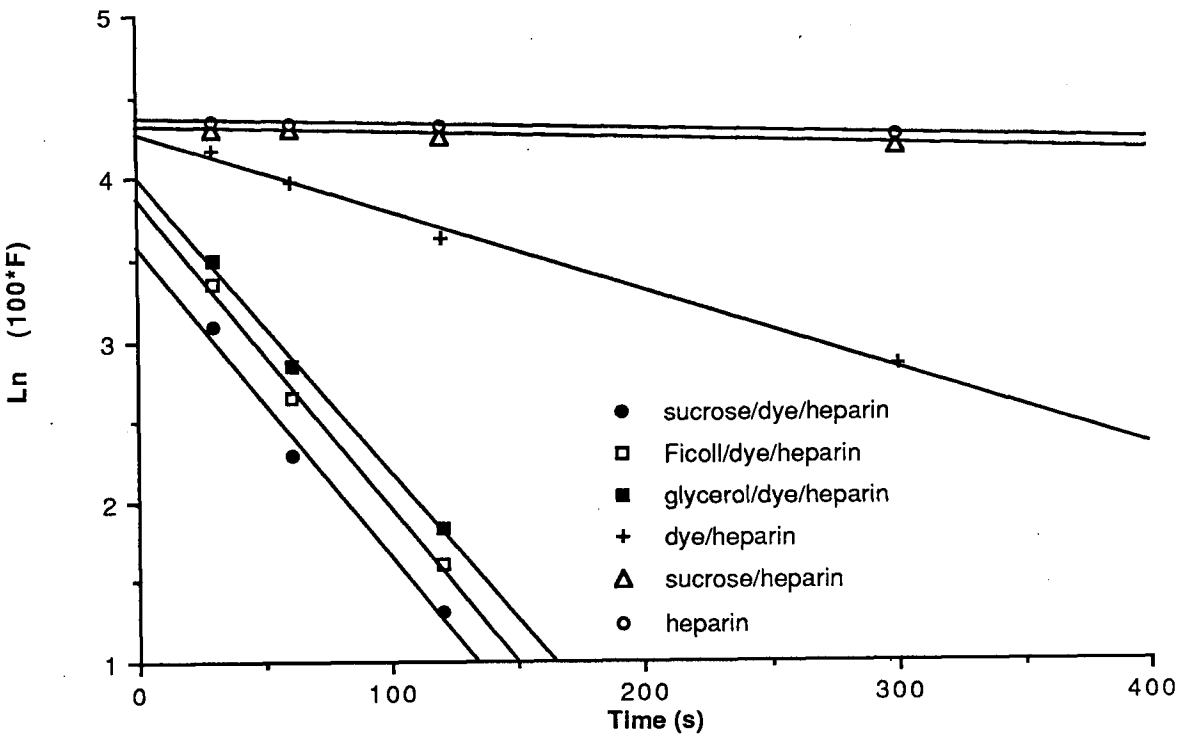
5
4
3
2
1
Ln (100*F)
0
100
200
300
400
Time (s)
sucrose/dye/heparin
Ficoll/dye/heparin
glycerol/dye/heparin
dye/heparin
sucrose/heparin
heparin

Figure 8. Stability of polymerase/promoter complexes during vortexing and sample application to polyacrylamide gels.

Binding reactions were initiated under the same conditions as described in Figure 7. Reaction temperatures were 18° C for Figures 8A and 8B, and 35 °C for Figure 8C. Following complex formation, 20 µl samples were added to heparin (final concentration 50 µg/ml). Panel A. After the heparin challenge, the samples were vortexed from 0 - 5 s, and analyzed by gel retardation as described in the Materials and Methods. Results were expressed as the fraction (F) of total DNA which remained in heparin resistant complexes with RNA polymerase after a given time of sample vortexing, and a plot of Ln(100*F) versus time is shown. The observed dissociation rate constant (k_{obs}) was calculated as described in Figure 7 (k_{obs} = 3.11 x 10^{-2} s^{-1}). Panel B. Samples were added to heparin at intervals over a 19 min period, and loaded immediately onto a 4% polyacrylamide gel (1 x TBE) running at 17 volts/cm. After the last sample was applied to the gel, electrophoresis was continued for one minute. The gel-wells were then thoroughly rinsed to remove any DNA that had not yet entered the gel matrix. Results were expressed as the cpm recovered versus the time of sample electrophoresis. The cpm recovered equals the radioactivity recovered from the gel slices divided by the radioactivity added to the well. Panel C. Samples were added to heparin at intervals over a 20 min period, loaded into separate polyacrylamide gel wells (1 x TBE, gel buffer temperature 22° C), and allowed to remain there prior to the onset of electrophoresis. Electrophoresis was initiated immediately following the application of the last sample. Results were expressed as the fraction (F) of total DNA which remained in heparin resistant complexes with RNA polymerase after a given time of sample residence in the gel-well, and a plot of Ln(100*F) versus time is shown. The observed dissociation rate constant (k_{obs}) was calculated as described in Figure 7 (k_{obs} = – 4.39 x 10^{-5} s^{-1}).

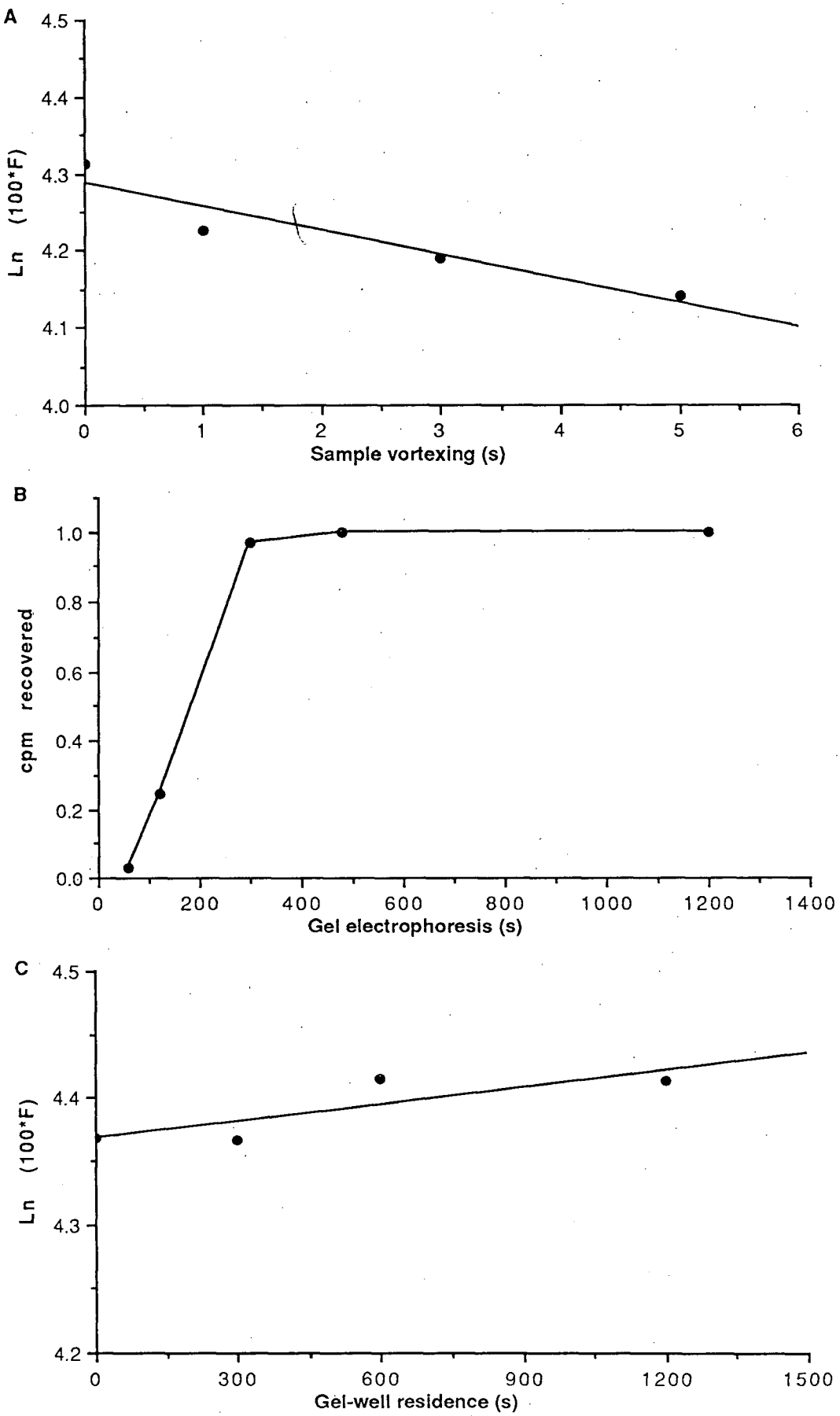
A
4.5
4.4
4.3
4.2
4.1
4.0
Ln (100*F)
0
1
2
3
4
5
6
Sample vortexing (s)
B
1.0
0.8
0.6
0.4
0.2
0.0
cpm recovered
0
200
400
600
800
1000
1200
1400
Gel electrophoresis (s)
C
4.5
4.4
4.3
4.2
Ln (100*F)
0
300
600
900
1200
1500
Gel-well residence (s)

Most complexes, even those involving low affinity protein/DNA associations, appear to be stabilized within the gel matrix during electrophoresis (Garner and Revzin, 1981; Fried and Crothers, 1981). This can be seen in Figure 3, where bound complexes (RP) exist as distinct bands, and display none of the 'smearing' effects that are indicative of complex dissociation. However, prior to entering the gel matrix, the sample must sit in the electrophoresis buffer of the gel well. The following experiments determine whether the exposure of the sample to the electrophoresis buffer destabilized complexes in the gel well.

To determine the time it takes a sample to enter the gel matrix, polymerase/promoter complexes were formed as described above in the dye stability experiments. Samples were removed to a heparin challenge at intervals over a 19 min period, and loaded immediately onto a 4% polyacrylamide gel (1x TBE) running at 17 volts/cm. After the last sample was applied to the gel, electrophoresis was continued for one minute, and then the gel-wells were thoroughly rinsed to remove any residual complexes that had not yet entered the gel matrix. Results were expressed as the fraction of total radioactivity added to the well which had entered the gel after electrophoresis for a given length of time. As Figure 8B shows, it took 5 minutes for complexes between polymerase and the BP2 promoter (449 bp) to completely enter the standard 4% polyacrylamide gel.

Figure 8C shows data on the stability of complexes in the gel electrophoresis buffer (1x TBE) during the time it takes the sample to enter the gel matrix. Initial complexes were formed as described in the dye stability experiments, except that the reaction temperature was 35° C. Samples were removed to a heparin challenge at intervals over a 20 min period, loaded into separate polyacrylamide gel wells (gel buffer temperature 22° C) and allowed to remain there prior to the onset of electrophoresis. Electrophoresis was initiated immediately following the application of the last sample, and heparin resistant complexes were identified and measured as described in the dye stability experiment. As can be seen, there was a

minimal enhancement of complex formation during the residence time of the sample in the gel running buffer. However, over the 5 minutes it took the sample to enter the gel (Fig 8B), this enhancement would contribute a maximum of a 1% error to complex measurements, and was considered negligible for the purpose of these investigations.

In summary, RNA polymerase holoenzyme interactions with a DNA template are directed towards a given promoter sequence, and are not due to non-specific interactions. Secondly, at 80 mM KCl, the addition of heparin prevents any further complex formation from occurring, irreversibly binding free RNA polymerase at a rate that is much faster than that of closed complex formation. Finally, heparin resistant polymerase/promoter complexes are stable during all stages of the gel retardation analysis if a loading dye mixture is omitted from the sample. These observations would suggest that the amounts of bound complexes and free promoter measured after gel electrophoresis accurately reflect those same levels formed in solution following heparin addition.

II. Study of polymerase binding at the BP1 and BP2 promoters.

1. Titration of promoters with RNA polymerase.

In order to measure the affinity of the RNA polymerase for the BP1 and BP2 promoters, a fixed amount of promoter template was titrated with increasing concentrations of holoenzyme under standard binding conditions (see Materials and Methods). When present, ppGpp was at a final concentration of 0.1 mM. Following a 10 minute incubation at the reaction temperature, the complexes were challenged with heparin and the binding reactions were analyzed by gel retardation as described in the Materials and Methods. Results were expressed as the fraction (F) of total DNA which formed a heparin resistant complex with RNA polymerase at a given enzyme concentration (R). The relationship between the equilibrium levels of

bound complexes and the concentration of active RNA polymerase is shown in Figures 9 and 10. Often, the results from such a titration experiment can be used to estimate the binding equilibrium constant (K1) for the bimolecular reaction between free RNA polymerase and promoter fragments (for a review, see Appendix A). The value for K1 is derived from a double reciprocal plot of F versus the equilibrium concentration of free RNA polymerase (Appendix A). However, further analysis of the data presented in Figures 9 and 10 was complicated by two factors, which are discussed below in turn.

Firstly, the treatment of a binding reaction at equilibrium is usually based on a single step reaction mechanism involving a simple bimolecular collision between the free reactants (see Appendix A). When isomerizations occur after the bimolecular collision, an assumption is usually made that the concentrations of intermediate complexes are negligible, effectively reducing (from a mathematical standpoint) the overall mechanism down to a single step. However, under conditions where the concentrations of intermediate complexes are significant, then this form of analysis is invalid. To address this problem, the treatment discussed in Appendix A makes no assumptions about the equilibrium concentrations of the reaction intermediates, allowing a full solution for any (n + 1) step mechanism (where $n \geq 1$ represents the number of isomerization steps following the initial bimolecular collision).

Secondly, as the overall equilibrium constant of a reaction increases, the estimation of K1 based on the methods described above becomes subject to large errors. Under conditions of DNA excess, the equilibrium concentration of free RNA polymerase (R), which is proportional to the term $R_T - P_TF$ (Appendix A.III, equation A-9b), approaches zero as the overall equilibrium constant increases, and therefore becomes sensitive to errors in the measurement of the absolute values of F. Consequently, the plots of 1/F versus 1/R display a large amount of scatter between the individual data points (data not shown). Although great care was taken

Figure 9. Saturation of the *B. subtilis rrnB* P1 promoter with RNA polymerase at 15 °C and 35 °C.

A constant amount of DNA template (0.5 nM, derived from pKK115B) was incubated with increasing concentrations of RNA polymerase under standard binding conditions (see Materials and Methods). When present in the reactions, ppGpp (closed symbols) was at a final concentration of 0.1 mM. Absence of ppGpp is denoted by the open symbols. RNA polymerase holoenzyme was obtained from either Batch #233 (circles) or Batch #176 (squares) (see Table III). Following a 10 min incubation at the reaction temperature (Panel A. Reaction temperature was 15 °C. Panel B. Reaction temperature was 35 °C), the complexes were challenged with heparin (final concentration 100 μg/ml) and the binding reactions were analyzed by gel retardation as described in the Materials and Methods. Results were expressed as the fraction (F) of total DNA which formed a heparin resistant complex with RNA polymerase at a given enzyme concentration (R). Error bars associated with enzyme concentration were calculated from the ± 1 S. D. values obtained from the active binding concentrations of the RNA polymerase holoenzyme stocks (Table III; ± 10% and ± 25% for Batch #233 and #176 respectively). Absence of an error bar indicates that the error range was less than the width of the symbol.

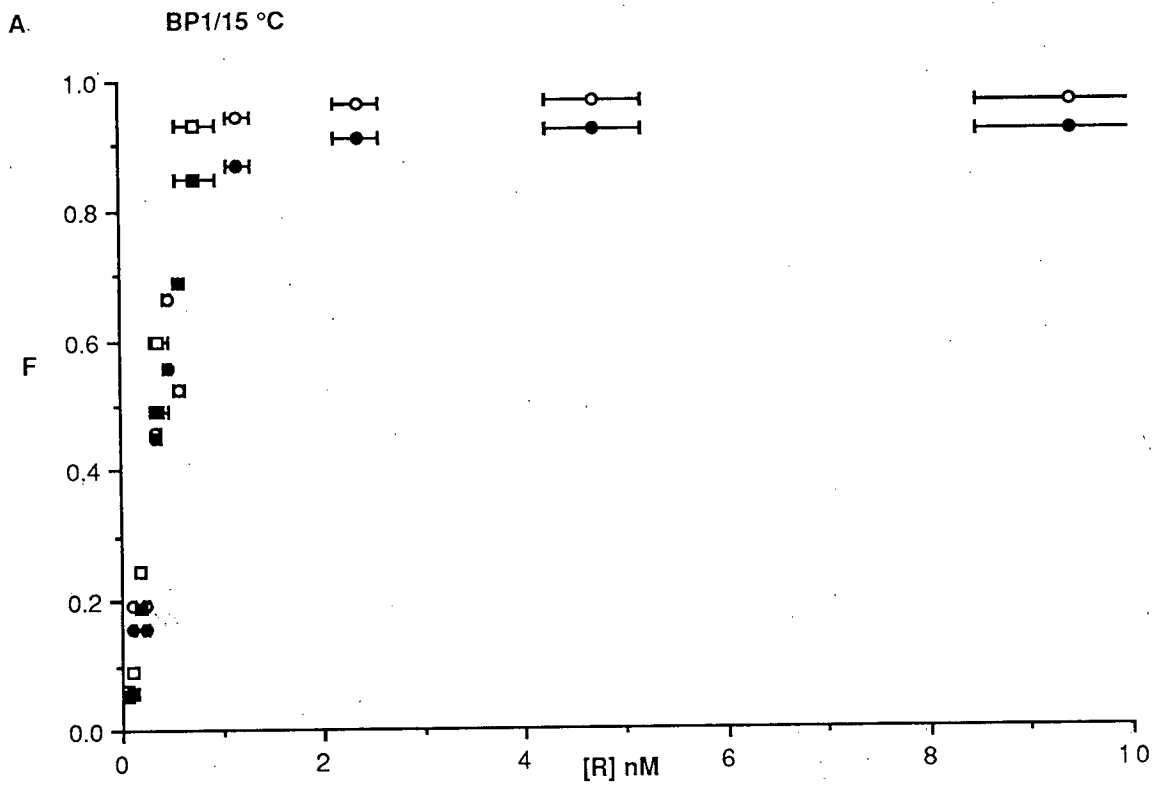
A
BP1/15 °C
F
[R] nM
0.0
0.2
0.4
0.6
0.8
1.0
0
2
4
6
8
10

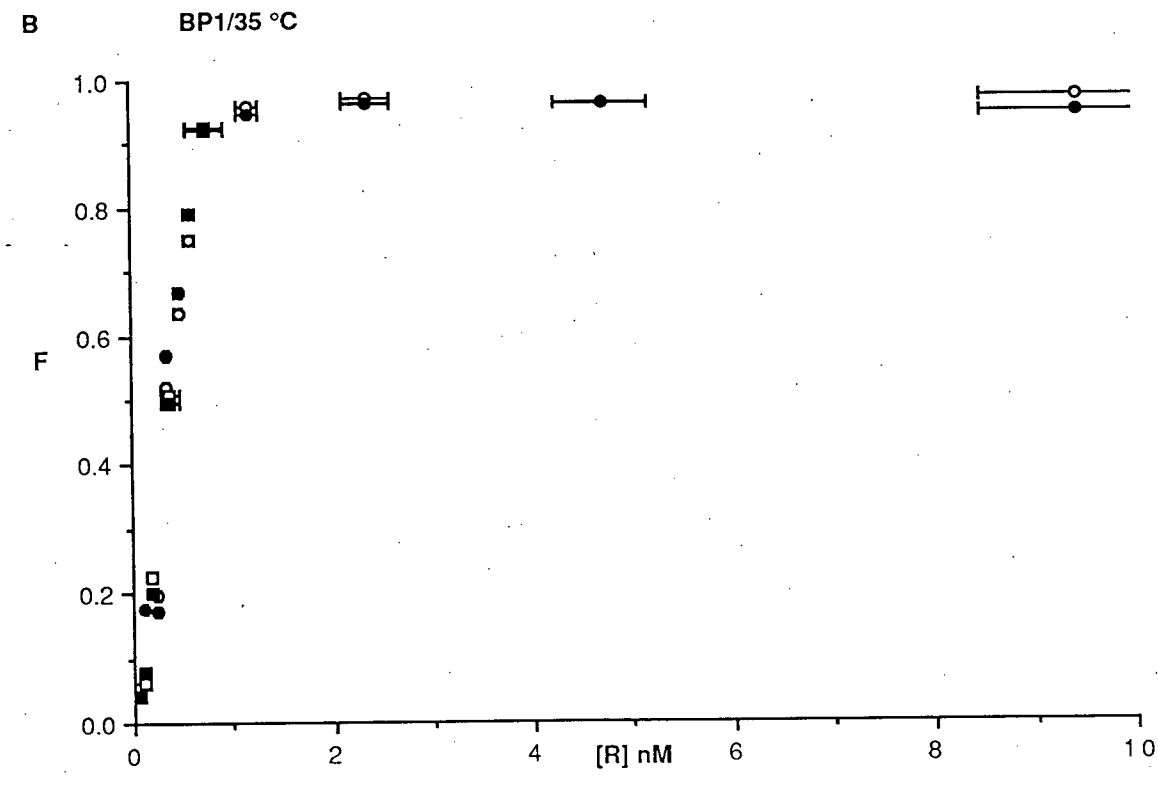
B
BP1/35 °C
F
[R] nM
0.0
0.2
0.4
0.6
0.8
1.0
0
2
4
6
8
10

Figure 10. Saturation of the *B. subtilis rrnB* P2 promoter with RNA polymerase at 10 ° C and 35 °C.

A constant amount of DNA template (0.5 nM, derived from pKK183B) was incubated with increasing concentrations of RNA polymerase as described in Figure 9. For Panel A, the reaction temperature was 10 °C, while for Panel B, the reaction temperature was 35 °C.

A

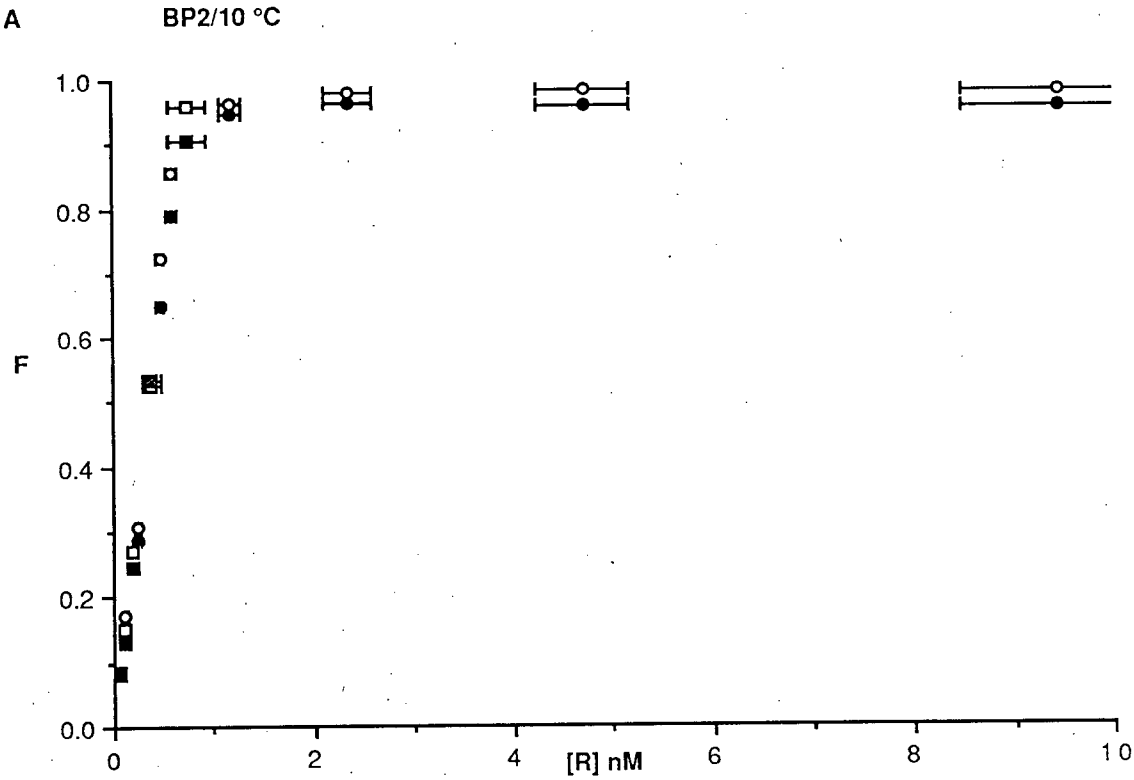
BP2/10 °C
F
[R] nM
0.0
0.2
0.4
0.6
0.8
1.0
0
2
4
6
8
10

B

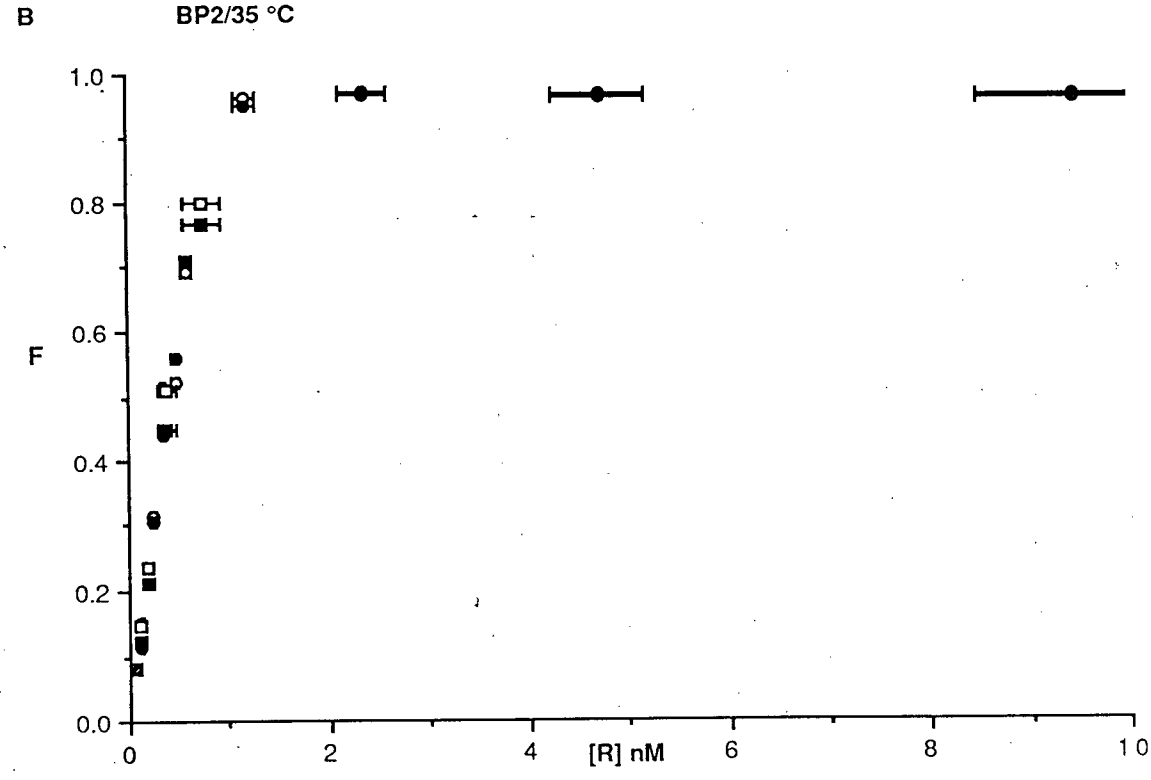
BP2/35 °C
F
[R] nM
0.0
0.2
0.4
0.6
0.8
1.0
0
2
4
6
8
10

to ensure that the gel loading conditions did not disturb the pre-formed complexes (see Results section I.2c above), it is still possible that a systematic decay occurred. For this reason, no great emphasis was placed on the results obtained from these titration experiments. As will be discussed later, rate studies provide a more reliable description of the equilibrium constant, since they use a relative measurement of F, which should obviate any systematic error that may occur during gel loading (Results section 4, and Appendix B.II.1).

Several qualitative conclusions from the titration results can be made. First, the results were very reproducible when using two different holoenzyme preparations (Figs. 9 and 10). Second, the estimated value for K1 was quite high for both the BP1 and BP2 promoters (10^8 - 10^9 M^{-1}), although it was associated with a high error (± 1 S.D. = 40-103%, data not shown). Interestingly, K1 did not appear to change very much with either temperature, or on addition of ppGpp. However, the plateau value of F at saturating levels of polymerase did change, and decreased slightly when ppGpp was added at the lower reaction temperatures (Figs. 9A and 10A). As mentioned in Appendix A.III, this plateau level is a function of the equilibrium position of steps following the bimolecular collision. A more accurate description of these steps is presented in Results sections II.3 and II.4.

2. Partitioning of RNA polymerase between BP1 and BP2.

It has been proposed that ppGpp exerts its effect by altering the equilibrium of RNA polymerase between growth-rate regulated and non-growth-rate regulated promoters (see also Introduction sections II.3 and III.1). This partitioning effect has been suggested based on observations made both *in vivo* (Ryals *et al.*, 1982; Little *et al.*, 1983a, 1983b) and *in vitro* (Travers, 1976; Glaser *et al.*, 1983; Kajitani and Ishihama, 1984). In particular, Kajitani and Ishihama (1984) reported that by employing a mixed-template assay *in vitro*, addition of ppGpp shifted the transcription preference between various growth-rate regulated and non-growth-

rate regulated promoters. To investigate whether ppGpp could alter the binding preference of polymerase between BP1 and BP2, a mixed-template assay was set up using a gel retardation assay.

In the mixed-template experiment, BP1 and BP2 were combined in equimolar amounts and incubated with decreasing concentrations of RNA polymerase under standard binding conditions at 35 ° C (see also Materials and Methods). When present, ppGpp was at a final concentration of 0.1 mM. Figure 11 shows the results of the gel retardation analysis. The difference in size between BP1 (381 bp), and BP2 (449 bp) allowed resolution of the bound complexes at these two promoters. For each promoter in a mixed template binding reaction, results were expressed as the fraction (F) of that promoter's total DNA which was found in heparin resistant complexes with RNA polymerase at a given enzyme concentration (R). These results are summarized in Table IV.

The addition of ppGpp at 35° C had no dramatic effect on the equilibrium position for either BP1 or BP2 in the mixed template assays (Table IV), confirming the independent promoter results obtained in Results section II.1 (see Figs. 9B and 10B). To investigate whether ppGpp had a differential effect on polymerase/promoter complex formation, the value of F obtained for each promoter under a particular reaction condition was expressed as a ratio between BP2 and BP1 (i.e. $F_{(BP2)}/F_{(BP1)}$). The term $(F_{(BP2)}/F_{(BP1)})$ was then compared between + ppGpp and – ppGpp conditions, and this final ratio is reported in the fourth column of Table IV. If there was no differential effect of ppGpp on the partitioning of RNA polymerase between the growth rate versus the non growth rate regulated promoters, the ratio of the term $(F_{(BP2)}/F_{(BP1)})$ under ± ppGpp conditions would have a value of 1.00. As can be seen in Table IV, the ratio was 1.00 for all concentrations of polymerase tested. These results suggest that ppGpp does not effect the overall equilibrium partitioning of heparin-resistant complex formation between BP2 and BP1 as measured by gel retardation, even under conditions of

Figure 11. Partitioning of RNA polymerase between the *B. subtilis rrnB* P1 and P2 promoters.

DNA fragments containing the *B. subtilis rrnB* P1 (BP1 derived from pKK115B) and P2 (BP2 derived from pKK183B) promoters were combined in equimolar amounts (0.5 nM each) and incubated with decreasing concentrations of RNA polymerase under standard binding conditions (Materials and Methods). When present in the reactions, ppGpp was at a final concentration of 0.1 mM. Following a 10 minute incubation at 35 °C, the complexes were challenged with heparin (final concentration 100 μg/ml), and the binding reactions were immediately loaded onto a 4% polyacrylamide gel (1 x TBE) running at 17 volts/cm (see Materials and Methods). Figure 11 shows a picture of the autoradiograph of this gel retardation analysis. The positions of heparin resistant complexes (RP) and unbound promoter fragments (P) are indicated to the left of the figure for both the BP1 and BP2 templates. In control experiments (Lanes 1 and 2), binding reactions contained either BP1 or BP2 respectively, without added RNA polymerase. For the experiments in Lanes 3 and 4, binding reactions contained either BP1 or BP2 respectively, with RNA polymerase present at a final concentration of 5.0 nM. Lanes 5 - 12: Binding reactions contained both BP1 and BP2 templates. Reactions loaded onto odd and even numbered lanes were performed in the absence and presence of ppGpp respectively. RNA polymerase was present at the following concentrations: Lanes 5, 6: 5.0 nM. Lanes 7, 8: 1.0 nM. Lanes 9, 10: 0.5 nM. Lanes 11, 12: 0.25 nM.

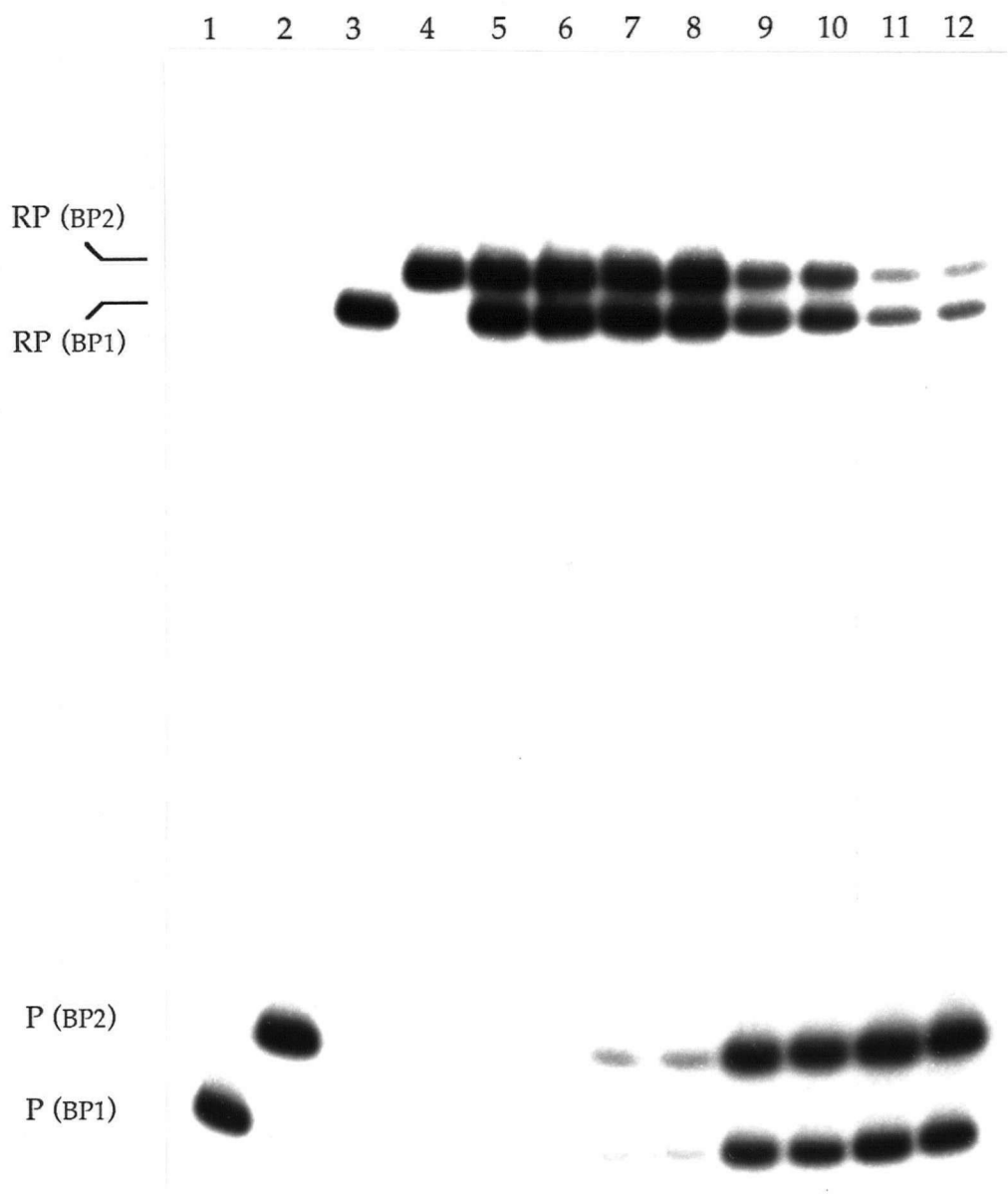
1 2 3 4 5 6 7 8 9 10 11 12
RP (BP2)
RP (BP1)
P (BP2)
P (BP1)

Table IV. Partitioning of RNA polymerase between the *B. subtilis rrnB* P1 and P2 promoters.

nM Polymerase (R) ± ppGpp	$F_{(BP2)}$	$F_{(BP1)}$	Relative partitioning [a]
BP1 (R = 0)		0	
BP2 (R = 0)	0		
BP1 (R = 5.0)		0.96	
BP2 (R = 5.0)	0.96		
5.0 –	0.96	0.96	1.01
5.0+	0.97	0.96	
1.0 –	0.87	0.92	0.99
1.0 +	0.86	0.92	
0.5 –	0.39	0.52	0.99
0.5 +	0.41	0.55	
0.25 –	0.23	0.31	0.99
0.25 +	0.22	0.30	

The data for Table IV was obtained from Figure 11. For each promoter in a mixed template binding reaction, results were expressed as the fraction (F) of that promoter's total DNA which was found in heparin resistant complexes with RNA polymerase at a given enzyme concentration (R). Results from binding reactions which contained only the individual BP1 or BP2 promoters (Lanes 1 - 4 of Figure 11) were also included in Table IV. The presence (+) or absence (–) of ppGpp in a binding reaction is noted accordingly.

a) The value of F obtained for each promoter under a particular reaction condition was expressed as a ratio between BP2 and BP1 (i.e. $F_{(BP2)}/F_{(BP1)}$). The term $(F_{(BP2)}/F_{(BP1)})$ was then compared between (+ ppGpp)/(– ppGpp) conditions.

limiting RNA polymerase. However, without affecting the equilibrium position at these promoters, ppGpp might still exert differential control by altering the absolute rates of heparin-resistant complex formation and decay. This possibility is considered in the following sections.

3. Dissociation rates of polymerase from BP1 and BP2.

As discussed in Appendix B.II.2, the irreversible conversion of heparin-resistant (HR) complexes into a heparin-sensitive (HS) state can be described by

$$HR \xrightarrow{k_d} HS \qquad (3)$$

where k_d is the overall dissociation rate constant, and the time-dependent concentration of HR is related to the initial (time zero) concentration according to

$$Ln[HR] = -(k_d)\, t + Ln[HR]_0 \qquad (4)$$

There were four main objectives of the studies in this section. First, equations 3 and 4 assume that the interaction of heparin with the heparin-sensitive complex was irreversible, and that the conversion of heparin resistant complexes to a heparin sensitive state was limited by a single reaction step (see also Appendix B sections II.2 and V). Note that the ability of heparin to irreversibly bind free RNA polymerase (Results section I.2b) does not guarantee that this competitor will interact as effectively with other heparin sensitive complexes which might occur in the overall reaction mechanism (equation 3). However, the above assumptions could be tested by investigating whether the dissociation plots of heparin resistant complexes versus reaction times were linear when analyzed according to equation 4. Second, it was important to determine whether the observed dissociation rate constant (k_{obs}) was 'intrinsic' to a given polymerase/promoter complex (i.e. $k_{obs} = k_d$), or whether there were contributions to this observed dissociation rate constant which originated from other sources. Third, additional information regarding the dissociation reaction mechanism could be obtained from a

thermodynamic analysis of k_d. From such studies, the minimum number of heparin resistant and heparin sensitive complexes could be estimated, and k_d could be interpreted as a function of the individual forward and reverse rate constants which defined this minimum dissociation mechanism (see Appendix B.II and B.III). The final objective was to determine whether ppGpp could exert a differential effect on the dissociation rate of polymerase from the BP1 and BP2 promoters.

3a. Observed dissociation rates.

The object of the studies in this section was to measure the rate constant k_{obs}, and determine whether the assumptions of equation 4 were met under the assay conditions of this thesis. To measure the dissociation rates of polymerase/promoter complexes, a large reaction stock of RNA polymerase and promoter fragment was mixed under standard conditions (Materials and Methods) and allowed to equilibrate for 10 min at the reaction temperature. At time zero, heparin was added (see Results sections II.3b and II.3d for concentrations) and, after a brief vortex, the stock was returned to the reaction temperature. Samples were removed at intervals, and analyzed by gel retardation as described in the Materials and Methods. Results were expressed as the fraction (F) of total DNA which remained in a heparin resistant complex with RNA polymerase at a given time following heparin addition.

A plot of Ln(100*F) versus time is shown in Figures 12 and 13, and the corresponding observed dissociation rate constants, together with error estimates (± 1 S. D.), are summarized in Table V (k_{obs}). As can be seen from Figures 12 and 13, the observed dissociation rates were linear over the reaction timecourse, which in some cases represented over 80% dissociation of initial complexes (Ln(100*F) = 3.0). As Figure 13 shows, the rate of dissociation was highly reproducible between two independent enzyme preparations (see BP2/15°/± ppGpp). Indeed, the standard deviation calculations in Table V indicate that, except for three reactions, k_{obs} values

Figure 12. Dissociation rate of RNA polymerase from the *B. subtilis rrnB* P1 promoter at various temperatures.

A binding reaction of RNA polymerase (final concentration 2.5 nM) and promoter fragment (0.5 nM of *B. subtilis rrnB* P1 derived from pKK115B) was mixed under standard conditions (Materials and Methods) and allowed to equilibrate for 10 min at the reaction temperature (15 - 35 °C). Unless otherwise specified in the figure insets, RNA polymerase was from Batch #233. At time zero, heparin (final concentration 50 μg/ml) was added, and after a brief vortex, the mixture was returned to the reaction temperature. Samples were removed at intervals, and analyzed by gel retardation as described in the Materials and Methods. Results were expressed as the fraction (F) of total DNA which remained in heparin resistant complexes with RNA polymerase at a given time following the addition of heparin, and a plot of Ln(100*F) versus time is shown. The lines through each data set were calculated by linear least-squares analysis, and the slopes from these lines yielded the observed dissociation rate constants (k_{obs}). The reaction temperatures are summarized in the figure insets, and the values for k_{obs} (± 1 S. D.) are reported in Table V. Panel A. Dissociation experiments were performed in the absence of ppGpp. Panel B. Dissociation experiments were performed in the presence of ppGpp (final concentration 0.1 mM).

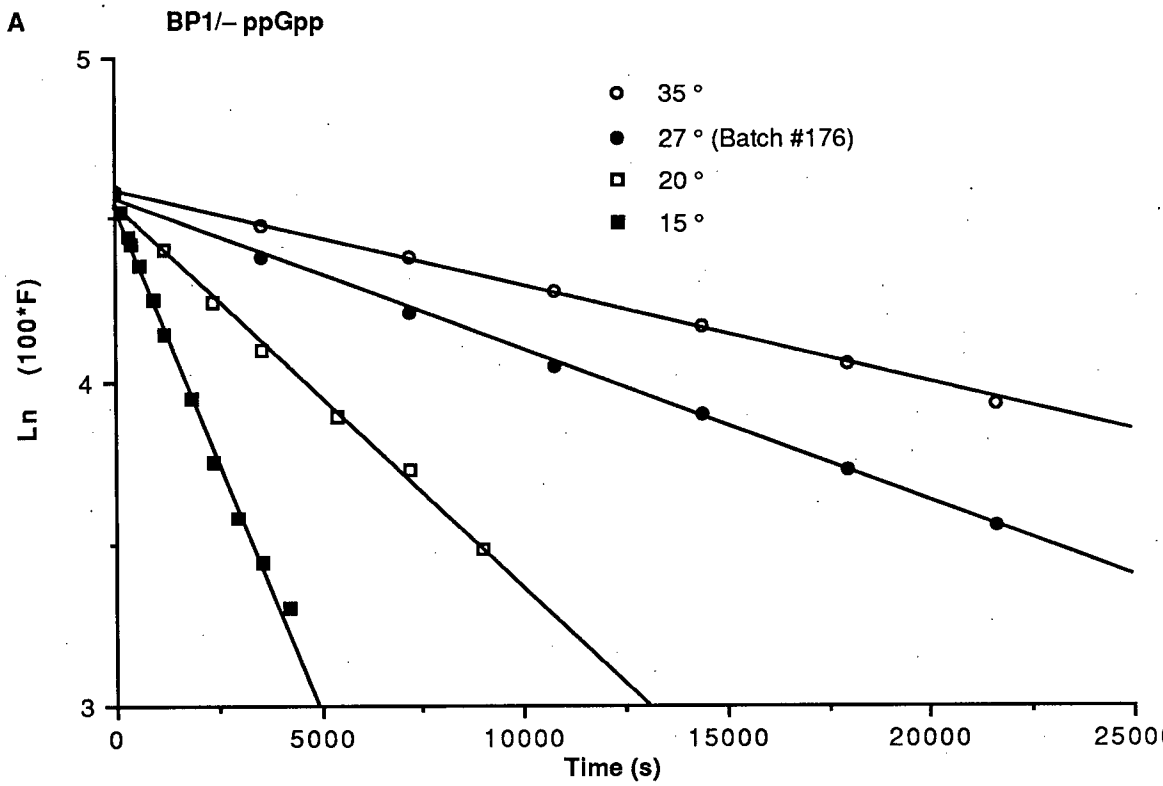
A
BP1/– ppGpp
35 °
27 ° (Batch #176)
20 °
15 °
Ln (100*F)
5
4
3
0
5000
10000
15000
20000
25000
Time (s)

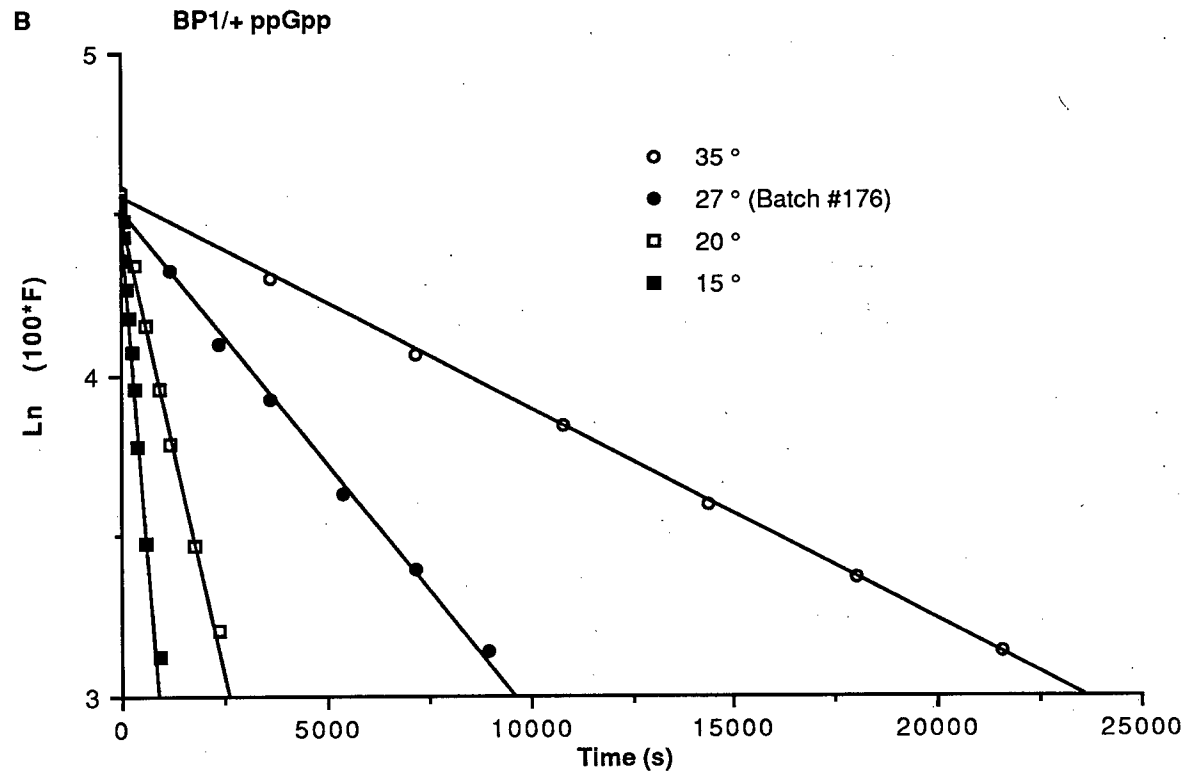
B
BP1/+ ppGpp
35 °
27 ° (Batch #176)
20 °
15 °
Ln (100*F)
5
4
3
0
5000
10000
15000
20000
25000
Time (s)

Figure 13. Dissociation rate of RNA polymerase from the *B. subtilis rrnB* P2 promoter at various temperatures.

Dissociation rate experiments were performed as described in Figure 12, using DNA templates derived from pKK183B. Reactions at 15 °C were performed in duplicate, using RNA polymerase from either Batch #233 (closed circles) or #176 (open circles) (see also Table III). To calculate the dissociation rate constant (k_{obs}) at 15 °C, the results from the two enzyme preparations were treated as a single data set. The reaction temperatures are summarized in the figure insets, and the values for k_{obs} (± 1 S. D.) are reported in Table V. Panel A. Dissociation experiments were performed in the absence of ppGpp. Panel B. Dissociation experiments were performed in the presence of ppGpp (final concentration 0.1 mM).

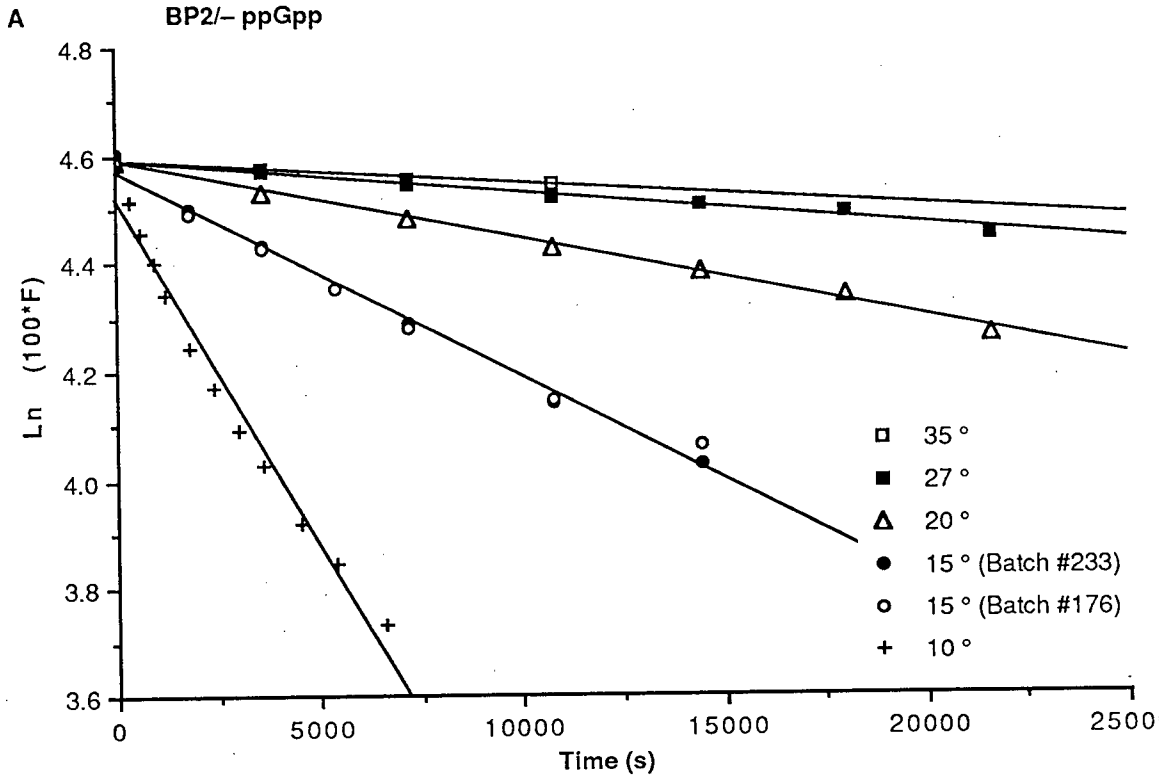
A
BP2/– ppGpp
4.8
4.6
4.4
4.2
4.0
3.8
3.6
Ln (100*F)
0
5000
10000
15000
20000
25000
Time (s)
35 °
27 °
20 °
15 ° (Batch #233)
15 ° (Batch #176)
10 °

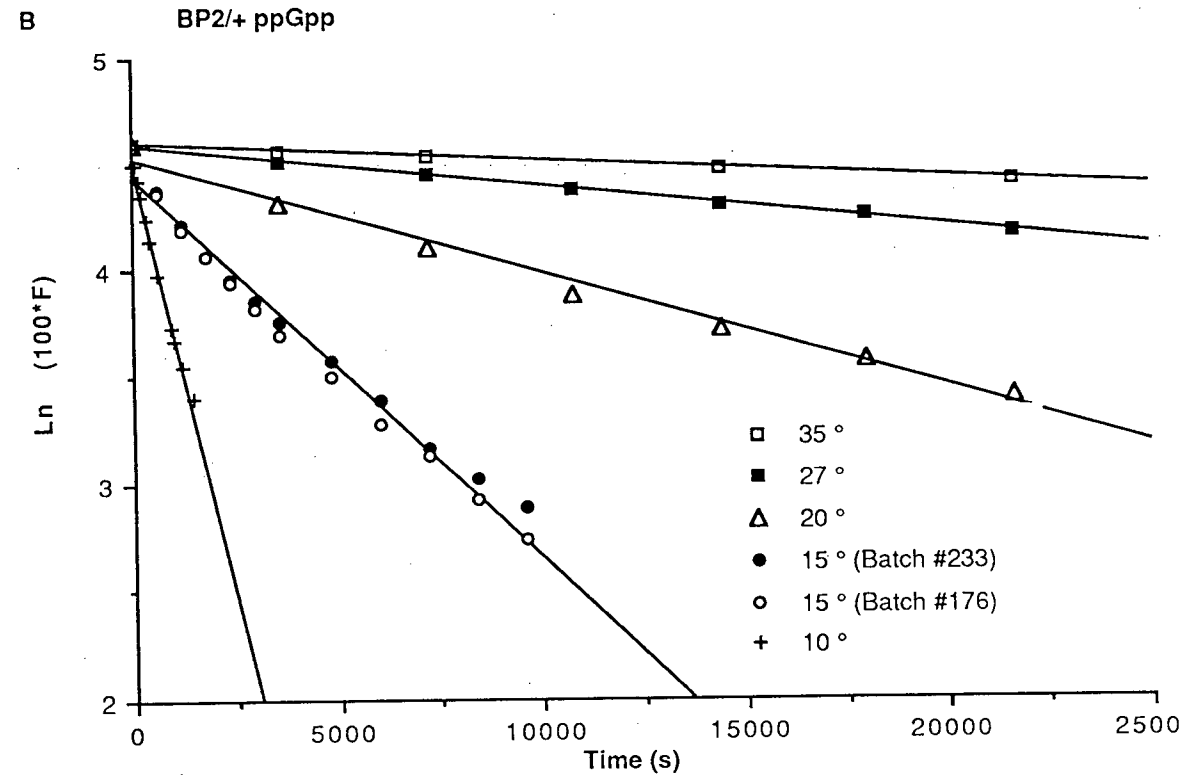
B
BP2/+ ppGpp
5
4
3
2
Ln (100*F)
0
5000
10000
15000
20000
25000
Time (s)
35 °
27 °
20 °
15 ° (Batch #233)
15 ° (Batch #176)
10 °

Figure 14. Heparin dependence of the dissociation rate of RNA polymerase from the *B. subtilis rrnB* P1 promoter at 35 °C.

Panels A and B. Dissociation rate experiments were performed as described in Figure 12, at a reaction temperature of 35 °C. The final concentrations of heparin which were added to the reactions are summarized in the figure insets, and the corresponding observed dissociation rate constants are indicated below. The dissociation reactions illustrated in Panels A and B were performed in the respective absence and presence of ppGpp (final concentration 0.1 mM).

[Heparin] (μg/ml)	Panel A (– ppGpp) k_{obs} (s^{-1})	Panel B (+ ppGpp) k_{obs} (s^{-1})
50	3.0×10^{-5}	6.6×10^{-5}
100	4.2×10^{-5}	9.0×10^{-5}
200	6.1×10^{-5}	1.1×10^{-4}

Panel C. The observed dissociation rate constants from Panels A (open circles) and B (closed circles) were plotted against their corresponding heparin concentrations. The lines through each data set were calculated by linear least-squares analysis, and the ordinate value at zero heparin (Y-axis intercept) yielded the 'intrinsic' dissociation rate constant (k_d). The values for k_d (± 1 S. D.) are reported in Table V.

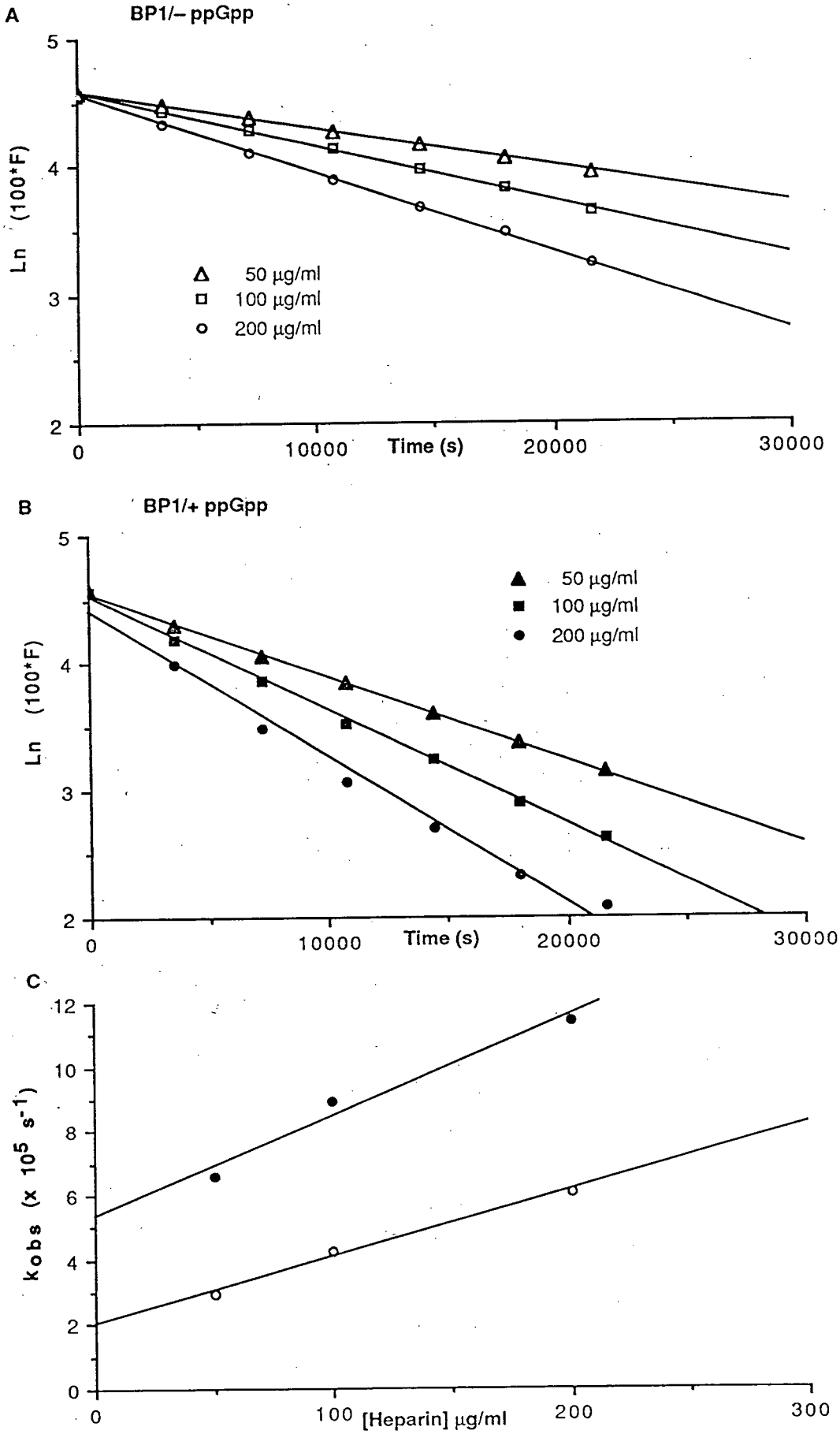
A
BP1/– ppGpp
Ln (100*F)
5
4
3
2
0
10000
Time (s)
20000
30000
50 µg/ml
100 µg/ml
200 µg/ml
B
BP1/+ ppGpp
Ln (100*F)
5
4
3
2
0
10000
Time (s)
20000
30000
50 µg/ml
100 µg/ml
200 µg/ml
C
kobs (x 10^5 s^-1)
12
10
8
6
4
2
0
0
100
[Heparin] µg/ml
200
300

Table V. Dissociation and inactivation rates of RNA polymerase from the *B. subtilis rrnB* P1 and P2 promoters at various temperatures.

Temperature (°C)		BP1 (- ppGpp) s^{-1}	BP1 (+ ppGpp) s^{-1}	BP1 (+/-) ppGpp ratio	BP2 (- ppGpp) s^{-1}	BP2 (+ ppGpp) s^{-1}	BP2 (+/-) ppGpp ratio
35	k_{obs} [a]	2.9×10^{-5}	6.6×10^{-5}	2.2	$4.4 \pm 0.8 \times 10^{-6}$	8.3×10^{-6}	
	k_d [b]	$2.0 \pm 0.2 \times 10^{-5}$	$5.3 \pm 0.7 \times 10^{-5}$		$3.2 \pm 0.5 \times 10^{-6}$	4.6×10^{-6}	
	c	$2.4 \pm 1.1 \times 10^{-6}$	$2.9 \pm 0.7 \times 10^{-6}$		$5.3 \pm 1.0 \times 10^{-6}$	$3.4 \pm 1.4 \times 10^{-6}$	
	d				6.9×10^{-7}	3.1×10^{-6}	4.5
27	k_{obs} [a]	4.7×10^{-5}	1.6×10^{-4}	3.4	$6.1 \pm 0.4 \times 10^{-6}$	1.9×10^{-5}	
	d				3.3×10^{-6}	1.6×10^{-5}	4.8
20	k_{obs} [a]	1.2×10^{-4}	5.6×10^{-4}	4.7	1.4×10^{-5}	5.4×10^{-5}	3.9
15	k_{obs} [a]	3.1×10^{-4}	1.6×10^{-3}	5.2	3.8×10^{-5}	1.8×10^{-4}	4.7
	k_d [b]	$2.1 \pm 0.6 \times 10^{-4}$	$1.3 \pm 0.6 \times 10^{-3}$				
	c	$7.0 \pm 1.7 \times 10^{-6}$	$2.4 \pm 0.2 \times 10^{-5}$		$0.7 \pm 1.5 \times 10^{-6}$	$3.3 \pm 1.2 \times 10^{-6}$	
10	k_{obs} [a]				1.3×10^{-4}	$8.1 \pm 0.5 \times 10^{-4}$	6.2
	k_d [b]				$1.0 \pm 0.4 \times 10^{-4}$	$6.7 \pm 3.2 \times 10^{-4}$	

Unless specified, the error in measurement (± 1 S. D.) of the rate constants listed in rows 'a - d' was < 5%.

a) Observed dissociation rates (k_{obs}) were measured at 50 µg/ml heparin (see Figs. 12 and 13).

b) Intrinsic dissociation rates (k_d) were calculated from the zero-heparin ordinate values extrapolated from plots of k_{obs} versus heparin concentration (see Fig. 14C).

c) The rate of RNA polymerase inactivation was measured as described in Results section II.3c.

d) The dissociation rates of polymerase/BP2 complexes at 35 °C and 27 °C were estimated by extrapolating the Arrhenius plots of the temperature dependences of k_{obs} for BP2 (see Fig. 15B). These extrapolated rate constants were also used to determine the (+/-) ppGpp ratio for BP2 at 35 °C and 27 °C.

obtained at 50 μg/ml heparin had associated errors of less than 5%, and that no error exceeded 20%. Together, these results indicate that at BP1 and BP2, the conversion of polymerase complexes to a heparin sensitive form was irreversible, and that a single step limited the overall dissociation mechanism.

3b. Dissociation rate versus heparin concentration.

The term 'heparin resistant' often refers to a comparative stability with respect to other complexes. Both Cech and McClure (1980) and Pfeffer *et al.* (1977) have demonstrated that the dissociation rates of certain heparin resistant complexes are dependent on the absolute heparin concentration, indicating that these polymerase/promoter interactions are subject to direct heparin attack. Figure 14 shows the response of the dissociation rate of polymerase from the BP1 promoter to varying heparin concentrations. In either the absence (Fig. 14A) or presence (Fig. 14B) of ppGpp, the observed decay rate increased with increasing heparin concentrations. This same dependency was observed for both the BP1 and BP2 promoters at both high and low reaction temperatures (primary data not shown, but for a given reaction condition, compare rows 'k_{obs}' and 'k_d' in summary Table V). This is similar to the findings reported by Cech and McClure (1980) and Pfeffer *et al.* (1977), and suggests that the polymerase in complexes at these two promoters is subject to direct heparin attack.

If the observed dissociation rate constants are plotted as a function of heparin concentration, then the 'intrinsic' dissociation rate can be calculated from the ordinate value at zero heparin (Y-axis intercept). This is illustrated for BP1 in Figure 14C, and summarized for both BP1 and BP2 in Table V (rows 'k_d' at 35°, 15°, and 10° C). Comparison of the observed dissociation rate constants at 50 μg/ml heparin (k_{obs}) to the calculated intrinsic dissociation rate constants (k_d) show that the average discrepancy between these two values was 40% (for a given reaction condition, compare rows 'k_{obs}' and 'k_d' in summary Table V). Similar findings

were made by Cech and McClure (1980) during the study of polymerase complex formation at bacteriophage T7 early promoters. Following their interpretation, the discrepancy between k_{obs} and k_d suggests that direct heparin attack occurs slowly relative to the intrinsic dissociation rate at both the BP1 and BP2 promoters.

3c. Rate of polymerase inactivation.

In the absence of ppGpp at 35° C, Table V (row 'k_{obs}') shows that the observed dissociation rates for polymerase/promoter complexes at 50 μg/ml heparin were very slow (Half life ≈ 7 - 44 h). To ensure that these observed decay rates were not due to enzyme inactivation over the course of the 6 hour assay, the rate of complex dissociation was measured in the absence of heparin, under conditions of DNA excess (promoter template = 0.5 nM, polymerase = 0.25 nM). Except for BP2/35° C, the rate of enzyme breakdown was always slower than the observed dissociation rate by a factor of 12 - 67 fold (see Table V rows 'k_{obs}' versus 'c'). This suggests that enzyme inactivation did not contribute to k_{obs} under any condition for BP1, or at the lower reaction temperatures (< 27° C) for BP2.

At the higher reaction temperatures for BP2, where the rate of enzyme inactivation contributed significantly to the observed dissociation rate of heparin resistant complexes, the intrinsic dissociation rates of heparin resistant complexes could not be accurately determined. It was decided that if the rate of enzyme inactivation contributed > 40% towards the observed dissociation rate at 50 μg/ml heparin (k_{obs}), then those k_{obs} values would not be used in subsequent analyses of either ppGpp or temperature effects. This meant that k_{obs} results obtained for BP2/35°/± ppGpp and BP2/27°/– ppGpp were discarded. For these three conditions, the intrinsic dissociation rate constants were estimated from extrapolation of the BP2/± ppGpp Arrhenius plots (see below).

3d. The temperature dependence of the observed dissociation rate constant.

The measurement of a single heparin resistant complex does not guarantee that such a complex represents a homogeneous population. There may be several heparin resistant complexes in the overall reaction mechanism corresponding to different reaction intermediates. Unless dramatic conformational differences exist between these heparin resistant isomers, they will not be separated by electrophoresis, and only one polymerase/promoter complex will be observed following gel retardation analysis. However, determining a secondary function of the observed single heparin resistant complex, such as the activation energy of dissociation, can often 'uncover' these physically hidden reaction intermediates (Kadesch *et al.*, 1982; Rosenberg *et al.*, 1982; Buc and McClure, 1985; Roe *et al.*, 1984, 1985; Duval-Valentin and Ehrlich, 1987).

In order to calculate the activation energy of dissociation, an Arrhenius plot (see also Appendix C) was made of the observed dissociation rate constants and absolute reaction temperatures from the data compiled in Table V. As discussed in section 3c, the results for BP2/35°/± ppGpp and BP2/27°/– ppGpp were not included, because it was determined that these values primarily reflected enzyme inactivation rates as opposed to the intrinsic dissociation rates of heparin resistant complexes. For the remaining results of Table V, the observed dissociation rate constants obtained at 50 μg/ml heparin (k_{obs}) were used as data points. In section 3b, it was determined that values for k_{obs} overestimated the intrinsic dissociation rate constants (k_d) by approximately 40% (see also Table V). However, the natural log function of the Arrhenius plot tends to reduce the discrepancy between k_{obs} and k_d (i.e. $Ln(k_{obs})/Ln(k_d) < k_{obs}/k_d$, also see Fig. 15). As a result, calculating the slope of the Arrhenius plot from k_{obs} values was felt to be an accurate reflection of the temperature dependence of the intrinsic dissociation rate of heparin resistant complexes at these promoters. Indeed, for the rate values and temperatures reported here, in no instance did the difference between the estimated maximum

Figure 15. Arrhenius plot of the temperature dependence of the dissociation rates of RNA polymerase from the *B. subtilis rrnB* P1 and P2 promoters.

The data for Figure 15 was taken from Table V. The natural log of the observed dissociation rate constants (k_{obs}) obtained at 50 μg/ml heparin (squares) were plotted against the reciprocal of their absolute reaction temperatures (Kelvin). An Arrhenius plot was also made using the intrinsic dissociation rate constants (k_d) (circles), however these points were not included during the linear least-squares analysis (see below). The absence and presence (final concentration 0.1 mM) of ppGpp during the dissociation experiments is indicated by open and closed symbols respectively. The lines through each data set were calculated by linear least-squares analysis, and the slopes from these lines were used to determine the activation energies of dissociation ($E_{a,d}$) as described in Appendix C (see also Table IX). Panel A. Arrhenius plot of the temperature dependence of complex dissociation at *B. subtilis rrnB* P1. Panel B. Arrhenius plot of the temperature dependence of complex dissociation at *B. subtilis rrnB* P2. Data from the 35 °C and 27 °C (- ppGpp) dissociation rate experiments were not included in Panel B, because it was determined that these values primarily reflected enzyme inactivation rates as opposed to the dissociation rates of heparin resistant complexes (see Results section II.3c and Table V).

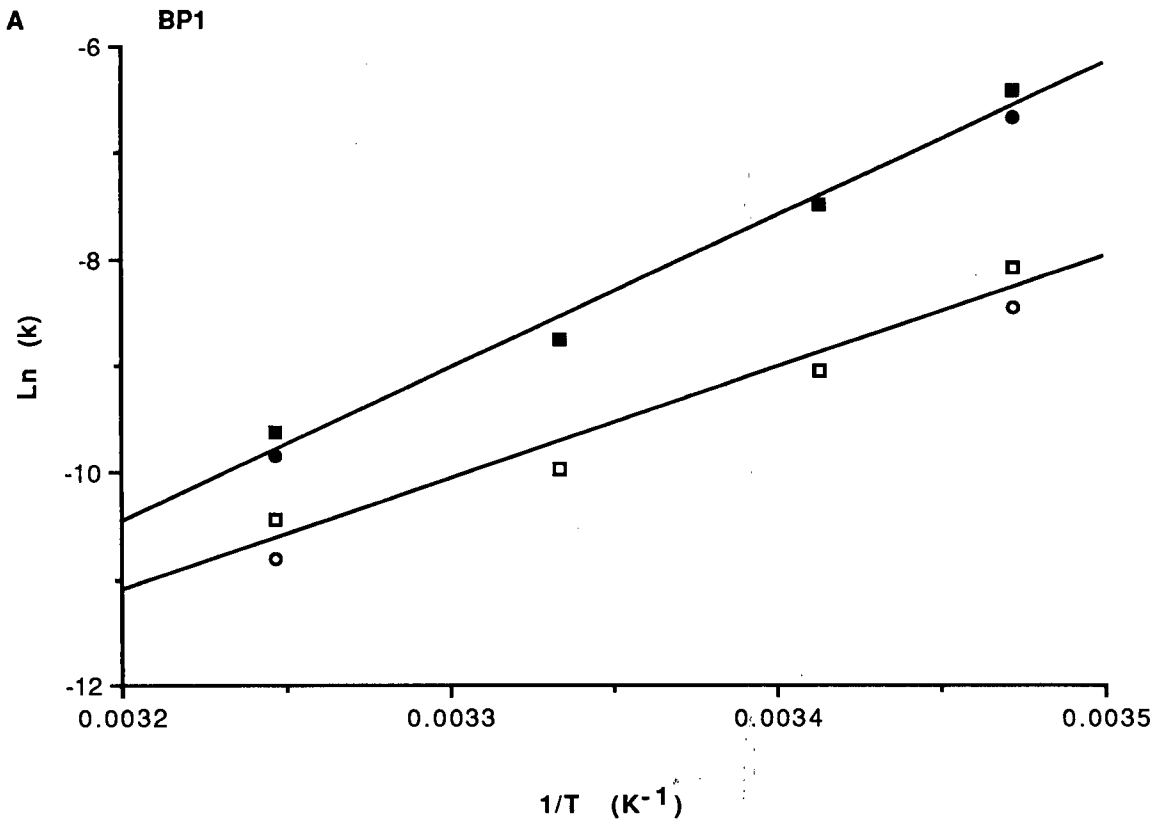
A
BP1
-6
-8
-10
-12
Ln (k)
0.0032
0.0033
0.0034
0.0035
1/T (K-1)

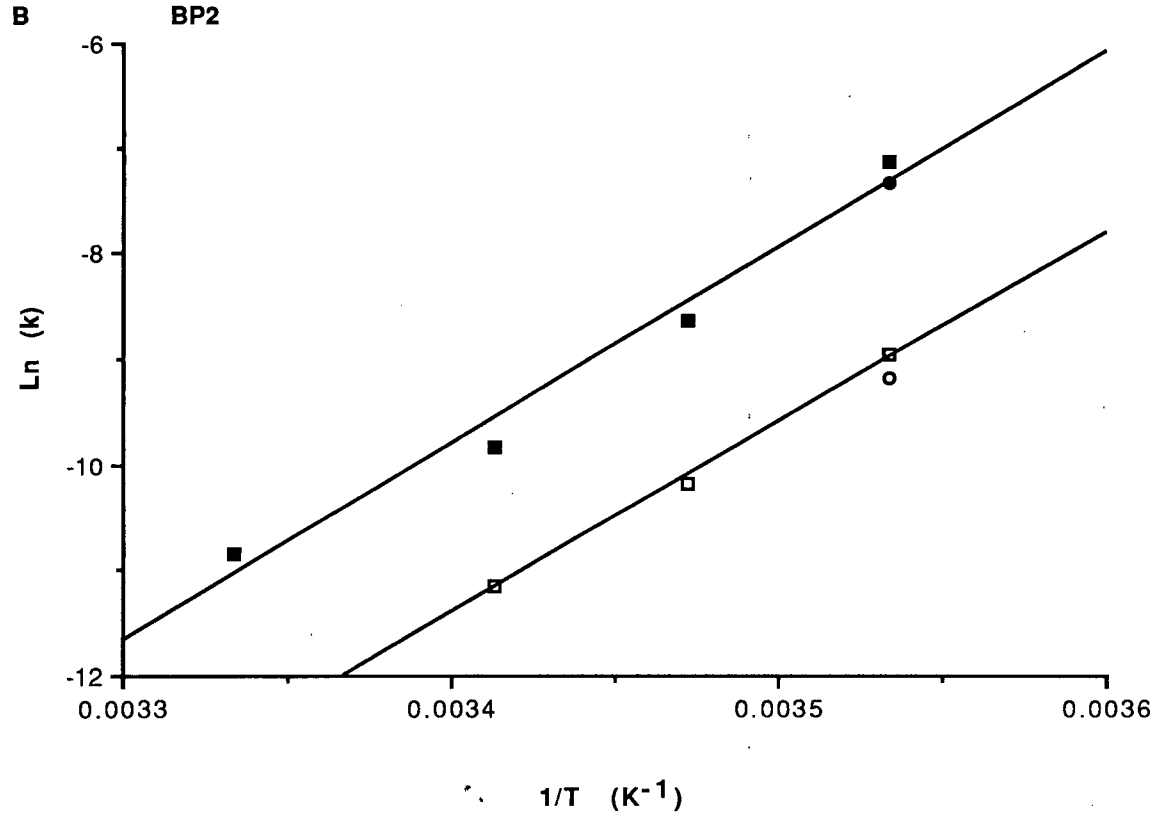
B
BP2
-6
-8
-10
-12
Ln (k)
0.0033
0.0034
0.0035
0.0036
1/T (K-1)

and minimum slopes (based on extreme limits between k_d and k_{obs} values) exceed the ± 1 S. D. error of the slope based solely on k_{obs} (data not shown).

Recall that the dissociation of complexes at the BP1 and BP2 promoters was apparently first-order for all of the reaction temperatures investigated (see Figs. 12 and 13), indicating that a single step limited the conversion of these complexes from a heparin resistant to a heparin sensitive state. However, the slopes obtained from the Arrhenius plots of BP1 and BP2 under ± ppGpp conditions were positive (see Fig. 15). The positive slopes meant that the activation energies of dissociation were strongly negative (see also Table IX). Except for certain rare reaction mechanisms (e.g. termolecular reactions), no single-step rate constant can have a negative activation energy, since this implies that the rate constant decreases with increasing temperature (Castellan, 1983). As a means to reconcile the apparent first-order dissociation reactions and the results from the Arrhenius plots, it is proposed that the overall dissociation mechanism consists of at least two steps:

$$HR2 \underset{k_3}{\overset{k_{-3}}{\rightleftharpoons}} HR1 \xrightarrow{k_r} HS \qquad (5)$$

Where k_3 and k_{-3} are the respective forward and reverse rate constants which describe the interconversion of the two heparin resistant complexes (HR1 and HR2), and k_r is the apparent reverse isomerization rate constant which describes the irreversible decay of HR1 to a heparin sensitive state. Note that under the assay conditions employed in this thesis, HR1 and HR2 were physically indistinguishable from one another, in that only one heparin resistant complex was ever observed following gel retardation analysis (see Figs. 3 - 5). If the two heparin resistant complexes are able to equilibrate ($k_3 >> k_r$) prior to the rate limiting formation of the heparin sensitive state, then the overall dissociation rate constant (k_d) for equation 5 can be interpreted as $k_r(1 + k_3/k_{-3})^{-1}$ (see Appendix B.III, equation B-34). If this

proposed mechanism for dissociation is correct, and if over the temperature range tested, $k_3/k_{-3} >> 1$, then the proposed overall dissociation rate constant can be simplified to $k_r(k_3/k_{-3})^{-1}$. The corresponding apparent activation energy ($E_{a,d}$) for dissociation can then be shown to be $E_{a,d} = E_{a,r} - \Delta H^\circ_3$ (see Appendix C, equations C-9 and C-10). This thermodynamic equation demonstrates how the overall dissociation rate constant (k_d) might increase with decreasing reaction temperature. The simplest example would be given if the enthalpy for the equilibrium between HR1 and HR2 was greater than the activation energy for k_r. In other words, the ratio of k_3/k_{-3} would decrease faster with decreasing reaction temperature than would k_r. Thus, the ratio of $k_r(k_3/k_{-3})^{-1}$ would increase with decreasing reaction temperature, and even though the overall dissociation rate constant (k_d) was apparently first-order, the activation energy of dissociation would be negative.

The preceding argument made use of two simplifying assumptions. First, it was assumed that $k_3/k_{-3} >> 1$ over the temperature range tested. It is felt that this assumption was valid, for if k_3/k_{-3} were less than 1, then the slope of the Arrhenius plot would become increasingly negative with decreasing reaction temperature as k_d approached k_r. Figure 15 clearly shows that this did not occur. Similarly, having $k_3/k_{-3} >> 1$ is consistent with the observation that at saturating polymerase, the formation of heparin resistant complexes were close to 100 % (see Figs. 9 - 10). The second assumption was that the enthalpy for the equilibrium between HR1 and HR2 was greater than the activation energy for k_r. This difference might be expected if the conversion of HR1 to HR2 reflects the formation of open complexes, as has been demonstrated at other promoters studied to date (Spassky *et al.*, 1985; Duval-Valentin and Ehrlich, 1987; Cowing *et al.*, 1989; Schickor *et al.*, 1990). Since the process of DNA melting at the transcription initiation site of a promoter is estimated to require 60 to 170 kcal (Roe *et al.*, 1984), it is reasonable to propose that $\Delta H^\circ_3 > E_{a,r}$.

3e. Effects of ppGpp on the dissociation rates of heparin resistant complexes.

Figure 14C shows that for BP1, the extrapolated intrinsic dissociation rate constants (k_d) under ± ppGpp conditions were different. This was also true for BP2 and for low reaction temperatures (see Table V rows 'k_d'). These results imply that the addition of ppGpp affects the intrinsic dissociation rate of the promoter/polymerase complexes, and not merely the sensitivity of those complexes to heparin attack. This interpretation follows from the analysis of Cech and McClure (1980), who proposed that the observed dissociation rate should be a sum of the intrinsic first-order rate of dissociation and the rate of heparin attack:

$$k_{obs} = k_d + k_{Hep}[Heparin] \qquad (6)$$

Where k_{Hep} is the second-order rate constant that describes the rate of heparin attack at the 'heparin resistant' complex. If the effect of ppGpp was limited to increasing the sensitivity of the complex to heparin (i.e. increasing k_{Hep}), then the values of k_{obs} extrapolated to zero heparin concentration under ± ppGpp conditions should intersect at the Y-axis (see Fig. 14C).

Inspection of Table V (row 'k_{obs}') reveals that addition of ppGpp increased the dissociation rate at 50 μg/ml heparin between 2 - 6 fold, depending on the reaction temperature. Except at 35° C, there was no evidence of a differential response between the BP1 and BP2 promoters, since at a given temperature, the stimulation of the dissociation rate by ppGpp was very similar for the two promoters. At 35° C there was an apparent twofold stimulation of the dissociation rate of heparin resistant complexes at BP2 compared to that dissociation rate at BP1. However, it must be noted that the dissociation rate constants obtained for BP2 at 35° C were based on an extrapolation of the Arrhenius plot for that promoter (see Fig. 15), and assumes that the activation energy for dissociation at BP2 was comparable over the entire temperature range investigated.

Figure 16. ppGpp dependence of the dissociation rates of RNA polymerase from the *B. subtilis rrnB* P1 and P2 promoters.

Dissociation rates (k_{obs}) of polymerase/promoter complexes were measured at 35 °C under standard binding conditions (Materials and Methods) as described in Figure 12. Plots of k_{obs} versus the final reaction concentrations of ppGpp are shown. Panel A. Dissociation experiments employed *B. subtilis rrnB* P1 (templates derived from pKK115B). Panel B. Dissociation experiments employed *B. subtilis rrnB* P2 (templates derived from pKK183B).

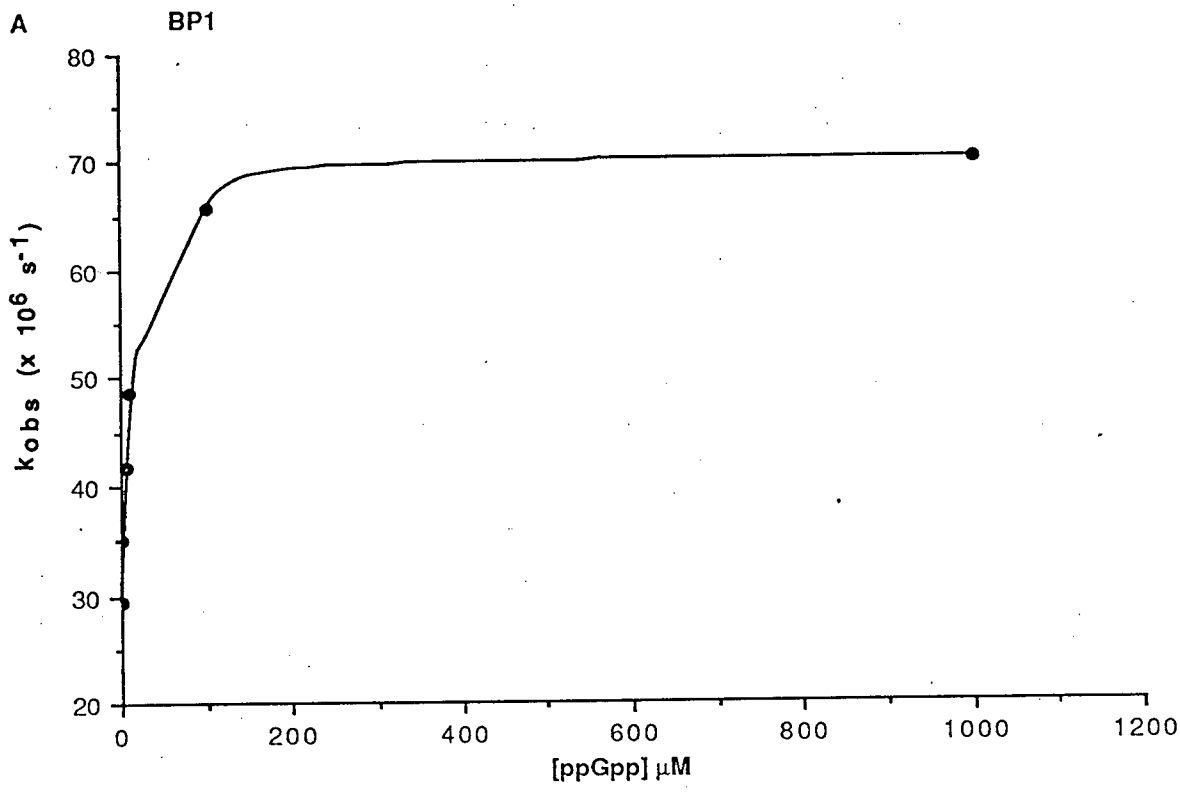
A
BP1
80
70
60
50
40
30
20
kobs (x 10^6 s^-1)
0
200
400
600
800
1000
1200
[ppGpp] μM

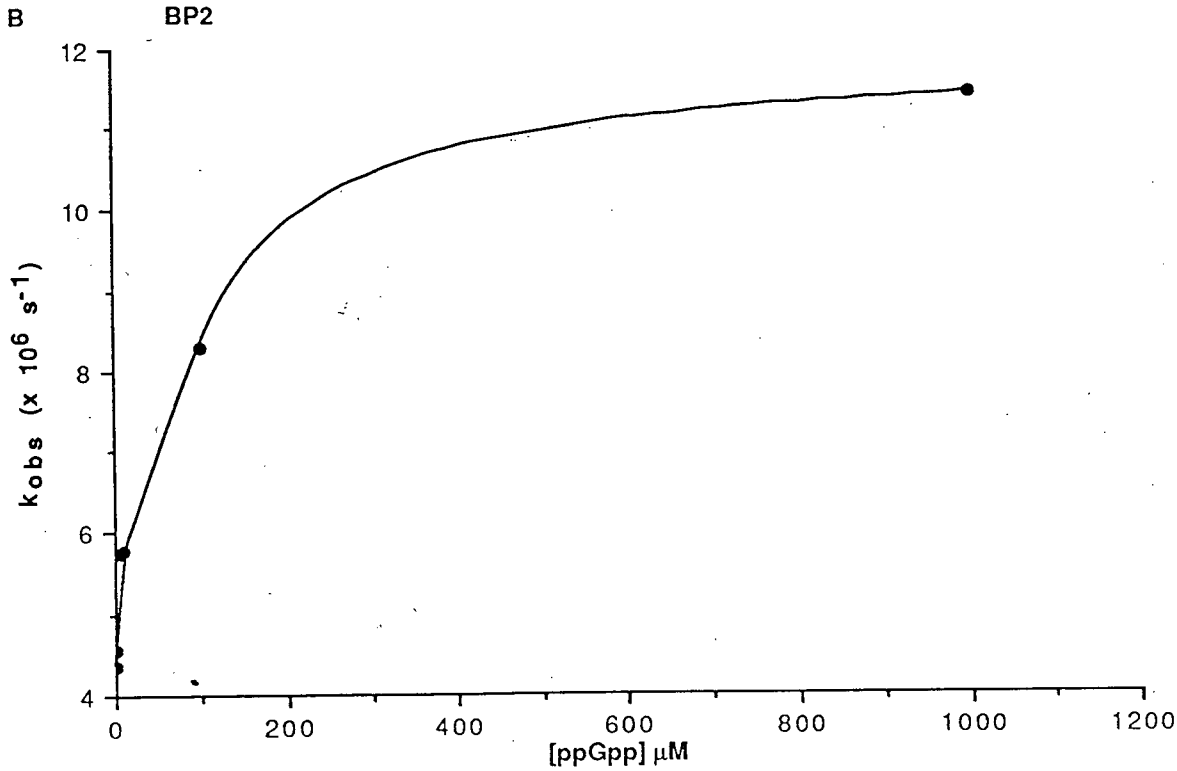
B
BP2
12
10
8
6
4
kobs (x 10^6 s^-1)
0
200
400
600
800
1000
1200
[ppGpp] μM

Assuming ppGpp to be the sole regulator of growth rate regulation in *E. coli* K12, it is possible to estimate that 0.1 mM ppGpp would be sufficient to cause ≥ 80% of the maximum inhibition of rRNA expression which is observed *in vivo* (Baracchini *et al.*, 1988; Hernandez and Bremer, 1990). This estimate is based on results from both r_s/r_t partitioning studies (Baracchini *et al.*, 1988) and promoter fusion experiments with the isolated *E. coli rrnB* P1 promoter (Hernandez and Bremer, 1990), and relies on the observation that 100 pmol ppGpp per OD_{460} unit of culture mass is approximately 0.3 mM (Baracchini *et al.*, 1988). However, it is possible that for the present *in vitro* assay, the BP1 and BP2 promoters require concentrations of ppGpp higher than 0.1 mM in order to effect a maximum response. To investigate this possibility, dissociation rates for complexes formed at BP1 and BP2 were measured as described in Results section II.3a (35° C, 50 μg/ml heparin) at a range of ppGpp concentrations (0 - 1000 μM). Figure 16 summarizes these results. As for section 3c, the dissociation rates of BP2 were difficult to interpret due to the significant contribution of polymerase breakdown at 35° C. However, Figure 16A demonstrates that for BP1, dissociation rates at 100 μM ppGpp were > 90% of the maximum response observed at 1000 μM ppGpp.

While the addition of ppGpp did not appear to create a significant differential response in the dissociation rates at BP1 and BP2, there was a difference between the absolute dissociation rates of complexes formed at these two promoters, with heparin resistant complexes formed at BP1 having rates of dissociation 7 - 10 fold higher than those of BP2 (Table V row 'k_{obs}'). From this, one might expect the final equilibrium position of polymerase binding at BP2 to be greater than that of BP1, even under conditions of polymerase excess. However, as the titration studies showed (see Results section II.1 and II.2), heparin resistant complex formation at BP1 and BP2 were both close to 100% at enzyme excess. This would suggest that the formation of heparin resistant complexes at BP1 and BP2 was so favorable, that even

large differences in the absolute dissociation rates have no measurable effect on the final equilibrium positions of these promoters.

4 Rate of association of RNA polymerase and the BP1 and BP2 promoters.

There are two points which should be considered during the analyses of the rates of formation of polymerase/promoter complexes. First, as discussed in Appendix B.II.1, there are only two states (i.e. heparin resistant and heparin sensitive) which are measured during the association reaction. Second, under conditions of enzyme excess, the initial bimolecular collision between free RNA polymerase and free promoter fragments will behave as a (pseudo) first-order reaction. As a consequence of these two points, the overall mechanism which describes the transitions between heparin resistant and heparin sensitive states can be expressed as a single isomerization reaction,

$$HS \rightleftharpoons HR \qquad (7)$$

Note that equation 7 does not comment on the number of heparin resistant and heparin sensitive complexes which exist in the overall reaction mechanism. This question will be addressed later in Results section 4b and the Discussion.

When an association reaction is initiated by the addition of RNA polymerase to a binding reaction containing promoter fragments (at time zero, it is assumed that $[HR]_0 = 0$), the approach of equation 7 to a state of equilibrium is described by

$$Ln(1 - [HR]/[HR]_\infty) = -(1/\tau)\, t\,, \qquad (8)$$

where $1/\tau$ is the overall association rate constant, and $[HR]_\infty$ represents the final equilibrium (time infinity) concentration of heparin resistant complexes.

There were three main objectives of the studies in this section. First, equations 7 and 8 assume that the overall rate at which heparin resistant complexes approached their final equilibrium concentrations is limited by a single reaction step (see also Appendix B sections II.1 and V). This assumption could be tested by

investigating whether the association plots of heparin resistant complexes versus reaction times were linear when analyzed according to equation 8. Second, additional information regarding the association reaction mechanism could be obtained from an analysis of the dependence of $1/\tau$ on polymerase concentration and reaction temperature. From such studies, the minimum number of heparin resistant and heparin sensitive complexes could be estimated, and $1/\tau$ could be interpreted as a function of the individual forward and reverse rate constants which defined this minimum association mechanism (see Appendix B.II and B.IV). The final objective was to determine whether ppGpp could exert a differential effect on the association rate of polymerase at the BP1 and BP2 promoters.

4a. Primary association rates.

The objects of the studies in this section were to measure the association rate constant $1/\tau$, and determine whether the assumptions of equations 7 and 8 were met under the assay conditions of this thesis. Experimentally, association rates were measured as follows. Various amounts of RNA polymerase were added to a standard binding reaction mixture (Materials and Methods) containing either BP1 or BP2. In all cases, the molar ratio of polymerase to promoter was five-fold or greater (see also Appendix B.II.1 and B.IV), and ppGpp, when present, was at a final concentration of 0.1 mM. After mixing briefly (vortex $\leq$ 1 s), samples were returned to the reaction temperature for increasing lengths of time. Note that timing was initiated upon the addition of polymerase. To stop the association reactions, heparin was added (final reaction concentration, 100 μg/ml), and the samples were analyzed by gel retardation as described in the Materials and Methods. Results were expressed as the fraction (F) of total promoter DNA which had formed heparin resistant complexes with RNA polymerase after a given association time. The final equilibrium concentration of heparin resistant complexes (F_∞) was based on the average value of at least two 'infinite' timepoints (generally between 5 - 10 min). In

Figure 17. Association rate of RNA polymerase and the *B. subtilis rrnB* P1 promoter at 15 °C.

Various amounts of RNA polymerase (Batch #233) were added to a standard binding reaction mixture (15 °C, see Materials and Methods) containing the *B. subtilis rrnB* P1 promoter (DNA templates derived from pKK115B). In all cases, the molar ratio of polymerase to promoter was ≥ 5. After mixing briefly (vortex ≤ 1 s), samples were returned to the reaction temperature for increasing lengths of time (timing was initiated upon the addition of polymerase). Heparin (final reaction concentration, 100 μg/ml) was added to stop the association reactions, and the samples were analyzed by gel retardation as described in the Materials and Methods. Results were expressed as the fraction of total promoter DNA (F) which had formed heparin resistant complexes with RNA polymerase after a given association time. The end-point concentration (F_∞) of polymerase/promoter complexes was based on the average value of at least two 'infinite' timepoints (generally between 5 - 10 min). In all cases, the infinite times were greater than 15 half lives of the overall association, and the standard deviation of F_∞ was always less than 2% (data not shown). Figure 17 illustrates the relationship between $Ln(1 - F/F_\infty)$ and the association time (see also Results section II.4a and Appendix B.II.1). The lines through each data set were calculated by linear least-squares analysis, and the slopes (± 1 S. D. ≤ 15%) from these lines yielded the association rate constants ($1/\tau$). The reaction concentrations of RNA polymerase (nM) are summarized in the figure insets, and the corresponding $1/\tau$ values are indicated below. Panel A. Association experiments performed in the absence of ppGpp. Panel B. Association experiments performed in the presence of ppGpp (final concentration 0.1 mM).

RNA polymerase (nM)	Panel A (BP1/15 °C/– ppGpp) $1/\tau$ (s^{-1})	Panel B (BP1/15 °C/+ ppGpp) $1/\tau$ (s^{-1})
0.184	1.6×10^{-2}	1.7×10^{-2}
0.276	2.7×10^{-2}	2.8×10^{-2}
0.367	2.6×10^{-2}	2.9×10^{-2}
0.735	3.6×10^{-2}	4.4×10^{-2}
1.102	3.7×10^{-2}	4.6×10^{-2}

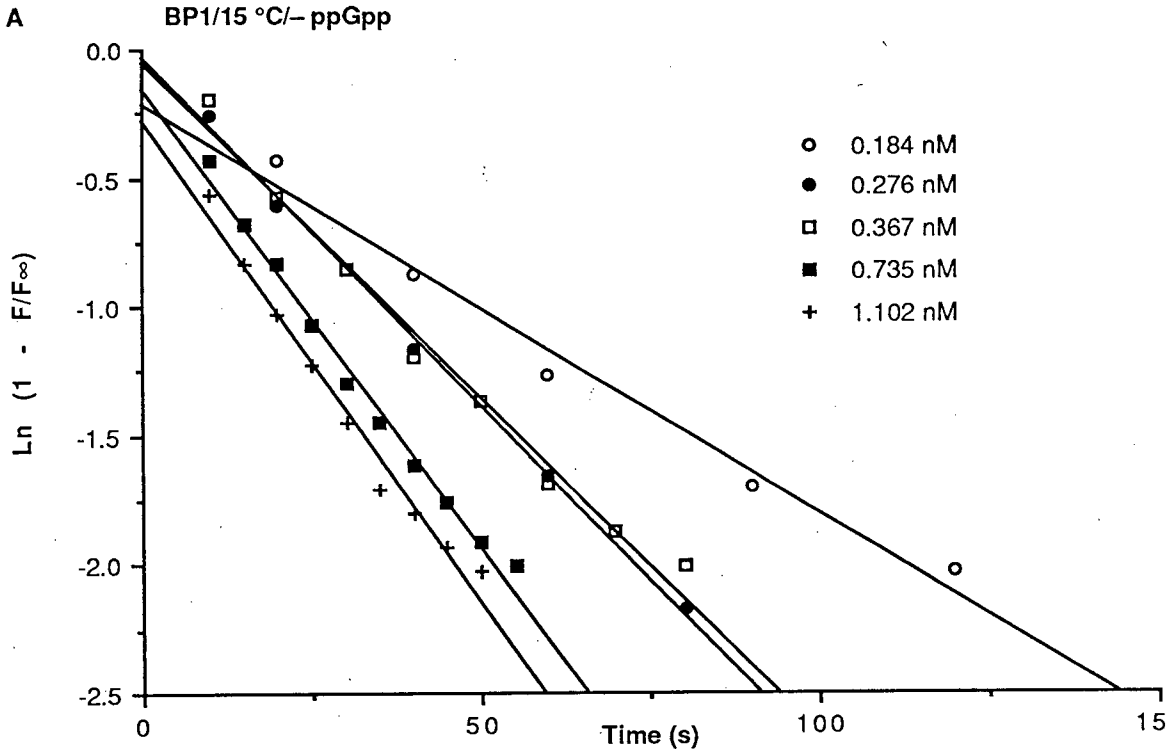
A
BP1/15 °C/– ppGpp
0.0
-0.5
-1.0
-1.5
-2.0
-2.5
Ln (1 - F/F∞)
0
50
100
150
Time (s)
0.184 nM
0.276 nM
0.367 nM
0.735 nM
1.102 nM

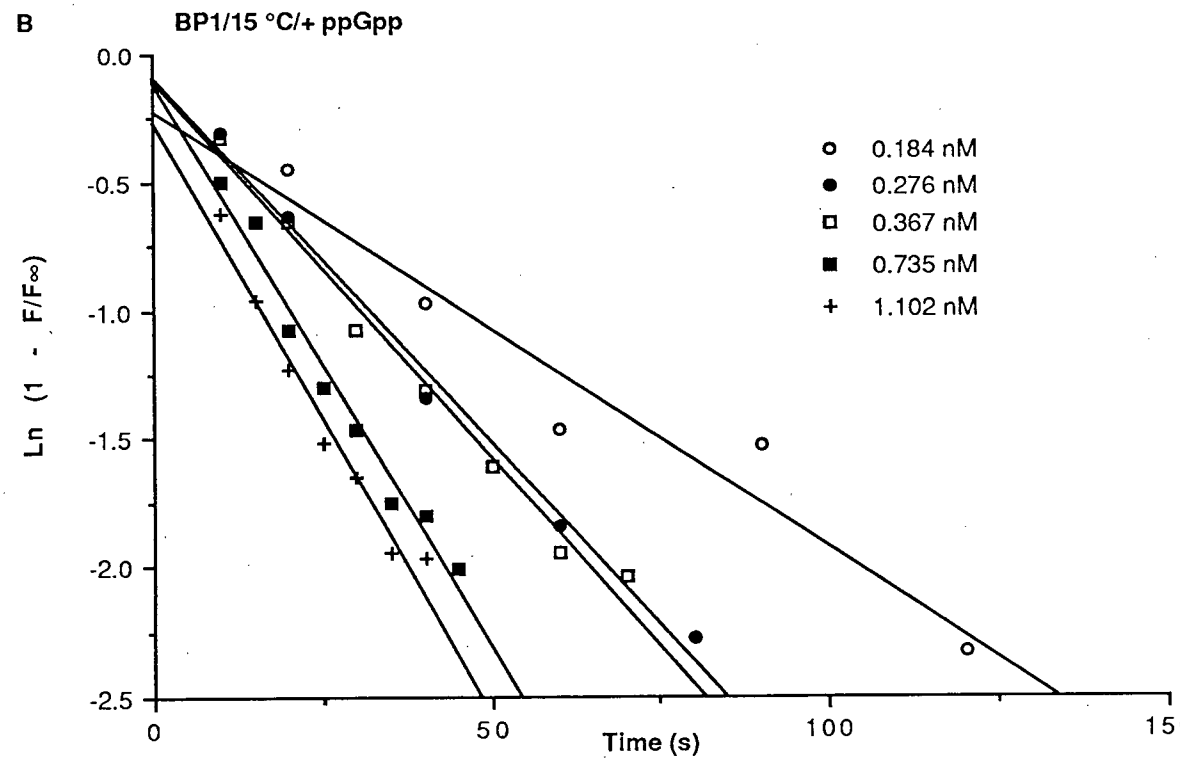
B
BP1/15 °C/+ ppGpp
0.0
-0.5
-1.0
-1.5
-2.0
-2.5
Ln (1 - F/F∞)
0
50
100
150
Time (s)
0.184 nM
0.276 nM
0.367 nM
0.735 nM
1.102 nM

Figure 18. Association rate of RNA polymerase and the *B. subtilis rrnB* P2 promoter at 10 °C.

Association reactions were performed as described in Figure 17, using the *B. subtilis rrnB* P2 promoter (10 °C, DNA templates derived from pKK183B). The reaction concentrations of RNA polymerase (nM) are summarized in the figure insets, and the corresponding $1/\tau$ values are indicated below. Panel A. Association experiments performed in the absence of ppGpp. Panel B. Association experiments performed in the presence of ppGpp (final concentration 0.1 mM).

RNA polymerase (nM)	Panel A (BP2/10 °C/– ppGpp) $1/\tau$ (s^{-1})	Panel B (BP2/10 °C/+ ppGpp) $1/\tau$ (s^{-1})
0.184	1.5×10^{-2}	1.5×10^{-2}
0.276	2.2×10^{-2}	2.4×10^{-2}
0.367	2.7×10^{-2}	3.1×10^{-2}
0.735	4.4×10^{-2}	4.7×10^{-2}
1.102	4.9×10^{-2}	6.5×10^{-2}

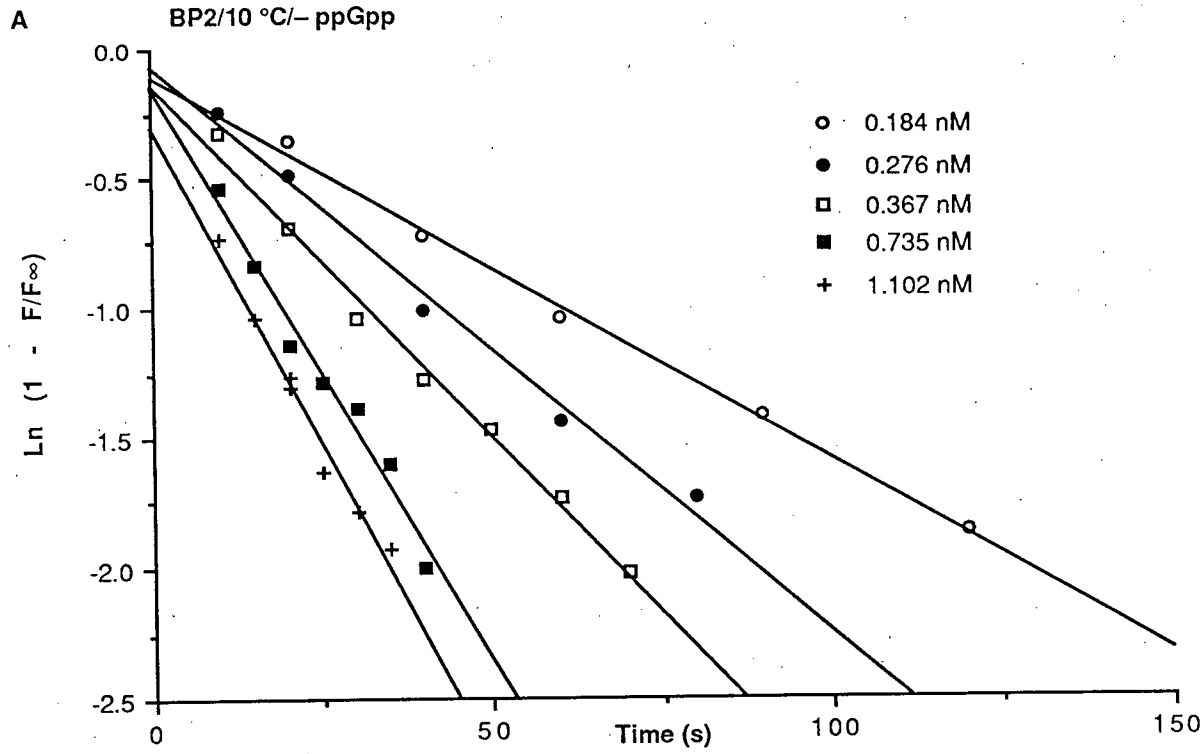
A
BP2/10 °C/– ppGpp
0.0
-0.5
-1.0
-1.5
-2.0
-2.5
Ln (1 - F/F∞)
0
50
100
150
Time (s)
0.184 nM
0.276 nM
0.367 nM
0.735 nM
1.102 nM

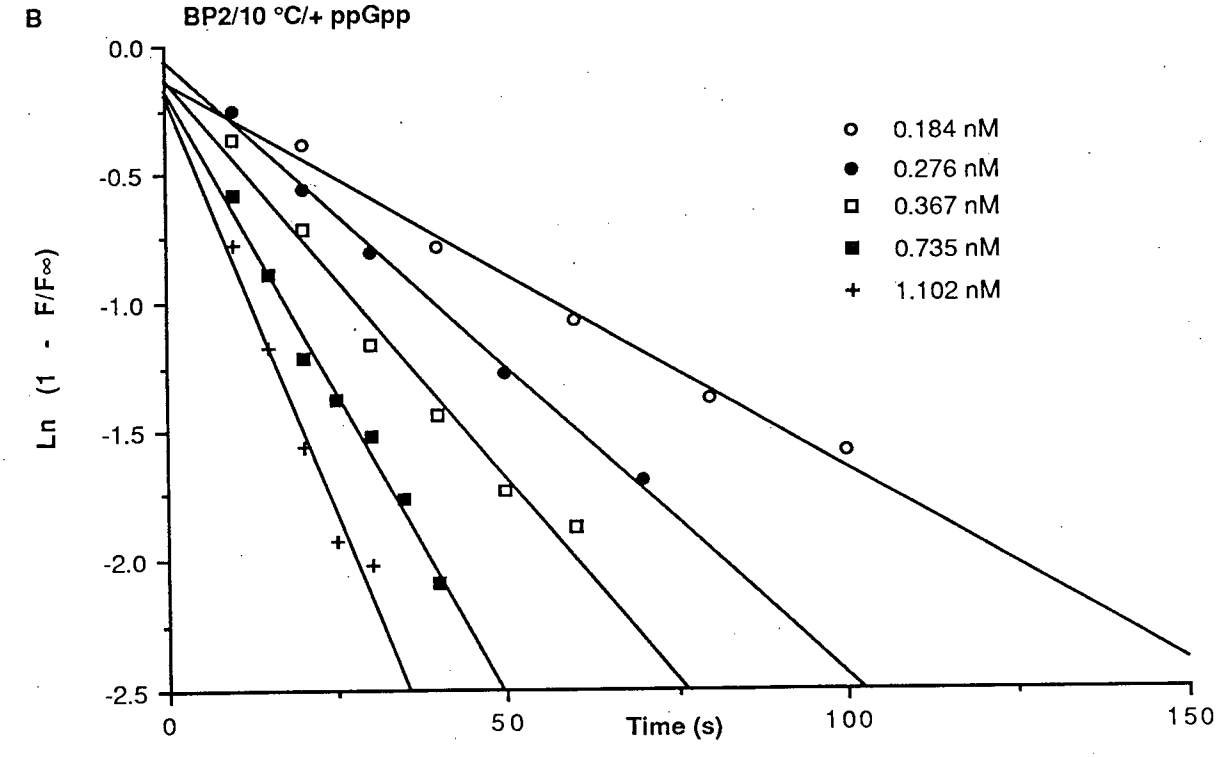
B
BP2/10 °C/+ ppGpp
0.0
-0.5
-1.0
-1.5
-2.0
-2.5
Ln (1 - F/F∞)
0
50
100
150
Time (s)
0.184 nM
0.276 nM
0.367 nM
0.735 nM
1.102 nM

Figure 19. Association rate of RNA polymerase and the *B. subtilis rrnB* P1 promoter at 35 °C.

Association reactions were performed as described in Figure 17, using the *B. subtilis rrnB* P1 promoter (35 °C, DNA templates derived from pKK115B). The reaction concentrations of RNA polymerase (nM) are summarized in the figure insets, and the corresponding $1/\tau$ values are indicated below. Panel A. Association experiments performed in the absence of ppGpp. Panel B. Association experiments performed in the presence of ppGpp (final concentration 0.1 mM).

RNA polymerase (nM)	Panel A (BP1/35 °C/– ppGpp) $1/\tau$ (s^{-1})	Panel B (BP1/35 °C/+ ppGpp) $1/\tau$ (s^{-1})
0.123	2.5×10^{-2}	2.9×10^{-2}
0.185	4.0×10^{-2}	3.8×10^{-2}
0.246	5.1×10^{-2}	5.1×10^{-2}
0.308	6.2×10^{-2}	6.9×10^{-2}

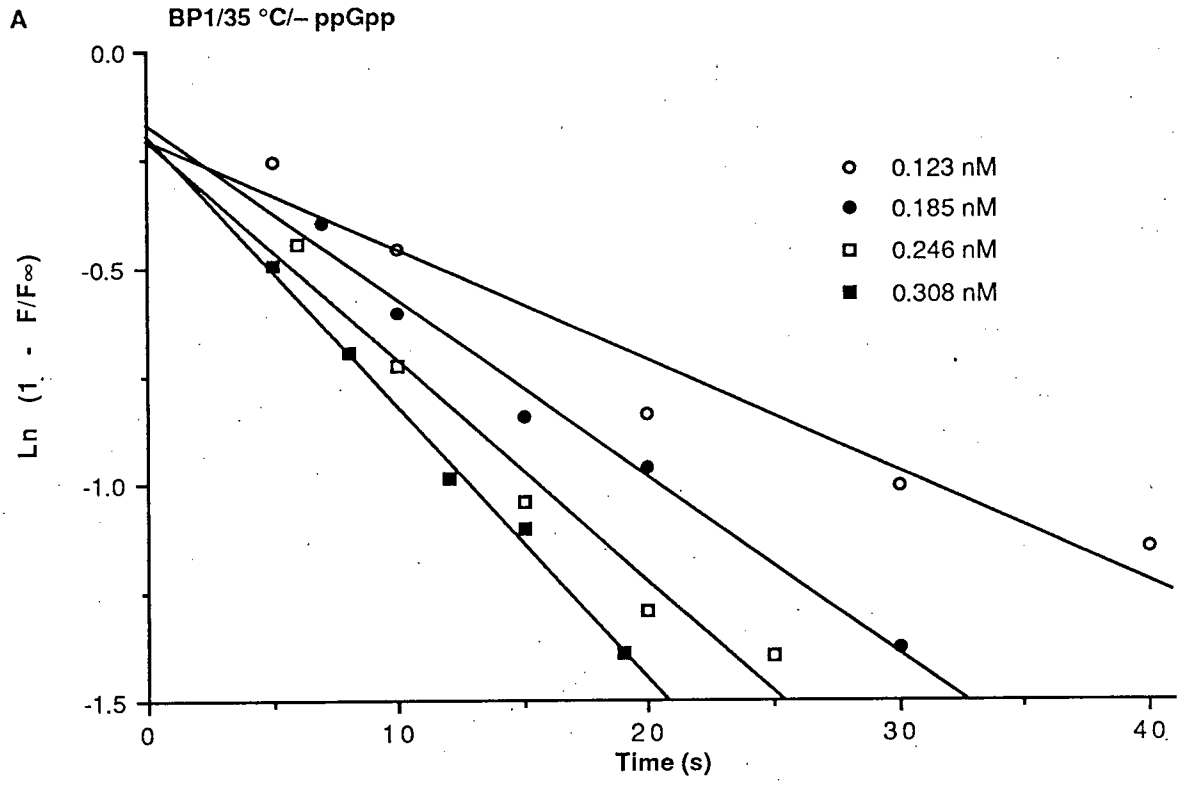
A
BP1/35 °C/– ppGpp
0.0
-0.5
-1.0
-1.5
Ln (1 - F/F∞)
0
10
20
30
40
Time (s)
0.123 nM
0.185 nM
0.246 nM
0.308 nM

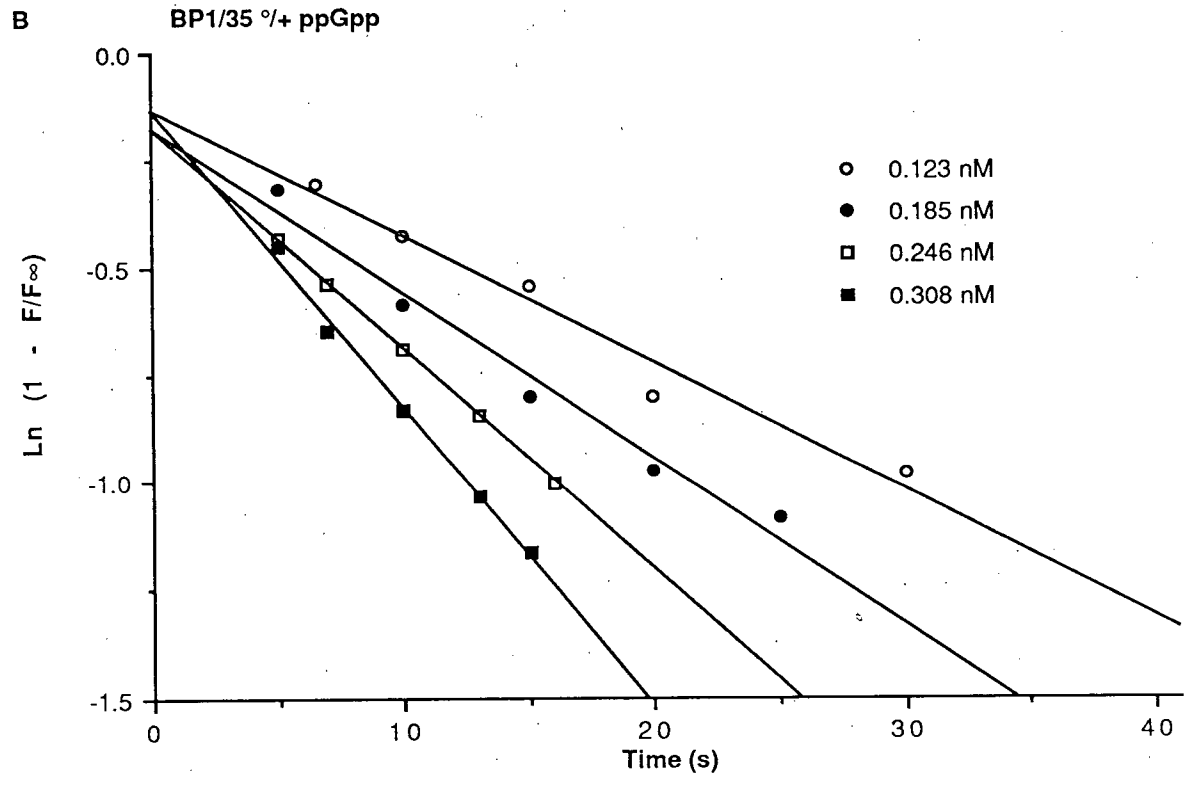
B
BP1/35 °/+ ppGpp
0.0
-0.5
-1.0
-1.5
Ln (1 - F/F∞)
0
10
20
30
40
Time (s)
0.123 nM
0.185 nM
0.246 nM
0.308 nM

Figure 20. Association rate of RNA polymerase and the *B. subtilis rrnB* P2 promoter at 35 °C.

Association reactions were performed as described in Figure 17, using the *B. subtilis rrnB* P2 promoter (35 °C, DNA templates derived from pKK183B). The reaction concentrations of RNA polymerase (nM) are summarized in the figure insets, and the corresponding $1/\tau$ values are indicated below. Panel A. Association experiments performed in the absence of ppGpp. Panel B. Association experiments performed in the presence of ppGpp (final concentration 0.1 mM).

RNA polymerase (nM)	Panel A (BP2/35 °C/– ppGpp) $1/\tau$ (s^{-1})	Panel B (BP2/35 °C/+ ppGpp) $1/\tau$ (s^{-1})
0.184	3.0×10^{-2}	2.0×10^{-2}
0.276	3.9×10^{-2}	3.3×10^{-2}
0.367	8.5×10^{-2}	7.5×10^{-2}
0.735	1.2×10^{-1}	1.2×10^{-1}
0.756		1.3×10^{-1}
1.102	1.9×10^{-1}	1.8×10^{-1}

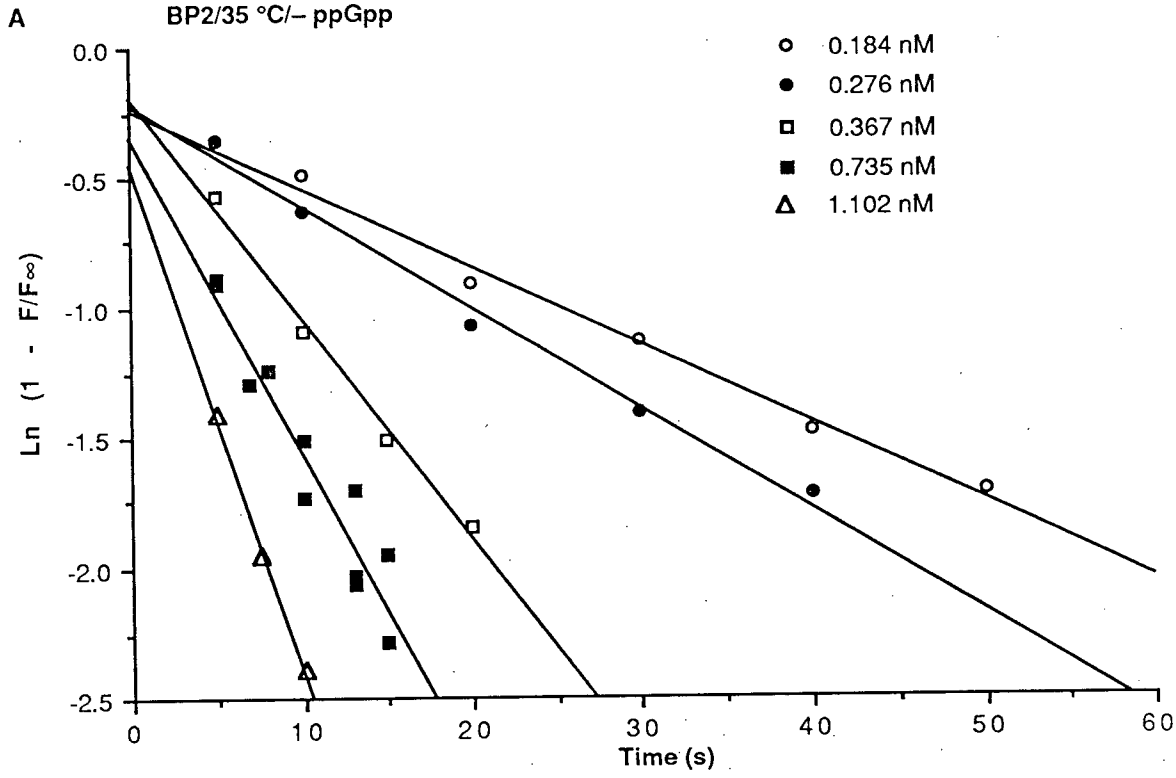
A
BP2/35 °C/– ppGpp
0.184 nM
0.276 nM
0.367 nM
0.735 nM
1.102 nM
Ln (1 - F/F∞)
0.0
-0.5
-1.0
-1.5
-2.0
-2.5
0
10
20
30
40
50
60
Time (s)

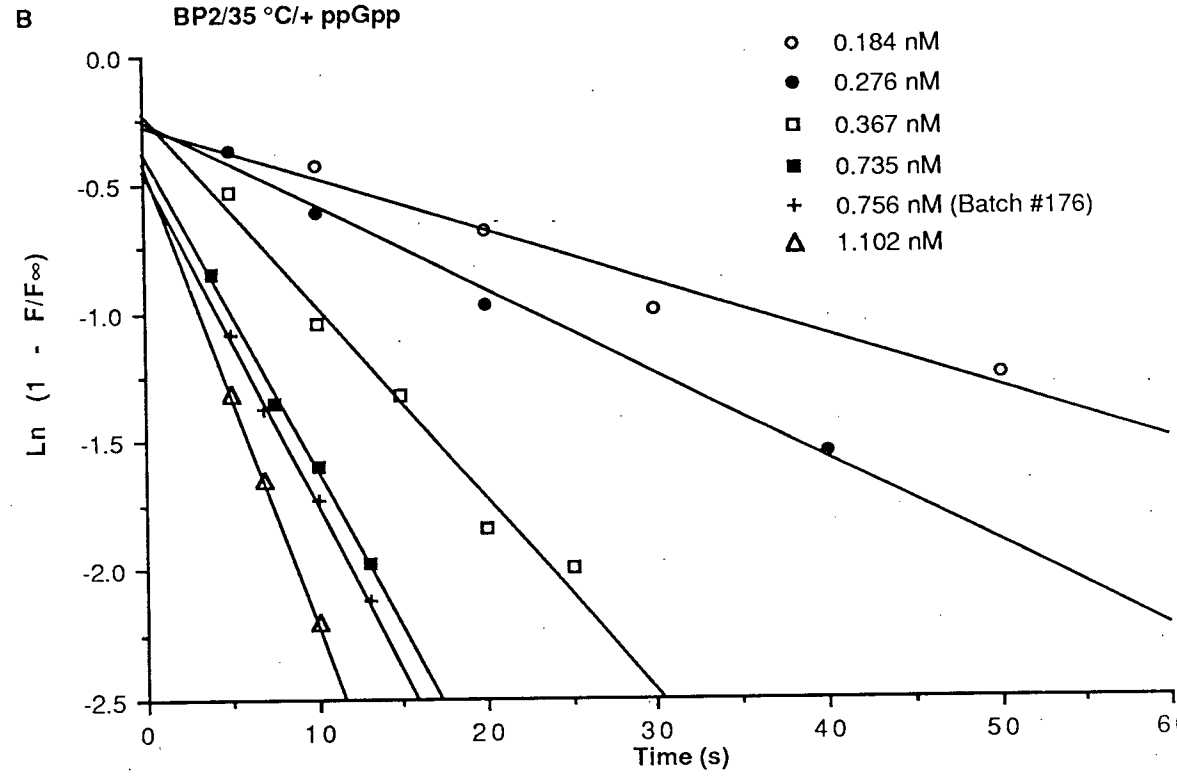
B
BP2/35 °C/+ ppGpp
0.184 nM
0.276 nM
0.367 nM
0.735 nM
0.756 nM (Batch #176)
1.102 nM
Ln (1 - F/F∞)
0.0
-0.5
-1.0
-1.5
-2.0
-2.5
0
10
20
30
40
50
60
Time (s)

all cases, the infinite times were greater than 15 half lives of the overall association, and the standard deviation of F_∞ was always less than 2% (data not shown). Note that the ratio of F/F_∞ is identical to the term $[HR]/[HR]_\infty$ of equation 8.

As Figures 17 - 20 show, the plots of $Ln(1 - F/F_\infty)$ versus association time were linear over the entire reaction timecourse, which in many cases followed the association process up to 85% of completion ($Ln(1 - F/F_\infty) \leq -2$). Based on a least squares analysis of the data, the slope determinations (which represent the association rate constant $1/\tau$) had standard deviations of less than 15% (data not shown). The linearity of the plot of $Ln(1 - F/F_\infty)$ versus association time suggested that only one step limited the overall rate at which heparin resistant complexes approached their final equilibrium concentrations (see also Appendix B sections II.1 and V). I felt that the non-zero $1/\tau$ intercepts observed under some reaction conditions were mostly due to the increased variance inherent in intercept calculations compared to that error obtained for slope determinations (Khazanie, 1979). For example, at 0.184 nM polymerase, the standard deviation in slope measurement for BP1 (Fig. 17B; 15 °C, + ppGpp) was only ± 15%, but this was magnified to a ± 84% error in the calculation of the intercept.

4b. 1/tau plots.

The single-step isomerization mechanism of equation 7 described the overall transition between the heparin sensitive and heparin resistant states of polymerase/promoter complexes during the association reactions. A more specific mechanism can be written by expanding equation 7 to show the contributions of free RNA polymerase (R) and free promoter fragments (P) to the overall association reaction. Two possible reaction mechanisms are considered. The first reaction mechanism assumes that a heparin resistant complex forms as a direct result of the bimolecular collision between free RNA polymerase and free promoter fragments such that

$$R + P \underset{k_d}{\overset{k_1}{\rightleftharpoons}} HR \qquad (9)$$

where k_1 is the second-order association rate constant which describes the formation of the initial polymerase/promoter complex, and k_d is the overall dissociation rate constant which describes the conversion of the heparin resistant complexes into a heparin sensitive state (recall that from Results section I.2b, free RNA polymerase is heparin sensitive under standard binding conditions). Since equation 9 only portrays the minimum number of heparin sensitive and heparin resistant complexes present in the overall reaction mechanism, k_d does not necessarily correspond to a single reaction step (see also Results section II.3d). For the mechanism of equation 9, the overall association rate constant ($1/\tau$) can be described as a function of the individual forward and reverse rate constants (Eisenberg and Crothers, 1969; Hammes and Schimmel, 1970) such that

$$1/\tau = k_1[R_T] + k_d \quad , \qquad (10)$$

where $[R_T]$ is the total concentration of RNA polymerase added to the binding reaction.

The second reaction mechanism which is considered, assumes that a heparin sensitive complex forms as a direct result of the bimolecular collision between free RNA polymerase and free promoter fragments, and that a heparin resistant state is not achieved until at least one additional isomerization step has occurred.

$$R + P \underset{k_{-1}}{\overset{k_1}{\rightleftharpoons}} HS \underset{k_d}{\overset{k_f}{\rightleftharpoons}} HR \qquad (11)$$

The rate constants k_1 and k_d were defined previously in equation 9, and k_{-1} is the reverse rate constant which describes the dissociation of the initial heparin sensitive complex into its separate components. The forward isomerization rate constant (k_f) describes the conversion of the heparin sensitive complexes into a heparin resistant state. Since equation 11 only portrays the minimum number of heparin sensitive and heparin resistant complexes present in the overall reaction mechanism, k_f does

not necessarily correspond to a single reaction step. Recall that under the conditions of this thesis (where the molar ratio of polymerase/promoter was ≥ 5), virtually 100% of the promoter fragments present in the association reactions were found as heparin resistant complexes following a 10 min incubation at the reaction temperature (see Results section II.1, Figs. 9 and 10). This suggests that $k_f >> k_d$ for the mechanism of equation 11, such that the overall association rate constant ($1/\tau$) can be described according to equation 12 (the derivation of equation 12 is presented in Appendix B.IV).

$$1/\tau = \frac{k_f k_1 [R_T]}{k_1 [R_T] + k_{-1} + k_f} \qquad (12)$$

The two association mechanisms presented in equations 9 and 11 can be distinguished from one another by observing the dependence of the overall association rate constant on enzyme concentration. If the mechanism of equation 9 describes the overall association reaction, then $1/\tau$ will be a linear function of enzyme concentration (see equation 10). However, if equation 11 describes the overall association reaction, then $1/\tau$ will approach a limiting (concentration independent) value at saturating levels of polymerase (see equation 12).

Figure 21 shows a plot of the association rate constants ($1/\tau$) for BP1 and BP2 versus active polymerase concentration. As the data of Figures 21A and 21B reveal, the dependence of the association rate constant on polymerase concentration displayed curvature at high enzyme concentrations for BP1 and BP2. This non-linear relationship suggested that at low reaction temperatures, the overall association mechanism behaved according to equation 11. It is assumed that the reaction mechanism for the BP1 and BP2 promoters does not change over the temperature range studied (i.e. that the number and order of heparin resistant and heparin sensitive complexes does not change). Therefore, at both low temperature and 35° C, the association rate data of the BP1 and BP2 promoters will be analyzed according to the two-step mechanism described by equations 11 and 12.

Figure 21. Dependence of the association rate constant ($1/\tau$) on RNA polymerase concentration.

The association rate constants ($1/\tau$) derived from Figures 17 - 20 are plotted against their corresponding RNA polymerase concentrations (nM). Squares and circles represent experiments which employed the *B. subtilis rrnB* P1 and P2 promoters respectively. The absence and presence (final concentration 0.1 mM) of ppGpp during the association experiment is indicated by open and closed symbols respectively. Panel A. Reaction temperature was 15 °C. Panel B. Reaction temperature was 10 °C. Panel C. Reaction temperature was 35 °C.

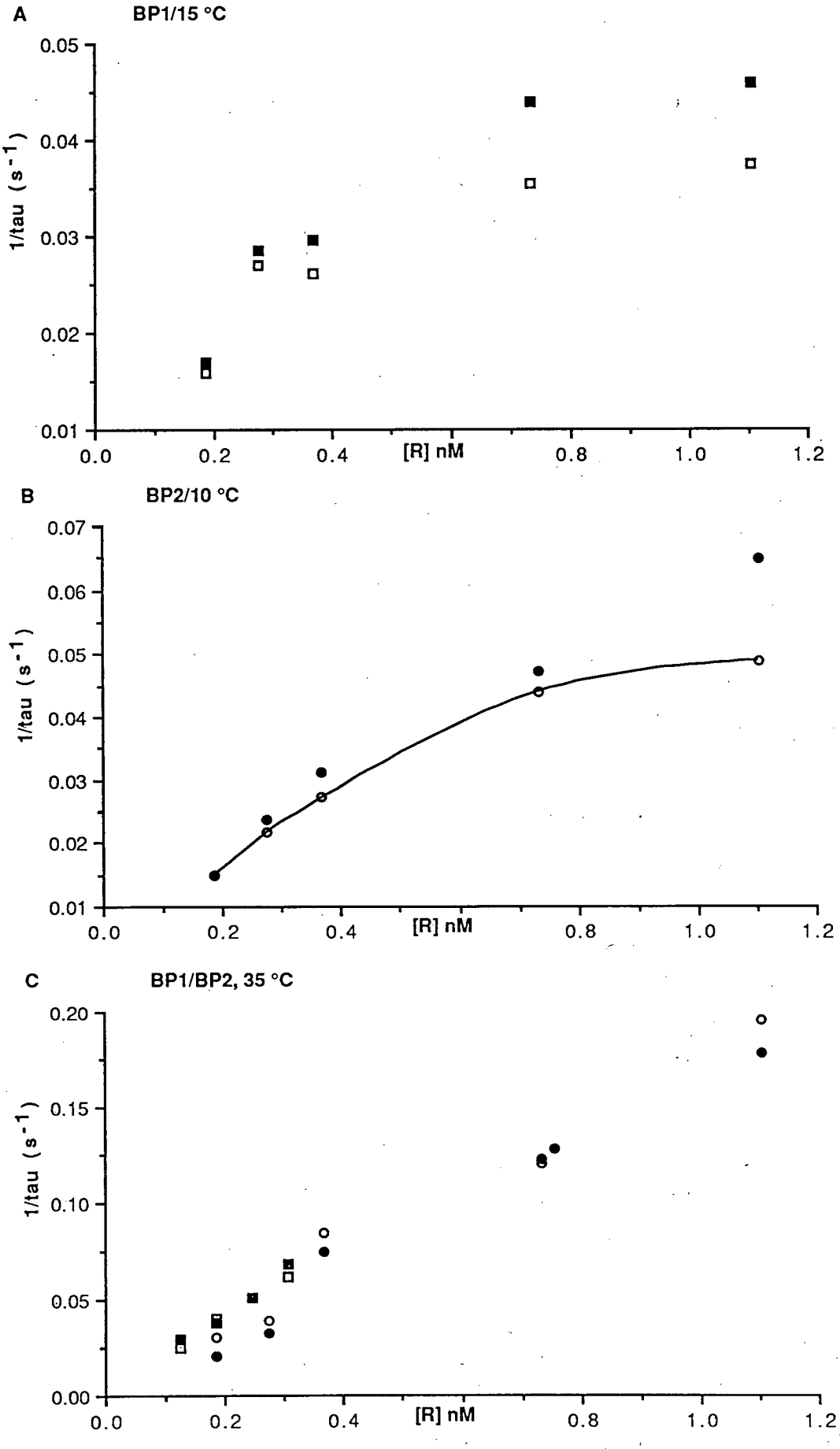
A
BP1/15 °C
1/tau (s-1)
0.05
0.04
0.03
0.02
0.01
0.0
0.2
0.4
[R] nM
0.8
1.0
1.2
B
BP2/10 °C
1/tau (s-1)
0.07
0.06
0.05
0.04
0.03
0.02
0.01
0.0
0.2
0.4
[R] nM
0.8
1.0
1.2
C
BP1/BP2, 35 °C
1/tau (s-1)
0.20
0.15
0.10
0.05
0.00
0.0
0.2
0.4
[R] nM
0.8
1.0
1.2

4c. Tau analysis

A more useful representation of equation 12 is the double reciprocal form.

$$\tau = \frac{k_{-1} + k_f}{k_f k_1 [R_T]} + \frac{1}{k_f} \qquad (13)$$

Thus, a plot of tau versus $[R_T]^{-1}$ will give a straight line, whose intercept equals $(1/k_f)$. The slope of the tau plot is sometimes referred to as the reciprocal of the (overall) second-order association rate constant (k_a). The expression for $(1/k_a)$ depends on the relative magnitudes of k_{-1} and k_f (see Appendix B.IV; Strickland *et al.*, 1975; McClure, 1980). If $k_{-1} >> k_f$, then the reaction between free RNA polymerase and the promoter is in rapid equilibrium, such that

$$R + P \underset{k_{-1}}{\overset{k_1}{\rightleftharpoons}} HS \xrightarrow{k_f} HR \qquad (14)$$

and the slope of the tau plot is $1/(k_f K1)$ (where the binding equilibrium constant $K1 = k_1/k_{-1}$). Alternatively, if $k_f >> k_{-1}$, then the formation of heparin resistant complexes will occur by a sequential mechanism, such that

$$R + P \xrightarrow{k_1} HS \xrightarrow{k_f} HR \qquad (15)$$

and the slope of the tau plot is $1/(k_1)$. An attempt to distinguish between the two mechanisms described in equations 14 and 15 will be presented in Results section II.4d.

Figures 22 and 23 show the representative tau plots for the association of RNA polymerase with the BP1 and BP2 promoters (± ppGpp), at both high (35° C) and low (10 - 15° C) reaction temperatures. Based on a least squares analysis of the data, the reciprocal of the slope and intercept values were calculated, and these results (± 1 S. D.) are summarized in Table VI. Because the determination of k_f was based upon intercept values, the average estimated error is greater (± 41%) than that of k_a, whose determination was based on the slope of the tau plot (average error ± 11%) (see also Results section II.4a). As a result, calculations which are based on k_f

Figure 22. Tau-plot analysis of the low temperature association kinetics of complexes between RNA polymerase and the *B. subtilis rrnB* P1 and P2 promoters.

The reciprocals of the association rate constants ($1/\tau$) derived from Figures 17 and 18 were plotted against the reciprocals of the corresponding RNA polymerase concentrations (nM). Open and closed symbols denote the respective absence and presence (final concentration 0.1 mM) of ppGpp during the association experiment, and the lines through each data set were calculated by linear least-squares analysis. The reciprocal of the slope yields the (overall) second-order association rate constant (k_a), and the τ-intercept at infinite polymerase concentration ($1/R = 0$) gives a value for $1/k_f$ (see Results section II.4c and Appendix B.IV). The results for k_a, k_f and their associated errors (± 1 S. D.) are summarized in Table VI. Panel A. Association reactions performed using the *B. subtilis rrnB* P1 promoter (15 °C, DNA templates derived from pKK115B). Panel B. Association reactions performed using the *B. subtilis rrnB* P2 promoter (10 °C, DNA templates derived from pKK183B).

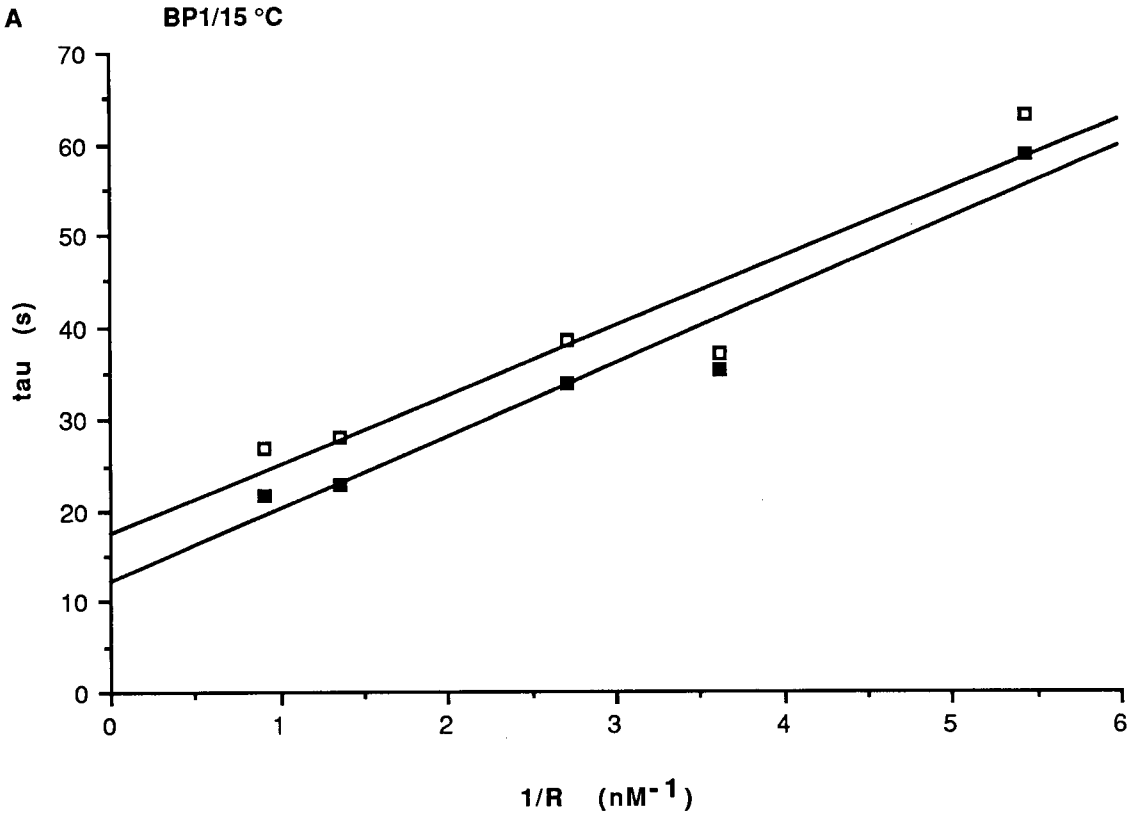
A
BP1/15 °C
tau (s)
70
60
50
40
30
20
10
0
0
1
2
3
4
5
6
1/R (nM-1)

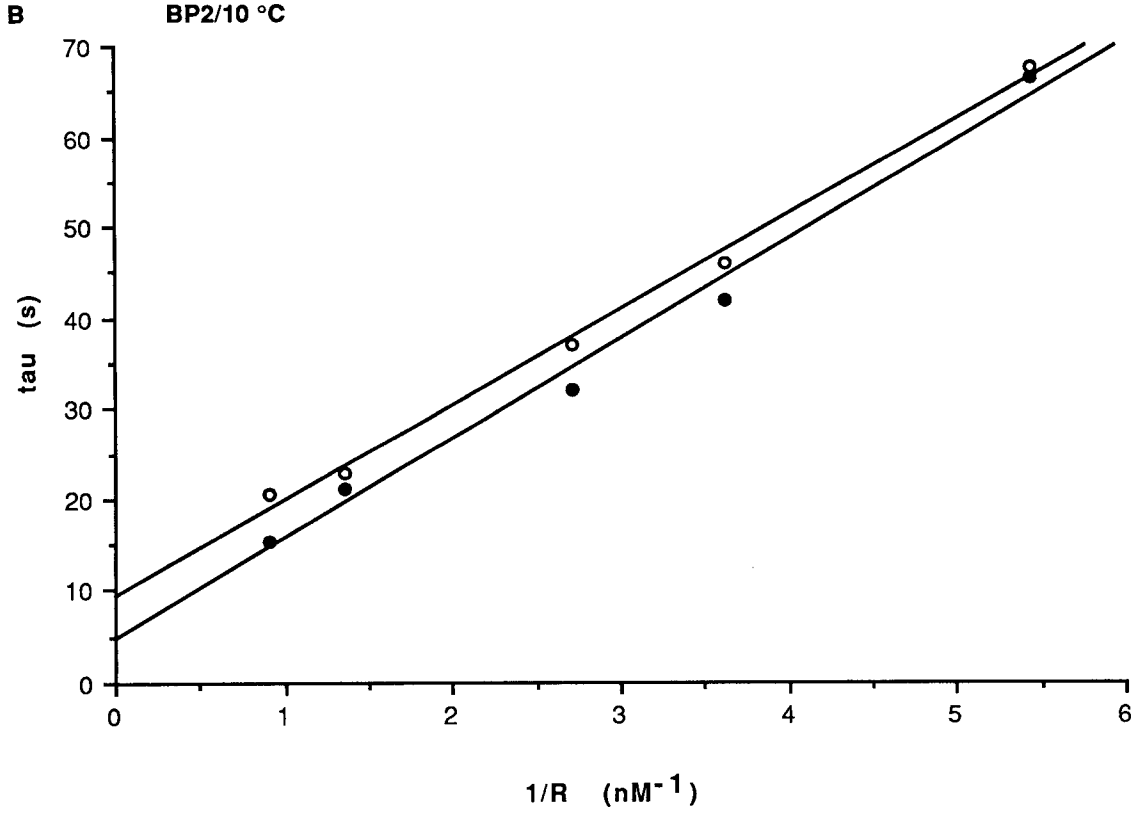
B
BP2/10 °C
tau (s)
70
60
50
40
30
20
10
0
0
1
2
3
4
5
6
1/R (nM-1)

Figure 23. Tau-plot analysis of the association kinetics of complexes between RNA polymerase and the *B. subtilis rrnB* P1 and P2 promoters at 35 °C.

The reciprocals of the association rate constants ($1/\tau$) derived from Figures 19 and 20 were plotted against the reciprocals of the corresponding RNA polymerase concentrations (nM) as described in Figure 22. The absence and presence (final concentration 0.1 mM) of ppGpp during the association experiment is indicated by open and closed symbols respectively. Panel A. Association reactions performed using the *B. subtilis rrnB* P1 promoter (35 °C, DNA templates derived from pKK115B). Panel B. Association reactions performed using the *B. subtilis rrnB* P2 promoter (35 °C, DNA templates derived from pKK183B).

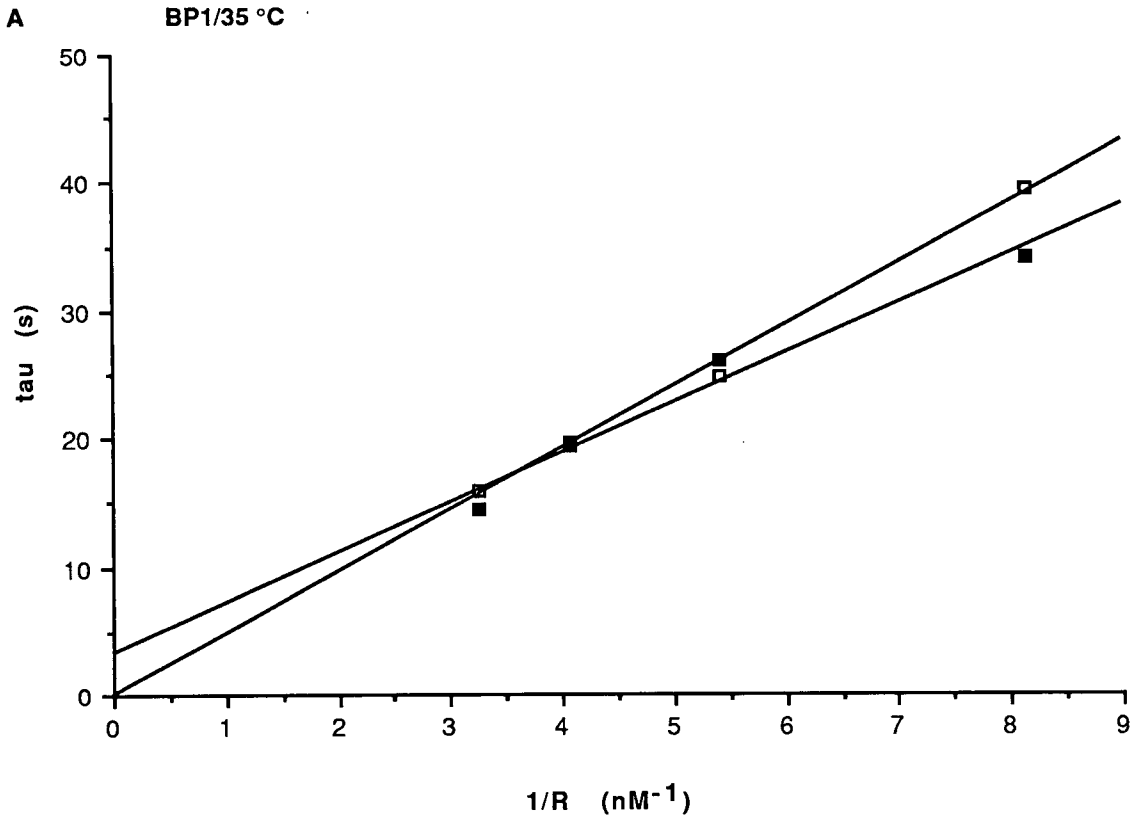
A
BP1/35 °C
tau (s)
1/R (nM-1)
0
10
20
30
40
50
0
1
2
3
4
5
6
7
8
9

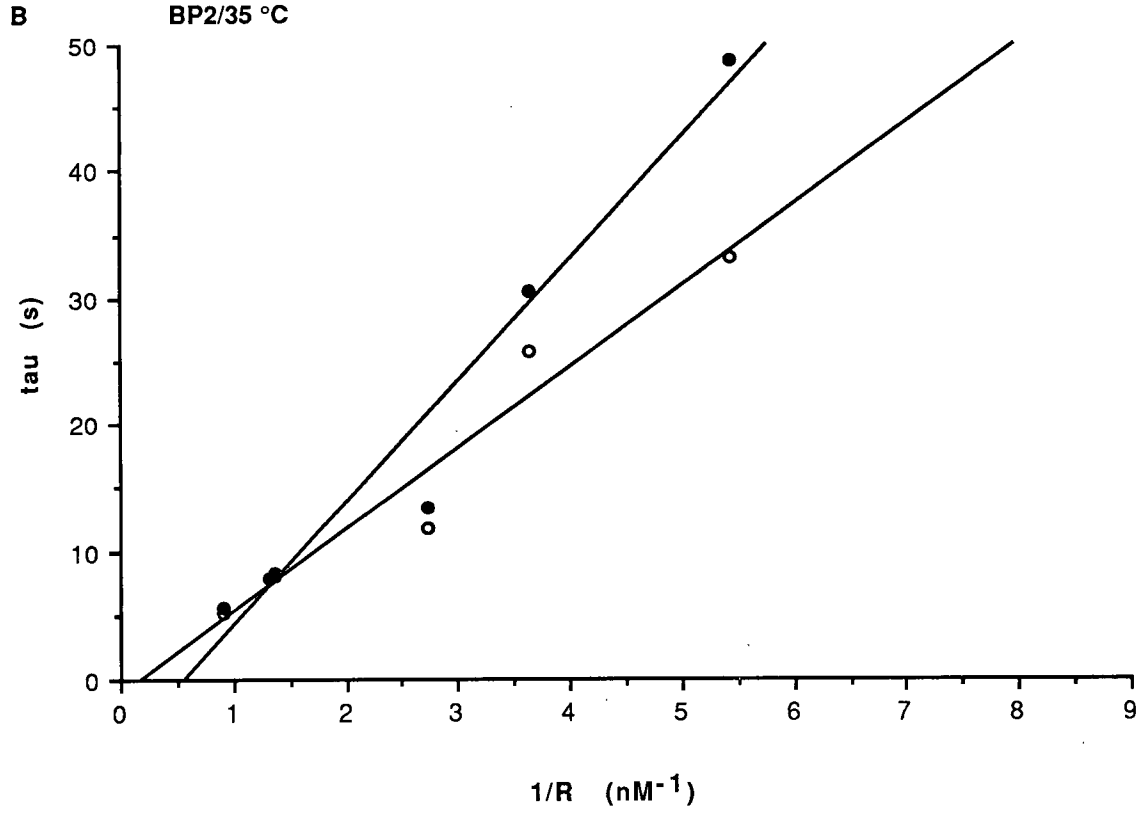
B
BP2/35 °C
tau (s)
1/R (nM-1)
0
10
20
30
40
50
0
1
2
3
4
5
6
7
8
9

Table VI. Derived rate constants from the tau-plot analyses of the association kinetics of complexes between RNA polymerase and the *B. subtilis rrnB* P1 and P2 promoters.

Template [a]	k_a [b] (M^{-1} s^{-1})	k_f [b] (s^{-1})	K1 [c] (M^{-1})
BP1/15 °C/–	$1.3 \pm 0.3 \times 10^8$	$5.7 \pm 1.6 \times 10^{-2}$	$2.3 \pm 0.8 \times 10^9$
BP1/15 °C/+	$1.3 \pm 0.2 \times 10^8$	$8.2 \pm 2.5 \times 10^{-2}$	$1.6 \pm 0.5 \times 10^9$
BP2/10 °C/–	$9.5 \pm 0.4 \times 10^7$	$1.1 \pm 0.2 \times 10^{-1}$	$8.6 \pm 1.4 \times 10^8$
BP2/10 °C/+	$9.1 \pm 0.6 \times 10^7$	$2.2 \pm 1.1 \times 10^{-1}$	$4.1 \pm 2.1 \times 10^8$
BP1/35 °C/–	$2.1 \pm 0.1 \times 10^8$	$\geq 6.5 \times 10^{-1}$	$\leq 3.4 \times 10^8$
BP1/35 °C/+	$2.6 \pm 0.3 \times 10^8$	$3.1 \pm 2.5 \times 10^{-1}$	$\geq 4.1 \times 10^8$
BP2/35 °C/–	$1.5 \pm 0.2 \times 10^8$	$\geq 5.6 \times 10^{-1}$	$\leq 3.0 \times 10^8$
BP2/35 °C/+	$1.0 \pm 0.1 \times 10^8$	≥ 1.0	$\leq 1.1 \times 10^8$

a) For a given association experiment, the DNA template, reaction temperature (°C), and presence (+) or absence (-) of ppGpp is indicated.

b) The results for k_a, k_f and their associated errors (± 1 S. D.) were obtained from the reciprocal of the respective slope and intercept values of Figures 22 and 23 (see also Results section II.4c and Appendix B.IV). In cases where the τ-intercept values were less than zero, a minimum value for k_f was estimated from the reciprocal of (τ intercept + 1 S. D.). For BP2/35 °C/+, a minimum value for k_f was estimated from the reciprocal of (τ intercept + 90% confidence limit for S. D.).

c) The equilibrium binding constant for the bimolecular collision between free RNA polymerase and promoter fragments (K1) was obtained from k_a/k_f. This relationship assumes that the reaction between free RNA polymerase and the promoter equilibrates rapidly, such that $k_a = k_f K1$ (see also Results section II.4c and Appendix B.IV). In situations where k_f represented a minimum threshold, K1 was expressed as a maximum, based on $(k_a + 1 \text{ S. D.})/k_{f(\text{minimum})}$. The exception to this was BP1/35°+, whose K1 value was expressed as a minimum, based on $(k_a - 1 \text{ S. D.})/(k_f + 1 \text{ S. D.})$.

values will also have a high associated error. The equilibrium constant for the bimolecular collision between free RNA polymerase and promoter fragments (K1 = k_1/k_{-1}) was estimated from a ratio of k_a/k_f (this assumes that the reaction between free RNA polymerase and the promoter is in rapid equilibrium, according to equation 14).

Comparison of Tables V and VI reveals that for a given reaction condition (promoter/temperature/± ppGpp), the ratio of k_f/k_d was always ≥ 60. This observation supports the original assumption made for equations 11 - 15 that $k_f >> k_d$ (Results section II.4b)

4d. Thermodynamics of RNA polymerase/promoter association rates.

In Results section II.4c, it was proposed that two alternative mechanisms could describe the association of free RNA polymerase and promoter fragments to form heparin resistant complexes (see also Appendix B.IV; Strickland *et al.*, 1975; McClure, 1980). In one mechanism (equation 14), the initial reaction between enzyme and promoter was governed by a rapid equilibration prior to the rate limiting formation of the heparin resistant complex. In the other mechanism (equation 15), the newly formed heparin sensitive intermediate could not equilibrate with the free reactants, since the conversion of the heparin sensitive complex to a heparin resistant state occurred more rapidly than the dissociation of bound enzyme (i.e. the formation of heparin resistant complexes occurred by a sequential mechanism).

Assuming that the first step exists as a rapid equilibration ($k_{-1} >> k_f$), the rate constants (k_a, k_f) and equilibrium constant ($K1 = k_1/k_{-1}$) which describe the overall association mechanism are summarized in Panel A of Table VII below (see also equations 13 and 14). The associated thermodynamic expressions which are derived from the rate and equilibrium constants are given in Panel B (a review of basic thermodynamic considerations is given in Appendix C).

Table VII. Rate and thermodynamic constants associated with a rapid equilibrium binding mechanism ($k_{-1} >> k_f$).

A. Rate constants	B. Thermodynamic constants
$k_a = k_f K1$	$E_{a,a} = E_{a,f} + \Delta H_1^\circ$
k_f	$E_{a,f}$
$K1 = k_a/k_f$	$\Delta H_1^\circ = E_{a,a} - E_{a,f}$

Assuming that a sequential ($k_f >> k_{-1}$) mode of binding describes the association mechanism, Table VIII shows that a different set of kinetic and thermodynamic expressions will be obtained (see also equations 13 and 15).

Table VIII. Rate and thermodynamic constants associated with a sequential binding mechanism ($k_f >> k_{-1}$).

A. Rate constants	B. Thermodynamic constants
$\mathbf{k_a = k_1}$	$\mathbf{E_{a,a} = E_{a,1}}$
k_f	$E_{a,f}$
$\mathbf{k_a/k_f}$	$\mathbf{E_{a,1} - E_{a,f}}$

Differences between Tables VII and VIII are in bold type. Note especially that the ratio of k_a/k_f, while representing the binding equilibrium constant (K1) under conditions of rapid equilibrium (Table VII: $k_{-1} >> k_f$), has no 'definition' under conditions of sequential binding (Table VIII: $k_f >> k_{-1}$). The enthalpy for the binding equilibrium (ΔH_1°) has been determined for several different promoter systems, and these enthalpies appear to share some general characteristics (see below). As a result, the characteristics of k_a/k_f for the BP1 and BP2 promoters offers a potential means to distinguish between the equilibrium and the sequential binding mechanisms (equations 14 and 15 respectively). This shall be considered below in Table IX, which summarizes the response of the rate and equilibrium constants obtained in Table VI to changes in temperature.

Table IX. Temperature dependence of the derived rate constants for the association of complexes between RNA polymerase and the *B. subtilis rrnB* P1 and P2 promoters.

Promoter (± ppGpp)	$E_{a,d}$ [a] (kcal/mol)	$E_{a,a}$ [a] (kcal/mol)	$E_{a,f}$ [a] (kcal/mol)	ΔH_1° [b] (kcal/mol)
BP1 –	- 20 ± 4	4 ± 1	≥ 21 ± 6	≤ - 17 ± 6
BP1 +	- 28 ± 2	6 ± 1	12 ± 10	- 6 ± 10
BP2 –	- 36 ± 2	3.2 ± 0.4	≥ 11 ± 2	≤ - 8 ± 2
BP2 +	- 37 ± 4	0.6 ± 0.1	≥ 10 ± 6	≤ - 9 ± 6

a) The general relationship used to obtain the activation energy (E_a) for a rate constant (k) is given by $E_a = -R$ [d Ln(k)/d (1/T)], where T = absolute reaction temperature (Kelvin), and R = gas constant (1.987 cal K^{-1} mol^{-1}) (Appendix C, equation C-6). $E_{a,d}$ was calculated from the slope of the Arrhenius plot for the dissociation rates (see Fig. 15), whereas $E_{a,a}$ and $E_{a,f}$ were calculated from the respective values of k_a and k_f (see Table VI).

b) The enthalpy for the bimolecular collision was obtained from the relationship $\Delta H_1^\circ = E_{a,a} - E_{a,f}$ (for example, see Appendix C equation C-8 to C-10). This relationship assumes that the reaction between free RNA polymerase and the promoter equilibrates rapidly, such that $k_a = k_f K1$ (see also Results section II.4c and Appendix B.IV).

Assuming that a rapid equilibrium mechanism described the binding of polymerase at BP1 and BP2, Table IX clearly shows that under both ± ppGpp conditions, ΔH_1° was negative for both BP1 and BP2 (i.e. the magnitude of K1 (= k_a/k_f) decreased with increasing temperature, see also Table VI). The interpretation of this negative ΔH_1° would be that the bimolecular collision occurs by way of an exothermic reaction. This contradicts what has been previously concluded about polymerase/promoter interactions. Indeed, for the pBR322 *tet* (Bertrand-Burggraf *et al.*, 1984), pSC101 *tetR* (Duval-Valentin and Ehrlich, 1987), *lac* UV5 (Buc and McClure, 1985; Straney and Crothers, 1987b), bacteriophage T7 A1 (Kadesch *et al.*, 1982), bacteriophage λ P_R (Roe *et al.*, 1985), and bacteriophage T7 A2 (Singer and Wu, 1988) promoters, the initial bimolecular collision was found to be either temperature insensitive or endothermic.

However, if the association mechanism occurs by way of sequential binding ($k_f >> k_{-1}$), then the ratio of k_a/k_f has no identifiable constraints, since it reflects the ratio of the forward rate constants k_1/k_f (see also Table VIII). Inspection of Table IX shows that the activation energy for k_f, (= $E_{a,f}$), was much larger than the activation energy for k_1, (= $E_{a,a}$). Under a sequential mechanism, the difference between ($E_{a,a}$ - $E_{a,f}$), does not reflect the enthalpy for the bimolecular reaction, however it would generate a negative result. These findings suggest that the initial bimolecular collision between RNA polymerase and either BP1 or BP2 promoter fragments occurs by way of a sequential binding mechanism. This view is also consistent with the behavior of the $1/\tau$ versus [R] plots made at 35° C. Figure 21C shows that the plot of $1/\tau$ versus polymerase concentration was linear for the BP1 and BP2 promoters at 35° C, as opposed to the curved plots which had been observed at the lower reaction temperatures (Figs. 21A and B). Since the concentration range of polymerase was the same at both high and low temperatures (Fig. 21, compare BP2/ – ppGpp at 10 °C and 35 °C), some component of the reaction mechanism must have changed during the shift to the higher reaction temperature. It is possible that the binding constant for the bimolecular collision ($K1 = k_1/k_{-1}$, equation 14) had decreased with increasing temperature. However, as discussed above, such behavior would suggest that the first step is exothermic, and contradicts other experimental observations that the polymerase/promoter bimolecular reaction is relatively temperature insensitive (Kadesch *et al.*, 1982; Roe *et al.*, 1985; Straney and Crothers, 1987b; Singer and Wu, 1988), or endothermic (Bertrand-Burggraf, *et al.*,1984; Buc and McClure, 1985; Duval-Valentin and Ehrlich, 1987). Alternatively, it might be that the forward rate constant for the second step (k_f) increased with increasing temperature. While an increase in k_f is expected based on thermodynamic considerations (see Appendix C, and Table IX), it would only lead to a linear $1/\tau$ plot if the first step of the reaction occurred by way of a sequential ($k_f >> k_{-1}$), instead of a rapid equilibrium ($k_{-1} >> k_f$) mechanism (see equations 13 - 15).

4e. Effects of ppGpp on association rates.

From Table VI it is evident that the addition of ppGpp had no significant impact on the magnitude of k_1 for either BP1 or BP2 at any reaction temperature (Table VI, $k_1 = k_a$). This suggests that ppGpp does not affect the overall rate of open complex formation at the level of the bimolecular collision.

The effect of ppGpp addition on the magnitude of k_f was more difficult to determine due to the large error associated with the tau-plot intercept values (see Table VI and Results section II.4c). For BP1 (at both 15° C and 35° C), differences in k_f under ± ppGpp conditions were not statistically significant as judged by the Student's *t* test (98% confidence, data not shown). Note that the data do not distinguish between the absence of a ppGpp-directed effect and an inability to resolve such an effect. However, under the same confidence limits, the addition of ppGpp produced a statistically significant change in k_f at the BP2 promoter, increasing k_f by approximately two-fold at both 10° C and 35° C. The exact magnitude of this stimulation is uncertain, because the k_f values represented an estimated minimum (see Table VI). It is not clear whether the stimulation of k_f by ppGpp represents a differential effect at the growth rate regulated promoter, since the response of BP1 to ppGpp was uncertain. Similarly, it is unknown whether the stimulation of k_f by ppGpp at BP2 has any regulatory significance, although the affect apparently contradicts the proposal that ppGpp acts as negative effector of growth rate regulated promoters.

5. DNase I protection analyses of complexes formed at BP1 and BP2.

The experiments discussed in Results section II have examined the effects of ppGpp on the overall equilibrium positions, the rates of dissociation, and the rates of association of RNA polymerase complexes at the BP1 and BP2 promoters. So far, no differential effect of ppGpp has been observed. One possible explanation for this would be if the effect of ppGpp acts on a step of the transcription initiation process

not measured by the gel retardation assay, that is, if ppGpp acts on a step following open complex formation. As mentioned in the Introduction, the commitment to transcript elongation *in vitro* is often preceded by a transitory phase of oligonucleotide synthesis and release, known as abortive initiation (Johnston and McClure, 1976; Carpousis and Gralla, 1980, 1985; Carpousis *et al.*, 1982). Since abortive cycling is a reversible step in the overall transcription initiation process, it represents a potential regulatory point (Carpousis and Gralla, 1980, 1985; Carpousis *et al.*, 1982; Kammerer *et al.*, 1986; Straney and Crothers, 1987a).

Resolution of open complexes from initiated complexes in a gel retardation assay can be technically difficult, because the open complex and initiated complex often have the same relative mobility on a polyacrylamide gel (Straney and Crothers, 1985; Krummel and Chamberlin, 1989; results this thesis section III.1). During gel retardation studies of the *lac* UV5 promoter, it was observed that a high-salt challenge could distinguish between open and initiated complexes (Straney and Crothers, 1985) However, a high-salt challenge was not effective in the present system (data not shown), most likely due to the heparin-escape that occurs at salt concentrations greater than 100 mM (see Figure 6).

In order to probe the steps which occur after open complex formation for sensitivity to ppGpp, I decided to use a DNase I protection analysis of complexes formed between RNA polymerase and the BP1 and BP2 promoters. Studies of other promoters have shown that the polymerase footprint is sensitive to the addition of initiating nucleotides (Straney and Crothers, 1987a; Krummel and Chamberlin, 1989). The DNase I protection analysis of polymerase complexes was performed as described in the Materials and Methods. End-labelled templates were constructed in the same manner as for the gel retardation assays (see Materials and Methods). Consequently, all footprints assay the bottom (or coding) strand of the DNA template. Heparin resistant complexes were not purified on a non-denaturing gel to lower the 'background' of the footprint (Krummel and Chamberlin, 1989), since the

percentage of formation of heparin resistant complexes at BP1 and BP2 was virtually 100% under the reaction conditions of this thesis.

Table X below summarizes the initiation conditions used at BP1 and BP2. Based on the published sequences and transcription initiation sites (Stewart and Bott, 1983; Deneer and Spiegelman, 1987) for these promoters, the probable oligonucleotide product (number of nucleotides formed) has been included. The nucleotides marked (in **bold**) denote the transcription initiation sites.

Table X. Initiating sequences for BP1 and BP2.

BP1: 5' C(**G**)UCGCUGA		BP2: 5' A(**A**)AGCUGCUUCA	
Initiating Nucleotides	Product Length (nt)	Initiating Nucleotides	Product Length (nt)
None	0	None	0
GTP	1	ATP	2
GTP, UTP	2	ATP, GTP	3
GTP, UTP, CTP	7	ATP, GTP, CTP	4
		ApA, GTP, CTP, UTP	10

Figure 24 shows the footprint results obtained for BP1. The numbering refers to the base position relative to the transcription initiation site (+ 1). In the absence of any polymerase (lanes L), there was a prominent gap in the DNase I footprint between positions - 53 and - 38, except for some slight reactivity at the - 44/- 45 position. This region corresponds to a 16 bp stretch of A and T residues, which has been shown to display anomalous electrophoretic mobility (Deneer, 1986). A defined footprint occurred on addition of polymerase, and was constant for the 0, GTP, and GTP/UTP initiating conditions. Complete protection of the promoter was observed between positions - 54 and + 17, including the previously sensitive positions at - 44/- 45. Weaker protection also extended to the + 22 site. Enhanced sensitivity was observed at positions - 47/- 46 (minor) and - 37 (major). These

Figure 24. DNase I protection analyses of complexes formed between RNA polymerase and the *B. subtilis rrnB* P1 promoter.

The DNase I protection analyses of complexes formed between RNA polymerase (20 nM) and the *B. subtilis rrnB* P1 promoter (2 nM, template derived from pKK115B) were performed at the indicated reaction temperatures as described in the Materials and Methods. DNase I treated promoter templates were electrophoresed on a 5% sequencing gel, and a picture of the autoradiograph of the sequencing gel is shown (the bottom (or coding) strands of the DNA templates are illustrated). The initiating nucleotide sequence for BP1 is 5'C(**G**)UCGCUGA, where (**G**) denotes the transcription start site (+ 1). The absence (-) or presence (+) of ppGpp during the binding reaction is shown above the reaction lanes, as are the initiating nucleotides and/or analogs present in the binding reaction (see also Table X). In the control reactions (lanes L), RNA polymerase was omitted. Sequence positions relative to the transcription initiation site (+ 1) are indicated to the left of the figure. The schematic to the right of the gel denotes the regions at which RNA polymerase fully (solid line) or partially (dashed line) protected the DNA template. Included in the schematic are the - 35 (closed box), - 10 (open box), and + 1 (closed circle) sites of the promoter. Regions of enhanced DNase I cleavage are indicated by arrows.

BP1: 5' C(G)UCGCUGA

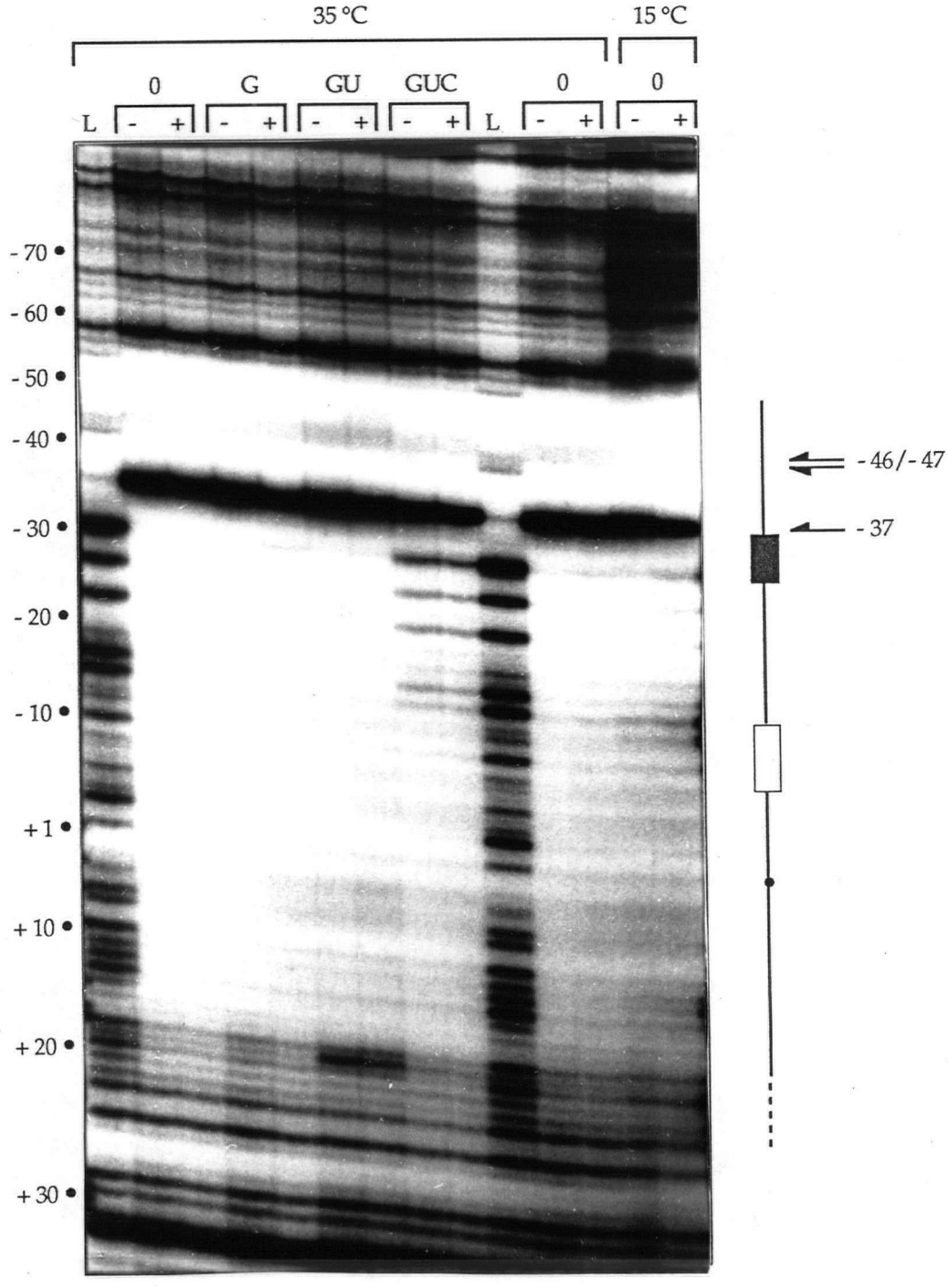

Figure 25. DNase I protection analyses of complexes formed between RNA polymerase and the *B. subtilis rrnB* P2 promoter.

The DNase I protection analyses of complexes formed between RNA polymerase (20 nM) and the *B. subtilis rrnB* P2 promoter (2 nM, template derived from pKK183B) were performed at the indicated reaction temperatures as described in the Materials and Methods. DNase I treated promoter templates were electrophoresed on a 5% sequencing gel, and a picture of the autoradiograph of the sequencing gel is shown (the bottom (or coding) strands of the DNA templates are illustrated). Figure 25 has been presented (with noted exceptions) according to the format described in Figure 24. The initiating nucleotide sequence for BP2 is 5'A(**A**)AGCUGCUUCA, where (**A**) denotes the transcription start site (+ 1). Lanes 1 - 4: The respective C, T, A, and G dideoxy sequencing reactions of the pKK183B template (see Materials and Methods).

BP2: 5' A(**A**)AGCUGCUUCA

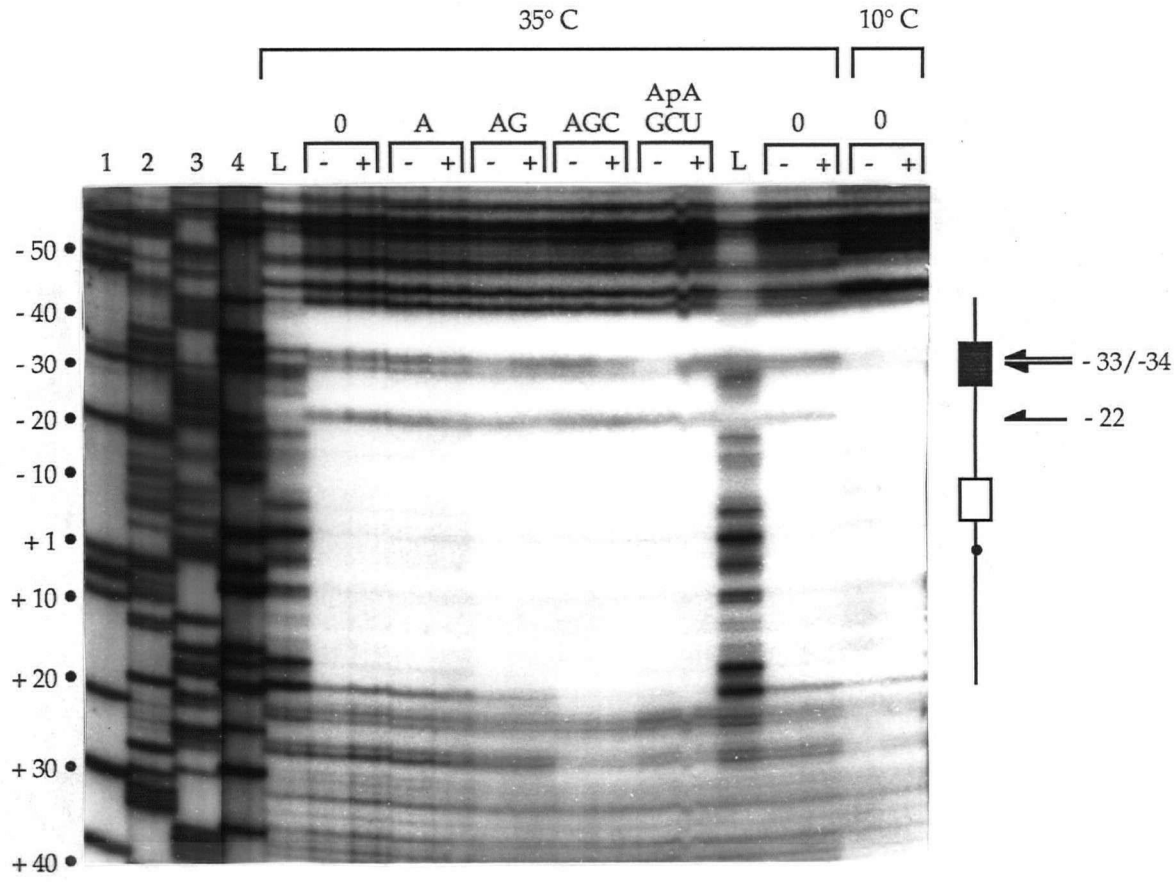

general features did not change under GTP/UTP/CTP initiation conditions, although specific protection of the - 32 to - 17 region was weakened, suggesting that some conformational change in the promoter complex had occurred. However, under no condition was ppGpp observed to significantly alter the pattern of DNase I sensitivity. Similarly, the footprints obtained at 15° C were identical to those formed at 35° C, and were insensitive to ppGpp.

Figure 25 shows the footprint results obtained for BP2. The numbering refers to the base position relative to the transcription initiation site (+ 1). A defined footprint occurred on addition of polymerase, and was constant for the 0, ATP, and ATP/GTP initiating conditions. Complete protection of the promoter was observed between positions - 43 and + 17, and weaker protection also extended to the + 18 site. Enhanced sensitivity was observed at positions - 34/- 33 and - 22. These specific features did not change under ATP/GTP/CTP or ApA/GTP/CTP/UTP initiation conditions, although protection of the + 18 position was now complete, suggesting that some conformational change in the promoter complex had occurred. However, under no condition was ppGpp observed to significantly alter the pattern of DNase I sensitivity. The overall digestion of the promoter complexes at 10° C was not as complete as for the 35° C reactions, which made interpretation of these results difficult. However in general, it appeared that no significant change occurred in the low temperature footprint compared to those obtained at 35° C.

III. Study of polymerase binding at the EP1 and EP2 promoters.

The results in section II suggest that ppGpp has no obvious differential effect on the formation of heparin resistant complexes at the BP1 and BP2 promoters, either in the presence or absence of initiating nucleotides. Since differential effects of ppGpp have been reported at *E. coli* ribosomal RNA promoters under some conditions (see Introduction section III.1), the question was raised whether the

present results are unique to the *B. subtilis* promoters, or whether they reflect the steps which are probed during the gel retardation analysis. To address this question, the effects of ppGpp on heparin resistant complex formation at the *E. coli rrnB* P1 and P2 promoters (EP1 and EP2 respectively) was investigated.

1. Requirements for complex formation.

Using a filter binding assay to measure polymerase complexes at the EP1 promoter, Gourse (1988) reported that stable complex formation at EP1 required low salt conditions (30 mM KCl), and the presence of the initiating nucleotides ATP and CTP. During gel retardation analysis, I found that three changes to the standard binding conditions (see Materials and Methods) had to be made for stable complex formation at the EP1 and EP2 promoters to occur. These are treated in turn below.

First, it was found that replacing 80 mM KCl with 80 mM potassium glutamate (KGlu) optimized heparin resistant complex formation, even when compared to 30 mM KCl (data not shown). This is in agreement with the observations of Leirmo *et al.*, 1987, which demonstrated that the replacement of chloride with glutamate dramatically enhanced polymerase/promoter interactions. The second finding was that complexes were unstable during gel loading, and would even decay within the confines of the gel matrix during electrophoresis (data not shown). This problem was solved by lowering the concentration of the gel buffer to 0.5 x TBE. Finally, both EP1 and EP2 required the addition of initiating nucleotides to form heparin resistant complexes. Table XI below summarizes the initiating conditions used at EP1 and EP2. Based on the published sequences and transcription initiation sites (Jinks-Robertson and Nomura, 1987) for these promoters, the probable oligonucleotide product (number of nucleotides formed) has been included. The nucleotides marked (in **bold**) denote the transcription initiation sites.

Table XI. Initiating sequences for EP1 and EP2.

EP1: 5' C(**A**)CUGA		EP2: 5' C(**C**)CGCGCCGCUGA	
Initiating Nucleotides	Product Length (nt)	Initiating Nucleotides	Product Length (nt)
None	0	None	0
ATP	1	CTP	2
ATP, CTP	2	CTP, OMeGTP	3
ATP, CTP, UTP	3	CTP, GTP	9
ATP, CTP, UTP, OMeGTP	4	CTP, GTP, UTP	11

To investigate the requirement of initiating nucleotides for heparin resistant complex formation at the EP1 and EP2 promoters, binding reactions were performed under standard conditions (Materials and Methods), except that KGlu was substituted for KCl in the reaction buffer. When present, nucleotides and analogs were each at a final concentration of 0.2 mM, and ppGpp was added to 0.1 mM. Following a 5 minute incubation at 35° C, the polymerase/promoter complexes were challenged with heparin and immediately loaded onto 4% polyacrylamide gel (0.5 x TBE) running at 17 volts/cm. Heparin resistant complexes and unbound promoter fragments were identified and measured as described in the Materials and Methods. Results were expressed as the fraction (F) of total DNA which formed a heparin resistant complex with RNA polymerase ($F = RP/P_{total}$), and these values are reported in Table XII. Note that under all conditions, the inclusion of heparin in the binding reaction prior to the addition of RNA polymerase prevented complex formation at both EP1 and EP2 (data not shown).

Figure 26A and Table XII show the binding results obtained for EP1. No complex formation occurred at EP1 in the absence of initiating nucleotides, or when only the single nucleotides were present. Stable complex formation at EP1 required the presence of both the initiating nucleotides ATP and CTP, confirming the observations of Gourse (1988). However, the inclusion of additional nucleotides led

Figure 26. Initiating nucleotide requirements for complex formation at the *E. coli rrnB* P1 and P2 promoters.

Complexes between RNA polymerase and the *E. coli rrnB* P1 (EP1 derived from pKK96E) and P2 (EP2 derived from pKK131E) promoters were formed under standard binding conditions (Materials and Methods), except that K-glutamate was substituted for KCl. Final concentrations of polymerase and promoters were 10 nM and 0.5 nM respectively. When present, initiating nucleotides and analogs were each at a final concentration of 0.2 mM, and ppGpp at 0.1 mM. Following a 5 min incubation at 35° C, heparin was added (final concentration 100 μg/ml) and the binding reaction was immediately loaded onto 4% polyacrylamide gel (0.5 x TBE) running at 17 volts/cm. Figure 26 shows the picture of the autoradiograph of this gel retardation analysis. The positions of heparin resistant complexes (RP) and unbound promoter fragments (P) are indicated to the left of the figure. The absence (-) or presence (+) of ppGpp during the binding reaction is shown above the reaction lanes, as are the initiating nucleotides and/or analogs present in the binding reaction (see also Table XI). Panel A. Initiating nucleotide requirements for EP1. The initiating nucleotide sequence for EP1 is 5'C(**A**)CUGA, where (**A**) denotes the transcription start site (+ 1). Panel B. Initiating nucleotide requirements for EP2. The initiating nucleotide sequence for EP2 is 5'C(**C**)CGCGCCGCUGA, where (**C**) denotes the transcription start site (+ 1).

A

EP1: 5' C(**A**)CUGA

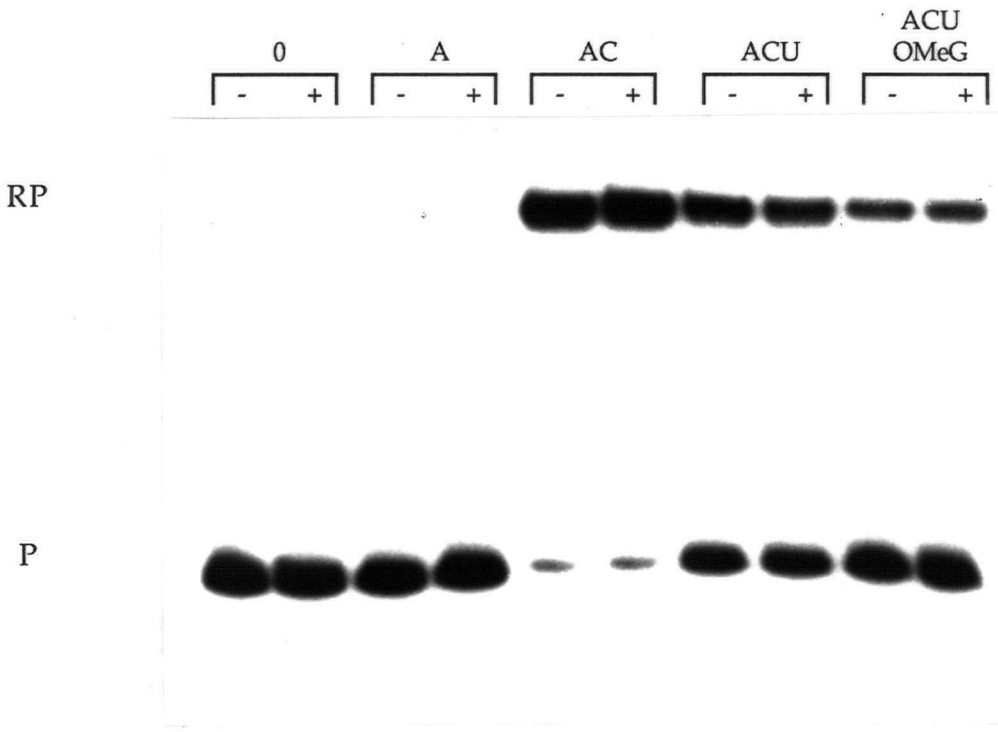

B

EP2: 5' C(**C**)CGCGCCGCUGA

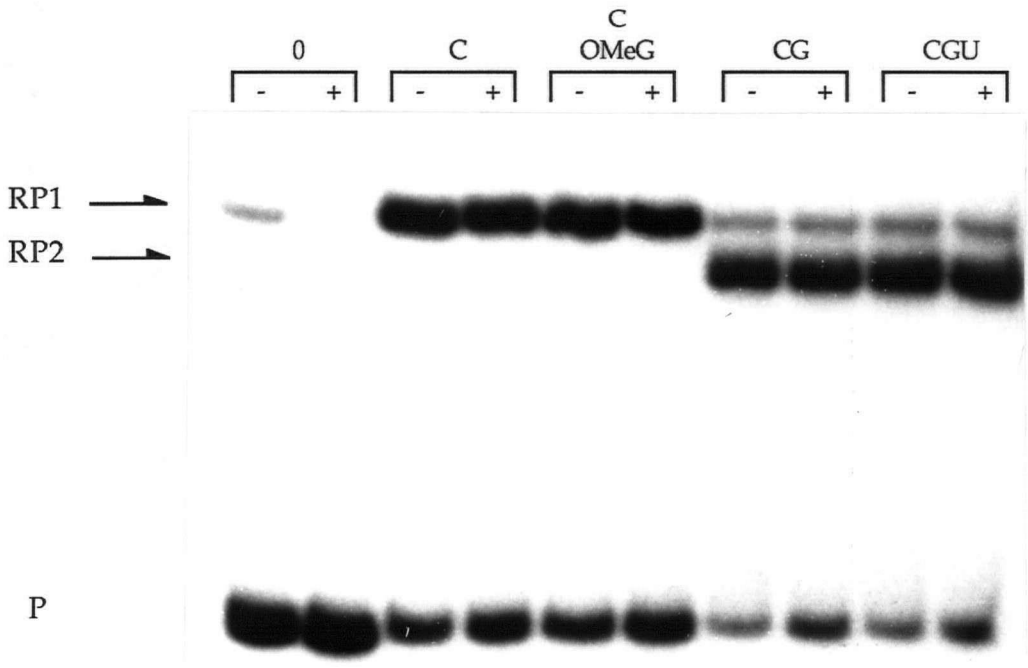

Table XII. Effect of initiating nucleotides on the yield of ternary complexes at the *E. coli rrnB* P1 and P2 promoters.

Promoter	Initiating nucleotides (± ppGpp)	F_1 (RP1/P_{total})	F_2 (RP2/P_{total})	Ratio +/− ppGpp
EP1	0 −	0.04		1.00
	0 +	0.04		
	ATP −	0.04		1.00
	ATP +	0.04		
	ATP, CTP −	0.85		1.00
	ATP, CTP +	0.85		
	ATP, CTP, UTP −	0.49		0.94
	ATP, CTP, UTP +	0.46		
	ATP, CTP, UTP, OMeGTP −	0.30		0.93
	ATP, CTP, UTP, OMeGTP +	0.28		
	CTP −	0.04		
	UTP −	0.04		
	GTP −	0.04		
	OMeGTP −	0.04		
EP2	0 −	0.15		0.40
	0 +	0.06		
	CTP −	0.65		0.89
	CTP +	0.58		
	CTP, OMeGTP −	0.59		0.86
	CTP, OMeGTP +	0.51		
	CTP, GTP −	0.18	0.56	1.00/*0.93* [a]
	CTP, GTP +	0.18	0.52	
	CTP, GTP, UTP −	0.21	0.57	0.86/*0.98* [a]
	CTP, GTP, UTP +	0.18	0.56	
	ATP −	0.13		
	UTP −	0.12		
	GTP −	0.12		
	OMeGTP −	0.12		

Following the gel retardation analyses of Figure 26, heparin resistant complexes and unbound promoter fragments were identified and measured as described in the Materials and Methods. Results were expressed as the fraction (F) of total DNA (P_{total}) which formed a heparin resistant complex with RNA polymerase under given initiating conditions. RP1 and RP2 are the respective upper and lower complexes illustrated in Figure 26B.

a) +/− ratios were calculated for both F_1 (plain) and F_2 (italics).

Figure 27. Yield of ternary complexes at the *E. coli rrnB* P1 and P2 promoters as a function of putative transcript length.

Following the gel retardation analyses of Figure 26, heparin resistant complexes and unbound promoter fragments were identified and measured as described in the Materials and Methods. Results were expressed as the fraction (F) of total DNA (P_{total}) which formed a heparin resistant complex with RNA polymerase under given initiating conditions (see also Table XII). From the published sequences of the *E. coli rrnB* P1 and P2 promoters, the putative transcript length formed under a given initiating condition was calculated (see also Table XI), and the relationship between F and the calculated length of the oligonucleotide product is presented in Figure 27. The absence and presence (final concentration 0.1 mM) of ppGpp during the binding experiment is indicated by open and closed symbols respectively. Circles represent EP1, whereas squares represent EP2. When calculating the value of (F) for EP2 at 9 and 11 nt, only the contributions of the upper complex (RP1) and free promoter fragments (P) were considered (see Fig. 26 and Results section III.1).

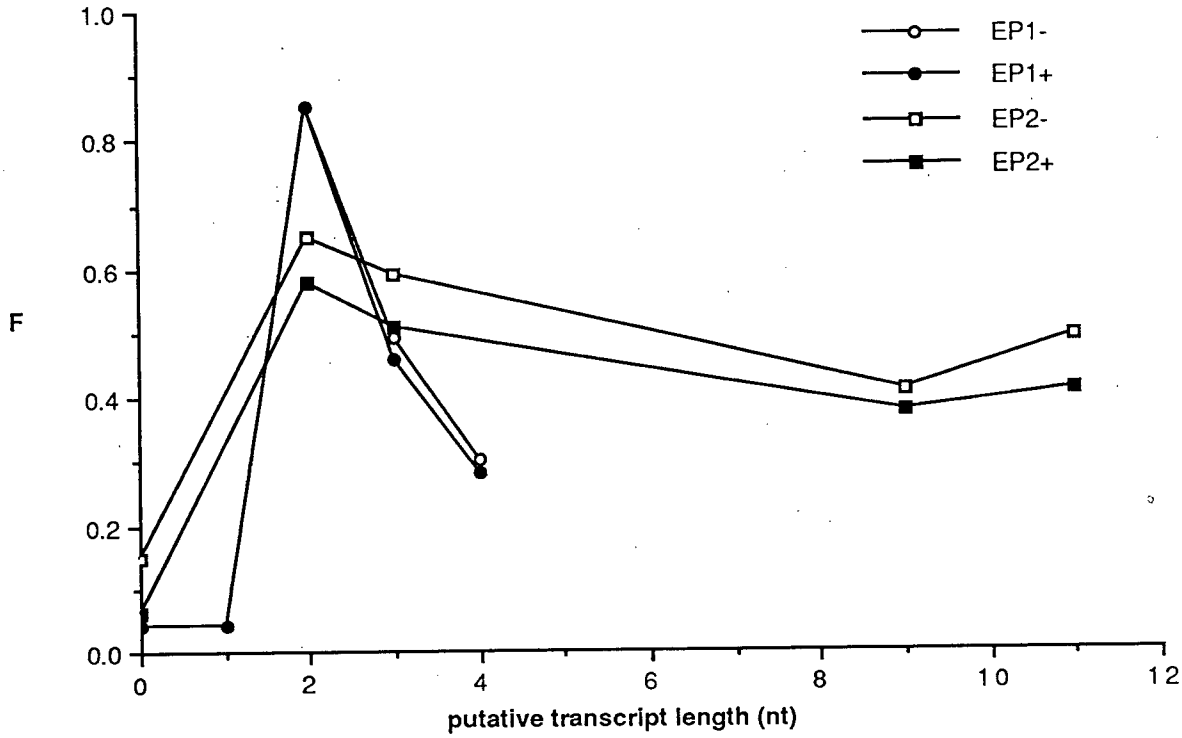
1.0
0.8
0.6
0.4
0.2
0.0
F
0
2
4
6
8
10
12
putative transcript length (nt)
EP1-
EP1+
EP2-
EP2+

to a progressive decrease in the final yield of heparin resistant complexes. As shown in Table XII, the addition of UTP and OMeGTP reduced the level of heparin resistant complexes from 85% to 30% (see also Fig. 27). It has been proposed that extension of the initiating chain length within a ternary complex leads to the formation of a stressed intermediate (Carpousis and Gralla, 1985; Straney and Crothers, 1987a). Since abortive cycling has been demonstrated at EP1 (Levin *et al.*, 1987), it is quite possible that the increased chain length, and hence an increase in polymerase/promoter 'stress', led to an overall decrease in the yield of heparin resistant complexes observed at EP1 (see also Discussion section IV and VI). This inverse correlation between putative chain length and complex formation was not reported by Gourse (1988), who observed a slight increase between ATP/CTP (79%) and ATP/CTP/UTP (84%) initiation conditions. The explanation for this discrepancy likely is due to an increased stringency of the present assay. If the EP1 complexes were sensitive to heparin concentration, then subtle changes in complex stability might be amplified in the present system, since the final concentration of heparin was 10-fold higher in this gel retardation system than in the previously reported filter-binding assay (Gourse, 1988). Whatever its cause, the inverse relationship between putative chain length and complex formation did not increase the sensitivity of EP1 complexes to ppGpp. This is clearly shown in Table XII, where the ratio of complexes formed under ± ppGpp conditions stayed essentially constant under all reaction conditions.

Complexes at EP2, like those at EP1, seemed to require the formation of at least one phosphodiester bond for maximal stability to heparin. Figure 26B and Table XII demonstrate that 15% of the maximal amount of complex formation was observed in the absence of any initiating nucleotides, and that the addition of CTP stimulated this by about 4-fold. The relative mobility of complexes formed under zero and plus CTP initiation conditions was the same (Fig. 26B), suggesting that open complexes were indistinguishable from abortive initiation complexes under

these electrophoresis conditions. When other single nucleotides were used, only background levels of binding were obtained, confirming that transcription at this promoter is specifically initiated by CTP (see Table XI). As with the experiments using EP1, extension of the putative chain length at EP2 decreased the level of heparin resistant complex formation, but not to the same degree (Fig. 27).

A dramatic change in both the complex yield (Table XII) and complex mobility (Fig. 26B) occurred when the initiating nucleotides CTP/GTP or CTP/GTP/UTP were used. The overall yield of heparin resistant complexes increased about 25%, and two distinct complexes were observed. The first complex (RP1) had a mobility identical to that of EP2 under CTP (or CTP/OMeGTP) initiation conditions, whereas the second complex (RP2) ran at an apparently lower molecular weight. It has been observed that the escape of a ternary complex from abortive cycling usually occurred when the chain length reached to about 8 - 14 nucleotides, and that this commitment to elongation was accompanied by the release of the σ factor (Hansen and McClure, 1980; Carpousis and Gralla, 1985; Straney and Crothers, 1985, 1987a; Stackhouse *et al.*, 1989; Krummel and Chamberlin, 1989). Since the CTP/GTP and CTP/GTP/UTP initiation conditions lead to the putative formation of a 9 - 11 nt transcript, it is quite possible that these EP2 complexes lack the σ subunit. Indeed, based on polymerase subunit analysis of complexes formed at the *E. coli* Tac promoter, Krummel and Chamberlin (1989) observed that the synthesis of an 11 nt transcript led to σ release and a shift in complex mobility similar to the one observed at EP2.

A commitment to elongation could also explain why the overall yield of heparin resistant complexes increased with the putative increase in chain length. It has been proposed that the strain energy associated with abortive cycling is lost upon σ release (Carpousis and Gralla, 1985; Straney and Crothers, 1987a), with the consequence that the formation of a ternary elongation complex is essentially irreversible (Rhodes and Chamberlin, 1974; Levin *et al.*, 1987). However, I found

that even under elongation conditions, a constant amount of RP1 existed, representing about 19% of total promoter DNA (Table XII). There are two likely explanations. First, it is possible that the conversion from RP1 to RP2 was not complete in the 5 minute incubation time. However, a time analysis showed that maximum levels of RP2 were obtained within 2 to 5 minutes, and that these levels were stable for at least 10 minutes (data not shown). Alternatively, it is possible that RP1 consisted of a fraction of the polymerase population that was unable to form an elongation ternary complex, but still able to initiate nucleotide incorporation. Inspection of Table XII suggests that at least 85% of the RNA polymerase was capable of initiating oligonucleotide synthesis (see EP1: ATP/CTP initiation), but that only about 55% of the enzyme population was able to commit to elongation (see EP2: RP2 formation during CTP/GTP and CTP/GTP/UTP initiation). If RP1 represents complexes trapped in an abortive cycling mode of transcription, then the ratio of RP1/(RP1 + free DNA) can be calculated as 42% (this value excludes any contribution from RP2 which, as discussed above, is assumed to be in an essentially irreversible elongation complex). This result is consistent with the proposal that the yield of the heparin resistant complexes decreases as the chain length of the abortive transcript increases (see also Fig. 27).

As with EP1, EP2 complexes showed no sensitivity to ppGpp. This is shown in Table XII where, except for in the absence of initiating nucleotides, the ratio of complexes formed under ± ppGpp conditions stayed relatively constant under all reaction conditions. In the absence of initiating nucleotides, the addition of ppGpp led to a 60% decrease in the amount of heparin resistant complex formation at EP2. It is difficult to determine the significance of this result, since direct comparison to EP1 is not possible under these initiating conditions, and EP2 is neither growth rate regulated nor subject to stringent control *in vivo* (Sarmientos and Cashel, 1983; Sarmientos *et al.*, 1983; Gourse *et al.*, 1986).

The results from Table XII are summarized in Figure 27. It is notable that the apparent complex stabilities at EP1 and EP2 were differentially sensitive to the putative transcript length. As the putative transcript length at EP1 increased from 2 to 4 nucleotides, the level of heparin resistant complex formation dropped nearly three-fold. However at EP2, an increase in putative transcript length from 2 - 10 nt led to only a 30% decrease in the level of heparin resistant complex formation. The possible implications that this differential response might have for growth rate regulation shall be discussed in a later section (see Discussion section VI).

2. Partitioning of RNA polymerase between EP1 and EP2.

To investigate whether ppGpp could alter the partitioning coefficient of polymerase between EP1 and EP2, a mixed-template assay was set up as described in Results section II.2, under modified binding conditions at 35 ° C (see Materials and Methods for standard conditions). Modifications included the replacement of KCl with KGlu, and the addition of the initiating nucleotides ATP and CTP. As discussed in Results section III.1, these conditions were sufficient to promote stable heparin resistant complex formation at both the EP1 and EP2 promoters (see Fig. 26 and Table XII).

Figure 28 shows the results of the gel retardation analysis. The difference in size between EP1 (362 bp), and EP2 (397 bp) resulted in the separation of the bound complexes at these two promoters, although the resolution was not as good as was obtained with the BP1 and BP2 promoters (see Fig. 11). As a result, it was concluded that the error in measurement of bound complexes at the mixed EP1 and EP2 promoters was slightly higher than at the individual templates. For each promoter in a mixed template binding reaction, results were expressed as the fraction (F) of that promoter's total DNA which formed heparin resistant complexes with RNA polymerase at a given enzyme concentration ($F = RP/P_{total}$). These results are summarized in Table XIII, and discussed below.

Figure 28. Partitioning of RNA polymerase between the *E. coli rrnB* P1 and P2 promoters.

DNA fragments containing the *E. coli rrnB* P1 (EP1 derived from pKK96E) and P2 (EP2 derived from pKK131E) promoters were combined in equimolar amounts (0.5 nM each) and incubated with decreasing concentrations of RNA polymerase under modified standard binding conditions (Materials and Methods). Modifications included the replacement of KCl with K-glutamate, and the inclusion of the initiating nucleotides ATP and CTP (0.2 mM each). When present in the reactions, ppGpp was at a final concentration of 0.1 mM. Following a 10 minute incubation at 35 °C, the complexes were challenged with heparin (final concentration 100 μg/ml), and the binding reactions were immediately loaded onto a 4% polyacrylamide gel (0.5 x TBE) running at 17 volts/cm (see Materials and Methods). Figure 28 shows a picture of the autoradiograph of this gel retardation analysis. The positions of heparin resistant complexes (RP) and unbound promoter fragments (P) are indicated to the left of the figure for both the EP1 and EP2 templates. In control experiments (Lanes 1 and 2), binding reactions contained either EP1 or EP2 respectively, without added RNA polymerase. For the experiments in Lanes 3 and 4, binding reactions contained either EP1 or EP2 respectively, with RNA polymerase present at a final concentration of 5.0 nM. Lanes 5 - 12: Binding reactions contained both EP1 and EP2 templates. Reactions loaded onto odd and even numbered lanes were performed in the absence and presence of ppGpp respectively. RNA polymerase was present at the following concentrations: Lanes 5, 6: 5.0 nM. Lanes 7, 8: 1.0 nM. Lanes 9, 10: 0.5 nM. Lanes 11, 12: 0.25 nM.

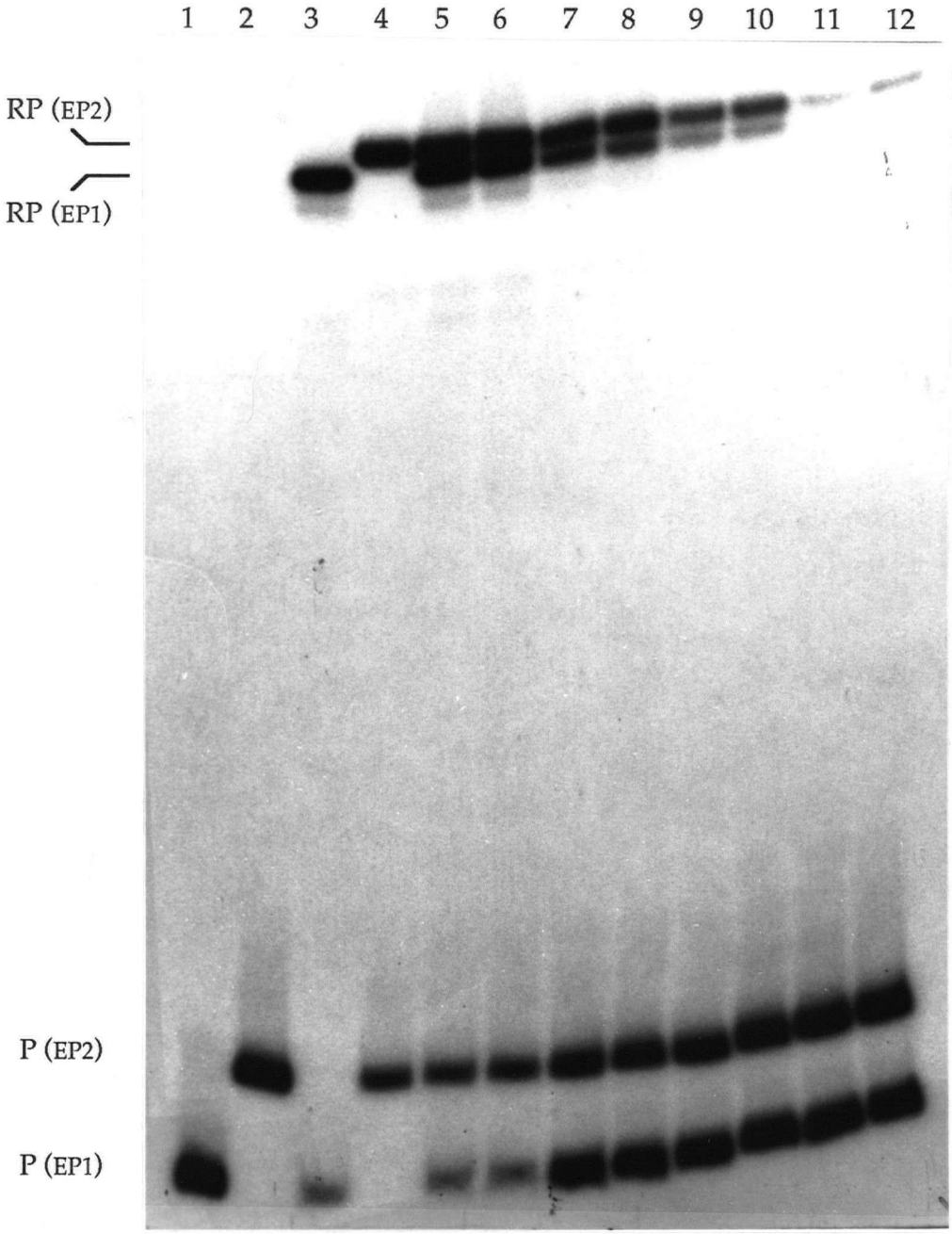
1 2 3 4 5 6 7 8 9 10 11 12
RP (EP2)
RP (EP1)
P (EP2)
P (EP1)

Table XIII. Partitioning of RNA polymerase between the *E. coli rrnB* P1 and P2 promoters.

nM Polymerase (R) ± ppGpp	$F_{(EP2)}$	$F_{(EP1)}$	Relative partitioning [a]
EP1 (R = 0)		0	
EP2 (R = 0)	0		
EP1 (R = 5.0)		0.81	
EP2 (R = 5.0)	0.64		
5.0 –	0.66	0.81	0.99
5.0+	0.63	0.77	
1.0 –	0.42	0.34	0.91
1.0 +	0.38	0.28	
0.5 –	0.24	0.16	1.20
0.5 +	0.20	0.16	
0.25 –	0.08	0.09	0.48
0.25 +	0.13	0.07	

The data for Table XIII was obtained from Figure 28. For each promoter in a mixed template binding reaction, results were expressed as the fraction (F) of that promoter's total DNA which was found in heparin resistant complexes with RNA polymerase at a given enzyme concentration (R). Results from binding reactions which contained only the individual EP1 or EP2 promoters (Lanes 1 - 4 of Figure 28) were also included in Table XIII. The presence (+) or absence (–) of ppGpp in a binding reaction is noted accordingly.

a) The value of F obtained for each promoter under a particular reaction condition was expressed as a ratio between EP1 and EP2 (i.e. $F_{(EP1)}/F_{(EP2)}$). The term $(F_{(EP1)}/F_{(EP2)})$ was then compared between (+ ppGpp)/(– ppGpp) conditions.

Except at the lowest polymerase concentration, the addition of ppGpp had no dramatic effect on the binding equilibrium for either EP1 or EP2, confirming the results obtained with each promoter independently (see Table XII). This is also seen by comparing the relative partitioning of RNA polymerase between EP1 and EP2 under ± ppGpp conditions (Table XIII). If there was no differential effect of ppGpp on the partitioning of RNA polymerase between EP1 and EP2, the relative partitioning coefficient would have a value of 1.00. Between the polymerase concentrations of 5 to 0.5 nM, there was no differential effect on the partitioning of RNA polymerase between EP1 and EP2 by ppGpp (see Table XIII). At 0.25 nM, there was an apparent increase in the absolute level of complex formation at EP2 when ppGpp was added. However, since the error in measurement was more significant at lower polymerase concentrations, and since the direction of the change at EP2 was opposite to that observed at all other polymerase concentrations, it was felt that this apparent shift was not significant.

3. DNase I protection analyses of complexes formed at EP1 and EP2.

To confirm the results obtained in section III.1, and to further compare complex formation between RNA polymerase and growth-rate versus non-growth rate regulated promoters, EP1 and EP2 complexes were assayed for their sensitivity to DNase I. The DNase I protection analysis of polymerase complexes was performed as described in the Materials and Methods, except that KCl was replaced with KGlu in the reaction buffer. End-labelled templates were constructed in the same manner as for the gel retardation assays (see Materials and Methods). Consequently, all footprints assayed the bottom (or coding) strand of the DNA template. Initiating conditions used at EP1 and EP2 were the same as those employed in Results section III.1 to test the nucleotide requirements for heparin resistant complex formation (see Table XI).

Figure 29 shows the footprint results obtained for EP1. The numbering refers to the base position relative to the transcription initiation site (+ 1). In the absence of any polymerase (lanes L), there was a prominent gap in the DNase footprint between positions - 58 and - 39, except for some slight sensitivity at the - 50 and - 45 position. This is strikingly similar to the pattern observed at the BP1 promoter (see Results section II.5, Fig. 24), and like BP1, corresponds to a 17 bp stretch of A and T residues, which has been shown to display anomalous electrophoretic mobility (Gourse *et al.*, 1986). The nucleotide requirements for the acquisition of a stable footprint were identical to those for complex formation in the gel retardation assay (see also Fig. 26A). Since the DNase I treatment assays the formation of polymerase/promoter complexes in the reaction tube, this observation suggests that no complex loss occured during the gel retardation experiments performed in sections III.1 and III.2 (i.e. the inability to detect complexes in the absence of initiating nucleotides was not due to complex instability in the 0.5 x TBE gel buffer).

Under ATP/CTP initiation conditions, complete protection of the EP1 promoter by RNA polymerase was observed between positions - 45 and + 18, and weaker protection was extended to the + 22 site (Fig. 29). Enhanced sensitivity was observed at positions - 46 (minor) and - 37 (major), as well as at position + 19. While these specific features did not change under ATP/CTP/UTP, or ATP/CTP/UTP/OMeGTP initiation conditions, the background protection of the - 34 to + 18 region was reduced. This is consistent with the observations made in Results section III.1, that increasing the putative chain length of the abortive transcript lowers the equilibrium level of complex formation. A similar reduction of this background protection was observed on addition of ppGpp.

Figure 30 shows the footprint results obtained for EP2. The numbering refers to the base position relative to the transcription initiation site (+ 1). The nucleotide requirements for the acquisition of a stable footprint at EP2 were identical to those

Figure 29. DNase I protection analyses of complexes formed between RNA polymerase and the *E. coli rrnB* P1 promoter.

The DNase I protection analyses of complexes formed between RNA polymerase (20 nM) and the *E. coli rrnB* P1 promoter (2 nM, template derived from pKK96E) were performed at 35 °C as described in the Materials and Methods (KCl replaced with K-glutamate). DNase I treated promoter templates were electrophoresed on a 5% sequencing gel, and a picture of the autoradiograph of the sequencing gel is shown (the bottom (or coding) strands of the DNA templates are illustrated). The initiating nucleotide sequence for EP1 is 5'C(**A**)CUGA, where (**A**) denotes the transcription start site (+ 1). The absence (-) or presence (+) of ppGpp during the binding reaction is shown above the reaction lanes, as are the initiating nucleotides and/or analogs present in the binding reaction (see also Table XI). Lanes 1 - 4: The respective C, T, A, and G dideoxy sequencing reactions of the pKK96E template (see Materials and Methods). In the control reactions (lanes L), RNA polymerase was omitted. Sequence positions relative to the transcription initiation site (+ 1) are indicated to the left of the figure. The schematic to the right of the gel denotes the regions at which RNA polymerase fully (solid line) or partially (dashed line) protected the DNA template. Included in the schematic are the - 35 (closed box), - 10 (open box), and + 1 (closed circle) sites of the promoter. Regions of enhanced DNase I cleavage are indicated by arrows.

EP1: 5' C(A)CUGA

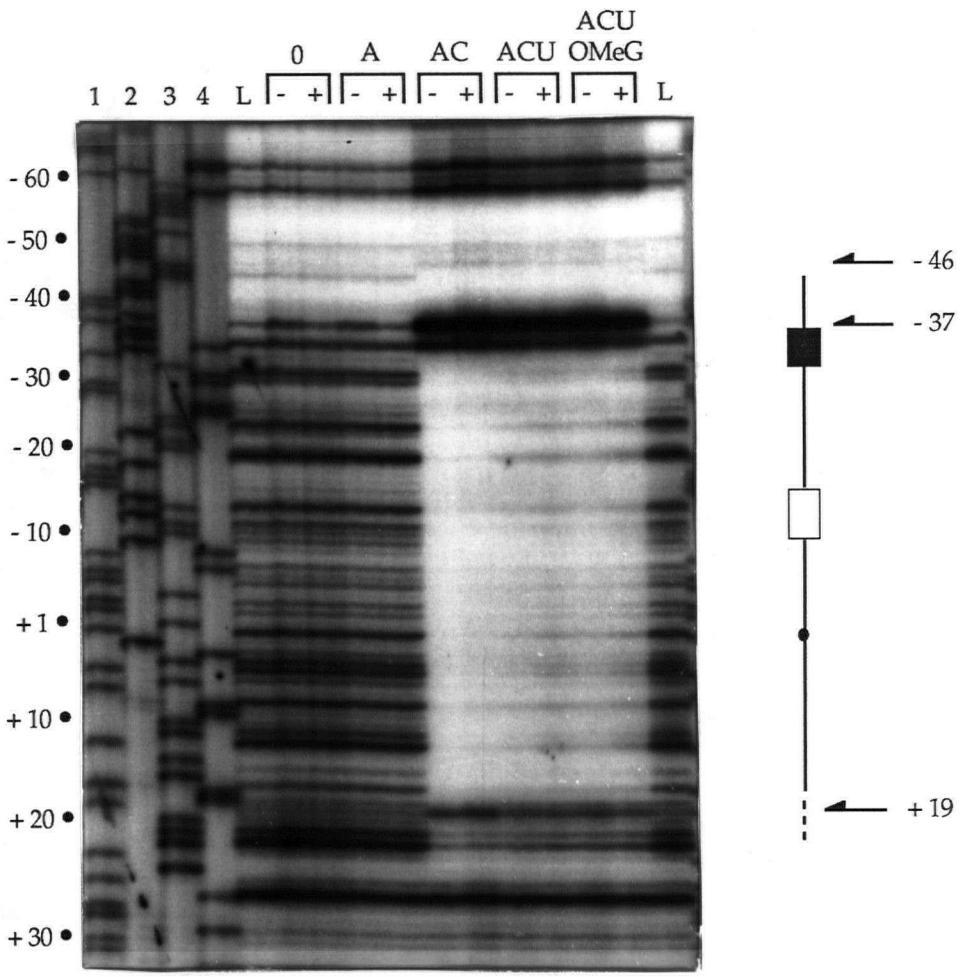

Figure 30. DNase I protection analyses of complexes formed between RNA polymerase and the *E. coli rrnB* P2 promoter.

The DNase I protection analyses of complexes formed between RNA polymerase (20 nM) and the *E. coli rrnB* P2 promoter (2 nM, template derived from pKK131E) were performed at 35 °C as described in the Materials and Methods (KCl replaced with K-glutamate). DNase I treated promoter templates were electrophoresed on a 5% sequencing gel, and a picture of the autoradiograph of the sequencing gel is shown (the bottom (or coding) strands of the DNA templates are illustrated). Figure 30 has been presented (with noted exceptions) according to the format described in Figure 29. The initiating nucleotide sequence for EP2 is 5'C(**C**)CGCGCCGCUGA, where (**C**) denotes the transcription start site (+ 1). Lanes 1 - 4: The respective C, T, G, and A dideoxy sequencing reactions of the pKK131E template (see Materials and Methods). The right-hand schematic represents DNase I protection under CTP and CTP/OMeGTP initiating conditions. The left-hand schematic represents DNase I protection under CTP/GTP and CTP/GTP/UTP initiating conditions.

EP2: 5' C(C)CGCGCCGCUGA

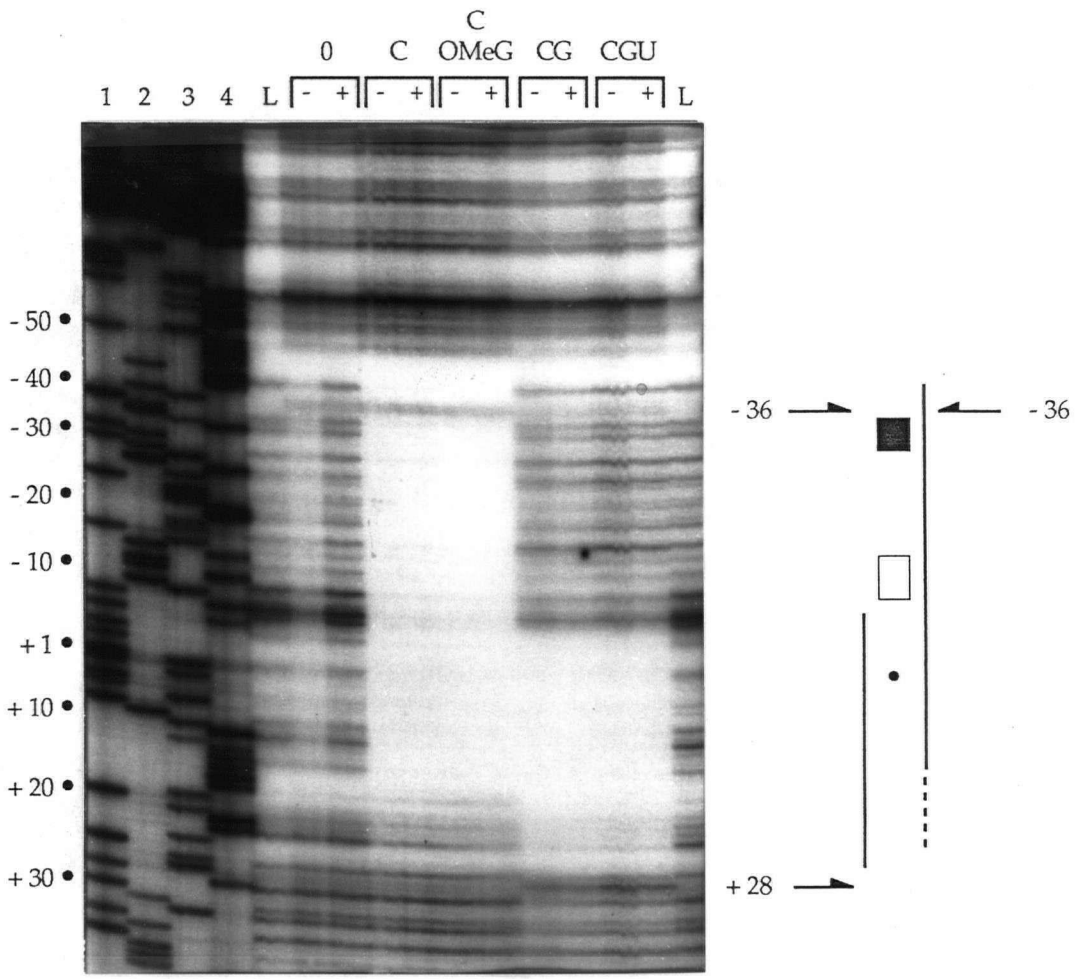

for complex formation in the gel retardation assay (see also Fig. 26B). A defined polymerase footprint occurred on addition of CTP, or CTP/OMeGTP. Complete protection of the promoter was observed between positions - 40 (upper limit of resolution is - 46) and + 15, and reduced protection was extended to the + 23 site. Enhanced sensitivity was observed at position - 36. A dramatic shift in this footprint occurred during CTP/GTP and CTP/GTP/UTP initiation conditions. Upstream protection between positions - 40 to - 5 was completely lost, whereas downstream protection now covered the promoter to the + 26 position. Furthermore, an increased sensitivity was observed at the + 28 site. These observations suggested that a major conformational change had occurred at the EP2 complex, and confirmed the results obtained from the gel retardation analysis (see Fig. 26B). Similar shifts in protection have been reported at other initiated promoters (Carpousis and Gralla, 1985; Straney and Crothers, 1985, 1987a; Krummel and Chamberlin, 1989; Metzger *et al.*, 1989a), and these have subsequently been found to involve the release of the σ subunit, and the commitment of the ternary complex to transcript elongation (Straney and Crothers, 1985; Krummel and Chamberlin, 1989). Except in the absence of initiating nucleotides, the addition of ppGpp had no effect on the overall footprint of the EP2 complexes. In the absence of initiating nucleotides, the addition of ppGpp reduced the overall level of DNase protection, suggesting that polymerase binding was reduced at EP2 (this point was discussed in section III.1 above).

Discussion

I. A model for open complex formation at the BP1 and BP2 promoters.

The results from this thesis suggest that the formation of heparin resistant complexes between *E. coli* RNA polymerase holoenzyme and the *rrnB* P1 and P2

promoters from *B. subtilis* proceeded by way of three kinetically significant reaction steps. The initial bimolecular collision between free RNA polymerase (R) and the promoter (P) led to the formation of a heparin sensitive (HS) complex, which subsequently isomerized to an intermediate (HR1) and then final (HR2) heparin resistant complex. This process is shown below in equation 16.

$$R + P \underset{k_{-1}}{\overset{k_1}{\rightleftharpoons}} HS \underset{k_r}{\overset{k_f}{\rightleftharpoons}} HR1 \underset{k_{-3}}{\overset{k_3}{\rightleftharpoons}} HR2 \qquad (16)$$

Note that the results from this thesis cannot rule out the existence of additional heparin resistant or heparin sensitive states which are physically (or kinetically) undetectable under the present assay conditions. Equation 16 represents a minimum reaction mechanism, and accounts for two observations:

1. From the temperature dependence of the dissociation rates of heparin resistant complexes, it was calculated that the dissociation process had a negative activation energy. This negative activation energy suggested that equilibration between two heparin resistant complexes could occur before the rate limiting formation of a heparin sensitive state (see Results section II.3d). The dissociation mechanism was summarized by equation 5, in which

$$HR2 \underset{k_3}{\overset{k_{-3}}{\rightleftharpoons}} HR1 \xrightarrow{k_r} HS$$

2. The response of the overall association rate constant ($1/\tau$) to polymerase concentration at low reaction temperatures was hyperbolic. This suggested that a heparin sensitive complex formed as a result of the bimolecular reaction between free RNA polymerase and promoter fragments, and that isomerization to a heparin resistant state was subsequent to this step (see Results section II.4b). The association mechanism was summarized by equation 11, in which

$$R + P \underset{k_{-1}}{\overset{k_1}{\rightleftharpoons}} HS \underset{k_d}{\overset{k_f}{\rightleftharpoons}} HR$$

To integrate the separate observations made in points 1 and 2, the respective dissociation and association mechanisms of equations 5 and 11 were combined in a linear fashion to produce the overall reaction mechanism of equation 16. Refinements to this overall reaction mechanism were based on the following three observations.

1. In studying the temperature dependence of the dissociation rates of heparin resistant complexes, the linear positive slopes of the Arrhenius plot at low temperatures indicated that $k_3 >> k_{-3}$ for all reaction temperatures tested (see Results section II.3d), suggesting that the reverse rate constant k_{-3} did not contribute significantly to the overall association rate. Having $k_3 >> k_{-3}$ was also consistent with the observation that at saturating polymerase, the formation of heparin resistant complexes were close to 100 % (see Figs. 9 and 10). If the equilibrium position of the final step of equation 16 lies far to the right, ultimately, all prior steps will proceed to the right as well. However, the overall equilibrium position of equation 16 does not determine the ability of the reverse rate constants k_{-1} and k_r to contribute to the overall rate of heparin resistant complex formation. Instead, the relationship between k_{-1} and k_f, and between k_r and k_3 determines the contribution of the reverse rate constants to the overall association kinetics. This is seen in points 2 and 3 below.

2. The ability of HR1 and HR2 to equilibrate prior to the formation of HS required that $k_3 >> k_r$ (i.e. a newly formed HR1 complex will isomerize to create HR2 faster than it can decay back to a heparin sensitive state; Results section II.3d). This relationship, in conjunction with the observation that $k_3 >> k_{-3}$ (see point 1 above), suggested that from a practical standpoint the contribution of k_r to the overall association kinetics was negligible.

3. The temperature dependence of k_f, and the temperature dependence of the (overall) second-order association rate constant for heparin resistant complex formation (k_a), were inconsistent with the proposal that free RNA polymerase and

promoter fragments existed in rapid equilibrium with HS (in this case, $k_{-1} >> k_f$, and $k_a = k_f K1$). If this rapid equilibrium existed, then the predicted equilibrium constant for the bimolecular step ($K1 = k_a/k_f$) would be exothermic, contradicting the temperature dependence of K1 observed at other promoters (see Results section II.4d). Consequently, it was proposed that a sequential ($k_f >> k_{-1}$, and $k_a = k_1$) mode of binding best described the bimolecular collision, and that the contribution of k_{-1} to the overall association rate was negligible.

II. Comparison to other promoter systems.

1. The mechanism.

The overall reaction mechanism outlined in equation 16 is entirely consistent with both kinetic and physical studies which have been performed at other promoter systems using *E. coli* RNA polymerase. Some of these other studies have been summarized below in Table XIV.

Table XIV. Kinetic and physical evidence to support a minimum three step reaction mechanism for open complex formation.

Promoter	Kinetic evidence	Physical evidence
groE		Cowing *et al.*, 1989.
lac UV5	Buc and McClure, 1985.	Spassky *et al.*, 1985; Straney and Crothers, 1985, 1987c.
λP_R	Roe *et al.*, 1984, 1985.	
λP_{RM}	Hawley and McClure, 1982.	
rrnB P1[a]	This thesis.	
rrnB P2[a]	This thesis.	
T7 A1	Kadesch *et al.*, 1982; Rosenberg *et al.*, 1982.	Schickor *et al.*, 1990.
tetR	Duval-Valentin and Ehrlich, 1987.	Duval-Valentin and Ehrlich, 1987.

[a]: Derived from *B. subtilis*.

Note that in all cases (including the results of this thesis), the presence and order of the reaction intermediates have been based on the observed differential stability or reactivity of RNA polymerase/promoter complexes to a variety of selective probes (e.g. the stability of a complex to a non-specific competitor template, or the reactivity of a complex to a modifying agent). Therefore, the equivalent reaction intermediates which have been based on different assays are not necessarily identical with one another. However, the collective information from these studies of polymerase/promoter interactions are the basis of the general three-step reaction mechanism for open complex formation which was described in the Introduction (section V.3 equation 1). Consequently, for the sake of comparison to other investigations of polymerase/promoter interactions, the initial heparin sensitive complex of this thesis is considered to be equivalent to the closed complex of equation 1. Similarly, HR1 and HR2 of equation 16 parallel the intermediate and open complexes of equation 1.

The majority of studies at other promoters have suggested that an equilibrium is rapidly established between the reactants and the closed complex. The reaction outlined in equation 16 is different, since the formation of the heparin sensitive (closed) complex proceeds by way of a sequential mechanism. For a sequential reaction, it might be expected that facilitating mechanisms, such as one-dimensional sliding, increase the rate of closed complex formation (for reviews, see Berg and von Hippel, 1985; Lohman, 1986). However, such facilitating mechanisms are only effective under diffusion-controlled conditions (i.e. when every collision between a polymerase/promoter active site forms a closed complex). Estimation of whether a particular reaction is diffusion-controlled is often based on a comparison of the observed reaction rate and the theoretical limit for the same process. When the observed reaction rate approaches or exceeds the theoretical limit, the bimolecular collision is often considered to be diffusion-controlled (Berg *et al.*, 1981). It has been estimated (von Hippel *et al.*, 1984) that the maximum rate for promoter-

specific closed complex formation is approximately 10^8 $M^{-1}s^{-1}$, which is in good agreement with the observed rates at 35° C for BP1 and BP2 (see Table VI: $k_a = k_1$). Therefore it is possible that the formation of the closed complex at BP1 and BP2 is controlled by the rate of diffusion.

There might be difficulties in comparing the rate constants derived for BP1 and BP2 if a diffusion-controlled reaction existed. Under a diffusion-controlled mechanism, closed complex formation rates could be influenced by several parameters, including general solution conditions, length of the DNA template, and relative positioning of the promoter within that template (Berg *et al.*, 1981; Berg and von Hippel, 1985; Lohman, 1986; Mazur and Record, 1989). While the solution conditions between BP1 and BP2 were identical, differences existed between these promoters in their template size and their relative positioning. However, the difference in template size between BP1 (381 bp) and BP2 (449 bp) was negligible ($\approx$ 18%), and it is not expected to produce a measurable difference in the association rate constant (k_1) (under comparable solution conditions, Winter *et al.* (1981) found that a $\geq$ 30 fold increase in template size led to only a 3 fold increase in the formation rate of *lac* repressor-operator complexes). Similarly, the theoretical effects of site position on association rates are only significant when the DNA template is long enough to form coiled domains (Mazur and Record, 1989). Since both BP1 and BP2 are shorter than 700 - 800 bp, they should display rod-like behavior in solution (Record *et al.*, 1975).

In summary, variations between the observed rate constants for BP1 and BP2 must reflect inherent differences between the specific polymerase/promoter complexes, and are not due to differences between the sizes or promoter locations of the two templates.

2. Magnitudes of the rate constants.

Several reviews have compiled the kinetic information obtained from *in vitro* transcription initiation studies at a variety of naturally occurring (mutant or hybrid promoters were not considered here) *E. coli* and bacteriophage promoters (von Hippel *et al.*, 1984; McClure, 1985; Travers, 1987). Two parameters are generally reported. The overall second-order association rate constant (k_a) governs the rate of closed complex formation. For the BP1 and BP2 promoters studied in this thesis, k_a was equal to k_1 (see Results section II.4d), however for the majority of promoters which have been studied, the bimolecular collision has been treated as a rapid equilibrium, and in these cases, k_a becomes a more complicated function (see also Appendix B, equations B-48 to B-50). The second parameter which is frequently reported is the forward isomerization rate constant (k_f). The rate constant k_f defines the isomerization step(s) following the bimolecular collision which lead to the formation of a stable polymerase/promoter complex. Note that the 'stable complex' is not necessarily equivalent to the formation of the open complex, but instead depends on the selection conditions used in the particular transcription assay (see also Discussion section II.1 above). In many cases, including this thesis, the first isomerization step leads to the formation of a stable complex, and k_f can be interpreted as k_2. Occasionally, however, there are more than one isomerization steps which exist between the closed complex and stable complex formation (Gourse, 1988). Under these circumstances, k_f can often be simplified to represent the slowest step in this series of isomerizations (Roe *et al.*, 1984, 1985). From the preceding discussion it seems clear that the interpretation of k_f and k_a depends on both the nature of the stable complex and the mechanism by which that complex is formed. Therefore, care must be taken when comparing the k_f and k_a values obtained at different promoters, or under different assay conditions.

Values reported for the forward isomerization rate constant (k_f) span between 10^{-3} - 10^{-1} s^{-1}, whereas values for the overall second-order association rate constant

(k_a) cover a range from 10^4 - 10^8 $M^{-1}s^{-1}$. The slowest k_a value reported was for the bacteriophage λP_{RM} promoter (Hawley and McClure, 1982; Shih and Gussin, 1983), while the fastest have been measured using the bacteriophage T7 A1 (Rosenberg *et al.*, 1982) and T5 P_{N25} (Bujard *et al.*, 1987) promoters, and the *E. coli rrnB* P1 promoter (Gourse, 1988). The relative *in vitro* activity of these last three promoters, while based on linear template analyses, closely resembles their relative strengths *in vivo* (Deuschle *et al.*, 1986). Comparing these reported values for k_a and k_f to those values obtained in this thesis (see Table VI), it is apparent that at 35 ° C, the BP1 and BP2 promoters can be classified among the fastest promoters for complex formation rates. Indeed, it is interesting to note that under some circumstances, the forward isomerization rate constant (k_f) approaches the theoretical maximum for promoter clearance rates at an individual rRNA promoter, which have been estimated at 1 s^{-1} (Table VI; Churchward *et al.*, 1982; Bremer and Dennis, 1987).

Only a few studies have investigated the individual kinetic steps during transcription initiation at growth rate regulated promoters (Ishihama, 1986; Gourse, 1988). Using the *lac* UV5 promoter as a reference, Ishihama (1986) compared the relative strengths of a variety of promoters (including *E. coli rrnE* P1 and P2) using a mixed template, single-round transcription assay. However, there are two aspects of this report which make comparison of the results difficult. First, in the individual transcription assays, either rifampicin or heparin was used to prevent reinitiation. While heparin resistance can be achieved prior to transcription initiation (Results this thesis), rifampicin resistance is apparently achieved only after the incorporation of at least the first two nucleotides into the nascent transcript (McClure and Cech, 1978). Therefore, two different criteria for stable complex formation were used by Ishihama (1986). Second, while initial complex formation was performed at low reaction temperatures, the rate studies were initiated by a temperature shift to 37° C. Therefore, the transcription initiation rates reported for 37° C were based on the relative distribution of polymerase between the various mixed templates at low

reaction temperatures. It is not apparent that the relative distribution of polymerase between the various template mixtures, and hence the relative transcription initiation rates, would be the same at both 37° C and low reaction temperatures. These two considerations would suggest that the relative values of (k_1/k_{-1}) and k_2 which were reported for the different promoters investigated by Ishihama (1986) cannot be so easily compared to one another (see also Ishihama *et al.*, 1987; Ishihama, 1988).

Using a filter-binding assay at 37 °C, Gourse (1988) studied the rate of heparin resistant complex formation between RNA polymerase and the growth rate regulated *E. coli rrnB* P1 promoter. Since the effects of ppGpp were not investigated by Gourse (1988), I shall only compare his study of EP1 with my findings under – ppGpp conditions (Table VI: BP2, 35° C). An important difference exists between the filter-binding assay of Gourse (1988) and the gel-retardation analysis performed in this thesis. While heparin resistant complex formation at the growth rate regulated BP2 promoter occurred at a step prior to the open complex (see Discussion section II.1 and equation 16), heparin resistant complex formation at the EP1 promoter required the presence of initiating nucleotides (Gourse, 1988; this thesis, Fig. 26A). Therefore, in studying growth rate regulated promoters, the present thesis measured the formation rate of the intermediate complex ($k_f \geq 5.6 \times 10^{-1}\ s^{-1}$), while the report of Gourse (1988) presumably investigated the formation rate of an initiated complex ($k_f = 1.7 \pm 0.6 \times 10^{-1}\ s^{-1}$). It is intriguing that the k_f of EP1 is ≥ 3-fold lower than the k_f of BP2, for it suggests that the rate limiting step for transcription initiation at a growth rate regulated promoter might occur after open complex formation. This speculation is based on three assumptions. First, that steps leading up to intermediate complex formation occur at similar rates for BP2 and EP1. Second, that the k_f of EP1 can be simplified to represent the slowest step in the series of isomerizations that leads to initiated complex formation (Roe *et al.*, 1984, 1985). Finally, that the rate of DNA melting (conversion from intermediate to

open complex) at a promoter is a rapid process at 37° C. While not determined for the EP1 or BP2 promoters, DNA melting has been shown to be rapid at the *lac UV5* promoter ($k_3 \approx 2\ s^{-1}$; Buc and McClure, 1985). The possibility that the transition from an open to an initiated complex is the rate limiting step for transcription initiation at growth rate regulated promoters shall be discussed further in a later section (Discussion section VI).

Although a thermodynamic analysis was not performed, the large magnitude of the overall second-order association rate constant led Gourse (1988) to suggest that the formation of the closed complex at EP1 might proceed by a sequential mechanism (i.e. $k_a = k_1$, see Results section II.4c). This is entirely consistent with the more detailed study of BP2 (see Results section II.4d), and it is pleasing to note that the magnitude of k_1 for the growth rate regulated BP2 promoter ($k_a = 1.5 \pm 0.2 \times 10^8\ M^{-1}\ s^{-1}$) is comparable to that reported by Gourse (1988) for EP1 ($k_a = 4.3 \pm 0.35 \times 10^8\ M^{-1}\ s^{-1}$). This lends support to the previous assumption that steps leading up to intermediate complex formation occur at similar rates for the BP2 and EP1 promoters. The k_a for EP1 is faster than that for BP2, but this is most likely due to the lower salt concentration (30 mM KCl versus 80 mM KCl) that the filter-binding assay employed (Gourse, 1988; Lohman, 1986).

3. Thermodynamic properties.

In either the presence or absence of ppGpp, the activation energy for the bimolecular collision at both BP1 and BP2 was ≤ 6 kcal/mol (see $E_{a,a}$ from Table IX). This small activation energy is in agreement with other studies which have demonstrated that the bimolecular collision is relatively temperature insensitive (Kadesch *et al.*, 1982; Roe *et al.*, 1985; Straney and Crothers, 1987b; Singer and Wu, 1988), although some researchers have reported an endothermic relationship for this step (Bertrand-Burggraf, *et al.*,1984; Buc and McClure, 1985; Duval-Valentin and Ehrlich, 1987). The small effect of temperature on k_1 is consistent with the idea that

closed complex formation is not thermodynamically driven by enthalpy, but by the increase in entropy that occurs during the release of counterions from the DNA of the promoter region as a result of polymerase binding (Shaner *et al.*, 1983; Lohman, 1986; Record and Mossing, 1987).

The forward rate constant k_f was associated with an activation energy range between 10 - 20 kcal/mol (see Table IX). This is similar to estimates obtained for the λP_R (Roe *et al.*, 1985), *lac* UV5 (Straney and Crothers, 1987b) and *tet* (Bertrand-Burggraf *et al.*, 1984) promoters, which have reported activation energies in the range of 13 - 20 kcal/mol for this isomerization step. If a small activation energy is assumed for k_r, then the overall enthalpy for the conversion of closed to intermediate complexes would be endothermic. A positive enthalpy would be consistent with evidence which suggests that the second step of equation 16 represents a temperature dependent conformational change of the RNA polymerase (Roe *et al.*, 1985; Spassky *et al.*, 1985; Straney and Crothers, 1985; Cowing, *et al.*, 1989; Schickor *et al.*, 1990). By using a small positive enthalpy as a limit for the second step (i.e. $\Delta H_2^\circ \approx 0$), it is possible to estimate the enthalpy for the conversion of intermediate to open complex formation (i.e. ΔH_3°). This is possible due to the relationship between the activation energy for dissociation ($E_{a,d} = E_{a,r} - \Delta H_3^\circ$) (see also Appendix C, equations C-7 to C-10), and the enthalpy for intermediate complex formation ($\Delta H_2^\circ = (E_{a,f} - E_{a,r}) \approx 0$); (see also Appendix C, equations C-10 and C-14). Using the results from Table IX, an estimate for ΔH_3° can be calculated for both BP1 (40 ± 10 kcal/mol) and BP2 (47 ± 7 kcal/mol). These values agree with other determinations for ΔH_3° made at the *lac* UV5 promoter (ΔH_3° = 41 kcal/mol; Buc and McClure, 1985; Spassky *et al.*, 1985), but are lower than measurements obtained at the *groE* promoter (ΔH_3° = 73 kcal/mol; Cowing *et al.*, 1989). It is not clear whether these differences reflect differences in the methods of determining ΔH_3°, or whether they reflect differences in the polymerase/promoter interactions themselves.

4. DNase I protection analyses.

At both the BP1 and EP1 promoters, there was a prominent gap in the control DNase I digest of the coding strand in the absence of RNA polymerase (Figs. 24 and 29, lanes L). The limits of these gaps were similar for both promoters, extending between - 53 to - 38 for BP1 and - 58 to - 39 for EP1 (similar limits at EP1 were reported by Gourse, 1988). At both promoters, this region corresponds to a 16 - 17 bp stretch of A and T residues, which have been shown to confer anomalous electrophoretic mobilities to their associated promoter fragments (Deneer, 1986; Gourse *et al.*, 1986). These mobility shifts are often indicative of a conformational change, and the bending of the DNA chain within an A:T-rich area is well documented (Wu and Crothers, 1984; Koo *et al.*, 1986; Burkhoff and Tullius, 1987). It is possible that such unusual structures were responsible for the inability of DNase I to cleave in this region. Although these structural similarities are interesting, they do not appear to be involved in growth rate regulation (Gourse *et al.*, 1986; Deneer and Spiegelman, 1987).

In the presence of RNA polymerase, all of the promoters analyzed displayed regions of enhanced DNase I sensitivity (see Figs. 24, 25, 29 and 30). In cases where more than one region occurred (BP1, BP2, EP1), the spacing between these sites was approximately 10 or 20 bp. From studies at the fd PV111, T7 A3 and *lac* UV5 promoters, it has been argued that a 10 bp periodicity of DNase I hypersensitive sites represents a polymerase-induced bend along one face of the DNA template (for a review see Travers, 1987). Using a mobility-shift assay to study holoenzyme complexes at the T7 A1 promoter, Heumann *et al.* (1988) have demonstrated that the potential axis for a bend occurs about 3 bp upstream of the transcription initiation site. There were differences in the relative intensities of the enhanced regions between the various promoters examined in this thesis. For example, all promoters studied had a DNase I hypersensitive site in the - 35 region (between - 33 to - 37), but the intensity of this site was much greater at BP1 and EP1 (Figs. 24 and

29) than at BP2 and EP2 (Figs. 25 and 30). At both BP1 and EP1, the - 37 hypersensitive sites were adjacent to an upstream A:T-rich sequence. As discussed above, this sequence may 'amplify' any bends in the promoter region which were caused by polymerase binding, thereby creating a 'super-enhanced' DNase I target site.

In the presence of RNA polymerase, the extent of DNase I protection was different between the BP1 and BP2 promoters. While protection of the coding strand covered 76 bp at the BP1 promoter (Fig. 24), the footprint at BP2 only protected 61 bp (Fig. 25). The smaller size of the BP2 footprint was mainly due to a shorter upstream protection endpoint compared to that of BP1 (- 43 versus - 54 respectively). These observations imply that the conformation of heparin resistant complexes were somehow different at the two promoters, however it is unknown whether such differences are important in growth rate regulation (see Discussion section VI).

From studies at other promoters, it would seem that the ability to detect movement of the polymerase during transcription initiation is a complex function of both the promoter sequence and the length of the initiating transcript. For example, upon formation of a 5 nt transcript at the Tac promoter, movement of the DNase I-protected area from the + 20 to + 24 position was observed (Krummel and Chamberlin, 1989). At the *lac* UV5 promoter, no shift in DNase I protection was observed when initiated complexes containing transcripts of up to 4 nt were formed (Carpousis and Gralla, 1985), however the formation of an 8 nt transcript at the same promoter resulted in an extension of protection by 4 base pairs (Straney and Crothers, 1987a). Therefore, it is not unusual that initiating conditions which generated putative transcript lengths between 1 - 7 nt did not result in significant downstream movement of the DNase I protection footprint at any of the promoters investigated in this thesis (Figs. 24, 25, 29 and 30).

The synthesis of a 9 nt transcript at the non growth rate regulated EP2 promoter resulted in a major change in both the upstream and downstream protection limits of the DNase I footprint (Fig. 30), shrinking the protected region from 66 ± 3 bp to 30 bp (the error associated with the first estimate is due to an inability to identify an exact protection endpoint within the - 46 to - 40 region of EP2). Similar shifts in protection have been reported at other initiated promoters (Carpousis and Gralla, 1985; Straney and Crothers, 1985, 1987a; Krummel and Chamberlin, 1989; Metzger *et al.*, 1989a), and these have subsequently been found to be associated with the release of the σ subunit, and the commitment of the ternary complex to transcript elongation (Straney and Crothers, 1985; Krummel and Chamberlin, 1989). While the change in DNase I protection was not as dramatic as for EP2, the putative synthesis of a 7 nt transcript at the non growth rate regulated BP1 promoter weakened specific upstream promoter contacts between the - 32 and - 17 positions (Fig. 24). In contrast, under initiating conditions at the BP2 promoter which allowed the putative synthesis of a 10 nt transcript, neither significant movement of protection limits nor weakened upstream promoter contact was detected (Fig. 25). It is not clear whether the differences between the initiated footprints of the EP2 and BP1 versus the BP2 templates are related to the non growth rate versus growth rate dependent control aspects of the respective promoters. However, these results suggest that under comparable initiating conditions (i.e. comparable transcript lengths), the ratio of upstream/downstream contact 'strengths' between RNA polymerase and a promoter is higher for the growth rate regulated BP2 promoter than for its two non growth rate regulated counterparts (see also Discussion section IV and VI). This differential in contact strength predicts that the growth rate regulated promoters may require the synthesis of a longer transcript before committing to elongation. Consistent with this view, it has been observed that the formation of a stable ternary complex at the *E. coli rrnB* P1 promoter does not occur until the synthesis of an 11 nt transcript (Levin *et al.*, 1987).

Gourse (1988) previously reported a DNase I protection analysis of heparin resistant complexes between RNA polymerase and the *E. coli rrnB* P1 promoter (during the following comparison of the report of Gourse (1988) to results in this thesis, refer to Fig. 29). Both Gourse (1988) and the data in this thesis found the same initiating nucleotide requirements in order to form stable complexes at EP1, and in the presence of RNA polymerase, the locations and intensities of DNase I hypersensitive sites on the coding strand were very similar. Both reports have a major DNase I enhancement at either - 39/40 (Gourse, 1988) or - 37, and a minor enhancement at either + 17 (Gourse, 1988) or + 19. I observed a minor enhancement at - 46 which was not reported by Gourse (1988). One difference between these two studies was the reported size of the protected region of the coding strand. The footprint of this thesis was 67 bp (- 45 to + 22), whereas that reported by Gourse (1988) covered 78 bp (- 58 to + 20). This difference was largely due to an inability to identify an exact protection endpoint within the upstream A:T rich region observed in both studies. For this thesis, the last protected base which could be observed (- 45) was chosen as the minimum estimate for the upstream protection endpoint, while Gourse (1988) chose the - 58 border of the A:T-rich region as an upper limit for the same endpoint. Therefore, the 11 bp discrepancy between these two reports reflects the upper and lower bounds of protection for the upstream DNase I protection border of the coding strand. From the two studies, an average footprint of 72 ± 6 bp can be estimated for the EP1 coding strand.

III. Regulation by ppGpp.

At this time, limited conclusions concerning the effects of ppGpp on the rate of transcription initiation at the BP1 and BP2 promoters can be made. In part, the limitation is due to the assay which was employed. While the mechanism for open complex formation consists of three steps (see equation 16), only the first two steps

were thoroughly investigated by the assay used, because the functional test for promoter specific complex formation was heparin resistance. Since both the intermediate (HR1) and open (HR2) complexes were indistinguishable under the electrophoresis conditions employed, the conversion rate of HR1 to HR2 could not be determined. The inability to measure the the individual rate constants k_3 and k_{-3} complicated the investigation of the effects of ppGpp on open complex formation. However, given the nature of the overall reaction mechanism (see equation 16), some simplifying assumptions were possible. For each reaction step for open complex formation at BP1 and BP2, it appeared that the contribution of the reverse rate constant to the overall association rate was negligible (see Discussion section I). Consequently, for ppGpp to have a functional effect on the rate of open complex formation as measured in this work, it would have to act on one of the forward rate constants (k_1, k_f, or k_3). Given this simplification, the possible role of ppGpp as a differential effector of transcription initiation is considered for each step in turn.

1. From Table VI it is evident that the addition of ppGpp had no significant impact on the magnitude of k_1 for either BP1 or BP2 at any reaction temperature (Table VI, $k_1 = k_a$). This suggests that ppGpp does not affect the overall rate of open complex formation at the level of the bimolecular collision. This result argues against the growth rate regulation model of Travers (1987), which proposed that growth rate regulated promoters are more difficult to saturate with polymerase than their non growth rate regulated counterparts, with the consequence that a ppGpp-directed shift in polymerase/promoter affinity would lead to a large change in the steady state transcription initiation rate at growth rate dependent promoters compared to that change observed at non growth rate regulated ones.

2. The effect of ppGpp addition on the magnitude of k_f was more difficult to determine due to the larger error associated with the measurement of the tau-plot intercept values (see Table VI and Results section II.4c). Indeed, for BP1 (at both 15° C and 35° C), differences in k_f under ± ppGpp conditions were not statistically

significant as judged by the Student's *t* test (98% confidence, data not shown). This analysis cannot distinguish between the absence of a ppGpp-directed effect versus an inability to resolve such an effect. However, under the same confidence limits, the addition of ppGpp produced a statistically significant change in k_f at the BP2 promoter, increasing k_f by approximately two-fold at both 10° C and 35° C. It is not clear whether the stimulation of k_f by ppGpp represents a differential effect at the growth rate regulated promoter, since the response of BP1 to ppGpp is uncertain. Similarly, it is unknown whether this stimulation by ppGpp has any regulatory significance. It has been reported that the repressor of the *lac* operon can act as a transient gene-activating protein, enhancing polymerase occupancy of the *lac* promoter while the repressor is bound, and thereby increasing the initial rate of transcription when repression is released (Straney and Crothers, 1987d). If the effector of growth rate regulation acts to block transcription initiation at a step which follows intermediate complex formation, it is conceivable that the stimulation of k_f by ppGpp might serve an analogous purpose. However, irrespective of any other regulatory function that ppGpp might have, the results presented here on the response of the growth rate regulated BP2 promoter suggests that ppGpp does not act as a negative effector of transcription initiation during the conversion of closed to initiated complexes.

3. As mentioned at the beginning of this section, the gel retardation assay is limited in probing steps which occur after intermediate complex formation at the BP1 and BP2 promoters. However, it is possible to use the dissociation rate experiments from Results section II.3 to provide some indirect information regarding the third step of equation 16. The response of the dissociation rates to changes in heparin concentration indicated that ppGpp increased the intrinsic dissociation rate constant (k_d) of heparin resistant complexes, and not just the sensitivity of those complexes to heparin (see Fig. 14C and Results section II.3e). A similar ppGpp-mediated increase in the dissociation rates of polymerase/promoter

complexes has been reported for the *E. coli rrnE* operon (Hamming *et al.*, 1980). Since the overall dissociation rate was a function of the three rate constants k_r, k_3, and k_{-3} (from Appendix B.III, equation B.34: $k_d \approx k_r(k_3/k_{-3})^{-1}$, see also Results section II.3d), the effect of ppGpp on k_d results from the effects of ppGpp on any combination of the steps governed by these rate constants. At the beginning of this Discussion section, it was pointed out that the rate of open complex formation at the BP1 and BP2 promoters would only be functionally regulated by ppGpp if one of the forward rate constants was altered (see equation 16). It is apparent that the only forward rate constant represented by the overall dissociation is k_3. Therefore, the observed effect of ppGpp on the overall dissociation rate might represent a functional change in the rate of open complex formation, but only if the conversion of HR1 to HR2 were rate limiting, and the action of ppGpp was confined to k_3. However, even if all these conditions were met, Table V indicates that at 35° C, the addition of ppGpp would only lead to a 2-fold decrease in the formation rate of open complexes at BP2 as compared to those formed at BP1 (since k_3 occurs in the denominator of equation B.34, an observed increase in k_d implies that k_3 must have decreased). This modest decrease is insufficient to account for the estimated 10-fold differential in specific promoter activity that is observed *in vivo* between these two promoters over a growth rate range of 0.4 - 1.25 doublings per hour (Deneer and Spiegelman, 1987). Studies using bacterial strains derived from *E. coli* K12 suggest that if ppGpp were the sole effector of growth rate regulation, an intracellular concentration of 0.1 mM ppGpp is sufficient to cause ≥ 80% of the maximum inhibition of rRNA expression which is observed *in vivo* (Baracchini *et al.*, 1988; Hernandez and Bremer, 1990). Therefore, it is unlikely that higher concentrations of ppGpp would have increased this differential response between BP1 and BP2 (see also Results section II.3e, Fig. 16).

The evidence presented so far would suggest that ppGpp does not act to differentially inhibit transcription initiation at a growth rate regulated promoter.

This observation is true for steps leading up to and (most likely) including open complex formation at the BP1 and BP2 promoters. In order to investigate the effect of ppGpp on steps following open complex formation, DNase I protection analyses were used to study polymerase/promoter complexes under initiating conditions (see Results section II.5). The results from these studies did not reveal any obvious changes in the protection pattern of initiated complexes under ± ppGpp conditions (Figs. 24 and 25), but the ability of the footprint technique to resolve ternary complexes (containing short oligonucleotide transcripts) from uninitiated complexes was clearly limited, and the conclusions from these footprint analyses must be viewed as incomplete. However, at the EP1 and EP2 promoters, significant amounts of heparin resistant complexes formed only in the presence of initiating nucleotides (Results section III.1). This made the *E. coli* promoters more suitable for studying the effects of ppGpp on the steps of transcription initiation which follow open complex formation. Heparin resistant complex formation at EP1 and EP2 will be discussed in the next section.

IV. The EP1 and EP2 promoters.

Optimum heparin resistant complex formation between RNA polymerase and the *E. coli rrnB* P1 and P2 promoters (EP1 and EP2 respectively) appeared to require the synthesis of at least one phosphodiester bond (Results section III.1 and Gourse, 1988). Qualitatively, this suggests that open complexes formed at the EP1 and EP2 promoters are much more unstable than those formed at the BP1 and BP2 promoters. This view is further supported by the different requirements of the *E. coli* and *B. subtilis rrnB* operons for optimum transcription *in vivo* within an *E. coli* host (see also the Introduction to this thesis). While the *E. coli rrnB* P1 promoter employs an upstream activating region to optimize its transcription *in vivo* (Gourse *et al.*, 1986; Gaal *et al.*, 1989; Ross *et al.*, 1990), there is no evidence of a similar

requirement for either of the *B. subtilis rrnB* P1 or P2 promoters (Deneer and Spiegelman, 1987), and the *in vivo* promoter activity of the individual BP2 promoter is comparable to that of the EP1 promoter associated with its upstream activating sequence (Deneer and Spiegelman, 1987; Deneer, 1986). Thus, the different sensitivities of the open complexes to heparin *in vitro* appears consistent with the overall promoter characteristics observed *in vivo*. However, although the upstream activating sequence is necessary to optimize transcription from EP1, it is not required for growth rate regulation (Gourse *et al.*, 1986). Therefore, while there are intrinsic differences between the open complex stabilities of EP1 and BP2, these differences do not prevent the promoters from being regulated in a growth rate dependent manner in *E. coli*.

It was mentioned previously that heparin resistant complex formation at EP1 and EP2 required the addition of nucleotides which would permit the formation of a short transcript. The fraction of heparin resistant complexes at EP1 and EP2 decreased as a function of putative transcript length (Fig. 27), and the growth rate regulated EP1 promoter appeared to be more sensitive to changes in the putative transcript length than was EP2. These findings are similar to observations made at the *lac* UV5 promoter (Carpousis and Gralla, 1980), in which the yield of a particular abortive oligonucleotide transcript decreased as the length of that transcript increased. However, Carpousis and Gralla (1980) measured the levels of released transcripts, which measures a different event than does the gel retardation assay, which measures the level of bound complexes. The results of these two reports would be consistent if one assumes that the bound promoter complexes at EP1 and EP2 become increasingly sensitive to displacement by heparin as the putative transcript length increases (i.e. as the transcript length of a ternary complex is increased, the oligonucleotide is less likely to be released, however the polymerase complex itself becomes more sensitive to a heparin challenge). The concept that a 'stressed' ternary complex is formed during transcription initiation has been

previously suggested (Carpousis and Gralla, 1985; Straney and Crothers, 1987a), and the possible contribution of such an intermediate to growth rate regulation shall be discussed in a later section.

The addition of ppGpp did not change the sensitivity of complexes at either EP1 or EP2 to the increase in transcript length (Fig. 27). These preliminary studies would suggest that ppGpp does not individually affect the forward and reverse rate constants which govern polymerase/promoter interactions following open complex formation. However these findings cannot rule out the possibility that ppGpp affects these same forward and reverse rate constants simultaneously, possibly slowing the the rate of heparin resistant complex formation, while leaving the final equilibrium position of these complexes unaltered.

V. Perspective.

The work of this thesis has attempted to investigate transcription initiation at both growth rate regulated and non growth rate regulated promoters, and ascertain whether ppGpp could act as a specific inhibitor of this process. The gel retardation assay described in this thesis examined a select number of steps in the overall path of transcription initiation. For the promoters in question, this analysis provided direct information regarding the formation of the closed and intermediate complexes, and indirect information regarding the formation of open and initiated ternary complexes. The cumulative results from studies of the *B. subtilis* and *E. coli rrnB* P1 and P2 promoters would suggest that ppGpp does not act to differentially inhibit transcription initiation at any of the steps investigated. How is it that other studies have reported a differential effect of ppGpp on the transcription from growth rate regulated promoters (see Introduction section III.1), whereas the results from this thesis would suggest that no such effect is detectable?

The majority of *in vitro* studies which have reported the differential response of stable RNA promoters to ppGpp have relied upon the synthesis of an RNA transcript in order to investigate the polymerase/promoter interactions (Travers, 1976; van Ooyen *et al.*, 1976; Glaser *et al.*, 1983; Kajitani and Ishihama, 1984). Consequently, these other assays included additional steps in the transcription process which were not measured in the present thesis. Some of these extra steps involve the commitment of the initiated ternary complex to elongation, and the elongation process itself, both of which may be sensitive functions of the assay conditions *in vitro* (Mangel and Chamberlin, 1974; Gralla, *et al.*, 1980, Munson and Reznikoff, 1981). For example, in experiments using a mixed template assay, Kajitani and Ishihama (1984), presented evidence that 0.1 mM ppGpp differentially altered the equilibrium partitioning of RNA polymerase between the *E. coli rrnE* P1 and P2 promoters by as much as 2.5-fold. However, under analogous conditions, I found that ppGpp did not have any effect on the relative partitioning of RNA polymerase between either BP1/BP2 (Fig. 11, Table IV) or EP1/EP2 (Fig. 28, Table XIII) promoters. Since Kajitani and Ishihama (1984) employed a single-round transcription assay to measure the degree of promoter occupancy, one means to reconcile their results and mine is to suggest that the differential effects of ppGpp are limited to a step of transcription that occurs after the formation of the open, and possibly even the initiated, complex (see also Discussion sections III and IV).

VI. Models for growth rate regulation: comments and speculation.

The studies by Bremer and co-workers (Ryals *et al.*, 1982; Little *et al.*, 1983a, 1983b) demonstrated a strict relationship between the intracellular concentration of ppGpp and the specific stable RNA gene activity. However, as noted by the authors (Ryals *et al.*, 1982), an observed response between two parameters does not guarantee a specific causal relationship. This last point was emphasized by the report of Gaal

and Gourse (1990), which demonstrated *in vivo* growth rate dependent control of the *E. coli rrnB* P1 promoter in the absence of any detectable ppGpp. The authors pointed out that their results might be compatible with those of Ryals *et al.* (1982) if cells had developed redundant systems for regulating rRNA transcription (Gaal and Gourse, 1990). However, it seems clear that any proposed mechanism for growth rate regulation must be able to operate in the absence of ppGpp. This latter view is reinforced by the results of the present thesis, and based on these results, one possible model for growth rate regulation is given below.

Analysis of complex formation between RNA polymerase and the *E. coli rrnB* promoters suggested that the fraction of heparin resistant ternary complexes at both EP1 and EP2 decreased as a function of putative transcript length (Fig. 27). Furthermore, the growth rate regulated EP1 promoter appeared to be more sensitive to changes in the putative transcript length than was EP2 (Fig. 27). This differential stability in response to increasing transcript length is intriguing, for it suggests that RNA polymerase molecules which pause in this early transcribed region will be more likely to continue from EP2 than from EP1. There are at least two conditions which may lead to paused ternary complexes at these promoters. First, ppGpp has been shown to increase the *in vitro* pausing of RNA polymerase as it transcribes from the *E. coli rrnB* operon (Kingston and Chamberlin, 1981). However, the distal pause sites mapped by these investigators are unnecessary for growth rate regulation *in vivo* (Gourse *et al.*, 1986). A second condition that might cause initiated ternary complexes to stall is limiting concentration of initiating nucleotides. The *in vitro* synthesis of abortive transcripts (McClure *et al.*, 1978; Carpousis and Gralla, 1980) and the rate of transcription initiation (Mangel and Chamberlin, 1974; Gralla, *et al.*, 1980, Munson and Reznikoff, 1981) have been demonstrated to be sensitive functions of the concentration of initiating nucleotides. Related to these last points, Levin and Chamberlin (1987) observed that the affinity of an initiating ternary complex for a particular nucleotide can vary up to 500-fold depending on the

positioning of that nucleotide within the initiating transcript. It is quite possible that the concentration of nucleotides plays an important regulatory role *in vivo*, since it has been observed that the intracellular concentrations of UTP and GTP are apparently below those levels required for the saturation of the transcribing RNA polymerase *in vitro* (Kingston *et al.*, 1981; Jensen *et al.*, 1982; Jensen *et al.*, 1986), and that the regulation of transcription at certain pyrimidine nucleotide biosynthetic genes appears to be controlled by the concentrations of nucleotides (Jensen *et al.*, 1982). Therefore, changes in the concentrations of nucleotides might lead to increased pausing of RNA polymerase in the early transcribed region of the EP1 and EP2 promoters. Consequently, the different stability of paused ternary complexes at EP1 and EP2 might lead to a differential response at the level of steady state transcription initiation rates, where it is predicted that EP1 would be down-regulated in comparison to EP2.

From the results of this thesis, it cannot be determined what the source of this differential stability of ternary complexes at EP1 versus EP2 might be. However from the intensive studies at other promoters, it is possible to speculate. The commitment of a promoter bound RNA polymerase to transcript elongation *in vitro* does not occur until after the synthesis of 8 - 14 nucleotides, when the complex has released its upstream promoter contacts by ejection of the σ subunit (Hansen and McClure, 1980; Carpousis and Gralla, 1985; Straney and Crothers, 1985, 1987a; Stackhouse *et al.*, 1989; Krummel and Chamberlin, 1989). Until this occurs however, the ternary complex is thought to exist in a state of 'stress', with the decision of whether to abort or commit to transcription being influenced by a delicate balance of opposing upstream and downstream promoter contacts (McClure *et al.*, 1978; Carpousis and Gralla, 1985; Straney and Crothers, 1987a, 1987c). While upstream promoter interactions are expected to be influenced by polymerase-σ-DNA contacts, the downstream interactions would be influenced by polymerase-RNA-DNA contacts. This view is supported both *in vivo* (Kammerer *et al.*, 1986) and *in*

vitro (Straney and Crothers, 1987a), where it has been observed that changes to the transcribed region of a promoter can influence its overall promoter activity.

With these observations in mind, one can inspect the EP1 and EP2 promoters for evidence of differences that may lead the growth rate regulated promoter to be more 'stressed' during transcription initiation, and hence more sensitive to subtle differences in the intracellular environment than would EP2. The optimal spacing between the – 35 and – 10 regions of a promoter seems to be 17 bp (Hawley and McClure, 1983; Harley and Reynolds, 1987). This spacing is demonstrated by the non growth rate regulated EP2 promoter (Jinks-Robertson and Nomura, 1987), but the growth rate regulated EP1 promoter has a sub-optimal spacing of 16 bp (Jinks-Robertson and Nomura, 1987). Moreover, Dickson *et al.* (1989) showed that this separation was essential for growth rate regulation, since an increase in spacing at EP1 from 16 to 17 bp led to an increase in promoter activity *in vivo*, but eliminated growth rate regulation. At EP2, commitment to elongation does not appear to occur until the synthesis of about 9 nt (Fig 30), whereas for EP1, abortive cycling continues until the ternary complex has synthesized 11 nt (Levin *et al.*, 1987). Since every G:C residue that is transcribed is expected to increase the strength of downstream promoter contacts (Straney and Crothers, 1987a), one can compare the G:C content of the initiation region for EP1 (+ 1 to + 11) and EP2 (+ 1 to + 9) as an estimate of downstream promoter contact stability. For EP1, the G:C content in this region is 54%, but for EP2 it is 100%. Thus, from the considerations of spacing between the – 35 and – 10 regions, and the estimated downstream promoter contact strengths, it might be expected that initiating complexes at EP1 are subject to a more delicate balance of opposing upstream and downstream promoter contacts than those at EP2, and hence more susceptible to regulation at the level of abortive initiation. Note that this is consistent with the observations of Gourse *et al.* (1986), who replaced the downstream region of the *E. coli rrnB* P1 promoter without altering the G:C content of the + 1 to + 11 sequence, and found that the resulting fusion was still growth rate

regulated *in vivo*. At the time, their conclusions were that this region was not required for growth rate dependent synthesis of rRNA, but their results do not rule against the present model.

If a common mechanism governs growth rate regulation, then a comparison of the BP2 and BP1 promoters should reveal a similar difference in the predicted 'stress' levels as found for EP1 and EP2 respectively. Based on the footprint results of BP2 (Fig. 25), it would appear that greater than 10 nt are required to facilitate a major conformational change indicative of σ release, and for the present discussion, 14 nt is taken as the upper limit for σ release (Stackhouse *et al.*, 1989) at both BP1 and BP2. The differential G:C content between the + 1 to + 14 sites at the BP2 and BP1 promoters is unremarkable (43% versus 57% respectively) compared to that of EP1 and EP2 (see above). Similarly, the – 35 to – 10 spacing at both the BP2 and BP1 promoters is 17 bp (Stewart and Bott, 1983). However, the spacing between the – 35 to + 1 site is only 27 bp for BP2 (see also Deneer and Spiegelman, 1987), whereas for BP1, this spacing is 30 bp. A survey of 83 promoters with single start sites revealed that 64% of the start sites are located either 28 or 29 bp from the downstream side of the – 35 consensus region (von Hippel *et al.*, 1984). While the deviation of BP2 and BP1 from 'consensus' may not appear significant, each additional base pair will require the RNA polymerase to somehow span an extra 0.34 nm of distance and compensate for an additional 34° of rotation (this assumes that B-DNA in solution has an average of 10.5 bp/turn; Wang, 1979). Thus, the same differential in promoter stress may exist at the BP2 and BP1 promoters, even though the structural features which contribute to this stress may be different from those features which contribute at the EP1 and EP2 promoters. This view is also supported by the differences in the BP1 and BP2 DNase I protection footprints (Results section II.5). While the BP1 promoter had an open complex footprint which extended 76 bp (Fig. 24), the growth rate regulated promoter had a much more 'compressed' footprint of 61 bp (Fig. 25). Furthermore, the synthesis of a putative 7 nt transcript led to

weakened upstream protection of the BP1 promoter (Fig. 24), whereas no changes were obtained when a putative 10 nt transcript was formed at BP2 (Fig. 25).

If growth rate regulation occurs at the level of commitment to elongation, then the conversion from open to committed complexes has to be potentially rate limiting. This has been demonstrated specifically at the *lac* UV5 promoter under conditions of polymerase excess (Stefano and Gralla, 1979; Straney and Crothers, 1987b). Additionally Carpousis *et al.* (1982) have shown that there is an apparent inverse correlation between the rate of open complex formation and the rate of productive transcription initiation. If this last point is true for most promoters, then the very rapid heparin resistant complex formation rates found at the BP1 and BP2 promoters would suggest that promoter escape limits their overall transcription initiation rate. This view is generally supported by the observation that at growth rate regulated promoters, the rate limiting step for ternary complex formation (at EP1) is slower than the formation of the intermediate complex (at BP2) (see Discussion section II.2).

References

Atherly, A. G. (1979). *Escherichia coli* mutant containing a large deletion from *relA* to *argA*. J. Bacteriol. **138**, 530-534.

Atkinson, T., and Smith, M. (1984). Purification of oligonucleotides obtained by small scale (0.2 μmol) automated synthesis by gel electrophoresis. In Oligonucleotide synthesis: A practical approach, M. J. Gait, ed. (IRL Press, Oxford). pp 70-72.

Aoyama, T., and Takanami, M. (1988). Supercoiling response of *E. coli* promoters with different spacer lengths. Biochim. Biophys. Acta **949**, 311-317.

Auble, D. T., Allen, T. L., and deHaseth, P. L. (1986). Promoter recognition by Escherichia coli RNA polymerase: Effects of substitutions in the spacer DNA separating the - 10 and - 35 regions. J. Biol. Chem. **261**, 11202-11206.

Auble, D. T., and deHaseth, P. L. (1988). Promoter recognition by *Escherichia coli* RNA polymerase. Influence of DNA structure in the spacer separating the -10 and -35 regions. J. Mol. Biol. **202**, 471-482.

Ayers, D. G., Auble, D. T., and deHaseth, P. L. (1989). Promoter recognition by *Escherichia coli* RNA polymerase. Role of the spacer region in functional complex formation. J. Mol. Biol. **207**, 749-756.

Babinet, C. (1967). A new method for the purification of RNA-polymerase. Biochem. Biophys. Res. Commun. **26**, 639-644.

Baracchini, E., Glass, R., and Bremer, H. (1988). Studies *in vivo* on *Escherichia coli* RNA polymerase mutants altered in the stringent response. Mol. Gen. Genet. **213**, 379-387.

Barnes, W. M. (1987). Sequencing DNA with dideoxyribonucleotides as chain terminators: Hints and strategies for big projects. Methods in Enzymology **152**, 538-556.

Batschelet, E. (1973). Introduction to mathematics for life sciences. (Springer-Verlag, New York). Chapter 11, pp 307-309.

Benson, S. W. (1960). The foundations of chemical kinetics. (McGraw-Hill Book Co. Inc., New York). Chapter 3, pp 39-42.

Berg, O. G. and von Hippel, P. H. (1985). Diffusion-controlled macromolecular interactions. Ann. Rev. Biophys. Chem. **14**, 131-160.

Berg, O. G., Winter, R. B., and von Hippel, P. H. (1981). Diffusion-driven mechanisms of protein translocation on nucleic acids. 1. Models and theory. Biochemistry **20**, 6929-6948.

Bertrand-Burggraf, E., Lefevre, J. F., and Duane, M. (1984). A new experimental approach for studying the association between RNA polymerase and the *tet* promoter of pBR322. Nucl. Acids Res. **12**, 1697-1706.

Beutel, B. A., and Record, M. T. Jr. (1990). *E. coli* promoter spacer regions contain nonrandom sequences which correlate to spacer length. Nucl. Acids Res. **18**, 3597-3603.

Borowiec, J. A., and Gralla, J. D. (1987). All three elements of the *lac* p^s promoter mediate its transcriptional response to DNA supercoiling. J. Mol. Biol. **195**, 89-97.

Bremer, H., and Dennis, P. P. (1987). Modulation of chemical composition and other parameters of the cell by growth rate. In *Escherichia coli* and *Salmonella typhimurium*: Cellular and molecular biology, F. C. Neidhardt, J. L. Ingraham, K. Brooks Low, B. Magasanik, M. Schaecter, and H. E. Umbarger, eds. (American Society for Microbiology, Washington D. C.), pp. 1527-1542.

Brewer, B. J. (1988). When polymerases collide: Replication and the transcriptional organization of the *E. coli* chromosome. Cell **53**, 679-686.

Brosius, J. (1984). Plasmid vectors for the selection of promoters. Gene **27**, 151-160.

Buc, H., and McClure, W. R. (1985). Kinetics of open complex formation between *Escherichia coli* RNA polymerase and the *lac* UV5 promoter. Evidence for a sequential mechanism involving three steps. Biochemistry **24**, 2712-2723.

Bujard, H., Brunner, M., Deuschle, U., Kammerer, W., and Knaus, R. (1987). Structure-function relationship of *Escherichia coli* promoters. In RNA polymerase and the regulation of transcription, W. S. Reznikoff, R. R. Burgess, J. E. Dahlberg, C. A. Gross, M. T. Record, Jr., and M. P. Wickens, eds. (Elsevier Science Publishing, Inc., New York), pp. 95-103.

Burgess, R. R. (1969). Separation and characterization of the subunits of ribonucleic acid polymerase. J. Biol. Chem. **244**, 6168-6176.

Burgess, R. R. (1976). Purification and physical properties of *E. coli* RNA polymerase. In RNA polymerase, R. Losick, and M. Chamberlin, eds. (Cold Spring Harbor, New York: Cold Spring Harbor Laboratory). pp 69-101.

Burgess, R. R., Erickson, B., Gentry, D., Gribskov, M., Hager, D., Lesley, S., Strickland, M., and Thompson, N. (1987). Bacterial RNA polymerase subunits and genes. In RNA polymerase and the regulation of transcription, W. S. Reznikoff, R. R. Burgess, J. E. Dahlberg, C. A. Gross, M. T. Record, Jr., and M. P. Wickens, eds. (Elsevier Science Publishing, Inc., New York), pp. 3-15.

Burgess, R. R., Travers, A. A., Dunn, J. J., and Bautz, E. K. F. (1969). Factor stimulating transcription by RNA polymerase. Nature (London) **221**, 43-46.

Burkhoff, A. M., and Tullius, T. D. (1987). The unusual conformation adopted by the adenine tracts in kinetoplast DNA. Cell **48**, 935-943.

Castellan, G. W. (1983). Physical chemistry, 3rd Ed., (Addison-Wesley Pub. Co., California), Chapters 11 and 33.

Carpousis, A. J., and Gralla, J. D. (1980). Cycling of ribonucleic acid polymerase to produce oligonucleotides during initiation *in vitro* at the *lac* UV5 promoter. Biochemistry **19**, 3245-3253.

Carpousis, A. J., and Gralla, J. D. (1985). Interaction of RNA polymerase with *lac* UV5 promoter DNA during mRNA initiation and elongation. J. Mol. Biol. **183**, 165-177.

Carpousis, A. J., Stefano, J. E., and Gralla, J. D. (1982). 5' nucleotide heterogeneity and altered initiation of transcription at mutant *lac* promoters. J. Mol. Biol. **157**, 619-633.

Cashel, M., and Gallant, J. (1969). Two compounds implicated in the function of the RC gene of *Escherichia coli*. Nature **221**, 838-841.

Cashel, M., and Rudd, K. E. (1987). The stringent response. In *Escherichia coli* and *Salmonella typhimurium*: Cellular and molecular biology, F. C. Neidhardt, J. L. Ingraham, K. Brooks Low, B. Magasanik, M. Schaecter, and H. E. Umbarger, eds. (American Society for Microbiology, Washington D. C.), pp. 1410-1438.

Cech, C. L., and McClure, W. R. (1980). Characterization of ribonucleic acid polymerase-T7 binary complexes. Biochemistry **19**, 2440-2447.

Chamberlin, M. J. (1974). The selectivity of transcription. Ann. Rev. Biochem. **43**, 721-775.

Churchward, G., Bremer, H., and Young, R. (1982). Transcription in bacteria at different DNA concentrations. J. Bacteriol. **150**, 572-581.

Cole, J. R., and Nomura, M. (1986). Changes in the half-life of ribosomal protein messenger RNA caused by translational repression. J. Mol. Biol. **188**, 383-392.

Cole, J. R., Olsson, C. L., Hershey, J. W. B., Grunberg-Manago, M. (1987). Feedback regulation of rRNA synthesis in *Escherichia coli*: Requirement for initiation factor IF2. J. Mol. Biol. **198**, 383-392.

Cowing, D. W., Mecsas, J., Record, M. T. Jr., and Gross, C. A. (1989). Intermediates in the formation of the open complex by RNA polymerase holoenzyme containing the sigma factor σ^{32} at the *groE* promoter. J. Mol. Biol. **210**, 521-530.

Darst, S. A., Kubalek, E. W., and Kornberg, R. D. (1989). Three-dimensional structure of *Escherichia coli* RNA polymerase holoenzyme determined by electron crystallography. Nature **340**, 730-732.

Davison, B. L., Leighton, T., and Rabinowitz, J. C. (1979). Purification of *Bacillus subtilis* RNA polymerase with heparin-agarose. J. Biol. Chem. **254**, 9220-9226.

de Boer, H., and Nomura, M. (1979). *In vivo* transcription of rRNA operons in *E. coli* initiates with purine nucleoside triphosphates at the first promoter and with CTP at the second promoter. J. Biol. Chem. **254**, 5609-5612.

Debenham, P. G., Buckland, R., and Travers, A. A. (1979). The regulation of RNA polymerase by guanosine 5'-diphosphate 3'-diphosphate. In Regulation of macromolecular synthesis by low molecular weight mediators, G. Koch and D. Richter, eds. (Academic Press, New York, New York). pp 77-84.

Debenham, P. G., Pongs, O., and Travers A. A. (1980). Formylmethionyl-tRNA alters RNA polymerase specificity. Proc. Nat. Acad. Sci. USA. **77**, 870-874.

Deneer, H. G. (1986). Cloning and expression of *Bacillus subtilis* ribosomal RNA gene promoters in *Escherichia coli*. Ph.D. thesis, microbiology, University of British Columbia, Vancouver, p. 76-81.

Deneer, H. G., and Spiegelman, G. B. (1987). *Bacillus subtilis* rRNA promoters are growth rate regulated in *Escherichia coli*. J. Bacteriol. **169**, 995-1002.

Deuschle, U., Kammerer, W., Gentz, R., and Bujard, H. (1986). Promoters of *Escherichia coli*: A hierarchy of *in vivo* strength indicates alternate structures. EMBO J. **5**, 2987-2994.

Dickson, R. R., Gaal, T., deBoer, H. A., deHaseth, P. L., and Gourse, R. L. (1989). Identification of promoter mutants defective in growth-rate-dependent regulation of rRNA transcription in *Escherichia coli*. J. Bacteriol. **171**, 4862-4870.

Dix, D. B., and Thompson, R. C. (1986). Elongation factor Tu.guanosine 3'-diphosphate 5'-diphosphate complex increases the fidelity of proofreading in protein biosynthesis: Mechanism for reducing translational errors introduced by amino acid starvation. Proc. Nat. Acad. Sci. USA. **83**, 2027-2031.

Dobinson, K. F., and Spiegelman, G. B. (1987). Effect of the δ subunit of *Bacillus subtilis* RNA polymerase on initiation of RNA synthesis at two bacteriophage ϕ29 promoters. Biochemistry **26**, 8206-8213.

Duval-Valentin, G., and Ehrlich, R. (1987). Dynamic and structural characterisation of multiple steps during complex formation between *E. coli* RNA polymerase and the *tetR* promoter from pSC101. Nucl. Acids Res. **15**, 575-594.

Eisenberg, D., and Crothers, D. (1979). Physical chemistry with applications to the life sciences, (The Benjamin/Cummings Pub. Co. Inc., California), Chapter 6.

Ellwood, M. and Nomura, M. (1980). Deletion of a ribosomal nucleic acid operon in *Escherichia coli*. J. Bacteriol. **143**, 1077-1080.

Ellwood, M. and Nomura, M. (1982). Chromosomal locations of the genes for rRNA in *Escherichia coli* K-12. J. Bacteriol. **149**, 458-468.

Engbaek, F., Gross, C., and Burgess, R. R. (1976). Quantitation of RNA polymerase subunits in *E. coli* during exponential growth and after bacteriophage T4 infection. Mol. Gen. Genet. **143**, 291-295.

Fried, M. and Crothers, D. M. (1981). Equilibria and kinetics of *lac* repressor-operator interactions by polyacrylamide gel electrophoresis. Nucl. Acids Res. **9**, 6505-6525.

Friefelder, D. (1982). Physical biochemistry. Applications to biochemistry and molecular biology, 2nd Ed., (W. H. Freeman and Co.), Chapter 18.

Friesen, J., An, G.,, and Fiil, N. P. (1978). Nonsense and insertion mutants in the *relA* gene of *E. coli*: Cloning *relA*. Cell **15**, 1187-1197.

Gaal, T., and Gourse, R. L. (1990). Guanosine 3'-diphosphate 5'-diphosphate is not required for growth rate-dependent control of rRNA synthesis in *Escherichia coli*. Proc. Nat. Acad. Sci. USA. **87**, 5533-5537.

Gaal, T., Barkei, J., Dickson, R. R., deBoer, H. A., deHaseth, P. L., Alavi, H., and Gourse, R. L. (1989). Saturation mutagenesis of an *Escherichia coli* rRNA promoter and initial characterization of promoter variants. J. Bacteriol. **171**, 4852-4861.

Gallant, J. A. (1979). Stringent control in *E. coli*. Ann. Rev. Genet. **13**, 393-415.

Gamper, H. B., and Hearst, J. E. (1982). A topological model for transcription based on unwinding angle analysis of *E. coli* RNA polymerase binary, initiation and ternary complexes. Cell **29**, 81-90.

Garner, M. M., and Revzin, A. (1981). A gel electrophoresis method for quantifying the binding of proteins to specific DNA regions: Application to components of the *Escherichia coli* lactose operon regulatory system. Nucl. Acids Res. **9**, 3047-3060.

Gausing, K. (1977). Regulation of ribosome production in *Escherichia coli*: Synthesis and stability of ribosomal RNA and of ribosomal protein messenger RNA at different growth rates. J. Mol. Biol. **115**, 335-354.

Glaser, G., Sarmientos, P., and Cashel, M. (1983). Functional interrelationship between two tandem E. coli ribosomal RNA promoters. Nature **302**, 74-76.

Glass, R. E., Jones, S. T., Ishihama, A. (1986). Genetic studies on the β subunit of *Escherichia coli* RNA polymerase. VII. RNA polymerase is a target for ppGpp. Mol. Gen. Genet. **203**, 265-268.

Gonzalez, N., Wiggs, J., and Chamberlin, M. (1977). A simple procedure for resolution of *Escherichia coli* RNA polymerase holoenzyme from core polymerase. Arch. Biochem. Biophys. **182**, 404-408.

Gourse, R. L. (1988). Visualization and quantitative analysis of complex formation between *E. coli* RNA polymerase and an rRNA promoter *in vitro*. Nucl. Acids Res. **16**, 9789-9809.

Gourse, R. L., and Nomura, M. (1984). Level of rRNA, not tRNA, synthesis controls transcription of rRNA and tRNA operons in *Escherichia coli*. J. Bacteriol. **160**, 1022-1026.

Gourse, R. L., deBoer, H. A., and Nomura, M. (1986). DNA determinants of rRNA synthesis in *E. coli*: Growth rate dependent regulation, feedback inhibition, upstream activation, antitermination. Cell **44**, 197-205.

Gralla, J. D. (1990). Promoter recognition and mRNA initiation by *Escherichia coli* $E\sigma^{70}$. Methods in Enzymology **185**, 37-54.

Gralla, J. D., Carpousis, A. J., and Stefano, J. E. (1980). Productive and abortive initiation of transcription *in vitro* at the *lac* UV5 promoter. Biochemistry **19**, 5864-5869.

Ha, J.-H., Spolar, R. S., and Record, M. T. Jr. (1989). Role of the hydrophobic effect in stability of site-specific protein-DNA complexes. J. Mol. Biol. **209**, 801-816.

Hammes, G. G., and Schimmel, P. R. (1970). Rapid reactions and transient states. In The enzymes Vol. II, 3rd Ed., P. D. Boyer, ed. (Academic Press New York, New York). Chapter 2, pp 87-91.

Hamming, J., Geert, A. B., and Gruber, M. (1980). *E. coli* RNA polymerase-rRNA promoter interaction and the effect of ppGpp. Nucl. Acids Res. **8**, 3947-3963.

Hansen, U. M., and McClure, W. R. (1980). Role of the σ subunit of *Escherichia coli* RNA polymerase in initiation. II. Release of σ from ternary complexes. J. Biol. Chem. **255**, 9564-9570.

Harley, C. B., and Reynolds, R. P. (1987). Analysis of *E. coli* promoter sequences. Nucl. Acids Res. **15**, 2343-2361.

Haseltine, W. A., and Block, R. (1973). Synthesis of guanosine tetra- and penta-phosphate requires the presence of a codon-specific uncharged transfer ribonucleic acid in the acceptor site of ribosomes. Proc. Nat. Acad. Sci. USA. **70**, 1564-1568.

Hawley, D. K., and McClure, W. R. (1982). Mechanism of activation of transcription initiation from the λP_{RM} promoter. J. Mol. Biol. **157**, 493-525.

Hawley, D. K., and McClure, W. R. (1983). Compilation and analysis of *Escherichia coli* promoter DNA sequences. Nucl. Acids Res. **11**, 2237-2255.

Hernandez, V. J., and Bremer, H. (1990). Guanosine tetraphosphate (ppGpp) dependence of the growth rate control of *rrnB* P1 promoter activity in *Escherichia coli*. J. Biol. Chem. **265**, 11605-11614.

Heumann, H., Ricchetti, M., and Werel, W. (1988). DNA-dependent RNA polymerase of *Escherichia coli* induces bending or an increased flexibility of DNA by specific complex formation. EMBO J. **7**, 4379-4381.

Hinkle, D. C., and Chamberlin, M. J. (1972). Studies of the binding of *Escherichia coli* RNA polymerase to DNA. I. The role of sigma subunit in site selection. J. Mol. Biol. **70**, 157-185.

Hinkle, D. C., Ring, J., and Chamberlin, M. J. (1972). Studies of the binding of *Escherichia coli* RNA polymerase to DNA. III. Tight binding of RNA polymerase holoenzyme to single-strand breaks in T7 DNA. J. Mol. Biol. **70**, 197-207.

Hsieh, T.-S., and Wang, J. C. (1978). Physicochemical studies on interactions between DNA and RNA polymerase. Ultraviolet absorption measurements. Nucl. Acids Res. **5**, 3337-3345.

Igarashi, K., Fujita, N., and Ishihama, A. (1989). Promoter selectivity of *Escherichia coli* RNA polymerase: Omega factor is responsible for the ppGpp sensitivity. Nucl. Acids Res. **17**, 8755-8765.

Ingraham, J. L., Maaløe, O., and Neidhardt, F. C. (1983). The growth of the bacterial cell. (Sinauer Associates, Inc., Sunderland MA). Chapter 5.

Ishihama, A. (1986). Transcription signals and factors in *Escherichia coli*. Adv. Biophys. **21**, 163-173.

Ishihama, A. (1988). Promoter selectivity of prokaryotic RNA polymerases. Trends in Genetics **4**, 282-286.

Ishihama, A., Fujita, N., Nomura, T. (1987). Promoter selectivity of *Escherichia coli* RNA polymerase. In RNA polymerase and the regulation of transcription, W. S. Reznikoff, R. R. Burgess, J. E. Dahlberg, C. A. Gross, M. T. Record, Jr., and M. P. Wickens, eds. (Elsevier Science Publishing, Inc., New York), pp. 397-401.

Ishihama, A., Murakami, S., Fukuda, R., Matsukage, A. and Kameyama, T. (1971). The nature of initiation sites on DNA for the core RNA polymerase. Mol. Gen. Genet. **111**, 66-77.

Iwakura, Y., Ito, K, and Ishihama, A. (1974). Biosynthesis of RNA polymerase in *E. coli*. I. Control of RNA polymerase content at various growth rates. Mol. Gen. Genet. **133**, 1-23.

Jensen, K. F., Neuhard, J., and Schack, L. (1982). RNA polymerase involvement in the regulation of expression of the *Salmonella typhimurium pyr*-genes. Isolation and characterization of a flurouracil-resistant mutant with high constitutive expression of the *pyrB* and *pyrE* genes due to a mutation in *rpoBC*. EMBO J. **1**, 69-74.

Jensen, K. F., Fast, R., Karlström, O., and Larsen, J. N. (1986). Association of RNA polymerase having increased Km for ATP and UTP with hyperexpression of the *pyrB* and *pyrE* genes of *Salmonella typhimurium*. J. Bacteriol. **166**, 857-865.

Jensen, K. F., and Pedersen, S. (1990). Metabolic growth rate control in *Escherichia coli* may be a consequence of subsaturation of the macromolecular biosynthetic apparatus with substrates and catalytic components. Microbiol. Rev. **54**, 89-100.

Jinks-Robertson, S. and Nomura, M. (1987). Ribosomes and tRNA. In *Escherichia coli* and *Salmonella typhimurium*: Cellular and molecular biology, F. C. Neidhardt, J. L. Ingraham, K. Brooks Low, B. Magasanik, M. Schaecter, and H. E. Umbarger, eds. (American Society for Microbiology, Washington D. C.), pp. 1358-1385.

Jinks-Robertson, S., Gourse, R. L., and Nomura, M. (1983). Expression of rRNA and tRNA genes in *Escherichia coli*:: Evidence for feedback regulation by products of rRNA operons. Cell **33**, 865-876.

Johnson, R. C., Glasgow, A. C., and Simon, M. I. (1987). Spatial relationship of the Fis binding sites for Hin recominational enhancer activity. Nature **329**, 462-465.

Johnston, D. E., and McClure, W. R., (1976). In RNA Polymerase (Losick, R., and Chamberlin, M., Eds.) p 413, Cold Spring Harbor Laboratory, Cold Spring Harbor, NY.

Kadesch, T. R., Rosenberg, S., and Chamberlin, M. J. (1982). Binding of *Escherichia coli* RNA polymerase holoenzyme to bacteriophage T7 DNA: Measurements of binding at bacteriophage T7 promoter A1 using a template competition assay. J. Mol. Biol. **155**, 1-29.

Kajitani, M., and Ishihama, A. (1984). Promoter selectivity of *Escherichia coli* RNA polymerase. J. Biol. Chem. **259**, 1951-1957.

Kammerer, W., Deuschle, U., Gentz, R., and Bujard, H. (1986). Functional dissection of *Escherichia coli* promoters: Information in the transcribed region is involved in late steps of the overall process. EMBO J. **5**, 2995-3000.

Khazanie, R. (1979). Elementary statistics in a world of applications. Goodyear Publishing Co. Inc., Santa Monica, California. Chapter 11.

Kingston, R. E., and Chamberlin, M. J. (1981). Pausing and attenuation of *in vitro* transcription in the *rrnB* operon of *E. coli*. Cell **27**, 523-531.

Kingston, R. E., Nierman, W. C., and Chamberlin, M. J. (1981). A direct effect of guanosine tetraphosphate on pausing of *Escherichia coli* RNA polymerase during RNA chain elongation. J. Biol. Chem. **256**, 2787-2797.

Kirkegaard, K., Buc, H., Spassky, A., and Wang, J. C. (1983). Mapping of single-stranded regions in duplex DNA at the sequence level: Single-strand-specific cytosine methylation in RNA polymerase-promoter complexes. Proc. Natl. Acad. Sci. USA. **80**, 2544-2548.

Koo, H.-S., Wu, H.-M., and Crothers, D. M. (1986). DNA bending at adenine-thymidine tracts. Nature **320**, 501-506.

Kovacic, R. T. (1987). The 0 °C closed complexes between *Escherichia coli* RNA polymerase and two promoters, T7-A3 and *lac* UV5 J. Biol. Chem. **262**, 13654-13661.

Krummel, B., and Chamberlin M. J. (1989). RNA chain initiation by *Escherichia coli* RNA polymerase. Structural transitions of the enzyme in early ternary complexes. Biochemistry **28**, 7829-7842.

Kuhnke, G., Fritz, H. J., and Ehring, R. (1987). The unusual properties of promoter-up mutations in the *Escherichia coli* galactose operon and evidence suggesting RNA polymerase-induced DNA bending. EMBO J. **6**, 507-513.

Leduc, E., Hoekstra, M., and Spiegelman, G. B. (1982). Relationship between synthesis of ribosomes and RNA polymerase in *Bacillus subtilis*. Can. J. Microbiol. **28**, 1280-1288.

Leirmo, S., Harrison, C., Cayley, D. S., Burgess, R. R., and Record, M. T. Jr. (1987). Replacement of potassium chloride by potassium glutamate dramatically enhances protein-DNA interactions *in vitro*. Biochemistry **26**, 2095-2101.

Levin, J. R., and Chamberlin, M. J. (1987). Mapping and characterization of transcriptional pause sites in the early genetic region of bacteriophage T7. J. Mol. Biol. **196**, 61-84.

Levin, J. R., Krummel, B., and Chamberlin, M. J. (1987). Isolation and properties of transcribing ternary complexes of *Escherichia coli* RNA polymerase positioned at a single template base. J. Mol. Biol. **196**, 85-100.

Lindahl, L., and Zengel, J. M. (1985). Understanding a 26-year old paper: Studies on the relationship between autogenous control and growth-rate regulation of r-protein synthesis. In The molecular biology of bacterial growth, M. Schaecter, F. C. Neidhardt, J. L. Ingraham, and N. O. Kjeldgaard, eds. (Jones and Bartlett Publishing, Inc.), pp. 4-12.

Lindahl, L., and Zengel, J. M. (1986). Ribosomal genes in *Escherichia coli*. Ann. Rev. Genet. **20**, 297-326.

Little, R., Ryals, J., and Bremer, H. (1983a). *rpoB* mutation in *Escherichia coli* alters control of ribosome synthesis by guanosine teraphosphate. J. Bacteriol. **154**, 787-792.

Little, R., Ryals, J., and Bremer, H. (1983b). Physiological characterization of *Escherichia coli rpoB* mutants with abnormal control of ribosome biosynthesis. J. Bacteriol. **155**, 1162-1170.

Lohman, T. M. (1986). Kinetics of protein-nucleic acid interactions: Use of salt effects to probe mechanisms of interaction. CRC Critical Rev. Biochem. **19**, 191-245.

Lund, E. and Dahlberg, J. E. (1979). Initiation of *Escherichia coli* ribosomal RNA synthesis *in vivo*. Proc. Nat. Acad. Sci. USA. **76**, 5480-5484.

Maaløe, O. (1969). An analysis of bacterial growth. Dev. Biol. Suppl. **3**, 33-58.

Mangel, W. F., and Chamberlin, M. J. (1974). Studies of ribonucleic acid chain initiation by *Escherichia coli* ribonucleic acid polymerase bound to T7 deoxyribonucleic acid. I. An assay for the rate and extent of ribonucleic acid chain initiation. J. Biol. Chem. **249**, 2995-3001.

Maniatis, T., Fritsch, E. F., and Sambrook, J. (1982). Molecular Cloning: A laboratory manual. Cold Spring Harbor Laboratory, Cold Spring Harbor, N. Y.

Mazur, S. J. and Record, M. T. Jr. (1989). Association kinetics of site-specific protein-DNA interactions: Roles of nonspecific DNA sites and of the molecular location of the specific site. Biopolymers **28**, 929-953.

McClure, W. R. (1980). Rate-limiting steps in RNA chain initiation. Proc. Natl. Acad. Sci. USA **77**, 5634-5638.

McClure, W. R. (1985). Mechanism and control of transcription initiation in prokaryotes. Ann. Rev. Biochem. **54**, 171-204.

McClure, W. R. and Cech, C. L. (1978). On the mechanism of rifampicin inhibition of RNA synthesis. J. Biol. Chem. **253**, 8949-8956.

McClure, W. R., Cech, C. L., and Johnston, D. E. (1978). A steady state assay for the RNA polymerase initiation reaction. J. Biol. Chem. **253**, 8941-8948.

McDaniel, D. H., and Smoot, C. R. (1956). Approximations in the kinetics of consecutive reactions. J. Phys. Chem. **60**, 966-969.

Melnikova, A. F., Beabealashivilli, R., and Mirzabekov, A. D. (1978). A study of unwinding of DNA and shielding of the DNA grooves by RNA polymerase by using methylation with dimethylsulphate. Eur. J. Biochem. **84**, 301-309.

Metzger, W., Schickor, P., and Heumann, H. (1989a). A cinematographic view of *Escherichia coli* RNA polymerase translocation. EMBO J. **8**, 2745-2754.

Metzger, S., Schreiber, G., Aizenman, E., Cashel, M., and Glaser, G. (1989b). Characterization of the relA1 mutation and a comparison of relA1 with new relA null alleles in *Escherichia coli*. J. Biol. Chem. **264**, 21146-21152.

Mukai, R., and Iida, Y, (1973). Separation of RNA polymerase holoenzyme from core enzyme on DNA-cellulose column. Biochem. Biophys. Res. Commun. **54**, 134-139.

Mulligan, M. E., Hawley, D. K., Entriken, R., and McClure, W. R. (1984). *Escherichia coli* promoter sequences predict *in vitro* RNA polymerase selectivity. Nucl. Acids Res. 12, 789-800.

Munson, L. M., and Reznikoff, W. S., (1981). Abortive initiation and long ribonucleic acid synthesis. Biochemistry **20**, 2081-2085.

Nilsson, L., Vanet, A., Vijgenboom, E., and Bosch, L. (1990). The role of FIS in trans activation of stable RNA operons of *E. coli*. EMBO J. **9**, 727-734.

Noller, H. F. and Nomura, M. (1987). Ribosomes. In *Escherichia coli* and *Salmonella typhimurium*: Cellular and molecular biology, F. C. Neidhardt, J. L. Ingraham, K. Brooks Low, B. Magasanik, M. Schaecter, and H. E. Umbarger, eds. (American Society for Microbiology, Washington D. C.), pp. 104-125.

Nomura, M., Gourse, R., and Baughman, G. (1984). Regulation of the synthesis of ribosomes and ribosomal components. Ann. Rev. Biochem. **53**, 75-117.

Nüsslein, C., and Heyden, B. (1972). Chromatography of RNA polymerase from *Escherichia coli* on single stranded DNA-agarose columns. Biochem. Biophys. Res. Commun. **47**, 282-289.

Owens, J. R., Woody, A. Y., and Haley, B. E. (1987). Characterization of the guanosine-3'-diphosphate-5'-diphosphate binding site on *E. coli* RNA polymerase using a photoprobe, 8-azidoguanosine-3'-5'-bisphosphate. Biochem. Biophys. Res. Comm. **142**, 964-971.

Pedersen, S. (1984). *Escherichia coli* ribosomes translate *in vivo* with variable rate. EMBO J. **3**, 2895-2898.

Petho, A., Belter, J., Boros, I., and Venetianer, P. (1986). The role of upstream sequences in determining the strength of an rRNA promoter of *E. coli*. Biochim. Biophys. Acta. **866**, 37-43.

Pfeffer, S. R., Stahl, S. J., and Chamberlin, M. J. (1977). Binding of *Escherichia coli* RNA polymerase to T7 DNA. J. Biol. Chem. **252**, 5403-5407.

Record, M. T. Jr., and Mossing, M. C. (1987). Physical-chemical origins of stability, specificity, and control of protein-DNA interactions. In RNA polymerase and the regulation of transcription, W. S. Reznikoff, R. R. Burgess, J. E. Dahlberg, C. A. Gross, M. T. Record, Jr., and M. P. Wickens, eds. (Elsevier Science Publishing, Inc., New York), pp. 61-83.

Record, M. T. Jr., Anderson, C. F., and Lohman, T. M. (1978). Thermodynamic analysis of ion effects on the binding and conformational equilibria of proteins and nucleic acids: The roles of ion association or release, screening, and ion effects on water activity. Q. Rev. Biophys. **11**, 103-178.

Record, M. T. Jr., Woodbury, C. P., and Inman, R. B. (1975). Characterization of rodlike DNA fragments. Biopolymers **14**, 393-408.

Rhodes, G., and Chamberlin, M. J. (1974). Ribonucleic acid chain elongation by *Escherichia coli* ribonucleic acid polymerase. J. Biol. Chem. **249**, 6675-6683.

Roe, J-H, Burgess, R. R., and Record, M. T. Jr. (1984). Kinetics and mechanism of the interaction of *Escherichia coli* RNA polymerase with the λP_R promoter. J. Mol. Biol. **176**, 495-521.

Roe, J-H., Burgess, R. R., and Record, M. T. Jr., (1985). Temperature dependence of the rate constants of the *Escherichia coli* RNA polymerase-λP_R promoter interaction: Assignment of the kinetic steps corresponding to protein conformational change and DNA opening. J. Mol. Biol. **184**, 441-453.

Rojiani, M. V., Jakubowski, H., and Goldman, E. (1989). Effect of variation of charged and uncharged $tRNA^{Trp}$ levels on ppGpp synthesis in *Escherichia coli*. J. Bacteriol. **171**, 6493-6502.

Rojiani, M. V., Jakubowski, H., and Goldman, E. (1990). Relationship between protein synthesis and concentrations of charged and uncharged $tRNA^{Trp}$ in *Escherichia coli*. Proc. Natl. Acad. Sci. USA. **87**, 1511-1515.

Rosenberg, S., Kadesch, T. R.,and Chamberlin, M. J. (1982). Binding of *Escherichia coli* RNA polymerase holoenzyme to bacteriophage T7 DNA: Measurements of the rate of open complex formation at T7 promoter A1. J. Mol. Biol. **155**, 31-51.

Ross, W., Thompson, J. F., Newlands, J. T., and Gourse, R. L. (1990). *E. coli* Fis protein activates ribosomal RNA transcription *in vitro* and *in vivo*. EMBO J. **9**, 3733-3742.

Ryals, J., Little, R., and Bremer, H. (1982). Control of rRNA and tRNA synthesis in *Escherichia coli* by guanosine tetraphosphate. J. Bacteriol. **151**, 1261-1268.

Sambrook, J., Fritsch, E. F., and Maniatis, T. (1989). Molecular Cloning: A laboratory manual (2nd Edition). Cold Spring Harbor Laboratory Press, Cold Spring Harbor, N. Y.

Sandermann, H. Jr., and Strominger, J. L. (1972). Purification and properties of C_{55}-isoprenoid alcohol phosphokinase from *Staphylococcus aureus*. J. Biol. Chem. **247**, 5123-5131.

Sarmientos, P., and Cashel, M. (1983). Carbon starvation and growth rate-dependent regulation of the *Escherichia coli* ribosomal RNA promoters: Differential control of dual promoters. Proc. Nat. Acad. Sci. USA. **80**, 7010-7013.

Sarmientos, P., Sylvester, J. E., Contente, S., and Cashel, M. (1983). Differential stringent control of the tandem *E. coli* ribosomal RNA promoters from the *rrnA* operon expressed *in vivo* in multicopy plasmids. Cell **32**, 1337-1346.

Saucier, J.-M., and Wang, J. C. (1972). Angular alteration of the DNA helix by *E. coli* RNA polymerase. Nature New Biol. **239**, 167-170.

Schachtele, C. F., Oman, R. W., and Anderson, D. L. (1970). Effect of elevated temperature on deoxyribonucleic acid synthesis in bacteriophage ϕ29 infected *Bacillus amyloliquefaciens*. J. Virol. **6**, 430-437.

Schickor, P., Metzger, W., Werel, W., Lederer, H., and Heumann, H. (1990). Topography of intermediates in transcription initiation of *E.coli*. EMBO J. **9**, 2215-2220.

Seeman, N., Rosenberg, J., and Rich, A. (1976). Sequence-specific recognition of double helical nucleic acids by proteins. Proc. Natl. Acad. Sci. USA. **73**, 804-808.

Shaner, S. L., Melançon, P., Lee, K. S., Burgess, R. R., and Record, M. T. Jr. (1983). Ion effects on the aggregation and DNA-binding reactions of *Escherichia coli* RNA polymerase. Cold Spring Harbor Symp. Quant. Biol. **47**, 463-472.

Shih, M.-C., and Gussin, G. N. (1983). Mutations affecting two different steps in transcription initiation at the phage λP_{RM} promoter. Proc. Natl. Acad. Sci. USA **80**, 496-500.

Siebenlist, U. (1979). RNA polymerase unwinds an 11-base pair segment of a phage T7 promoter. Nature **279**, 651-652.

Siebenlist, U, Simpson, R. B., and Gilbert, W. (1980). *E. coli* RNA polymerase interacts homologously with two different promoters. Cell **20**, 269-281.

Singer, P. T., and Wu, C-W. (1988). Kinetics of promoter search by *Escherichia coli* RNA polymerase. J. Biol. Chem. **263**, 4208-4214.

Spassky, A., Kirkegaard, K., and Buc, H. (1985). Changes in the DNA structure of the *lac*UV5 promoter during formation of an open complex with *Escherichia coli* RNA polymerase. Biochemistry **24**, 2723-2731.

Spiegelman, G. B. (1972). The kinetics of DNA-RNA membrane filter hybridizations. Ph.D. thesis, molecular biology, University of Wisconsin, Madison. p. 167-172, and Appendix 3.

Spiegelman, G. B., and Whiteley, H. R., (1974). Purification of ribonucleic acid polymerase from SP82-infected *Bacillus subtilis*. J. Biol. Chem. **249**, 1476-1482.

Stackhouse, T. M., Telesnitsky, A. P., and Meares, C. F. (1989). Release of the σ subunit from *Escherichia coli* RNA polymerase transcription complexes is dependent on the promoter sequence. Biochemistry **28**, 7781-7788.

Stefano, J. E. and Gralla, J. D. (1979). *Lac*UV5 transcription *in vitro*. Rate limitation subsequent to formation of an RNA polymerase-DNA complex. Biochemistry **18**, 1063-1067.

Stefano, J. E. and Gralla, J. D. (1982a). Mutation-induced changes in RNA polymerase-*lac* p^s promoter interactions. J. Biol. Chem. **257**, 13924-13929.

Stefano, J. E. and Gralla, J. D. (1982b). Spacer mutations in the *lac* p^s promoter. Proc. Natl. Acad. Sci. USA. **79**, 1069-1072.

Sternbach, H., Engelhardt, R., and Lezius, A. G. (1975). Rapid isolation of highly active RNA polymerase from *Escherichia coli* and its subunits by matrix-bound heparin. Eur. J. Biochem. **60**, 51-55.

Stewart, G., and Bott, K. 1983. DNA sequence of the tandem ribosomal RNA promoters of the *B. subtilis* operon *rrnB*. Nucl. Acids Res. **11**, 6289-6300.

Straney, D. C., and Crothers, D. M. (1985). Intermediates in transcription initiation from the *E. coli lac* UV5 promoter. Cell **43**, 449-459.

Straney, D. C., and Crothers, D. M. (1987a). A stessed intermediate in the formation of stably initiated RNA chains at the *Escherichia coli lac* UV5 promoter. J. Mol. Biol. **193**, 267-278.

Straney, S. B., and Crothers, D. M. (1987b). Kinetics of the stages of transcription initiation at the *Escherichia coli lac* UV5 promoter. Biochemistry **26**, 5063-5070.

Straney, D. C., and Crothers, D. M. (1987c). Comparison of the open complexes formed by RNA polymerase at the *Escherichia coli lac* UV5 promoter. J. Mol. Biol. **193**, 279-292.

Straney, S. B., and Crothers, D. M. (1987d). Lac repressor is a transient gene-activating protein. Cell **51**, 699-707.

Strauss, H. S., Burgess, R. R., Record, M. T. Jr. (1980). Binding of *Escherichia coli* ribonucleic acid polymerase holoenzyme to a bacteriophage T7 promoter-containing fragment: Evaluation of promoter binding constants as a function of solution conditions. Biochemistry **19**, 3504-3515.

Strickland, S., Palmer, G., and Massey, V. (1975). Determination of dissociation constants and specific rate constants of enzyme-substrate (or protein-ligand) interactions from rapid reaction kinetic data. J. Biol. Chem **250**, 4048-4052.

Sutcliffe, J. G. (1979). Complete nucleotide sequence of the *Escherichia coli* plasmid pBR322. Cold Spring Harbor Symp. Quant. Biol. **43**, 77-90.

Takebe, Y., Miura, A., Bedwell, D. M., Tam, M., and Nomura, M. (1985). Increased expression of ribosomal genes during inhibition of ribosome assembly in *Escherichia coli*. J. Mol. Biol. **184**, 23-30.

Thompson, J. F., and Landy, A. (1988). Empirical estimation of protein-induced DNA bending angles: Applications to λ site-specific recombination complexes. Nucl. Acids Res. **16**, 9687-9705.

Travers, A. A. (1976). Modulation of RNA polymerase specificity by ppGpp. Mol. Gen. Genet. **147**, 225-232.

Travers, A. A. (1987). Structure and function of *E. coli* promoter DNA. CRC Critical Rev. Biochem. **22**, 181-219.

Travers, A. A., and Burgess, R. R. (1969). Cyclic re-use of the RNA polymerase sigma factor. Nature (London) **222**, 537-540.

Travers, A. A., Buckland, R., and Debenham, P. G. (1980). Functional heterogeneity of *Escherichia coli* ribonucleic acid polymerase holoenzyme. Biochemistry **19**, 1656-1662.

Travers, A. A., Debenham, P. G., and Pongs, O. (1980). Translation initiation factor 2 alters *E. coli* ribonucleic acid polymerase holoenzyme. Biochemistry **19**, 1651-1656.

Vogt, V. (1969). Breaks in DNA stimulate transcription by core RNA polymerase. Nature (London) **223**, 854-855.

van Ooyen, A. J. J., Gruber, M., and Jørgensen, P. (1976). The mechanism of action of ppGpp on rRNA synthesis *in vitro*. Cell **8**, 123-128.

von Hippel, P. H., Bear, D. G., Morgan, W. D., and McSwiggen, J. A. (1984). Protein-nucleic acid interactions in transcription: A molecular analysis. Ann. Rev. Biochem. **53**, 389-446.

Wallace, R. B., and Miyada, C. G. (1987). Oligonucleotide probes for the screening of recombinant DNA libraries. Methods in Enzymology **152**, 432-442.

Walter, G., Zillig, W., Palm, P., and Fuchs, E. (1967). Initiation of DNA-dependent RNA synthesis and the effect of heparin on RNA polymerase. Eur. J. Biochem. **3**, 194-201.

Wang, J. C. (1979). Helical repeat of DNA in solution. Proc. Natl. Acad. Sci. **76**, 200-203.

Wang, J. C., Jacobsen, J. H., and Saucier, J.-M. (1977). Physicochemical studies on interactions between DNA and RNA polymerase. Unwinding of the DNA helix by *Escherichia coli* RNA polymerase. Nucl. Acids Res. **4**, 1225-1241.

Webb, V., and Spiegelman, G. B. (1984). Ribosomal RNA synthesis in uninfected and SPO1 am34 infected *Bacillus subtilis*. Mol. Gen. Genet. **194**, 98-104.

Winter, R. B., Berg, O. G., and von Hippel, P. H. (1981). Diffusion-driven mechanisms of protein translocation on nucleic acids. 3. The *Escherichia coli lac* repressor-operator interaction: Kinetic measurements and conclusions. Biochemistry **20**, 6961-6977.

Woodbury, C. Jr., Hagenbüchle, O., and von Hippel, P. (1980). DNA site recognition and reduced specificity of the *Eco* R1 endonuclease. J. Biol. Chem. **255**, 11534-11546.

Wu, H.-M., and Crothers, D. M. (1984). The locus of sequence-directed and protein-induced DNA bending. Nature **308**, 509-513.

Yamagishi, M., de Boer, H. A., and Nomura, M. (1987). Feedback regulation of rRNA synthesis: A mutational alteration in the anti-Shine-Dalgarno region of the 16S rRNA gene abolishes regulation. J. Mol. Biol. **198**, 547-550.

Yates, J. L., and Nomura, M. (1981). Feedback regulation of ribosomal protein synthesis in *E. coli*: Localization of the mRNA target sites for repressor action of ribosomal protein L1. Cell **24**, 243-249.

Appendix A: Binding Equilibria

A.I: Mechanisms with the equivalent of one step.

Regular treatments of binding reactions at equilibrium are usually based on a single step reaction mechanism involving a simple bimolecular collision (for a review see Freifelder, 1982). When isomerizations occur after the bimolecular collision, an assumption is usually made that the concentration of intermediate complexes is negligible, effectively reducing, from a mathematical standpoint, the overall mechanism back down to a single step. This is illustrated below in a two-step mechanism

$$R + P \rightleftharpoons C \rightleftharpoons O \qquad \text{(A-1)}$$

where R, P, C, and O are equilibrium concentrations of RNA polymerase, free promoter fragment, closed complex (heparin sensitive), and open complex (heparin resistant) respectively. When [C] is negligible, it can be shown that the total concentration of promoter [P_T] and polymerase [R_T] are given as

$$P_T \approx P + O \qquad \text{(A-2a)}$$

$$R_T \approx R + O. \qquad \text{(A-2b)}$$

Furthermore, the equilibrium constants for the first (K1) and second (K2) steps of equation (A-1) are defined as

$$K1 = \frac{[C]}{[R][P]} \qquad \text{(A-2c)}$$

and $$K2 = \frac{[O]}{[C]}. \qquad \text{(A-2d)}$$

If $$F = \frac{[O]}{P_T} \qquad \text{(A-3a)}$$

= (measurable fraction of heparin resistant complexes formed at a given polymerase concentration)

then by substitution of equations (A-2a,c, and d) into equation (A-3a), it can be shown that

$$F = \frac{K1K2[R][P]}{[P] + K1K2[R][P]} \qquad \text{(A-3b)}$$

and $$\frac{1}{F} = \frac{1}{K1K2[R]} + 1. \qquad \text{(A-3c)}$$

Finally, from equations (A-2b) and (A-3a) it can be shown that

$$[R] = R_T - P_T F. \qquad \text{(A-3d)}$$

Thus, a plot of $1/F$ versus $1/(R_T - P_T F)$ will give a straight line whose slope is equal to $1/K1K2$.

A.II: Mechanisms with two steps.

The following treatment makes no assumptions about the equilibrium concentrations of the reaction intermediates. For the same mechanism (A-1), all descriptions are as listed above, except that

$$P_T = P + O + C \qquad \text{(A-4a)}$$

and $$R_T = R + O + C. \qquad \text{(A-4b)}$$

As a result, it can be demonstrated that

$$F = \frac{K1K2[R][P]}{[P] + K1K2[R][P] + K1[R][P]} \qquad \text{(A-5a)}$$

and $$\frac{1}{F} = \frac{1}{K1K2[R]} + \left(1 + \frac{1}{K2}\right) \qquad \text{(A-5b)}$$

where $$[R] = R_T - P_T F\left(1 + \frac{1}{K2}\right) \qquad \text{(A-5c)}$$

Note: (A-5c) is derived from the relationship ($R = R_T - O - C$) (equation A-4b), where ($O = P_T F$) (equation A-3a), and ($C = P_T F/K2$) (equation A-2d, A-3a).

At saturating enzyme, it is assumed that all available promoter fragments (P_T) exist as complexes of either C or O. If F* represents the fraction of heparin resistant complexes formed at saturating enzyme, it can be shown that

$$F^* = \frac{O}{O + C} \qquad \text{(A-6a)}$$

and $$\frac{F^*}{1 - F^*} = \frac{O}{C} = K2 \qquad \text{(A-6b)}$$

Substitution of (A-6b) into equations (A-5b+c) allows an exact solution for both K1 and K2.

A.III: Mechanisms with three steps (general solution).

$$R + P \rightleftharpoons C \rightleftharpoons I \rightleftharpoons O \qquad \text{(A-7)}$$

If both I and O form heparin resistant complexes, then it can be shown that

$$F = \frac{[O] + [I]}{P_T},\ K1 = \frac{[C]}{[R][P]},\ K2 = \frac{[I]}{[C]},\ \text{and } K3 = \frac{[O]}{[I]}.$$

Also $P_T = P + P_TF + C$

and $R_T = R + P_TF + C.$

From the same considerations given to Case II, it can be shown that

$$F = \frac{K1K2[R](1 + K3)}{K1K2[R](1 + K3) + K1[R] + 1} \qquad \text{(A-8a)}$$

$$\frac{1}{F} = \frac{1}{K1K2(1 + K3)[R]} + \left(1 + \frac{1}{K2(1 + K3)}\right) \qquad \text{(A-8b)}$$

$$[R] = R_T - P_TF\left(1 + \frac{1}{K2(1 + K3)}\right) \qquad \text{(A-8c)}$$

and

$$\frac{F^*}{1 - F^*} = K2(1 + K3). \qquad \text{(A-8d)}$$

As for section A.II, F* represents the fraction of heparin resistant complexes formed at saturating enzyme. From inspection of Case II and III, one can write a general solution.

$$\frac{1}{F} = \frac{1}{K1Ka[R]} + \left(1 + \frac{1}{Ka}\right) \qquad \text{(A-9a)}$$

$$[R] = R_T - P_TF\left(1 + \frac{1}{Ka}\right) \qquad \text{(A-9b)}$$

and

$$\frac{F^*}{1 - F^*} = Ka \qquad \text{(A-9c)}$$

Note that equation (A-9c) reflects the contribution of equilibria following the bimolecular collision, but that the term Ka does not describe the overall equilibrium position of those steps (e.g. In equation A-8d, Ka = K2 + K2K3. This is not the overall equilibrium position for these two steps, which is defined as K2K3).

Therefore, knowledge of R_T and P_T, combined with measurements of F and F*, allows the calculation of K1 for any (n + 1) step mechanism (where $n \geq 1$ represents the number of isomerization steps following the initial bimolecular collision). It should be noted, that as the K1 and/or Ka of a reaction increases, the estimation of K1 based on the methods described above becomes subject to large errors. This is because the term $R_T - P_TF$ approaches zero as the overall equilibrium position of a reaction increases, and therefore becomes more sensitive to errors in the measurement of the absolute value of F.

Appendix B: Reaction Kinetics

B.I: First-order reactions.

Mathematically, the treatment of first-order reactions is relatively simple, and much of the work involved in studying the kinetics of biological mechanisms is based on expressing the overall system in terms of a first-order reaction. A brief review of first-order reaction mechanisms is given below (see also Batschelet, 1973; Eisenberg and Crothers, 1979). The decomposition reaction

$$A \xrightarrow{k} B \qquad \text{(B-1)}$$

can be described by the differential rate equation

$$\frac{d[A]}{dt} = -k[A]. \qquad \text{(B-2)}$$

The object is to find the mathematical equation which can solve for the concentration of A at any time (t), in terms of the concentration of A at time zero ($[A] = [A]_0$ = constant at t = 0). This is accomplished by first rearranging the variables,

$$\frac{d[A]}{[A]} = -k\,dt \qquad \text{(B-3)}$$

and integrating both sides,

$$\int_{A_0}^{A} \frac{d[A]}{[A]} = -k \int_0^t dt \qquad \text{(B-4)}$$

to give the final solution,

$$Ln[A] - Ln[A]_0 = -kt \qquad \text{(B-5)}$$

or, the equivalent form,

$$[A] = [A]_0 e^{-kt} \qquad \text{(B-6)}$$

Thus, for a first-order reaction, the concentration of A decreases exponentially with time. A plot of Ln[A] versus time (t) will yield a straight line, with a slope equal to the negative of the reaction rate constant k.

B.II: Solutions to the overall reaction mechanisms.

The reactions investigated in this thesis are quite straightforward, since there are only two states which are measured (i.e. all detectable complexes are either heparin resistant (HR) or heparin sensitive (HS)). Because of this (and under certain conditions which will be discussed below), overall rate equations can be derived without knowledge of the detailed reaction mechanisms (i.e. the exact number of HS or HR intermediates). These rate equations are discussed below for the overall association and dissociation reactions.

1. Association rates.

The overall mechanism which describes the transitions between heparin resistant and heparin sensitive states can be expressed as a single isomerization reaction,

$$HS \underset{k_d}{\overset{k_{HS}}{\rightleftharpoons}} HR \qquad \text{(B-7)}$$

Where k_{HS} and k_d represent the overall forward and dissociation rate constants respectively. There are three assumed conditions which apply to equation (B-7). First, that the concentration of total promoter fragment $[P_T]$ and polymerase $[R_T]$ remains constant during the course of the reaction. Second, that the individual forward and reverse reactions of the mechanism are either true or pseudo first-order. Finally, that there is one reaction step in the overall mechanism which equilibrates slowly relative to all other steps (the significance of this last condition will be treated in section B.V). There is also one assumed initial condition which is specific to the association reaction of this thesis, such that at time zero, when the association reaction is initiated by mixing the polymerase with the promoter fragments, the concentration of HR is zero (i.e. $[HR]_0 = 0$). Under these conditions, it can be shown that for equation (B-7),

$$[P_T] = [HS] + [HR] \qquad \text{(B-8)}$$

and $$\frac{d[HR]}{dt} = k_{HS}[HS] - k_d[HR]. \qquad \text{(B-9)}$$

Rearrangement of equation (B-8), followed by substitution into (B-9), allows the differential equation to be solved in terms of HR, such that

$$\frac{d[HR]}{dt} = k_{HS}([P_T] - HR]) - k_d[HR] \qquad \text{(B-10)}$$

or

$$\frac{d[HR]}{dt} = -(k_{HS} + k_d)[HR] + k_{HS}[P_T]. \qquad \text{(B-11)}$$

Equation (B-11) has the general form

$$\frac{d[HR]}{dt} = -(1/\tau)[HR] + \beta, \qquad \text{(B-12)}$$

or upon rearrangement,

$$\frac{d[HR]}{dt} = -(1/\tau)([HR] - \beta\tau). \qquad \text{(B-13)}$$

This last equation has the same form as a first-order reaction (B-2), with the corresponding solution

$$\mathrm{Ln}([HR] - \beta\tau) - \mathrm{Ln}([HR]_0 - \beta\tau) = -(1/\tau)\, t, \qquad \text{(B-14)}$$

or the equivalent form

$$\mathrm{Ln}\left\{\frac{[HR] - \beta\tau}{[HR]_0 - \beta\tau}\right\} = -(1/\tau)\, t. \qquad \text{(B-15)}$$

After an 'infinite' reaction time, the association reaction (B-7) will reach a stable equilibrium. From equation (B-12), this means that at infinite reaction time, $d[HR]/dt = 0$, and the product of $\beta\tau$ represents the final equilibrium concentration of the heparin resistant complex $[HR]_\infty$. From the initial reaction conditions for (B-7), it was assumed that $[HR]_0 = 0$. Substituting these expressions for $\beta\tau$ and $[HR]_0$ back into equation (B-15) and rearranging, one can show that

$$\mathrm{Ln}(1 - [HR]/[HR]_\infty) = -(1/\tau)\, t. \qquad \text{(B-16)}$$

This final equation describes the approach of the overall reaction mechanism (B-7) to a state of equilibrium in terms of the time-dependent formation of heparin resistant complexes, where $1/\tau$ is the overall association rate constant. Two important points must be made regarding equation (B-16). First, the rate equation will describe the formation of heparin resistant complexes irrespective of the actual number of HS or HR intermediates in the overall reaction mechanism (B-7). Second, the overall association rate constant $1/\tau$ is a function of the individual forward and reverse rate constants which define the overall reaction mechanism.

Therefore, while measurement of $1/\tau$ does not require knowledge of the detailed reaction mechanism, interpretation of $1/\tau$ will (see also section IV below).

2. Dissociation rates.

The overall dissociation reaction described in this thesis takes the form

$$HR \xrightarrow{k_d} HS \qquad \text{(B-17)}$$

Where k_d represents the overall dissociation rate constant. The three assumed conditions which were previously described for the association reaction (B-7), also apply to equation (B-17). Furthermore, it is assumed that the interaction between heparin and a heparin-sensitive complex is irreversible. Under these conditions, it can be shown that for equation (B-17),

$$\frac{d[HR]}{dt} = - k_d[HR]. \qquad \text{(B-18)}$$

As for the association reaction, it can be shown that equation (B-18) also has the general form

$$\frac{d[HR]}{dt} = - (k_d)[HR] + \beta, \qquad \text{(B-19)}$$

where $\beta = 0$.

Equation (B-19) can be solved according to the treatment applied to equation (B-12), such that

$$Ln\left\{\frac{[HR] - \beta/k_d}{[HR]_0 - \beta/k_d}\right\} = - (k_d)\, t. \qquad \text{(B-20)}$$

Since $\beta = 0$, it is obvious that the final 'equilibrium' concentration of the heparin-resistant complex ($\beta/k_d = [HR]_\infty$) will be zero, as would be expected for an irreversible dissociation reaction, and the description of the overall dissociation mechanism (B-17) will be

$$Ln[HR] = -(k_d)\, t + Ln[HR]_0. \qquad \text{(B-21)}$$

As for the association reaction, equation (B-21) will describe the dissociation rate of heparin resistant complexes irrespective of the actual number of HS or HR intermediates in the overall reaction mechanism (B-17). Similarly, the overall dissociation rate constant (k_d) is a function of the individual forward and reverse rate constants which define the overall reaction mechanism. Note that the rate equation (B-21) could have been obtained directly by integrating equation (B-18). However, the forms of equations B-20 and B-15 emphasize an important consideration. Both the association and dissociation reactions measure the concentration of heparin resistant complexes relative to the reference concentrations of $[HR]_0$ and $[HR]_\infty$. In cases where the plots of equations (B-16) or (B-21) give unexpected results, the assumptions regarding $[HR]_0$ and $[HR]_\infty$ should be re-examined. For example, the dissociation reactions in this thesis were originally performed under conditions of 125 mM KCl, and the corresponding plots of Ln[HR] versus time displayed marked curvature (data not shown). This was because the final equilibrium position of heparin resistant complexes $[HR]_\infty$ was not zero, as originally assumed (see above). Instead, the association of heparin with the heparin-sensitive complex was reversible under these reaction conditions (see also Result section I.2b, Figs. 5 and 6).

In the next two sections, interpretation of the overall rate constants k_d and $1/\tau$ will be considered in relation to the detailed dissociation and association reaction mechanisms which were consistent with the findings of the present thesis.

B.III: Interpreting k_d of the dissociation mechanism.

It has been proposed that complexes between RNA polymerase and promoter fragments can form two types of heparin resistant (HR) isomers which exist in rapid equilibrium with one another, compared to subsequent steps in the dissociation mechanism (see Results section II.3d), such that

$$HR2 \underset{k_3}{\overset{k_{-3}}{\rightleftharpoons}} HR1 \xrightarrow{k_r} HS \qquad \text{(B-22)}$$

Where k_3 and k_{-3} are the respective forward and reverse rate constants which describe the interconversion of the two heparin resistant complexes (HR1 and HR2), and k_r is the apparent reverse rate constant which describes the irreversible decay of HR1 to a heparin sensitive state. This general reaction mechanism has been treated exhaustively in the literature. The treatment outlined here generally follows that of McDaniel and Smoot (1956), but alternative solutions are also available (Benson, 1960; Spiegelman, 1972).

If the concentration of total promoter fragment $[P_T]$ remains constant during the course of the reaction, it follows that

$$[HR2] + [HR1] + [HS] = [P_T] = \text{constant} \qquad \text{(B-23)}$$

$$\frac{d[HR2]}{dt} = k_3[HR1] - k_{-3}[HR2] \qquad \text{(B-24)}$$

$$\frac{d[HR1]}{dt} = k_{-3}[HR2] - (k_3 + k_r)[HR1] \qquad \text{(B-25)}$$

$$\frac{d[HS]}{dt} = k_r[HR1] \qquad \text{(B-26)}$$

and $$\frac{d[HR2]}{dt} + \frac{d[HR1]}{dt} + \frac{d[HS]}{dt} = 0. \qquad \text{(B-27)}$$

As a consequence of equation (B-27), it is apparent that the dissociation rate of all heparin resistant complexes equals the formation rate of the heparin sensitive complex, such that

$$-\frac{d[HR2 + HR1]}{dt} = \frac{d[HS]}{dt}. \qquad \text{(B-28)}$$

From equation (B-26) it is clear that equation (B-28) can also be written as

$$\frac{d[HR2 + HR1]}{dt} = -k_r[HR1]. \qquad \text{(B-29)}$$

A solution for [HR1] in terms of [HR2 + HR1] is possible if d[HR1]/dt is negligible (steady state assumption), such that equation (B-25) can be expressed as

$$(k_3 + k_r)[HR1] = k_{-3}[HR2]. \qquad \text{(B-30)}$$

From equation (B-23), $[HR2] = [P_T - HR1 - HS]$. Substitution of this expression into equation (B-30), followed by rearrangement, yields a solution for [HR1].

$$[HR1] = \frac{k_{-3}[P_T - HS]}{k_{-3} + k_3 + k_r}. \qquad \text{(B-31)}$$

From equation (B-23), $[P_T - HS] = [HR2 + HR1]$. Furthermore, the original mechanism outlined in equation (B-22) suggested that HR1 and HR2 existed in a rapid equilibrium relative to the rate limiting formation of HS (i.e. $k_3 >> k_r$). With these considerations, substitution of equation (B-31) into equation (B-29) yields

$$\frac{d[HR2 + HR1]}{dt} = -\left(\frac{k_r}{1 + k_3/k_{-3}}\right)[HR2 + HR1]. \qquad \text{(B-32)}$$

It can be seen that (B-32) takes the form of a first-order differential equation (see B-2), with the corresponding solution

$$Ln[HR2 + HR1] = -\left(\frac{k_r}{1 + k_3/k_{-3}}\right)t + Ln[HR2 + HR1]_0. \qquad \text{(B-33)}$$

As expected, the form of this last equation is equivalent to the solution (B-21) for the overall dissociation reaction (B-17). The corresponding overall dissociation rate constant (k_d) will be related to the individual forward and reverse rate constants of the detailed mechanism (B-22) such that

$$k_d = \frac{k_r}{1 + k_3/k_{-3}}. \qquad \text{(B-34)}$$

B.IV: Interpreting 1/τ of the association mechanism.

It has been proposed that a heparin sensitive complex forms as a direct result of the bimolecular collision between free RNA polymerase (R) and free promoter fragments (P), and that a heparin resistant state is not achieved until at least one additional isomerization step has occurred (see Results section II.4b).

$$R + P \underset{k_{-1}}{\overset{k_1}{\rightleftharpoons}} HS \underset{k_d}{\overset{k_f}{\rightleftharpoons}} HR \qquad (35)$$

The second-order association rate constant (k_1) describes the formation of the initial HS complex, and k_{-1} is the reverse rate constant which describes the dissociation of the initial HS complex into its separate components. The forward rate constant (k_f) describes the conversion of the heparin sensitive complexes into a heparin resistant state, and the overall dissociation rate constant (k_d) was previously described in section B.II.2. Under conditions where total RNA polymerase (R_T) is in molar excess over total promoter fragments (P_T), the kinetics of the bimolecular collision will be pseudo first-order, since the concentration of [R] does not change over the course of the reaction (i.e. $[R] \approx [R_T]$ = constant). Consequently, equation (B-35) can be reduced, such that

$$P \underset{k_{-1}}{\overset{k_1 R_T}{\rightleftharpoons}} HS \underset{k_d}{\overset{k_f}{\rightleftharpoons}} HR \qquad (36)$$

If the total promoter concentration is constant over the course of the association reaction, the following equations will describe mechanism (B-36).

$$[P] + [HS] + [HR] = [P_T] \qquad (B\text{-}37)$$

$$\frac{d[P]}{dt} = k_{-1}[HS] - k_1[R_T][P] \qquad (B\text{-}38)$$

$$\frac{d[HS]}{dt} = k_1[R_T][P] - (k_{-1} + k_f)[HS] + k_d[HR] \qquad (B\text{-}39)$$

and $$\frac{d[HR]}{dt} = k_f[HS] - k_d[HR]. \qquad \text{(B-40)}$$

The formation rate of heparin resistant complexes is given by equation (B-40). The exercise is to solve equation (B-40) in terms of HR. The solution to this problem is given below, and closely follows the general treatment of Strickland *et al.*, (1975) as adapted by McClure (1980).

If d[HS]/dt is negligible (steady state assumption), then equation (B-39) can be rearranged such that

$$(k_{-1} + k_f)[HS] = k_1[R_T][P] + k_d[HR]. \qquad \text{(B-41)}$$

From equation (B-37), $[P] = [P_T - HS - HR]$. Substitution of this expression into (B-41), followed by rearrangement, yields an expression for [HS].

$$[HS] = \frac{k_1[R_T][P_T] + (k_d - k_1[R_T])[HR]}{k_1[R_T] + k_{-1} + k_f}. \qquad \text{(B-42)}$$

Substitution of (B-42) into (B-40), followed by rearrangement will yield

$$\frac{d[HR]}{dt} = -\left\{\frac{k_1[R_T](k_f + k_d) + k_{-1}k_d}{k_1[R_T] + k_{-1} + k_f}\right\}[HR] + \frac{k_f k_1[R_T][P_T]}{k_1[R_T] + k_{-1} + k_f}. \qquad \text{(B-43)}$$

This differential equation takes the general form

$$\frac{d[HR]}{dt} = -(1/\tau)[HR] + \beta. \qquad \text{(B-44)}$$

The solution to (B-44) has been treated in detail for the association reaction in section B.II.1, and can be written as

$$\text{Ln}(1 - [HR]/[HR]_\infty) = -(1/\tau)\, t. \qquad \text{(B-45)}$$

Thus, the exponential approach of the heparin resistant complex to its final equilibrium position will be described by the overall association rate constant $(1/\tau)$. In turn, $(1/\tau)$ can be related to the individual forward and reverse rate constants which describe the detailed reaction mechanism (B-36). Referring back to equations (B-43) and (B-44), it is apparent that

$$1/\tau = \frac{k_1[R_T](k_f + k_d) + k_{-1}k_d}{k_1[R_T] + k_{-1} + k_f}. \qquad \text{(B-46)}$$

If it is assumed that $k_f >> k_d$ (see also Tables V and VI), and that the term $(k_{-1}k_d)$ is negligible compared to $k_fk_1[R_T]$, then equation (B-46) simplifies to

$$1/\tau = \frac{k_fk_1[R_T]}{k_1[R_T] + k_{-1} + k_f}. \qquad \text{(B-47)}$$

A more useful representation of equation (B-47) is the double reciprocal form.

$$\tau = \frac{k_{-1} + k_f}{k_fk_1[R_T]} + \frac{1}{k_f}. \qquad \text{(B-48)}$$

Thus, a plot of tau versus $[R_T]^{-1}$ will give a straight line, whose intercept equals $(1/k_f)$. The slope of the tau plot is sometimes referred to as the reciprocal of the (overall) second-order association rate constant (k_a). The expression for $(1/k_a)$ depends on the relative magnitudes of k_{-1} and k_f. If $k_{-1} >> k_f$, then the reaction between free RNA polymerase and the promoter is in rapid equilibrium, such that

$$R + P \underset{k_{-1}}{\overset{k_1}{\rightleftharpoons}} HS \xrightarrow{k_f} HR \qquad (49)$$

and the slope of the tau plot is $1/(k_fK1)$ (where the binding equilibrium constant $K1 = k_1/k_{-1}$). Alternatively, if $k_f >> k_{-1}$, then the formation of heparin resistant complexes will occur by a sequential mechanism, such that

$$R + P \xrightarrow{k_1} HS \xrightarrow{k_f} HR \qquad (50)$$

and the slope of the tau plot is $1/(k_1)$.

Note that if the term $(k_{-1}k_d)$ of (B-46) were significant compared to $k_fk_1[R_T]$, then the subsequent plots of τ versus $[R_T]^{-1}$ would have a decrease in slope at low concentrations of polymerase (Strickland *et al.*, 1975). Inspection of Figures 22 and 23 clearly shows that such a decrease did not occur, suggesting that the original assumption that $k_{-1}k_d << k_fk_1[R_T]$ was valid.

B.V: Are the steady-state approximations accurate reflections of the exact solutions?

It is notable that both the dissociation (B-22) and association (B-36, where $k_f >> k_d$) mechanisms treated in this thesis take the form:

$$A \underset{k_{21}}{\overset{k_{12}}{\rightleftharpoons}} B \xrightarrow{k_{23}} C \qquad (51)$$

As discussed in section B.II, the detailed reaction mechanism will be described by an overall rate constant (k_d or $1/\tau$ for the respective dissociation and association mechanisms). Approximate solutions to these overall rate constants were obtained in sections B.III and B.IV by applying a steady-state assumption to the equivalent of the intermediate 'B' of equation (B-51) (where B = HR1 in section B.III and HS in section B.IV). How well do these approximate solutions reflect the exact solutions in terms of the individual rate constants which define a reaction mechanism of the form outlined in equation (B-51)? It can be shown that the exact solution (Benson, 1960; Hammes and Schimmel, 1970; Batschelet, 1973) to the two-step mechanism outlined in equation (B-51) will be described by a spectrum of two overall reaction rate constants, designated here as λ_f (fast) and λ_s (slow):

$$[C] = X + Ye^{-(\lambda_f)t} + Ze^{-(\lambda_s)t} \qquad (B\text{-}52)$$

The coefficients X, Y, and Z are functions whose exact values will depend on the initial reaction conditions. The two overall rate constants λ_f and λ_s are defined by the individual forward and reverse rate constants of mechanism (B-51) such that:

$$\lambda_{f,s} = \frac{(k_{12} + k_{21} + k_{23}) \pm \sqrt{(k_{12} + k_{21} + k_{23})^2 - 4(k_{12}k_{23})}}{2} \qquad (B\text{-}53)$$

Where λ_f and λ_s are the respective positive and negative roots of equation (B-53), and are therefore related to one another such that:

$$\lambda_f + \lambda_s = k_{12} + k_{21} + k_{23} \qquad (B\text{-}54)$$

and $$(\lambda_f)(\lambda_s) = k_{12}k_{23}. \qquad (B\text{-}55)$$

Under conditions where $\lambda_f >> \lambda_s$, it can be seen that the exact solution to equation (B-52) will be dominated by the single exponential term containing λ_s. This is because the exponential term in equation (B-52) which contains λ_f will rapidly approach zero before any significant change has occurred in the term containing λ_s. Furthermore, since $\lambda_f + \lambda_s \approx \lambda_f$, a solution to λ_s can be obtained from division of equation (B-55) by (B-54), such that:

$$\lambda_s = \frac{k_{12}k_{23}}{k_{12} + k_{21} + k_{23}}. \qquad \text{(B-56)}$$

This last expression is identical in form to the definitions of k_d and $1/\tau$ obtained in sections B.III and B.IV using a steady-state approximation (e.g. compare equation B-56 with B-47). Therefore under conditions where $\lambda_f >> \lambda_s$, the steady-state approximation will accurately reflect the exact solution to the overall rate constant which describes a reaction mechanism of the form outlined in equation (B-51). In their treatment of equation (B-51), McDaniel and Smoot (1956) demonstrated that the steady-state approximation will accurately reflect the exact solution under any of the following circumstances (equation B-57a-d):

(a) $k_{21} >> k_{23}$

(b) $k_{21} >> k_{12}$

(c) $k_{23} >> k_{12}$

(d) $k_{12} >> k_{23}$

For the dissociation mechanism (B-22) it was proposed that the two heparin resistant complexes existed in a state of rapid equilibrium compared to subsequent steps in the reaction (i.e. $k_3 >> k_r$). This is equivalent to condition (B-57a) listed above, and suggests that the definition of k_d (B-34) obtained by steady-state approximation will accurately reflect the exact solution to the dissociation reaction. For the association mechanism outlined in equation (B-36), the situation was more complicated. From the thermodynamic analysis of the association rates (see Results section II.4d), it was concluded that the formation of heparin resistant complexes

occurred by a sequential mechanism (B-50) such that $k_f >> k_{-1}$. This implies that the definition of $1/\tau$ obtained by steady-state approximation (B-47) will accurately reflect the exact solution to the association reaction only if conditions (B-57c) or (B-57d) are satisfied. Equations (B-57c and B-57d) are equivalent to comparing $k_1[R_T]$ to k_f for the association mechanism (B-36). Using the calculated values for k_1 and k_f obtained from the tau analyses (see Table VI), and the maximum polymerase concentration that was employed in each study, Table XV below investigates the predicted relationship between $k_1[R_T]$ and k_f.

Table XV. Relationship between $k_1[R_T]$ and k_f.

Promoter/ °C/± ppGpp	$[R_T]$ (M) x 10^9	k_1 ($M^{-1}s^{-1}$) x 10^{-8}	$k_1[R_T]$ (s^{-1})	k_f (s^{-1})	$k_1[R_T]/k_f$
BP1/15°-	1.1	1.3	0.14	0.06	2.4
BP1/15°+	1.1	1.3	0.14	0.08	1.8
BP2/10°-	1.1	0.95	0.1	0.11	0.91
BP2/10°+	1.1	0.91	0.1	0.22	0.46
BP1/35°-	0.31	2.1	0.065	≥0.65	≤0.1
BP1/35°+	0.31	2.6	0.081	0.31	0.26
BP2/35°-	0.31	1.5	0.046	≥0.56	≤0.08
BP2/35°+	0.31	1.0	0.031	≥1.0	≤0.03

From Table XV it is apparent that at 35° C, $k_f > k_1[R_T]$ over the entire polymerase concentration range used at either BP1 or BP2. This satisfies condition (B-57c) and suggests that at 35° C, the definition of $1/\tau$ obtained by the steady-state approximation (B-47) will accurately reflect the exact solution to the association reaction. At the lower reaction temperatures, conditions may exist where the ratio $k_1[R_T]/k_f$ approaches 1.0. McDaniel and Smoot (1956) have calculated that under these circumstances, the steady-state approximation will be a poor reflection of the exact solution for approximately 61% of the association reaction, but that following this 'induction' period, values calculated by the steady-state approximation will be

within 5% of the exact solution. Practically, this means that $1/\tau$ determinations based on equation (B-45) can still be interpreted according to the steady-state approximation (B-47) as long as the $Ln(1 - [HR]/[HR]_\infty)$ values are ≤ -1 (i.e. the association reaction is $\geq 63\%$ complete). For example, at 1.1 nM polymerase and in the presence of ppGpp, the $k_1[R_T]/k_f$ ratio approaches 1.0 for BP1/15° (see Table XV), suggesting that equation (B-47) might inadequately represent the association reaction. However, Fig. 17B shows that under these conditions, the majority of the points calculated for $Ln(1 - [HR]/[HR]_\infty)$ are well below - 1. Therefore, the estimate of $1/\tau$ should still be interpreted according to the steady-state approximation (B-47). In general, the absence of any curvature in the plots of $Ln(1 - [HR]/[HR]_\infty)$ versus time would suggest that the association reaction (B-36) is represented by the steady-state approximation (B-47).

Appendix C: Thermodynamics

The study of thermodynamics is concerned with the energy changes that accompany a physical process (for a review see Castellan, 1983). These energy changes are expressed as a differential in free energy between the products and the reactants of the process in question. By convention, this differential is designated by the symbol Δ. When a reaction occurs under conditions of constant pressure (standard pressure = 1 atm), it can be shown that at equilibrium

$$Ln(Kc) = -\frac{\Delta G^\circ}{RT} \qquad \text{(C-1)}$$

where Kc = the equilibrium constant of the reaction.

ΔG° = the standard Gibbs energy of the reaction (cal mol^{-1}).

R = the gas constant (1.987 cal K^{-1} mol^{-1})

T = the absolute temperature of the reaction (Kelvin)

As can be seen from equation C-1, the value of ΔG° determines the position of equilibrium for a reaction. However, this relationship is only true under the

condition of constant temperature, since the term $\Delta G°$ is a function of temperature itself, wherein

$$\Delta G° = \Delta H° - T\Delta S° \qquad \text{(C-2)}$$

and $\Delta H°$ = the standard enthalpy of the reaction (cal mol^{-1}).

$\Delta S°$ = the standard entropy of the reaction (cal K^{-1} mol^{-1}).

Substituting this expression for $\Delta G°$ into equation C-1, one obtains the general relationship

$$\text{Ln(Kc)} = -\frac{\Delta H°}{RT} + \frac{\Delta S°}{R} \qquad \text{(C-3)}$$

Thus the temperature dependency of the equilibrium constant is based on $\Delta H°$, and a plot of Ln(Kc) versus 1/T will give a straight line whose slope is equal to $-\Delta H°/R$. Stated another way:

$$\frac{\text{d Ln(Kc)}}{\text{d (1/T)}} = -\frac{\Delta H°}{R} \qquad \text{(C-4)}$$

If the overall reaction is exothermic, $\Delta H°$ is negative, and the equilibrium constant decreases with increasing temperature. Conversely, when the reaction is endothermic, $\Delta H°$ is positive, and Kc increases with increasing temperature.

The equilibrium constant (Kc) can be defined as a ratio between the complementary forward (k_f) and reverse (k_r) rate constants of the reaction mechanism. As a result, the temperature dependence of an individual rate constant is very similar to that of an equilibrium constant, such that

$$\text{Ln(k)} = -\frac{E_a}{RT} + \text{Ln(A)} \qquad \text{(C-5)}$$

where k = the rate constant for the reaction step.

E_a = the activation energy for the reaction step.

A = the collision frequency factor of the reaction step.

This relationship is the Arrhenius equation, and like C-3, it can be written as

$$\frac{d\,Ln(k)}{d\,(1/T)} = -\frac{E_a}{R} \qquad (C\text{-}6)$$

Thus, for a single rate constant, the plot of Ln(k) versus 1/T will yield a straight line, whose slope can be used to calculate the activation energy of the reaction step. With very rare exceptions (e.g. some termolecular reactions, Castellan, 1983), an increase in temperature will cause an increase in the reaction rate. Therefore, E_a is almost always positive for the individual rate constants of a reaction step. However, the Arrhenius plot for an apparent rate constant can often yield an overall activation energy which is negative. Consider the dissociation reaction outlined in Appendix (B-34), where the rate limiting step (k_r) was preceded by a rapid equilibrium such that

$$k_d = \frac{k_r}{1 + k_3/k_{-3}} \qquad (C\text{-}7)$$

Assuming $k_3/k_{-3} >> 1$, then this equation reduces to

$$k_d = \frac{k_r}{(k_3/k_{-3})}. \qquad (C\text{-}8)$$

Under these conditions, the Arrhenius plot of k_d can be expanded as

$$-R\,\frac{d\,Ln(k_d)}{d\,(1/T)} = -R\,\frac{d\,Ln\left[\frac{k_r}{k_3/k_{-3}}\right]}{d\,(1/T)} = -R\,\frac{d\,Ln(k_r) - d\,Ln(k_3/k_{-3})}{d\,(1/T)} \qquad (C\text{-}9)$$

With consideration to equations C-4 and C-6, the last expression of (C-9) is equivalent to

$$E_{a,d} = E_{a,r} - \Delta H_3^\circ \qquad (C\text{-}10)$$

Therefore, the apparent activation energy for the rate constant k_d (= $E_{a,d}$) is a differential between the activation energy for k_r (= $E_{a,r}$), and the enthalpy for the equilibrium k_3/k_{-3} (= ΔH_3°). Under conditions when $\Delta H_3^\circ > E_{a,r}$, the overall activation energy for the dissociation rate will be negative.

Finally, Figure 31 below demonstrates that the activation energy for a reaction step is related to the enthalpy of the reaction equilibrium. For this exothermic reaction, the activation energy of the forward rate constant ($E_{a,f}$) and that of the reverse rate constant ($E_{a,r}$), are related to the enthalpy ($\Delta H°$) according to equations C-11 to C-14.

Figure 31. Variation of enthalpy during an exothermic reaction.

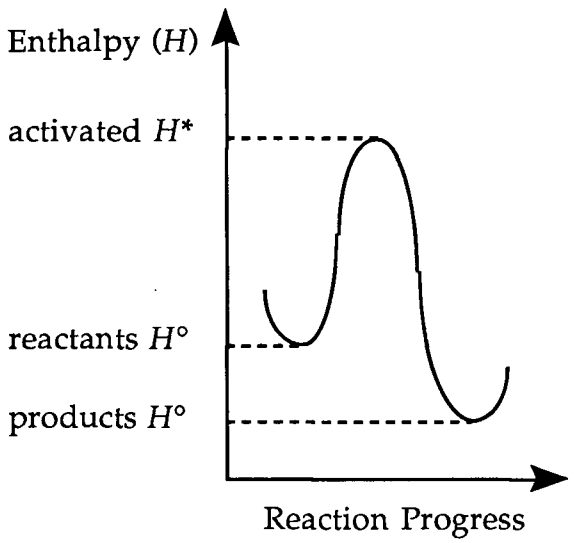

$$E_{a,f} = H^* - H°(\text{reactants}) \qquad \text{(C-11)}$$

$$E_{a,r} = H^* - H°(\text{products}) \qquad \text{(C-12)}$$

$$\Delta H° = H°(\text{products}) - H°(\text{reactants}) \qquad \text{(C-13)}$$

From this it follows that

$$\Delta H° = E_{a,f} - E_{a,r} \qquad \text{(C-14)}$$